HAL
open science

Rôle des complexes WASH et exocyste dans l'invasion tumorale

Pedro Monteiro

To cite this version:

Pedro Monteiro. Rôle des complexes WASH et exocyste dans l'invasion tumorale. Biologie cellulaire. Université Pierre et Marie Curie - Paris VI, 2014. Français. NNT : 2014PA066291 . tel-01205724

HAL Id: tel-01205724

https://theses.hal.science/tel-01205724

Submitted on 27 Sep 2015

HAL is a multi-disciplinary open access archive for the deposit and dissemination of scientific research documents, whether they are published or not. The documents may come from teaching and research institutions in France or abroad, or from public or private research centers.

L'archive ouverte pluridisciplinaire **HAL**, est destinée au dépôt et à la diffusion de documents scientifiques de niveau recherche, publiés ou non, émanant des établissements d'enseignement et de recherche français ou étrangers, des laboratoires publics ou privés.

THESE DE DOCTORAT DE

L'UNIVERSITE PIERRE ET MARIE CURIE

Spécialité : Complexité du vivant

Présentée par

M. Pedro Monteiro

Pour obtenir le grade de

DOCTEUR de l'UNIVERSITE PIERRE ET MARIE CURIE

Rôle des complexes WASH et exocyste dans l'invasion tumorale

Thèse effectuée à l'Institut Curie, Paris

Equipe « Dynamique de la membrane et du cytosquelette »

UMR 144 CNRS/Institut Curie

dirigée par le Dr. Philippe CHAVRIER

soutenue le 25 septembre 2014

<u>devant le jury composé de :</u>

Pr Thierry Soldati	Rapporteur
Dr Corinne Albigès-Rizo	Rapporteur
Pr Joëlle Sobczak-Thépot	Examinateur
Dr Ana-Maria Lennon Duménil	Examinateur
Dr Philippe Chavrier	Directeur de thèse

Table des matières

Table des figures.....7

Résumé 11

Introduction.....15

I. Cancer du sein et programme métastatique.....15
A. Histologie de l'épithélium de la glande mammaire.....15
B. Transition épithélio-mésenchymateuse.....19
II. La matrice extracellulaire.....23
A. Composition de la matrice extracellulaire.....23
1. La membrane basale.....23
a. Composition de la membrane basale.....23
b. Transmigration à travers la membrane basale.....25
2. Stroma.....26
a. La matrice extracellulaire du stroma.....26
b. Migration à travers le stroma.....28
3. Matrices extracellulaires reconstituées *in vitro*.....31
III. Les invadopodes : protrusions membranaires responsables de la dégradation de la matrice extracellulaire.....37
A. Découverte des invadopodes.....37
B. Composition en protéases.....39
C. Formation des invadopodes.....42
D. Polymérisation de filaments d'actine et maturation de l'invadopode.....45
1. Les filaments d'actine.....45
2. Régulation de la polymérisation de filaments d'actine à l'invadopode.....47
3. Maturation de l'invadopode.....51
IV. Les métalloprotéases matricielles.....55
A. Description de la famille des métalloprotéases.....55

B. MT1-MMP....60
1. Synthèse et structure de MT1-MMP....61
2. Activité de MT1-MMP....62
3. Endocytose de MT1-MMP....63
4. Régulation de MT1-MMP par le trafic intracellulaire....64
V. Le complexe exocyste....67
VI. Le complexe WASH....71

Objectifs....77

Article....81

Discussion....137

Remerciements....155

Références....159

Annexes....179

Table des Figures

Figure 1 : Cancer du sein et dissémination métastatique....13
Figure 2 : Coupe histologique transversale d'un canal galactophorique de la glande mammaire....16
Figure 3 : Polarité apico-basale au sein d'une cellule épithéliale de l'épithélium de la glande mammaire....17
Figure 4 : Transition épithélio-mésenchymateuse et changement de phénotype cellulaire....21
Figure 5 : Schéma de la composition et de l'organisation de la membrane basale....24
Figure 6 : Franchissement de la membrane basale en condition physiologique et pathologique....25
Figure 7 : Synthèse, maturation et assemblage des fibres de collagène de type 1....27
Figure 8 : Différents modes de migration à travers le stroma....30
Figure 9 : Exemples de matrices reconstituées *in vitro*....32
Figure 10 : Extraction en milieu acide ou enzymatique (pepsine) de collagène provenant de tendons de queues de rats : effets sur la capacité invasive des cellules....34
Figure 11 : Influence de la température de polymérisation des fibres de collagène sur la porosité du réseau tridimensionnel des fibres de collagène....36
Figure 12 : Premières observations d'invadopodes....38
Figure 13 : Formation d'invadopodes au niveau de cellules tumorales cultivées sur substrat artificiel....41
Figure 14 : Schéma représentant les étapes initiales de la formation des invadopodes....43
Figure 15 : La dynamique des filaments d'actine....46
Figure 16 : Localisation au niveau de l'invadopode de la machinerie de polymérisation d'actine et des métalloprotéases matricielles....50
Figure 17 : Maturation de l'invadopode dépendante de la présence de filaments d'actine et de protéases....53
Figure 18 : Evolution de la formation et de la maturation de l'invadopode....54
Figure 19 : Structure des métalloprotéases matricielles....56
Figure 20 : Tableau représentant les différentes caractéristiques des MMPs (catégorie, activateurs, cibles....58
Figure 21 : Synthèse, endocytose et trafic intracellulaire de MT1-MMP....62
Figure 22 : Adressage de MT1-MMP au niveau de la membrane plasmique de l'invadopode....66
Figure 23 : Le complexe exocyste est impliqué dans de nombreux processus cellulaires....70
Figure 24: Le complexe WASH localise à la surface des endosomes dont la nature dépend du type cellulaire....74

Figure 25: Le complexe WASH permet d'induire la polymérisation de filaments d'actine à la surface d'endosomes.....139
Figure 26: Mise en relation de deux réseaux branchés d'actine de polarité opposée.....142
Figure 27 : Carte des domaines d'interaction de Sec3 et Exo84 avec WASH obtenus par cribles double hybride.....143
Figure 28 : Mécanisme impliquant les aPKC et la dynamine lors de l'exocytose des endosomes contenant MT1-MMP.....146
Figure 29 : Rôle du noyau cellulaire dans la migration à travers un réseau de collagène fibrillaire.148
Figure 30 : Effet de l'inhibition de l'activité catalytique de MT1-MMP sur des cellules tumorales MDA-MB-231 cultivées dans un réseau de collagène fibrillaire.....150

Résumé

Le cancer du sein représente la première cause de décès par cancer chez la femme. La grande majorité de ces décès est due à la dissémination des cellules tumorales dans l'organisme, processus aboutissant à la colonisation de tissus sains et à la formation de métastases. Ce processus est appelé dissémination métastatique et peut être résumé en 3 principales étapes : la formation d'une tumeur primaire, l'invasion tumorale et la formation de métastases, également appelées tumeurs secondaires (voir Figure 1) (De Craene and Berx, 2013; Gupta and Massague, 2006; Hanahan and Weinberg, 2000). Dans les cancers du sein, la formation de la tumeur primaire a lieu au niveau de l'épithélium des canaux ou des lobules de la glande mammaire. Les cellules formant cet épithélium (cellules épithéliales, voir Figure 1a) subissent des altérations génétiques qui entrainent leur transformation. Ces cellules transformées se divisent, prolifèrent de manière incontrôlée et donnent naissance à un ensemble de cellules tumorales confinées dans les canaux de la glande mammaire (appelé carcinome canalaire *in situ*, voir Figure 1b). Ce carcinome canalaire *in situ* est séparé des tissus interstitiels sous-jacents (stroma) par la présence d'une lame basale (membrane basale). De par son organisation et son architecture, la membrane basale permet le maintien de la structure de l'épithélium mammaire et constitue un frein à la progression tumorale. La membrane basale est non-permissive au passage des cellules tumorales. Ces cellules tumorales vont devoir dégrader la membrane basale afin de la pénétrer.

Les cellules tumorales acquièrent cette capacité à dégrader les tissus environnants, et notamment la membrane basale, lors d'un processus cellulaire appelé transition épithélio-mésenchymateuse (TEM) (Thiery, 2002). La TEM s'accompagne notamment d'un réarrangement du cytosquelette de la cellule ainsi que de la surexpression de métalloprotéases matricielles (MMPs), enzymes dégradatives spécifiques des composants de la membrane basale (Kessenbrock et al., 2010).

Au cours de ces dernières années, de nombreuses études ont démontré l'importance d'un membre de la famille des MMPs, la métalloprotéase matricielle MT1-MMP (Hotary et al., 2006; Poincloux et al., 2009). MT1-MMP est surexprimée dans de nombreux cancers, notamment le cancer du sein (Jiang et al., 2006). MT1-MMP est présente dans

les cellules tumorales au niveau de compartiments intracellulaires appelés endosomes (Sakurai-Yageta et al., 2008; Steffen et al., 2008).

Lorsque des cellules tumorales de cancer du sein sont cultivées *in vitro* au contact de substrats artificiels reconstituant l'environnement physiologique de la cellule, les cellules tumorales dégradent le substrat (Artym et al., 2006; Hotary et al., 2006; Rowe and Weiss, 2008). La dégradation est circonscrite à des structures cellulaires appelées invadopodes (Artym et al., 2006; Chen, 1989; Sakurai-Yageta et al., 2008). Les invadopodes sont des protrusions membranaires enrichies en filaments d'actine ainsi qu'en métalloprotéase MT1-MMP et sont responsables de l'activité dégradative des cellules tumorales *in vitro*.

Les cellules tumorales invasives s'échappant de la tumeur primaire (on parle de carcinome infiltrant; voir Figure 1c) vont éventuellement atteindre et entrer dans les vaisseaux sanguins ou les vaisseaux lymphatiques (phénomène d'intravasation, voir Figure 1d), emprunter ces deux réseaux de circulation afin de migrer vers des sites distants, en ressortir (phénomène d'extravasation, voir Figure 1e) et coloniser les organes sains afin de proliférer et de former des métastases (voir Figure 1f). Ces différentes étapes constituent le programme de dissémination métastatique responsable de l'agressivité des cancers du sein.

Le but de mon travail a été de comprendre comment se fait l'adressage de la protéase MT1-MMP au niveau de la membrane plasmique de la cellule tumorale. L'identification du mécanisme moléculaire mis en jeu ainsi que les régulateurs de ce processus constitue une pièce importante dans la compréhension de l'invasion tumorale ainsi qu'une cible importante dans la lutte contre le cancer du sein.

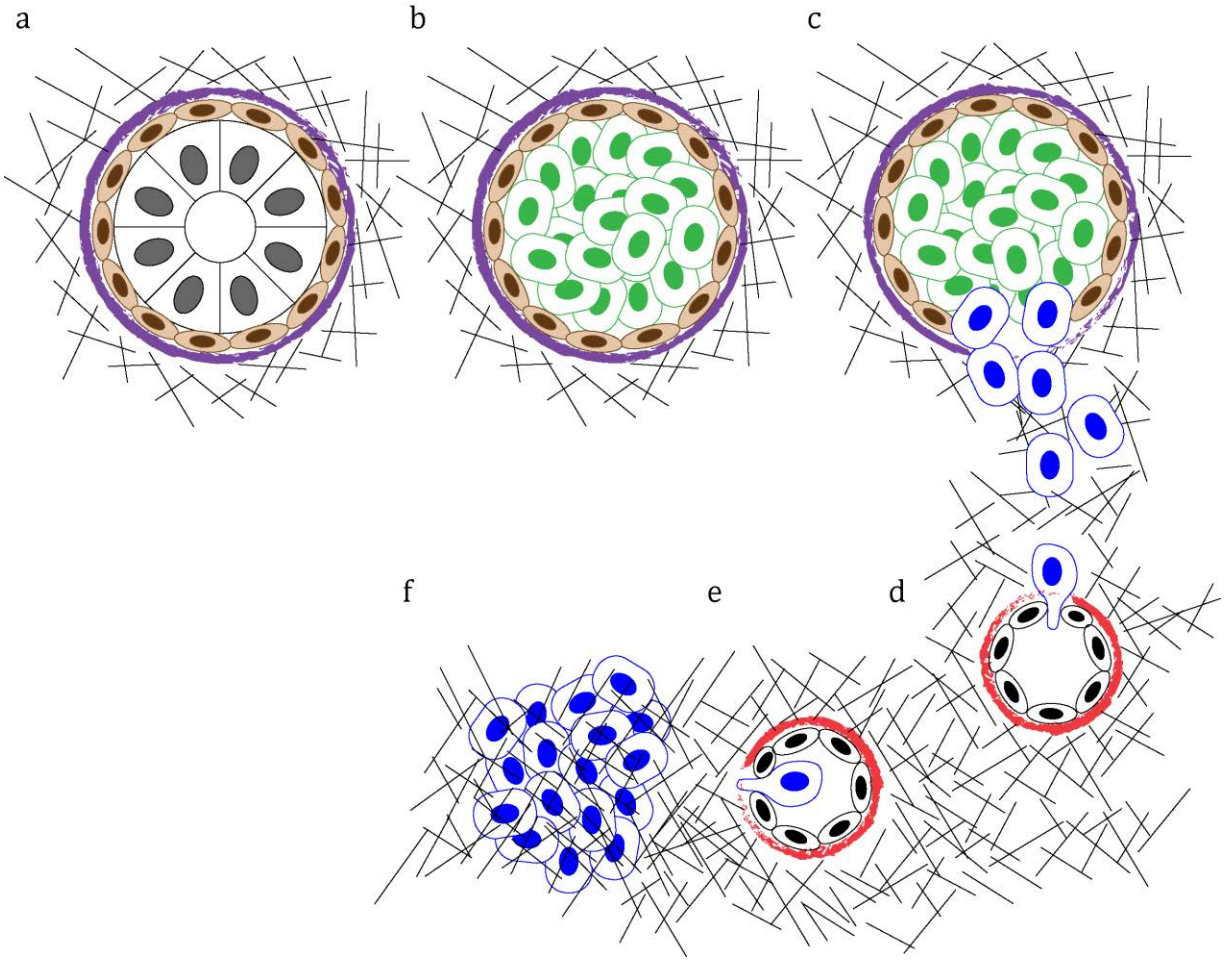

Figure 1 : Cancer du sein et dissémination métastatique

a) Les cellules épithéliales (gris) sont confinées dans le canal galactophorique de la glande mammaire notamment par la présence de cellules myoépithéliales (marron) et de la membrane basale (violet), permettant de délimiter le feuillet épithéliale du stroma (traits gris). **b)** Les cellules épithéliales subissent des changements entraînant une prolifération excessive, deviennent cancéreuses et forment un carcinome intracanalaire (ductal carcinoma *in situ*) (vert) confiné au niveau du canal galactophorique de la glande mammaire. **c)** Les cellules tumorales acquièrent des capacités invasives permettant le franchissement de la membrane basale et la migration à travers le stroma (bleu). **d)** Les cellules tumorales invasives atteignent la circulation lymphatique ou sanguine (rouge) et pénètrent dans les vaisseaux (intravasation). **e)** Les cellules tumorales invasives ressortent de la circulation lymphatique ou sanguine (extravasation). **f)** Les cellules tumorales invasives colonisent l'organe sain atteint où elles forment une métastase.

Introduction

I. Cancer du sein et programme métastatique

A. Histologie de l'épithélium de la glande mammaire

Chez les métazoaires, les cellules sont généralement organisées et regroupées en tissus dont on distingue quatre grands groupes: les tissus de soutien (tissu conjonctif, tissu cartilagineux et tissu osseux), le tissu musculaire, le tissu nerveux et le tissu épithélial. Un épithélium est un tissu non-vascularisé composé d'une seule couche de cellules ou bien stratifié (composé de plusieurs couches de cellules). Il existe deux types d'épithéliums : les épithéliums de revêtement qui tapissent les cavités de l'organisme et la surface du corps (la peau) et les épithéliums glandulaires, organisés en organes (glandes salivaires, foie, glandes endocrines, glande mammaire), ou associés à un épithélium de revêtement (glandes de la muqueuse digestive ou respiratoire). L'épithélium mammaire comprend une couche de cellules épithéliales luminales sécrétoires (impliquées dans la sécrétion du lait lors du processus de lactation) entourée d'une couche de cellules basales myoépithéliales au contact direct et reposant sur une membrane basale (Guinebretiere et al., 2005) (voir Figure 2).

Les cellules épithéliales sont jointives, juxtaposées, solidaires les unes des autres par des systèmes de jonction (jonctions serrées, jonctions adhérentes et desmosomes) qui permettent la cohésion des cellules entre elles (Green et al., 2010) (voir Figure 3). Ces jonctions cellulaires sont notamment enrichies en E-cadhérine, protéine transmembranaire impliquée dans l'adhésion cellule-cellule par formation de dimères de E-cadhérine au niveau de chaque cellule et interaction de ces dimères (Meng and Takeichi, 2009). Les jonctions cellulaires sont également impliquées dans l'organisation du cytosquelette de la cellule. Les jonctions adhérentes permettent de lier le cytosquelette d'actine à la membrane plasmique (Engl et al., 2014) tandis que les desmosomes sont impliqués dans l'ancrage des filaments intermédiaires à la membrane plasmique (Green et al., 2010). Le réseau de microtubules peut se lier à ses deux types de jonctions (Green et al., 2010; Shahbazi et al., 2013).

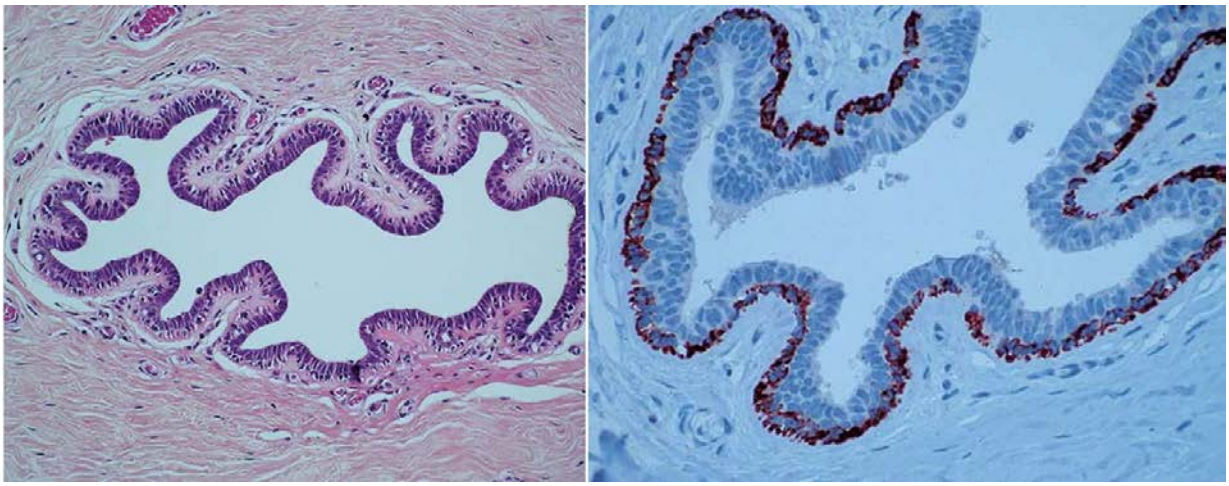

Figure 2 : Coupe histologique transversale d'un canal galactophorique de la glande mammaire

(Gauche) Coloration HES permettant de visualiser les noyaux cellulaire en bleu (hématéine), les cytoplasmes en rose (éosine) et les fibres de collagène en jaune (safran) (grossissement : x100).
Le feuillet de cellules épithéliales luminales (violet) fait face à la lumière du canal galactophorique.
(Droite) Immunomarquage de la myosine permettant de visualiser les cellules myoépithéliales (grossissement : x150).

Extrait de Guinebretière et al, "Normal and pathological breast, the histological basis", European Journal of Radiology 54 (2005) 6–14.

Comme toutes les cellules épithéliales, les cellules luminales sont polarisées avec un pôle apical tourné vers la lumière du canal galactophorique et un pôle basal au contact du feuillet de cellules myoépithéliales (Guinebretiere et al., 2005; Rodriguez-Boulan and Macara, 2014). Cette polarité est maintenue en place grâce à plusieurs complexes protéiques au niveau des jonctions cellulaire : les complexes Par et Crumbs sont présents au niveau des jonctions serrées au pôle apical tandis que le complexe Scribble est présent au pôle basal (Ellenbroek et al., 2012; Horikoshi et al., 2009; Khursheed and Bashyam, 2014) (voir Figure 3).

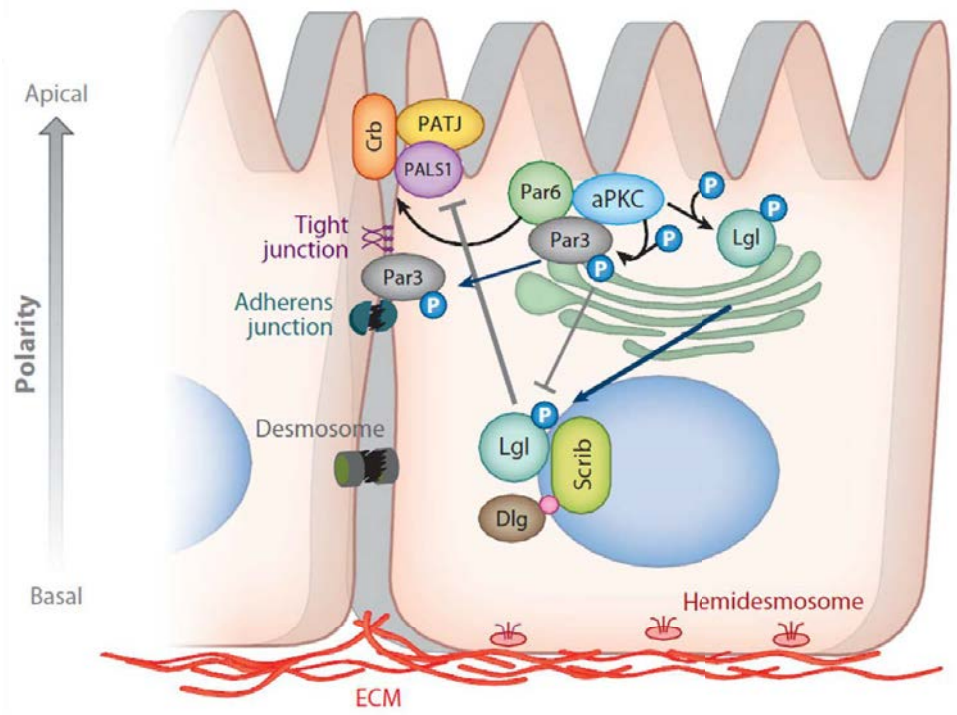

Figure 3 : Polarité apico-basale au sein d'une cellule épithéliale de l'épithélium de la glande mammaire

L'établissement d'une polarité apico-basale au sein d'une cellule épithéliale est le résultat d'une distribution spatiale de complexes protéiques nécessaires à l'établissement et au maintien de la polarité : le complexe Scribble (Lgl, lethal giant larvae ; Dlg, Discs large, Scrib), le complexe Par (Par-3 ; Par-6 ; aPKC, atypical protein kinase C) et le complexe crumbs (Crb ; Pals1 ; PATJ, Pals1 associated tight junction).
Tight junction : jonctions serrées ; *Adherens junction* ; jonctions adhérentes ; *ECM*, matrice extracellulaire ; P, phosphorylation).

Extrait de Muthuswamy et al, "Cell Polarity as a Regulator of Cancer Cell Behavior Plasticity", Annu. Rev. Cell Dev. Biol, (2012) 28:599-625

Les cellules myoépithéliales sont des cellules contractiles enrichies en actine musculaire lisse et en myosine, protéines caractéristiques des cellules contractiles comme les cellules musculaires lisses (Moumen et al., 2011). L'activité contractile des cellules myoépithéliales est dépendante de l'actine musculaire lisse et permet l'expulsion dans le canal galactophorique de la glande mammaire du lait produit par les cellules épithéliales, assurant ainsi la fonctionnalité de la glande mammaire (Haaksma et al., 2011; Moumen et al., 2011) (voir Figure 2).

La perte des caractéristiques des cellules épithéliales (jonctions intercellulaires et polarité apico-basale) est une étape clé dans la transformation cellulaire et la progression tumorale. Il a été montré que la perte des protéines de polarité provoque une perte des adhésions cellule-cellule, entraînant la formation de tumeurs et de métastases (McCaffrey et al., 2012; Xue et al., 2013). Ce processus est le résultat d'un programme cellulaire appelé transition épithélio-mésenchymateuse.

B. Transition épithélio-mésenchymateuse

La transition épithélio-mésenchymateuse (TEM) est un processus biologique fondamental dans de nombreux programmes développementaux tels que la formation du mésoderme lors de la gastrulation, la migration des cellules de la crête neurale et le développement du muscle cardiaque ainsi que dans la réparation tissulaire chez l'adulte (Kalluri and Weinberg, 2009; Thiery, 2002; Thiery et al., 2009).

La TEM est également impliquée dans les processus pathologiques tels que les cancers, au niveau desquels elle est réactivée peut être causale de l'initiation de la progression tumorale et de la dissémination métastatique (Kalluri and Weinberg, 2009; Peinado et al., 2007; Yang and Weinberg, 2008).

La TEM est la succession séquentielle de changements biochimiques et structurelles d'évènements qui vont conduire une cellule épithéliale polarisée à perdre ses caractéristiques épithéliales et (ré)acquérir un phénotype mésenchymateux (Kalluri and Weinberg, 2009; Thiery, 2002; Thiery et al., 2009) (voir Figure 4). Cette transition est notamment caractérisée par :

- la perte des jonctions cellule-cellule
- la perte de la polarisation cellulaire
- l'acquisition de propriétés migratoires et invasives

La transition épithélio-mésenchymateuse est induite par des facteurs extracellulaires présents dans l'environnement de la cellule : facteurs de croissance sécrétés par les cellules immunitaires, endothéliales ainsi que les fibroblastes (Hanahan and Weinberg, 2000; Thiery, 2002; Yilmaz and Christofori, 2009). Produits par les fibroblastes, les macrophages et les granulocytes, le TGFβ (*transforming growth factor β*) est le principal inducteur de la TEM (Hanahan and Weinberg, 2011; Zarzynska, 2014). Le TGFβ se lie à son récepteur de membrane qui, une fois activé, phosphoryle de nombreux effecteurs tels que les protéines cytosoliques SMAD (Lv et al., 2013). Les SMAD s'assemblent en complexes multiprotéiques transloqués dans le noyau où ils s'associent à des facteurs de transcription afin d'activer des gènes codant pour des facteurs de transcription tels que les protéines Snail, Zeb et Twist (Papageorgis et al., 2010; Peinado et al., 2007).

Au cours de la TEM, le principal rôle des facteurs de transcription Snail, Zeb et Twist réside dans la répression de l'expression de nombreux gènes codant pour des protéines

caractéristiques des cellules épithéliales, notamment la E-cadhérine, principale cible de la TEM (Thiery, 2002). La répression de l'expression de la E-cadhérine déstabilise d'une part les jonctions intercellulaires préexistantes et d'autre part, empêche la formation de nouvelles jonctions serrées. Cette répression de la E-cadhérine entraine une individualisation des cellules épithéliales (Thiery et al., 2009).

Lors de la réactivation de la TEM au cours du processus tumoral, les facteurs de transcription Snail, Zeb et Twist induisent l'expression de protéines impliquées dans la la transformation cellulaire et la progression tumorale. Parmi ces protéines, les métalloprotéases matricielles (MMPs) permettent aux cellules tumorales de remodeler les tissus environnants et de s'évader de la tumeur primaire afin de former des métastases. Les MMPs apparaissent surexprimées dans les cellules tumorales sous l'influence de facteurs de transcription tels que Snail, responsable notamment de la sur-expression des protéases MMP-2 (Yokoyama et al., 2003) et MMP-9 (Jorda et al., 2005). De manière intéressante, il a été reporté qu'au-delà de leur rôle de cible des facteurs de transcriptions, les MMPs - MMP-9 (Lin et al., 2011) et MMP-28 (Illman et al., 2006) - peuvent également interagir avec les facteurs de transcription afin d'induire la TEM, jouant ainsi un rôle pro-tumorale.

La réorganisation du cytosquelette de la cellule constitue une étape également critique au cours de la TEM (Yilmaz and Christofori, 2009) et il a été montré que le facteur de transcription Twist peut induire la formation d'invadopodes via la surexpression du récepteur au PDGF, conduisant à l'activation de la protéine à activité kinase Src, enzyme centrale dans la formation et l'activité des invadopodes (Eckert et al., 2011).

Les facteurs de croissance tels que l'HGF (*hepatocyte growth factor*) (Farrell et al., 2014), l'EGF (*epidermal growth factor*) (Ahmed et al., 2006; Docherty et al., 2006; Hardy et al., 2010) ou encore le FGF (*fibroblast growth factor*) (Billottet et al., 2008) sont également impliqués dans l'induction de la TEM.

La TEM peut être partielle, certaines jonctions cellule-cellule restant intactes ou simplement affaiblies (Thiery et al., 2009). Les cellules épithéliales peuvent rester partiellement liées les unes aux autres, ce qui pourra notamment affecter leur comportement migratoire.

Enfin, la TEM est un processus réversible ; au cours de « Transition Mésenchymateuse-Epithéliale » (TME) les cellules mésenchymales peuvent réacquérir des caractéristiques épithéliales et se différencier au niveau de leur site d'implantation (Thiery, 2002; Thiery et al., 2009). Dans les cancers, la TME est impliquée dans la recolonisation des foyers secondaire associée à la formation de tumeurs secondaires solides (également appelées métastases) (Gunasinghe et al., 2012).

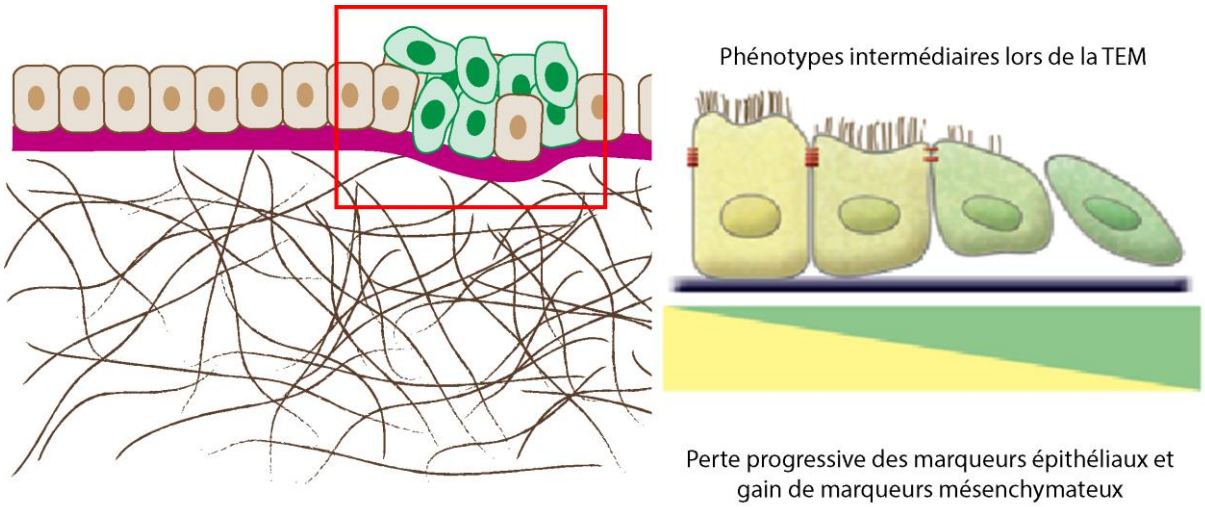

Figure 4 : Transition épithélio-mésenchymateuse et changement de phénotype cellulaire

(Gauche) Les cellules ayant subi la TEM prolifèrent et changent de morphologie (cellules vertes).
(Droite) Evolution de la perte du phénotype épithéliale (jaune) et acquisition du phénotype mésenchymateux avec perte de jonctions cellule-cellule (verte). *Extrait de Kalluri and Weinberg, "The basics of epithelial-mesenchymal transition", J. Clin. Invest. (2009) 119:1420–1428*

II. La matrice extracellulaire

A la suite de la transition épithélio-mésenchymateuse, les cellules tumorales sont plus ou moins individualisées et prêtes à s'échapper de la tumeur primaire afin de coloniser les tissus environnants. Au cours de ce processus, les cellules cancéreuses vont devoir franchir les différentes barrières tissulaires constituées de composants de la matrice extracellulaire que sont la membrane basale sur laquelle repose l'épithélium et le tissu interstitiel (stroma) (Rowe and Weiss, 2008).

A. Composition de la matrice extracellulaire

1. La membrane basale

a. Composition de la membrane basale

La membrane basale est un réseau de protéines matricielles impliqué dans le support et le maintien de l'épithélium (Rowe and Weiss, 2008). Elle est majoritairement composée de deux grandes catégories de molécules : les laminines et le collagène de type IV (Kalluri, 2003; Rowe and Weiss, 2008; Yurchenco, 2011).

Les laminines sont des protéines matricielles non-collagènique constituées d'un hétérotrimère composé d'une chaîne α, d'une chaine β et d'une chaîne γ (voir Figure 5A). Il existe 5 chaînes α, 4 chaînes β et 3 chaînes γ dont les différentes combinaisons α–β–γ sont à l'origine de 15 isoformes différents de laminines (exemple, laminine 111 est composé de la chaîne α1, β1 et γ1) (Yurchenco, 2011). Les chaînes α, β et γ possèdent des domaines « coiled-coil » impliqués dans l'assemblage des hétérotrimères (Aumailley et al., 2005). Plusieurs hétérotrimères s'associent entre eux et forment le réseau de laminines (voir Figure 5C). Les chaines α possèdent un domaine LG en position C-terminale qui permet de lier la surface de la cellule via les récepteurs de membrane tels que les intégrines (Berrier and Yamada, 2007; Kusuma et al., 2012; Yurchenco, 2011) (voir Figure 5C).

Le collagène de type IV est un collagène non-fibrillaire (contrairement aux autres collagènes de type I, II et III) pouvant s'auto-assembler. Le collagène de type IV

s'organise en hétérotrimère composé de 3 chaines α parmi les 6 formes de chaînes α existantes (α1-α6) et formant un protomère (voir Figure 5B). L'assemblage de plusieurs protomères (voir Figure 5B), est à l'origine d'un réseau de collagène de type IV (voir Figure 5C). Ce réseau est lié de manière covalente par des ponts disulfures (Rowe and Weiss, 2008; Rowe and Weiss, 2009).

Les polymères de laminines et de collagène de type IV s'associent et forment un réseau de macromolécules stabilisé par des glycoprotéines comme les nidogènes et le perlecan (Rowe and Weiss, 2008; Yurchenco, 2011) (voir Figure 5C).

De par l'organisation et l'agencement de ces macromolécules, la membrane basale constitue une structure très dense d'une épaisseur comprise entre 100 et 300nm comportant des pores de 10 à 90nm de diamètre (Rowe and Weiss, 2008; Rowe and Weiss, 2009). Ces pores sont permissifs au passage de molécules de petite taille comme des chémoattractants, permettant une communication entre les cellules de l'épithélium et les cellules présentes dans le stroma (Willis et al., 2013).

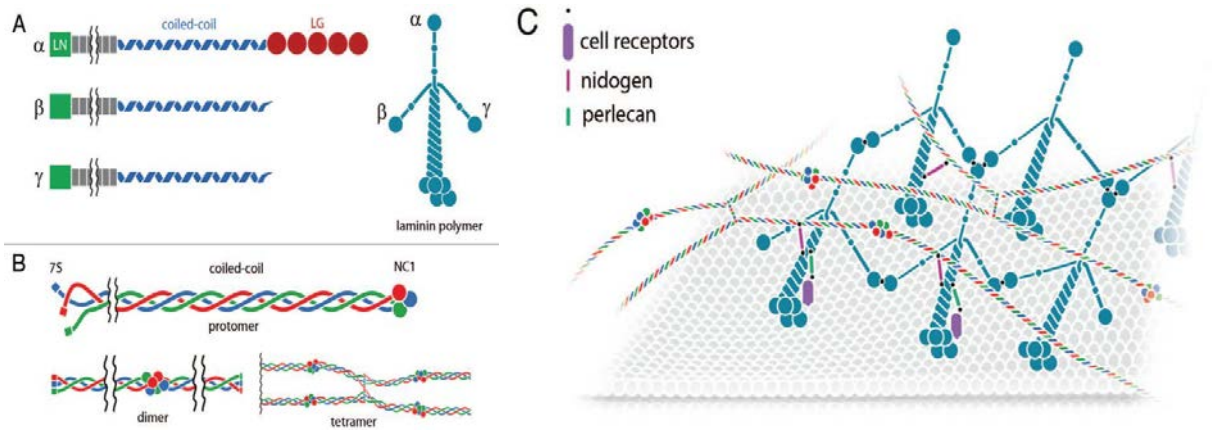

Figure 5 : Schéma de la composition et de l'organisation de la membrane basale

(a) Représentation schématique et organisation en trimères des chaînes α, β et γ de laminines.
(b) Représentation schématique et organisation en trimères des chaînes α de collagène de type IV, s'organisant en protomères, puis dimères et tétramères.
(c) Agencement et organisation tridimensionnelle des réseaux de laminines et de collagène de type IV formant la membrane basale.

Extrait de Glentis et al, "Assembly, heterogeneity, and breaching of the basement membranes", Cell Adhesion & Migration (2014) 8:3, 1–10

b. Transmigration à travers la membrane basale

Le passage de cellules à travers la membrane basale dépend du type cellulaire. Les cellules du système immunitaire franchissent quotidiennement la membrane basale de l'endothélium vasculaire lors des processus de surveillance immunitaire de l'organisme. La transmigration des leucocytes est indépendante de toute activité protéolytique (Friedl and Wolf, 2003; Rowe and Weiss, 2008; Willis et al., 2013) ; un des mécanismes sous-jacents est lié au fait que les leucocytes possèdent des noyaux souples pouvant se déformer lors du passage de la cellule à travers les pores de la membrane basale (voir Figure 6, droite). Cette déformabilité nucléaire est en partie due à l'absence d'expression des lamines par les leucocytes, protéine de la membrane nucléaire interne permettant la rigidification de la membrane du noyau associée à la protection du génome nucléaire (Harada et al., 2014; Shin et al., 2013; Swift et al., 2013). D'ailleurs certains leucocytes sont caractérisés par une durée de vie extrêmement brève (24 heures dans le cas des neutrophiles).

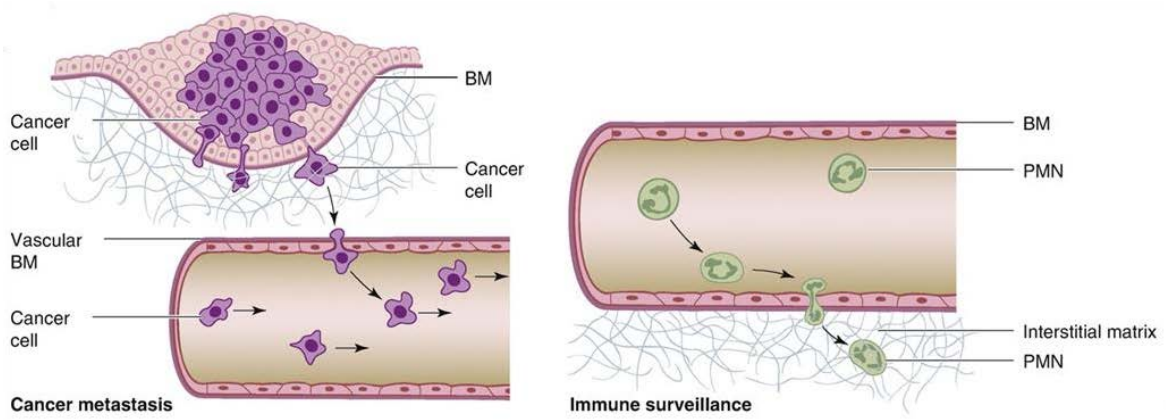

Figure 6 : Franchissement de la membrane basale en condition physiologique et pathologique

(Gauche) Cellules tumorales (*cancer cell*, violet) s'échappant de la tumeur primaire par franchissement de la membrane basale (BM), migration à travers le stroma et intravasation dans la circulation sanguine.
(Droite) Cellules du système immunitaire (vert) migrant à travers la membrane basale vasculaire.

Extrait de Rowe and Weiss, "Breaching the basement membrane: who, when and how?" Trens in Cell Biology, (2008) 18-11. 560-574

A contrario, les cellules exprimant les lamines possèdent des noyaux plus rigides et moins déformables (Wolf et al., 2013; Wolf et al., 2007). C'est le cas des cellules tumorales dont la rigidité nucléaire contrarie le passage à travers des pores de la matrice extracellulaire inférieurs à 3µm (Harada et al., 2014; Willis et al., 2013; Wolf et al., 2013). Par conséquent, le passage de la membrane basale nécessite une activité protéolytique de la part des cellules tumorales (Wolf et al., 2013). On parle de transmigration protéase-dépendante qui provoque des changements irréversibles de la membrane basale liés à l'activité protéolytique de ces enzymes (Hotary et al., 2006) (voir Figure 6, gauche).

2. Stroma

Après avoir franchi la membrane basale, les cellules tumorales se trouvent au contact du tissu interstitiel ou stroma. Le stroma est composé d'un réseau tridimensionnel de fibres de collagène de type I, de glycoprotéines et de protéoglycanes (Rowe and Weiss, 2009; Willis et al., 2013) colonisé par différents types cellulaires (fibroblastes et cellules du système immunitaire tel que les lymphocytes, les macrophages) dont la nature varie en fonction des organes. Dans les cancers, le stroma peut également être composé de vaisseaux sanguins nouvellement formés. Induite par les cellules cancéreuses et stromales, cette formation de vaisseaux est notamment importante pour l'apport en oxygène et en éléments nutritifs indispensables à la croissance tumorale et à la dissémination métastatique.

a. La matrice extracellulaire du stroma

Le collagène est le composé protéique le plus abondant chez les mammifères et le principal composant du stroma (Ricard-Blum, 2011; Rowe and Weiss, 2009). Le collagène de type 1 est synthétisé par les fibroblastes présents dans le stroma (voir Figure 7) et est sécrété sous formes d'hétérotrimères composé de 3 chaînes α, appelé procollagène (Sabeh et al., 2009) (voir Figure 7). Le procollagène est déposé dans le milieu interstitiel et clivé à ses 2 extrémités N- et C-terminale afin de permettre son assemblage aboutissant à la formation de fibres de collagène de type 1 (Kadler et al., 2008). Ces fibres de collagène sont liées entre elles par des enzymes, telles que les lysyl

oxydases (LOX) (Cox et al., 2013) ainsi que les transglutaminases (Chau et al., 2005), afin de renforcer le réseau fibrillaire tridimensionnel de collagène de type 1 (voir Figure 7).

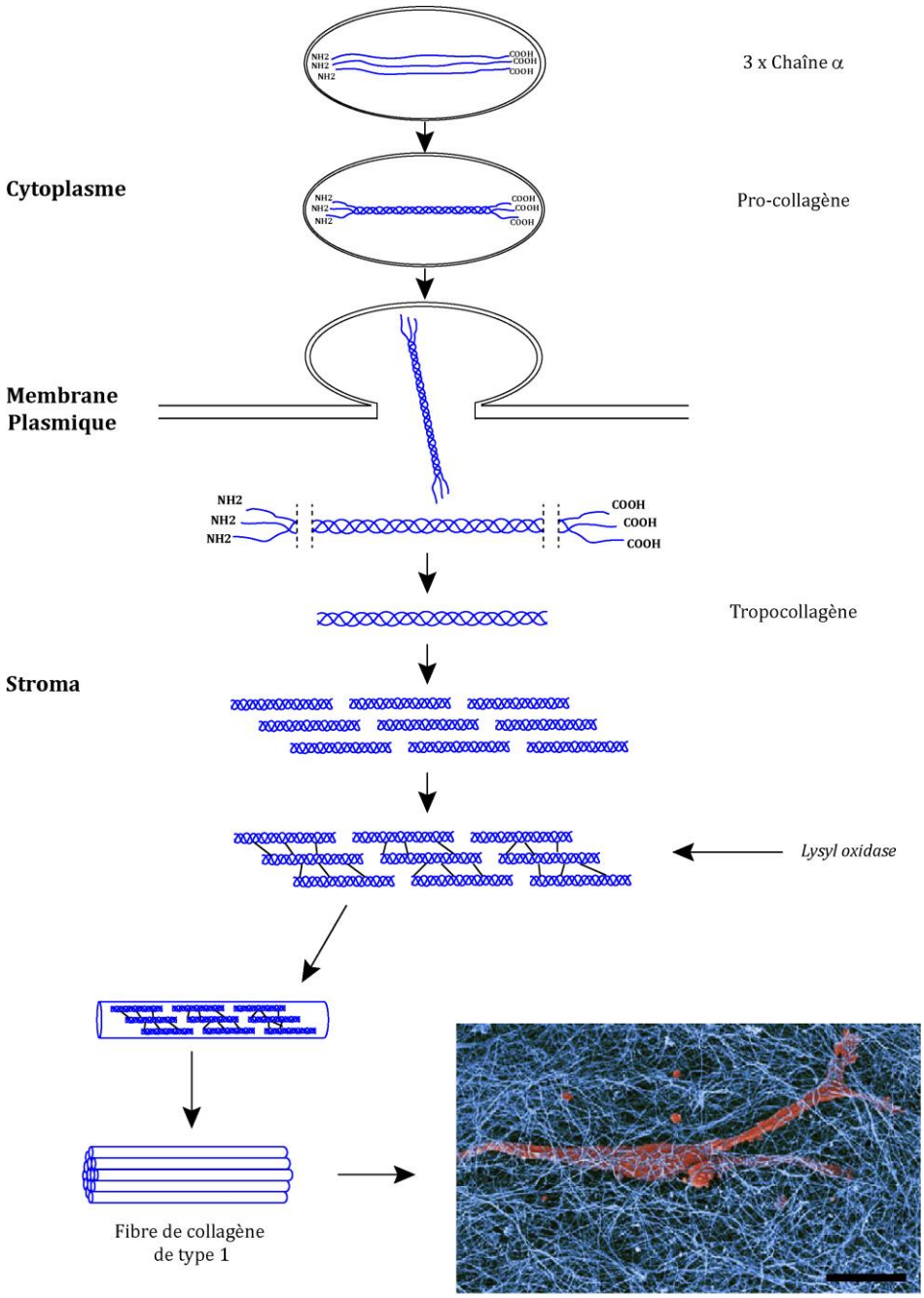

Figure 7 : Synthèse, maturation et assemblage des fibres de collagène de type 1

Représentation schématique de la synthèse intracellulaire des chaînes α de collagène de type 1. Ces chaînes s'assemblent en pro-collagène au sein de vésicules intracellulaires qui permettent la déposition par exocytose du pro-collagène dans le milieu extracellulaire. Le pro-collagène mature et s'assemble afin de donner naissance à des fibres de collagène de type 1 qui constituent le stroma. L'encart montre une cellule de cancer du sein (rouge) dans un environnement de fibres de collagène de type 1 (bleu ; Echelle : 10µm). *Extrait de Poincloux et al, "Matrix invasion by tumour cells: a focus on MT1-MMP trafficking to invadopodia", Journal of Cell Science 122 (2009) 3015-3024.*

b. Migration à travers le stroma

Une fois échappée de la tumeur primaire, les cellules tumorales vont migrer à travers le stroma afin d'atteindre les vaisseaux sanguins ou lymphatiques. L'agencement des fibres de collagène entre elles donne naissance à des espaces interfibrillaires (ou pores) dont la taille a été estimée de l'ordre de 1-3µm (Willis et al., 2013; Wolf et al., 2013). De par cette organisation, des contraintes physiques et mécaniques sont appliquées aux cellules en mouvement à travers ces matrices. Ces contraintes impactent entre autre sur le noyau de la cellule qui représente l'organelle le plus rigide (Harada et al., 2014; Shin et al., 2013; Swift et al., 2013) et dictent le mode migratoire des cellules (Friedl and Alexander, 2011; Friedl et al., 2011). Les cellules tumorales semblent utiliser principalement deux modes de migration à travers le stroma : la migration collective et la migration individuelle (de type mésenchymale ou amiboïde) (voir Figure 8) (Friedl and Wolf, 2009; Sabeh et al., 2009).

Migration cellulaire collective

A la suite d'une TEM partielle, des jonctions intercellulaires entre les cellules carcinomateuses persistent. Les cellules restent liées les unes aux autres et migrent en groupes ou en feuillets ; on parle de migration cellulaire collective (voir Figure 8e). Ce mode de migration est primordial au cours de développement embryonnaire et la morphogénèse en permettant la formation et l'organisation de structures tissulaires complexes tels que les épithéliums, les vaisseaux sanguins et lymphatiques. La migration cellulaire collective est également en jeu lors de processus pathologiques comme le cancer et l'invasion tumorale (Alexander et al., 2008; Friedl and Gilmour, 2009; Weijer, 2009).

Au cours de la migration cellulaire collective, les cellules de « tête » localisées au front de migration présentent des capacités plus importantes à interagir avec la matrice extracellulaire, notamment en percevant les signaux présents au niveau de l'environnement cellulaire (Friedl and Gilmour, 2009). Ces signaux entrainent un remodelage du cytosquelette de la cellule ainsi que la capacité à dégrader la matrice extracellulaire afin de créer des tunnels dans l'environnement tissulaire nécessaire au passage des autres cellules du groupe, plus solidaires entre elles et interagissant moins avec leur environnement (Wolf et al., 2003a; Wolf et al., 2007). Le maintien des jonctions

cellules-cellules impliqué dans la migration cellulaire collective facilite la communication paracrine entre les cellules, permettant d'optimiser la transmission des signaux au sein du tissu et uniformiser le déplacement du groupe de cellules (Friedl and Gilmour, 2009).

Par ailleurs, il a été reporté que les fibroblastes présents au niveau du stroma peuvent contribuer à la migration collective des cellules tumorales (Gaggioli et al., 2007). Une étude a montré que des fibroblastes particuliers – caractéristiques du microenvironement tumoral (CAF) - sont localisés au front d'invasion (à l'avant des cellules tumorales), et jouent ainsi un rôle de guide ou de pionnier pour ces cellules. Les fibroblastes produisent des facteurs de croissance, des cytokines ainsi que des métalloprotéases, permettant de modifier l'environnement matriciel et créer un passage pour l'invasion des cellules tumorales (Gaggioli, 2008; Gaggioli et al., 2007).

Migration cellulaire invdividuelle de type mésenchymale

La migration individuelle de type mésenchymateuse caractérise le déplacement de cellules individualisées à travers la matrice extracellulaire (voir Figure 8b, c). Ce mode migration est un processus cyclique caractérisé par :

- la mise en place d'une polarité cellulaire avant-arrière (polarité planaire),
- la formation d'une protrusion,
- la formation d'adhésions permettant l'attachement de la cellule à son environnement grâce à l'engagement de récepteurs d'adhésion,
- la mise en place d'un programme protéolityque permettant de remodeler l'environnement et de faciliter le mouvement de la cellule,
- l'avancement de la cellule par contraction du corps cellulaire,
- le désengagement des adhésions à l'arrière de la cellule, permettant l'avancement de la cellule et la mise en place d'un nouveau cycle (Friedl and Wolf, 2009; Friedl et al., 2011; Ridley et al., 2003; Sanz-Moreno and Marshall, 2010).

Migration individuelle de type amiboïde

La migration individuelle de type amiboïde est indépendante de toute activité protéolytique de la part des cellules (Sabeh et al., 2009; Wolf et al., 2003b) (voir Figure 8d). Les cellules possèdent la capacité de se faufiler à travers les pores formés par les

fibres de collagènes (Lammermann and Sixt, 2009). Ces cellules présentent une morphologie arrondie, due à de faibles interactions avec la matrice extracellulaire et une forte contractilité intracellulaire dépendante de l'actomyosine, permettant le mouvement cellulaire à travers les pores préexistants dans le stroma (Charras and Paluch, 2008; Sabeh et al., 2009).

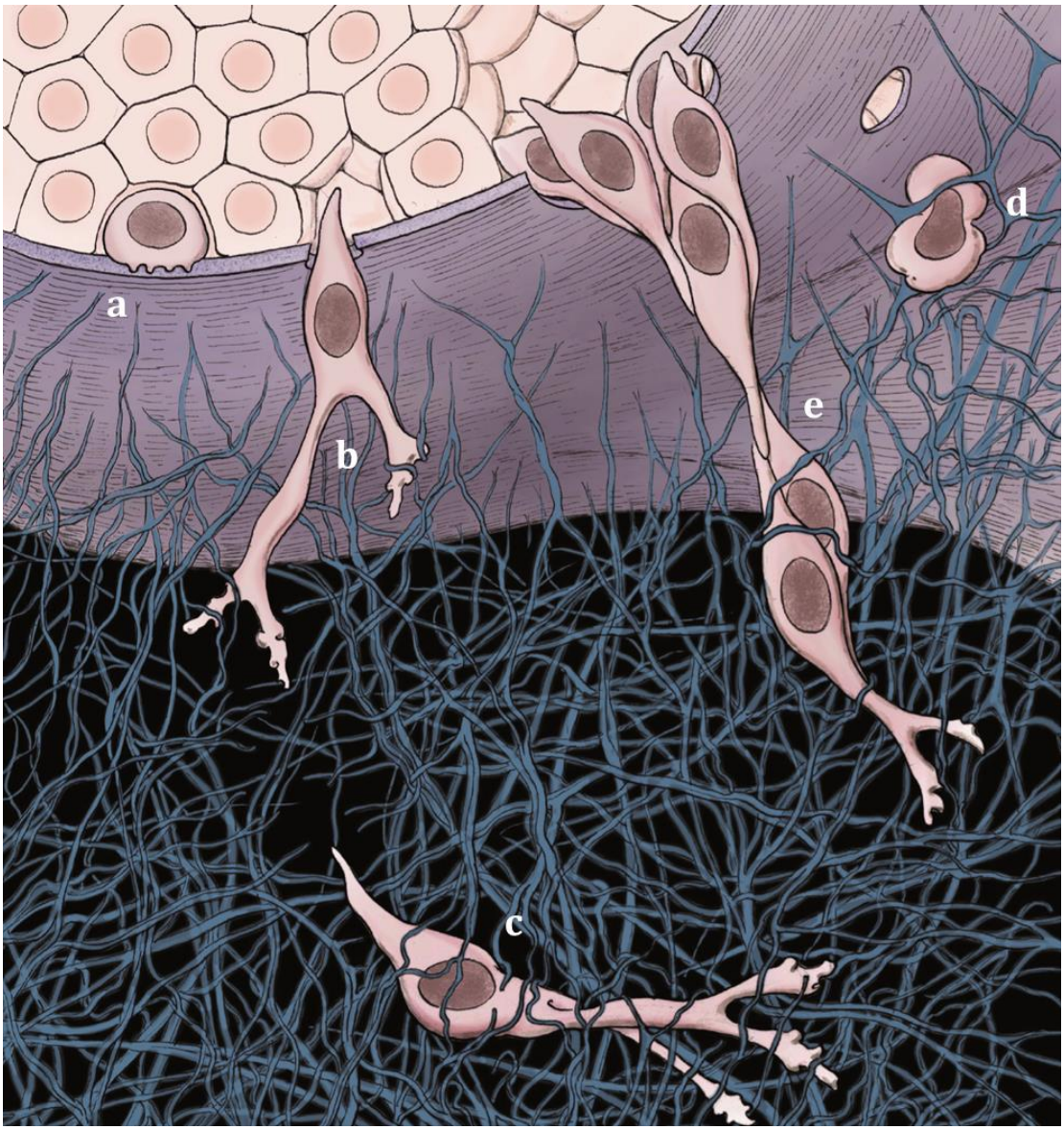

Figure 8 : Différents modes de migration à travers le stroma

Après avoir dégradé **(a)** et franchi **(b)** la membrane basale, les cellules migrent à travers le stroma de manière individuelle **(c, d)** ou bien collectivement **(e)**. Il existe deux modes de migration cellulaire individuelle : de type mésenchymale **(c)** ou de type amiboïde **(d)**.

Extrait de Poincloux et al, "Matrix invasion by tumour cells: a focus on MT1-MMP trafficking to invadopodia", Journal of Cell Science 122 (2009) 3015-3024.

3. Matrices extracellulaires reconstituées *in vitro*

Afin de comprendre comment *in vivo* les cellules abordent et dégradent la matrice extracellulaire, il est essentiel de pouvoir reconstituer *in vitro* des matrices extracellulaires mimant les conditions de l'environnement physiologique des cellules. Depuis de nombreuses années, les travaux portants sur la capacité des cellules tumorales à dégrader la membrane basale utilisent une matrice artificielle appelée Matrigel. Le Matrigel est un extrait soluble et acellulaire de protéines matricielles produit par des cellules tumorales du sarcome murin de Engelbreth-Holm-Swarm (EHS), formant un gel viscoélastique dense lorsqu'il est polymérisé à 37°C (Kleinman and Martin, 2005) (voir Figure 9A). La composition protéique du Matrigel est similaire à celle des membranes basales natives retrouvées dans l'organisme (laminines, collagène de type IV, nidogènes, perlecan et autres proteoglycans) (Kleinman and Martin, 2005; Rowe and Weiss, 2008). Toutefois, ce système présente des limites. Au niveau structurel, les liaisons observées dans le réseau de collagène de type IV présent sous forme native dans l'organisme ne sont pas retrouvées dans le Matrigel (Candiello et al., 2007; Rowe and Weiss, 2008; Willis et al., 2013). Il a également été montré que le Matrigel présente une élasticité nettement inférieure à celle retrouvée dans les tissus *in vivo* (Soofi et al., 2009). Ces différences peuvent se révéler importantes, notamment sur la capacité des cellules à engager ou non un programme protéolytique (Willis et al., 2013; Wolf et al., 2003a).

Concernant l'environnement interstitiel, les modèles développés *in vitro* reposent sur l'extraction de collagène – principalement de type I - présent dans les tendons de queue de rat. Cette solution de collagène possède la capacité de reformer de longues fibres dans des conditions précises de pH et de température (Sabeh et al., 2004; Sabeh et al., 2009; Willis et al., 2013) (voir Figure 9B, 10 et 11).

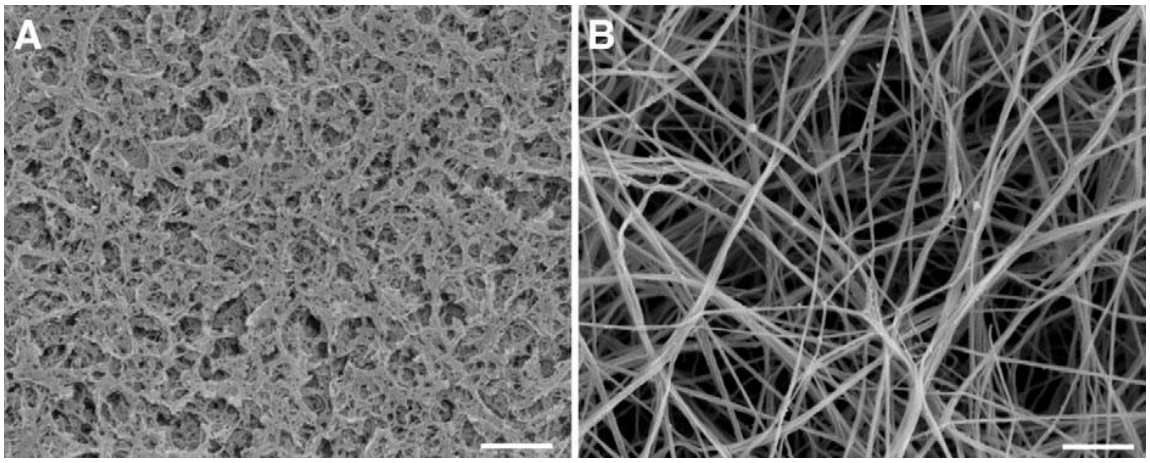

Figure 9 : Exemples de matrices reconstituées *in vitro*

(A) Image par microscopie électronique à balayage d'une matrice de Matrigel (échelle : 1µm).
(B) Image par microscopie électronique de fibres de collagène de type I (échelle : 1µm).

Extrait de Poincloux et al, "Matrix invasion by tumour cells: a focus on MT1-MMP trafficking to invadopodia", Journal of Cell Science 122 (2009) 3015-3024.

Il existe principalement deux modes d'extraction du collagène : une extraction en milieu acide et une extraction enzymatique faisant intervenir une endoprotéase digestive, la pepsine. Bien que le mode d'extraction ne perturbe pas la polymérisation de fibres de collagène de type 1 et la formation d'un réseau tridimensionnel (voir Figure 10B, extraction en milieu acide et Figure 10C, extraction enzymatique), il conditionne toutefois le comportement migratoire des cellules à travers la matrice.
L'extraction enzymatique du collagène médiée par la pespine ne permet pas de reformer les liaisons présentes au niveau de collagène natif (Sabeh et al., 2009) (voir Figure 10A). La pespine clive le tropocollagène au niveau des extrémités non-hélicoïdales, générant des télopeptides qui, en condition physiologique, sont impliqués dans les liaisons entre molécules de tropocollagène (voir Figure 10A). En condition d'extraction du collagène en milieu acide, la présence de protons permet de dissocier les liaisons natives (voir Figure 10A). Cette dissociation est réversible lorsque la (re)polymérisation des fibres de collagène a lieu en milieu basique, permettant notamment de lever cette inhibition et de reformer ces liaisons (Sabeh et al., 2009).

De manière fort intéressante, il a été montré que la migration de cellules tumorales à travers un réseau de fibres de collagène reconstituées à partir d'une solution de collagène extrait en milieu acide est dépendante d'une activité dégradative des cellules (Sabeh et al., 2009) (voir Figure 10D). *A contrario*, la migration à travers un réseau de fibres de collagène reconstituées à partir d'une solution de collagène extrait de manière enzymatique ne nécessite pas d'activité dégradative des cellules (Sabeh et al., 2009) (voir Figure 10E). Ces résultats montrent l'influence et l'impact de l'environnement cellulaire dans le mode migratoire de la cellule et suggèrent que du collagène extrait en milieu acide permet de reconstituer au mieux les conditions retrouvées au niveau du collagène natif.

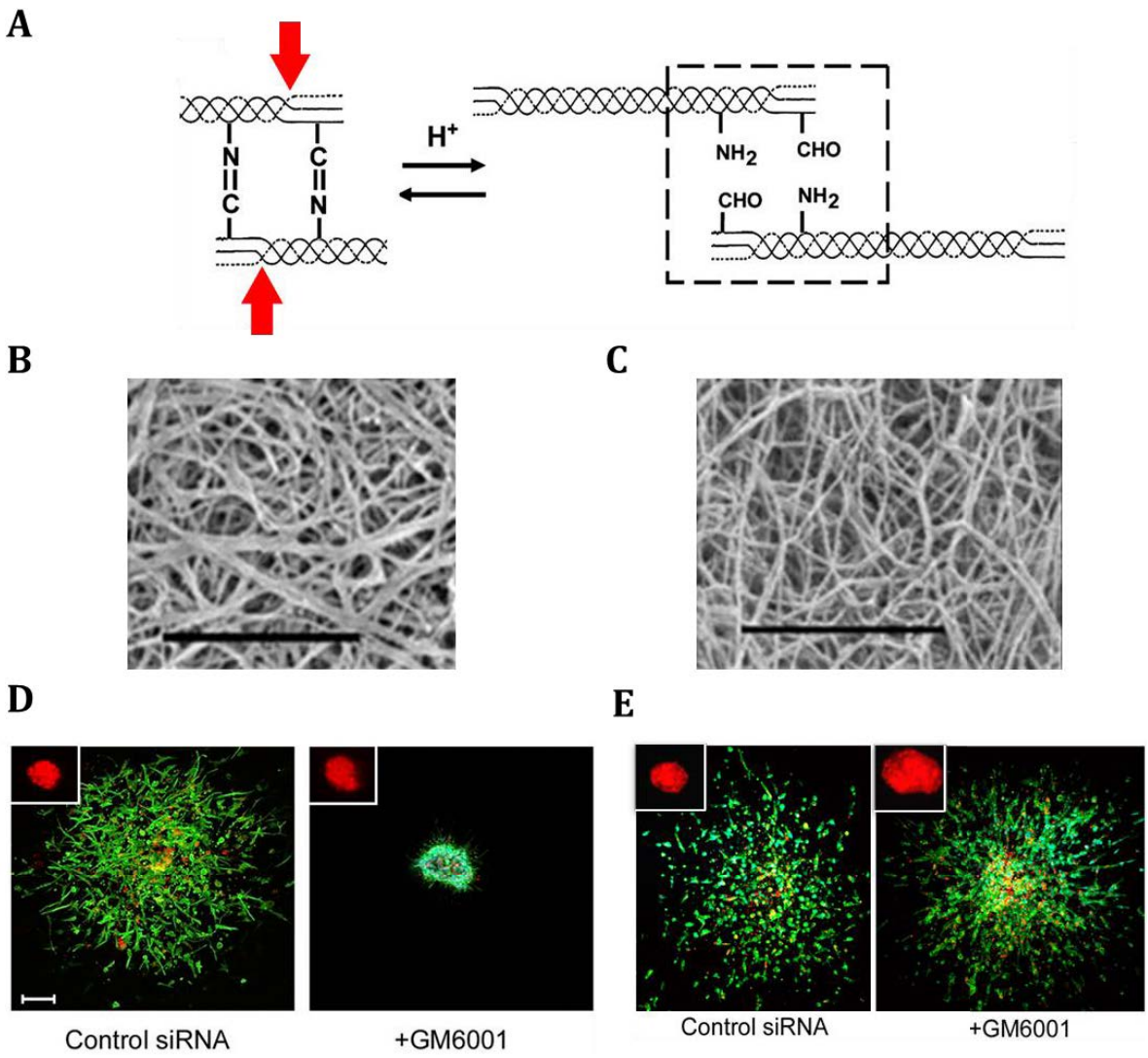

Figure 10 : Extraction en milieu acide ou enzymatique (pepsine) de collagène provenant de tendons de queues de rats : effets sur la capacité invasive des cellules.

(A) Schéma représentatif des liaisons mises en place entre molécules de collagène en condition native (gauche) et à la suite de l'extraction en milieu acide (H^+) (droite, encart). Les flèches rouges indiquent les sites d'activité de la pepsine lors de l'extraction enzymatique.
(B) Réseau de fibres de collagène obtenu après extraction en milieu acide. Echelle : 5 µm
(C) Réseau de fibres de collagène obtenu après extraction enzymatique (pepsine). Echelle : 5 µm
(D) Sphère de cellules HT-1080 cultivée dans un gel tridimensionnel de collagène obtenu après extraction en milieu acide. L'image montre la progression de l'invasion des cellules après 3 jours (vert) en condition contrôle (control siRNA) ou après inhibition des protéases MMPs (+GM6001). L'encart montre la sphère de cellules au temps 0 (rouge). Echelle : 100 µm
(E) Sphère de cellules HT-1080 cultivée dans un gel tridimensionnel de collagène obtenu après extraction enzymatique (pepsine). L'image montre la progression de l'invasion des cellules après 1 jour (vert) en condition contrôle (control siRNA) ou après inhibition des protéases MMPs (+GM6001). L'encart montre la sphère de cellules au temps 0 (rouge). Echelle : 100 µm

Extrait de Sabeh et al, "Protease-dependent versus -independent cancer cell invasion programs: three-dimensional amoeboid movement revisited", Journal of Cell Biology (2009) Vol. 185 No. 1 ; 11–19.

Dans la même perspective, une étude a récemment montré l'importance des conditions de polymérisation du collagène fibrillaire (Wolf et al., 2013). Au-delà des modalités d'extraction du collagène (en milieu acide ou enzymatique), la température de polymérisation de ces solutions de collagène est fondamentale dans l'établissement de l'architecture du réseau tridimensionnel de fibres de collagène (Wolf et al., 2013). Il a été montré que des fibres de collagène polymérisées à une température de 9°C s'associent et donnent naissance à des espaces interfibrillaires (pores) six fois plus larges (~ 30 μm^2 ; voir Figure 11A) que des pores formés par des fibres de collagène polymérisées à une température de 37°C (~5 μm^2 ; voir Figure 11A) (Wolf et al., 2013).
La migration de cellules tumorales à travers les larges pores du réseau de fibres de collagène polymérisées à une température de 9°C est plus rapide et surtout, est indépendante de l'activité protéolytique des cellules (voir Figure 11B). L'usage d'inhibiteurs des protéases n'a aucun effet sur la capacité des cellules à migrer à travers cette matrice (Wolf et al., 2013) (voir Figure 11B).

Ces résultats peuvent s'expliquer par le fait que les cellules possèdent la capacité d'adapter leur mode de migration aux conditions environnantes. De manière intéressante, une étude a montré que lorsque la capacité des cellules à dégrader la matrice extracellulaire est bloquée (par des inhibiteurs des protéases), les cellules permutent vers un mode de migration indépendant de la dégradation des fibres de collagène de type amiboïde (Wolf et al., 2003a), mettant ainsi en évidence le principe d'une transition mésenchymale-amiboïde. L'usage d'inhibiteurs pharmacologiques des protéases (notamment MMP) n'affecte pas la capacité des cellules à migrer à travers les fibres de collagène mais influence le mode migratoire des cellules (Wolf et al., 2003a). Cependant, la portée de ces résultats limitée par le fait que le collagène de type I utilisé pour les expériences ayant abouti à la mise en évidence de la transition mésenchymale-amiboïde était extrait par la pepsine et donc plus permissif à la migration invasive des cellules tumorales en absence d'activité protéolytique (Sabeh et al., 2009; Wolf et al., 2003a; Wolf et al., 2013).

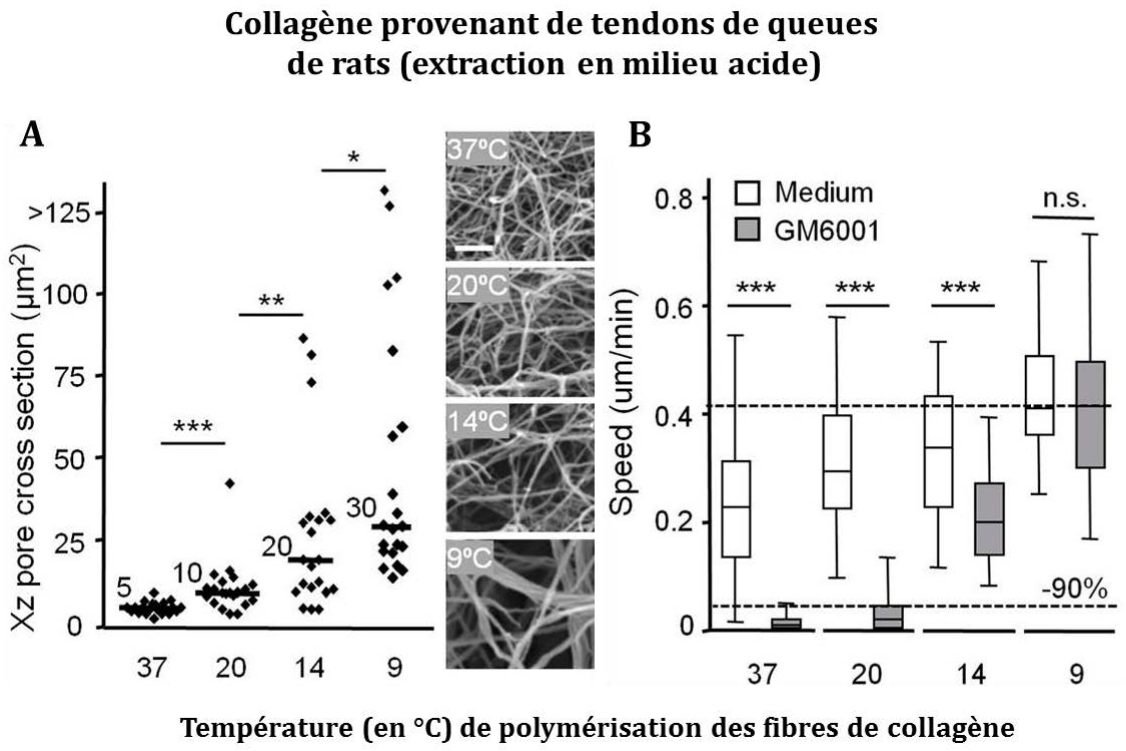

Figure 11 : Influence de la température de polymérisation des fibres de collagène sur la porosité du réseau tridimensionnel des fibres de collagène.

(A) Quantification de la taille des pores interfibrillaires formé par le réseau de fibres de collagènes selon la température de polymérisation (5, 10, 20, 30 représentent les tailles moyenne en µm² pour des températures de polymérisation de 37°C, 20°C, 14°C et 9°C respectivement). Observation par microscopie électronique à balayage des réseaux fibrillaires obtenus. Echelle : 1µm.
(B) Observation et quantification de la vitesse de migration de cellules HT-1080 dans des réseaux fibrillaires obtenus à des températures de polymérisation différentes. Plus la température de polymérisation est basse, plus les pores interfibrillaires sont larges et plus la migration est indépendante de l'activité protéolytique des cellules. (GM6001 : inhibiteurs des MMPs).

Extrait de Wolf et al, "Physical limits of cell migration: Control by ECM space and nuclear deformation and tuning by proteolysis and traction force", Journal of Cell Biology (2013) Vol. 201 No. 7 1069–1084.

L'ensemble de ces données montrent que la cellule possède la capacité à s'adapter à son environnement et à opter pour un mode de migration selon les caractéristiques et propriétés de l'environnement. Ces résultats soulignent également l'importance des techniques et conditions expérimentales mises en place lors de la préparation de substrats artificiels comme les matrices de collagène fibrillaire reconstituées, nécessaires à une interprétation correcte et cohérente des résultats.

III. Les invadopodes : protrusions membranaires responsables de la dégradation de la matrice extracellulaire

Lorsque les cellules tumorales sont cultivées *in vitro* au contact de substrats artificiels, elles développent des structures membranaires capables de dégrader la matrice extracellulaire appelées invadopodes. Les invadopodes sont des protrusions membranaires riches en filaments d'actine dont la particularité réside dans la présence et l'accumulation de protéases permettant de dégrader la matrice extracellulaire.

A. Découverte des invadopodes

Les invadopodes ont été observés pour la premières fois au cours des années 80 dans des fibroblastes provenant d'embryons de poulet transformés par le virus du sarcome de Rous (rétrovirus exprimant l'oncogène v-Src) (Chen, 1989; David-Pfeuty and Singer, 1980; Tarone et al., 1985). Une réorganisation des protéines du cytosquelette d'actine a été observée dans ces cellules et des protéines telles que la vinculine et l'α-actinine, initialement présentes au niveau des adhésions focales s'organisent en « rosettes » dans les cellules transformées (voir Figure 12) (David-Pfeuty and Singer, 1980). Ces structures sont enrichies en actine filamenteuse ainsi qu'en protéines à résidus tyrosine phosphorylée (Tarone et al., 1985) et sont capables de dégrader la matrice extracellulaire ou des substrats matriciels artificiels (Chen, 1989; Chen, 1996; Mueller and Chen, 1991). La notion d'invadopode a émergé progressivement et ces structures ont été observées dans des lignées de carcinomes mammaires (Bowden et al., 1999; Chen, 1996), confirmant l'existence de ces structures initialement observées dans des cellules transformées dans des cellules de carcinomes humains.

Il existe d'autres protrusions membranaires structurellement et fonctionnellement semblables aux invadopodes, appelées podosomes (Linder, 2007; Linder et al., 2011), qui contrairement aux invadopodes se forment dans les cellules saines et sont impliquées dans des processus de remodelage de la matrice extracellulaire physiologiques. Les macrophages, les cellules dendritiques, les ostéoclastes et les cellules endothéliales sont les principaux modèles cellulaires présentant des podosomes

(Linder et al., 2011; Murphy and Courtneidge, 2011). L'étude des podosomes a aidé à la compréhension des mécanismes impliqués au niveau de l'invadopode (et *vice versa*) (Artym et al., 2011; Linder et al., 2011).

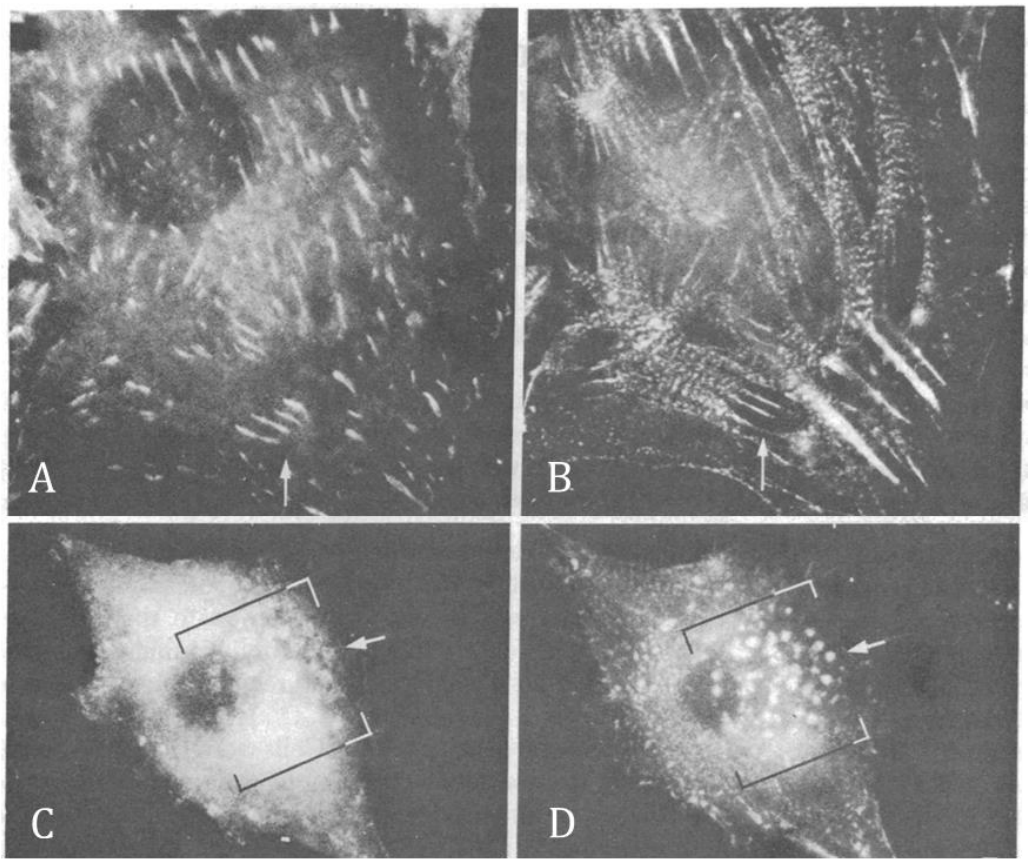

Figure 12 : Premières observations d'invadopodes

La vinculine et l'a-actinine initialement présentes au niveau de structures d'adhésion à la matrice extracellulaire (**A** et **B** respectivement, flèches) sont observées au niveau des invadopodes (**C** et **D** respectivement, flèches).

Extrait de David-Pfeuty and Singer, "Altered distributions of the cytoskeletal proteins vinculin and α-actinin in cultured fibroblasts transformed by Rous sarcoma virus", Proc. Nati. Acad. Sci. USA, (1980), Vol. 77, No. 11, pp. 6687-6691.

B. Composition en protéases

La particularité des invadopodes est leur capacité à dégrader la matrice extracellulaire (Artym et al., 2006; Buccione et al., 2009; Chen, 1989; Steffen et al., 2008) (voir Figure 13). Cette activité est due à la présence, au niveau de l'invadopode, de protéases permettant la dégradation de la matrice extracellulaire. Le génome humain comptabilise plus de 500 gènes codant pour des protéases ou protéines apparentées (Puente et al., 2003), certaines d'entre elles sont présentes à l'invadopode et sont impliquées dans les processus de dégradation de la matrice extracellulaire (Artym et al., 2006). Il existe 4 grandes catégories de protéases répertoriées à l'invadopode :

- les métalloprotéases régulées par le zinc : la famille des MMP.

Principaux acteurs de l'activité protéolytique des invadopodes, les MMPs font l'objet d'une description détaillée dans le chapitre suivant (Chapitre IV). Ces protéases fondamentales dans la progression tumorale sont indispensables à la formation de l'invadopode et à son activité. Une attention particulière sera portée à MT1-MMP, protéine clé du processus métastatique.

- métalloprotéases régulé par le zinc : la famille des ADAM.

Les protéases de la famille des ADAM (A Disintegrin and metalloproteinase) font partie des métalloprotéases régulées par le zinc. Leur implication directe dans la dégradation de la matrice n'est pas clairement élucidée mais il a été montré que dans des fibroblastes transformés, la protéase ADAM12 est présente à l'invadopode au niveau desquelles elle lie des protéines telles que Tks5 (Abram et al., 2003) et interagit avec des récepteurs de la membrane tels que l'intégrine β1 (Seals and Courtneidge, 2003). ADAM12 est localisée à l'invadopode en présence de la tyrosine kinase Src et régule son activité (Stautz et al., 2010) ainsi que le clivage des ligands du récepteur à l'EGF au niveau de l'invadopode (Albrechtsen et al., 2011; Diaz et al., 2013).

- Cathépsines

Les cathépsines sont des endopeptidases (11 membres appelés cathepsine A, C, D, F, H, J, K, L, L2, S et Z) résidentes des endosomes tardifs et des lysosomes. Elles sont présentes au niveau des podosomes des ostéoclastes (Vaananen and Laitala-Leinonen, 2008) et

des macrophages (Lopez-Castejon et al., 2010), ainsi qu'au niveau des invadopodes de fibroblastes transformés par v-Src (Tu et al., 2008) et de cellules tumorales (Brisson et al., 2011; Gillet et al., 2009; Jelassi et al., 2011). La cathépsine K possède une activité dégradative permettant de cliver et dégrader les collagène de type 1 (Han et al., 2009) et 2 (Dejica et al., 2008). La cathépsine S clive le nidogène 1 et empêche son attachement à la membrane basale (Sage et al., 2012).

- Les protéases à sérine

Les protéases à sérine sont des peptidases dont les membres présents à l'invadopode sont la séprase (connue également sous le nom de FAPα, pour fibroblastes activation protein α) et la DPP-4 (pour Dipeptidyl peptidase-4) (Artym et al., 2006). Ces 2 enzymes possèdent toutes deux des activités enzymatiques exopeptidase et sont présentes à l'invadopode (Ghersi et al., 2006; Kindzelskii et al., 2004; O'Brien and O'Connor, 2008) au niveau duquel leur implication demeure peu connue à ce jour.

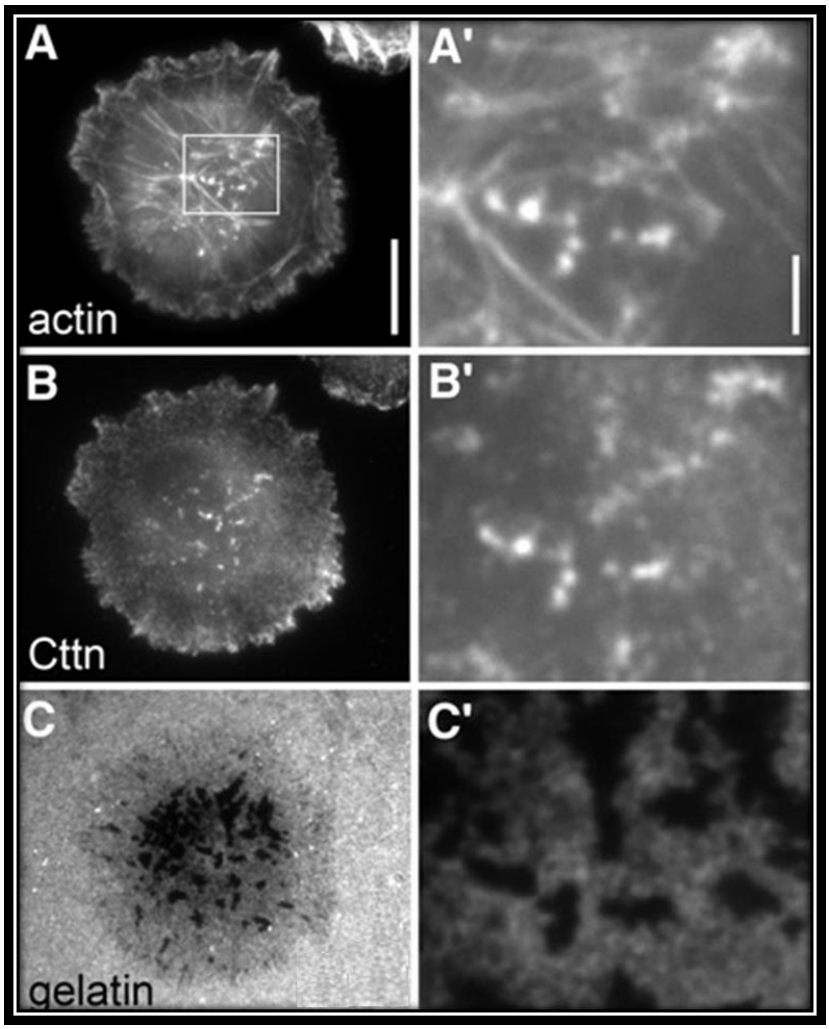

Figure 13 : Formation d'invadopodes au niveau de cellules tumorales cultivées sur substrat artificiel.

Des cellules d'adénocarcinomes mammaires MDA-MB-231 sont cultivées sur du collagène dénaturé (gelatine) couplé à un fluorophore permettant sa visualisation. Les cellules forment des invadopodes enrichis en actine **(A)** et en cortactine **(B)**, capables de dégrader le substrat **(C**, zones noires**)**.
Un grossissement des invadopodes est montré en **A'**, **B'** et **C'**.
Echelle en A (valable pour B et C) : 10µm ; Echelle en A' (valable pour B' et C') : 2µm.

Extrait de Steffen et al,"MT1-MMP-Dependent Invasion Is Regulated by TI-VAMP/VAMP7", Current Biology (2008) 18, 926–931.

C. Formation des invadopodes

Récepteurs membranaires à activité tyrosine kinase.

La membrane plasmique présente des récepteurs à activité tyrosine kinase (appelés RTK) permettant de lier des ligands présents dans le milieu extracellulaire appelées facteurs de croissance, comme le facteur de croissance épidermique (EGF) (Mader et al., 2011; Yamaguchi et al., 2005), le facteur de croissance des hépatocytes (HGF) (Rajadurai et al., 2012), le facteur de croissance vasculaire endothéliale (VEGF) (Lucas et al., 2010) ainsi que le facteur de croissance de transformation beta (TGFβ) (Mandal et al., 2008; Pignatelli et al., 2012). Ces facteurs constituent des signaux extracellulaires initiateurs de la formation des invadopodes (Buccione et al., 2009; Hoshino et al., 2013; Murphy and Courtneidge, 2011) (voir Figure 14). Après activation par ces facteurs, les RTK permettent le recrutement et l'activation de diverses protéines, notamment la protéine kinase Src, produit du proto-oncogène c-Src codant pour une protéine cytosolique à activité tyrosine kinase centrale dans la formation des invadopodes (Hauck et al., 2002; Mader et al., 2011; Summy and Gallick, 2003) (voir Figure 14). Les invadopodes ont été observés initialement comme des zones enrichies en protéine kinase Src (Chen, 1989; Chen et al., 1985) avec une forte accumulation de protéines à résidus tyrosines phosphorylées (Mueller et al., 1992). L'expression de formes mutantes de Src (domaine kinase inactif) abolit la formation des invadopodes ainsi que la dégradation de la matrice (Bowden et al., 2006; Hauck et al., 2002) démontrant le rôle de Src dans la formation des invadopodes. Des travaux ont mis en évidence une réduction du potentiel invasif de cellules traitées par des inhibiteurs de Src (Dasatinib, PP2 et SU6656) lorsqu'elles sont cultivées en Matrigel (Sanchez-Bailon et al., 2012). Une étude menée *in vivo* chez la souris a montré que l'expression de Src est essentielle pour la formation de métastases sans affecter la formation et la croissance des tumeurs primaires (Wang et al., 2009).

Il existe d'autres enzymes non-récepteurs à activité tyrosine kinase, notamment Abl et Arg (*Abl-related gene*) dont l'expression est corrélée avec le potentiel invasif des cellules tumorales (Srinivasan and Plattner, 2006). Il a été mis en évidence que la perte d'expression de Abl et Arg réduit la capacité des cellules tumorales à dégrader et à envahir la matrice extracellulaire (Smith-Pearson et al., 2010; Srinivasan and Plattner, 2006). Arg interagit à l'invadopode avec l'intégrine β1 (Beaty et al., 2013) et est

impliquée dans la phosphorylation de la cortactine de manière coordonnée avec Src (Mader et al., 2011).

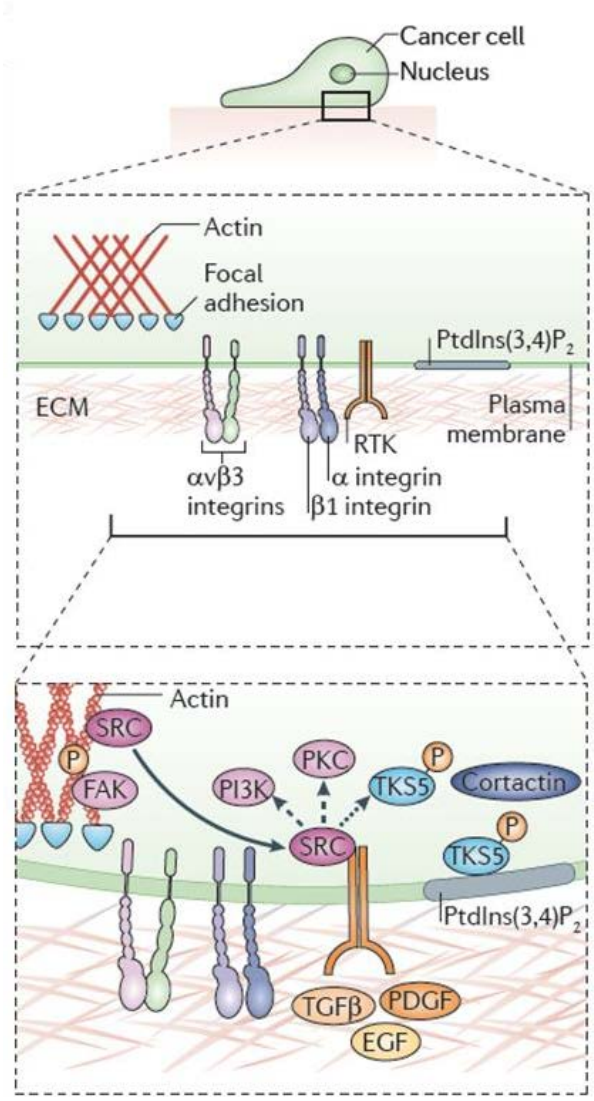

Figure 14 : Schéma représentant les étapes initiales de la formation des invadopodes

Les récepteurs membranaires à activité tyrosine kinase (RTK) sont activés par des facteurs de croissance présents dans le milieu extracellulaire et permettent l'activation des RTK. S'en suit un recrutement de certaines protéines, notamment la kinase Src, responsable de la phosphorylation de nombreuses protéines. Les récepteurs membranaires d'adhésion cellulaire (intégrines) sont également impliqués dans la formation de l'invadopode.

Extrait de Murphy and Courtneidge, "The 'ins' and 'outs' of podosomes and invadopodia: characteristics, formation and function", Nat. Rev. Mol. Cell. Biology (2011) 12, 413-426.

Rôle des récepteurs membranaires d'adhésion cellulaire

De façon attendue, les récepteurs membranaires impliqués dans la reconnaissance et l'adhésion de la cellule à la matrice extracellulaire sont également importants dans la formation des invadopodes (Buccione et al., 2009; Gimona et al., 2008; Hoshino et al., 2013; Murphy and Courtneidge, 2011). L'intégrine β1 fait partie des premiers composants observés et mis en évidence aux invadopodes dans les fibroblastes d'embryon de poulet transformés (Mueller and Chen, 1991). Il a été montré qu'en l'absence de l'intégrine β1 (et dans des conditions de surexpression de Src), les invadopodes ne se forment plus tandis que l'absence de l'intégrine β3 n'affecte pas la formation de ces structures (Destaing et al., 2010). L'interaction de l'intégrine β1 avec Arg est importante pour la stabilité des invadopodes (Beaty et al., 2013).

Organisation lipidique de la membrane plasmique au niveau de l'invadopode

La membrane plasmique au niveau de l'invadopode est caractérisée par des domaines lipidiques spécifiques et organisés appelés « radeaux lipidiques » (Caldieri et al., 2009; Yamaguchi et al., 2009). Ces domaines lipidiques sont notamment enrichis en cholestérol, dont la déplétion dans des cellules tumorales empêche la formation et l'activité des invadopodes (Caldieri et al., 2009). Ces domaines lipidiques sont également enrichis en nombreux phosphoinositides, lipides membranaires impliqués dans le trafic intracellulaire, la signalisation, l'arrangement du cytosquelette et dans l'organisation de la membrane plasmique (Di Paolo and De Camilli, 2006; Takenawa and Itoh, 2001). Les phosphoinositides sont phosphorylés, donnant naissance à différentes isoformes comme le PI_3P, PI_4P, PI_5P, $PI(3,4)P_2$, $PI(4,5)P_2$, $PI(3,5)P_2$ et $PI(3,4,5)P_3$ (Yamaguchi and Oikawa, 2010). Les principaux phosphoinositides impliqués dans la formation et l'activité des invadopodes sont le $PI(3,4)P_2$, $PI(4,5)P_2$, et $PI(3,4,5)P_3$ (Saengsawang et al., 2013; Yamaguchi and Oikawa, 2010). Une diminution du niveau de $PI(4,5)P_2$ dans des lignées cellulaires provenant d'adénocarcinomes mammaires empêche la formation des invadopodes ainsi que la dégradation de la matrice extracellulaire (Yamaguchi et al., 2010). La présence de $PI(4,5)P_2$ à la membrane plasmique induit le recrutement de protéines impliquées dans la formation des invadopodes telles que N-WASP, la cofiline et la dynamine-2 (Rivera et al., 2009; Takenawa and Itoh, 2001), démontrant une implication du $PI(4,5)P_2$ dans la polymérisation des filaments d'actine au niveau de l'invadapode (Yamaguchi and Oikawa, 2010).

Il a également été montré que le PI(3,4)P_2 permet le recrutement à la membrane plasmique de protéines telles que Tks5, Grb2 ou encore N-WASP qui sont également impliquées dans la formation des invadodpodes (Oikawa et al., 2008; Oikawa and Takenawa, 2009; Yamaguchi and Oikawa, 2010).
Ces résultats soulignent le rôle des lipides membranaires et de leur organisation à la membrane plasmique dans les étapes initiatrices de la formation des invadopodes, notamment dans le recrutement des partenaires de la polymérisation de filaments d'actine.

D. Polymérisation de filaments d'actine et maturation de l'invadopode

Les invadopodes sont des protrusions membranaires enrichies en filaments d'actine et en régulateurs de la polymérisation d'actine (Albiges-Rizo et al., 2009; Hoshino et al., 2013; Linder et al., 2011; Murphy and Courtneidge, 2011; Nurnberg et al., 2011; Ridley, 2011). Les filaments d'actine polymérisés à l'invadopode permettent de générer une protrusion membranaire (voir Figure 15 et 16). La polymérisation des filaments d'actine confère probablement à l'invadopode une certaine rigidité nécessaire à son maintien et à sa fonction de pénétration de la matrice (Schoumacher et al., 2010).

1. Les filaments d'actine

L'actine est une protéine globulaire d'environ 40 kDa qui existe sous deux formes : une forme monomérique, appelée actine-G, qui après assemblage, nucléation et élongation, peut former des filaments d'actine fibrillaire, appelée actine-F (Pollard and Borisy, 2003). L'assemblage des monomères d'actine nécessite l'intervention de machineries de polymérisation, donnant naissance à un polymère hélicoïdal constituée de monomères orientés, avec une extrémité + (ou « barbed end »), siège de la croissance du filament d'actine par addition de monomères d'actine et une extrémité – (ou « pointed end ») à partir de laquelle les monomères se désassemblent. Ces monomères sont réutilisés à l'extrémité +, suivant un mécanisme de tapis roulant (treadmealling). Cependant, la dynamique de ce mécanisme est lente (estimée à 0,04 µm/min) – notamment comparée à la vitesse de migration cellulaire (entre 1 et 10 µm/min selon le type cellulaire). Une multitude de protéines permettent d'accélérer et optimiser le

processus de polymérisation des filaments d'actine (Pollard and Borisy, 2003) (voir Figure 15).

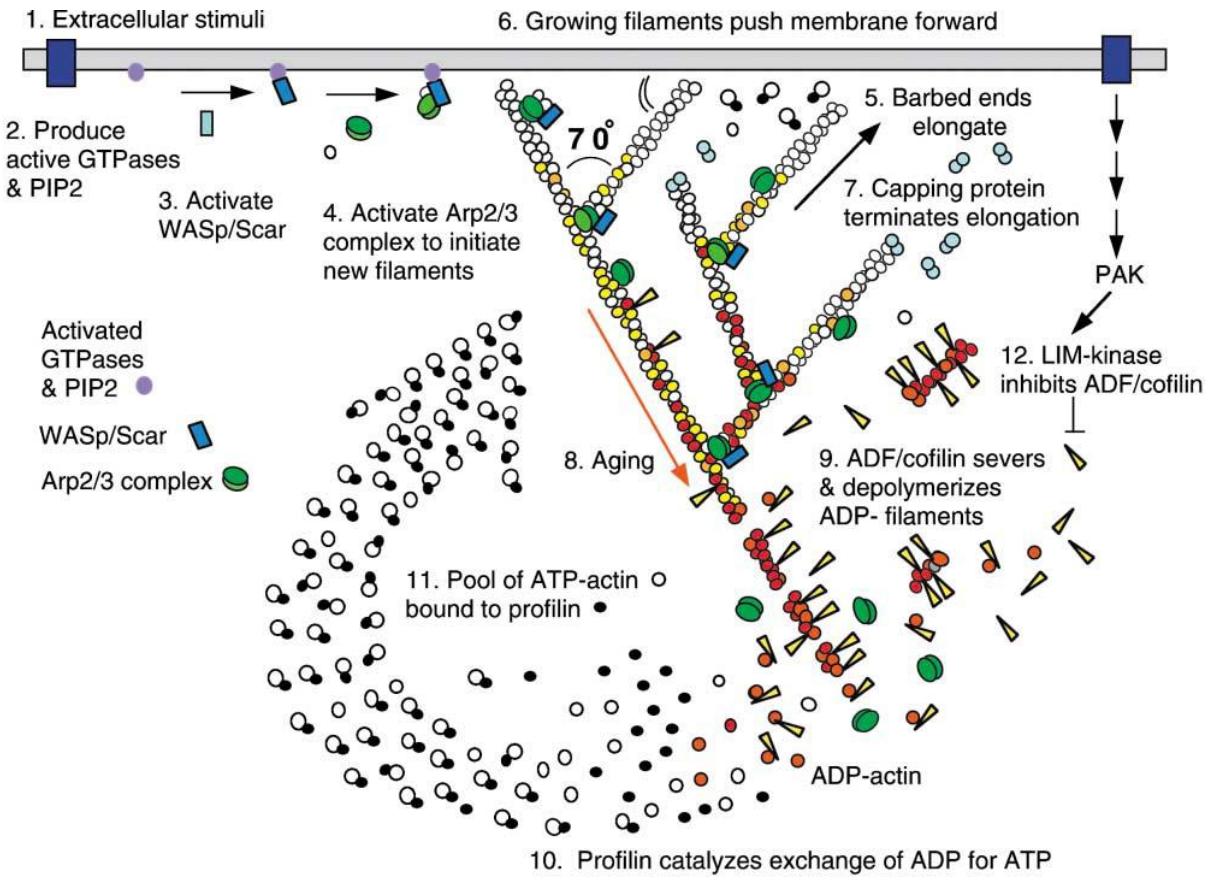

Figure 15 : La dynamique des filaments d'actine.

Des signaux extracellulaires activent des récepteurs membranaires **(1)** qui, par transduction de signaux activent les GTPases de la famille Rho et des phosphoinsositides tel que le PIP_2 **(2)** qui, à leur tour, activent les protéines WASp/Scar **(3)**. WASp/Scar interagit avec le complexe Arp2/3 qui s'associe à un filament d'actine préexistant afin d'induire la polymérisation d'un nouveau filament d'actine et forment un branchement **(4)**. L'élongation du filament d'actine se fait par l'extrémité + (barbed end) **(5)** et induit une pression sur la membrane plasmique **(6)**. Les protéines de coiffe terminent la croissance **(7)**. Les filaments d'actine vieillissent par l'hydrolyse de l'ATP (changement de couleur blanc-jaune des unités d'actine) puis par la dissociation du phosphate inorganique (unités rouges) **(8)**. Des protéines tel que l'ADF/cofiline favorise la dissociation du phosphate, coupe les filaments d'ADP-actine et favorise la dissociation de l'ADP-actine au niveau des extrémités **(9)**. La profiline catalyse l'échange ADP-ATP **(10)**, permettant de renouveler le réservoir d'ATP-actine prêt à allonger les extrémités barbées libres **(11)**. La LIM kinase est activée par les Rho-GTPases via PAK qui phosphoryle l'ADF/cofiline, ralentissant le renouvellement des filaments **(12)**.

Extrait de Pollard and Borisy, «Cellular Motility Driven by Assembly and Disassembly of Actin Filaments », Cell (2003), Vol. 112, 453–465.

2. Régulation de la polymérisation de filaments d'actine à l'invadopode

La polymérisation des filaments d'actine est un finement régulée et aboutit à deux types d'organisation distincts des réseaux de filaments d'actine (Pollard, 2007) : de longs filaments organisés en faisceaux parallèles dont la polymérisation est dépendante des formines ; des filaments d'actine branchés organisés en réseau dont la nucléation est dépendante du complexe Arp2/3 (Lorenz et al., 2004; Yamaguchi et al., 2005).
Le complexe Arp2/3 permet la formation d'un réseau branché de filaments d'actine, observable par microscopie électronique au niveau du lamellipode de cellules en migration (Svitkina and Borisy, 1999). Possédant une très faible activité de nucléation intrinsèque, le complexe Arp2/3 nécessite une activation par des protéines activatrices (Campellone and Welch, 2010). Le complexe Arp2/3 se lie à des filaments d'actine préexistants et, de concert avec ces protéines activatrices, induit la polymérisation de nouveaux filaments d'actine à partir des filaments préexistants pour constituer un réseau branché (Campellone and Welch, 2010; Pollard, 2007) (voir Figure 15 et 16).

Les membres de la famille WASP (Wiskott-Aldrich syndrome protein) sont des activateurs du complexe Arp2/3 (Kollmar et al., 2012; Rotty et al., 2013; Veltman and Insall, 2010). Parmi ces membres, N-WASP a été identifié comme étant l'activateur du complexe Arp2/3 à l'invadopode ; N-WASP est indispensable à la formation de cette structure en induisant la polymérisation des filaments d'actine via l'activation du complexe Arp2/3 (Desmarais et al., 2009; Lorenz et al., 2004; Oser and Condeelis, 2009; Pichot et al., 2010; Yamaguchi et al., 2005) (voir Figure 16). La localisation de N-WASP à la membrane plasmique est régulée par les protéines adaptatrices telles que Grb2, Nck (Kempiak et al., 2005) ainsi que par la cortactine (Oser et al., 2009) qui sont observées dans les invadopodes. D'autres membres de cette famille sont impliqués dans l'activation du complexe Arp2/3 à d'autres emplacements cellulaire : WAVE au lamellipode, WASH à la surface des endosomes (Rotty et al., 2013).

Parmi les nombreux régulateurs de la polymérisation d'actine présents à l'invadopode et impliqués dans la régulation de la nucléation, la cofiline joue un rôle important dans la dynamique des filaments d'actine (voir Figure 15 et 16). La cofiline est impliquée dans le sectionnement des filaments d'actine et leur dépolymérisation, permettant ainsi de

générer à la fois de nouvelles extrémités de filaments et un réservoir local d'actine monomérique nécessaire à la polymérisation de nouveaux filaments d'actine (Bravo-Cordero et al., 2011; Oser and Condeelis, 2009; Yamaguchi et al., 2005). La cofiline interagit avec la cortactine et cette interaction inhibe l'activité de la cofiline (Oser et al., 2009). La phosphorylation de la cortactine permet à la cofiline de se dissocier de la cortactine et de lever l'inhibition. La cofiline peut alors sectionner des filaments d'actine préexistant et induire la nucléation de nouveaux filaments (Oser et al., 2009).
Il a également été montré que la fascine est présente à l'invadopode où son activité de pontage des filaments d'actine entre eux joue sur la stabilité du réseau d'actine à l'invadopode (Li et al., 2010; Schoumacher et al., 2010).

Les filaments d'actine induits par le complexe Arp2/3 sont stabilisés par des protéines permettant le maintien du réseau d'actine branché. L'un des principaux acteurs de ce maintien est la cortactine, composant majeur de l'invadopode (Artym et al., 2006; Ayala et al., 2008; Oser et al., 2009; Yamaguchi and Condeelis, 2007) (voir Figure 16).
La cortactine est une protéine produite par un gène situé sur la région chromosomique 11q13, fréquemment amplifiée dans différents cancers. L'amplification de ce locus s'accompagne d'une augmentation du niveau d'expression de la cortactine, qui est effectivement surexprimée dans différents carcinomes, notamment du sein (Hui et al., 1998). Tout d'abord identifiée aux invadopodes avec la paxilline (Bowden et al., 1999), la cortactine a ensuite été considérée comme essentielle et indispensable à la formation des invadopodes et à la régulation de leur activité (Artym et al., 2006; Bowden et al., 2006; Clark et al., 2007), plaçant même cette protéine au centre des cascades de phosphorylation induites à l'invadopode notamment par Src et Arg (Ayala et al., 2008; Evans et al., 2012; Mader et al., 2011) (voir Figure 16). La cortactine possède à son extrémité N-terminale un domaine pouvant lier et activer très faiblement le complexe Arp2/3 (Uruno et al., 2001), suivi d'un domaine permettant de lier les filaments d'actine préexistants et de stabiliser les filaments d'actine néo-synthétisés (Weaver et al., 2002; Weaver et al., 2001). En position C-terminale se trouve un domaine SH3 permettant de lier directement des protéines contenant des domaines PRD (*proline-rich domain*) comme N-WASP (Martinez-Quiles et al., 2004; Oser et al., 2009) et la dynamine-2 (Baldassarre et al., 2003; McNiven et al., 2000). La surexpression de la cortactine dans des cellules tumorales en culture (MDA-MB-231) permet d'augmenter leur potentiel

migratoire et invasif (Li et al., 2001) tandis que l'inhibition de la cortactine par traitement avec des anticorps bloquant dirigés contre la cortactine dans des cellules préalablement perméabilisée empêche la formation des invadopodes ainsi que la dégradation de la matrice (Bowden et al., 1999).
De par sa structure, la cortactine joue un rôle important à l'invadopode au niveau duquel elle interagit avec de nombreux partenaire, permettant ainsi le maintien de la structure des filaments d'actine polymérisés, nécessaire à la formation de la protrusion membranaire.

La protéine Tks5 (également connue sous les noms de FISH et SH3PXD2A) est un composant de l'invadopode initialement identifié dans les fibroblastes transformés par Src (Abram et al., 2003; Seals et al., 2005). C'est un substrat de Src (Abram et al., 2003; Burger et al., 2014; Seals et al., 2005) important dans la formation des invadopodes ainsi que la dégradation de la matrice extracellulaire (Sharma et al., 2013) (voir Figure 16). La déplétion de Tks5 dans des lignées cellulaires en culture abolit la formation des invadopodes et la dégradation de la matrice extracellulaire (Seals et al., 2005; Sharma et al., 2013). La restauration par expression ectopique de Tks5 dans ces cellules déplétées restaure leurs capacités dégradatives et invasives (Seals et al., 2005; Sharma et al., 2013). A son extrémité N-terminale, Tks5 arbore un domaine qui lie les phosphoinositides, notamment $PI(3,4)P_2$, permettant le recrutement et la localisation de Tks5 à la membrane plasmique au niveau de l'invadopode (Murphy and Courtneidge, 2011; Oikawa et al., 2008). L'activation du récepteur à l'EGF est également impliquée dans le recrutement de Tks5 à la membrane plasmique (Fekete et al., 2013). Tks5 est une protéine d'échafaudage possédant 5 domaines SH3 (il existe un variant d'épissage à 4 domaines SH3 appelé Tks4, SH3PXD2B) (Buschman et al., 2009). Comme décrit pour la cortactine, ces domaines SH3 permettent de lier les protéines à domaine SH3, tel que N-WASP (Oikawa et al., 2008), la protéine adaptatrice Nck (Stylli et al., 2009) ainsi que les protéases de la famille des ADAMs (Abram et al., 2003; Buschman et al., 2009). Tks5 est impliquée dans le recrutement de la cortactine à l'invadopode (Crimaldi et al., 2009; Sharma et al., 2013). Tks5 peut également lier une sous unité du complexe NADPH oxydase ($p22^{phox}$) (Diaz et al., 2009), et est impliquée dans la production des espèces réactives de l'oxygène (ROS) par la NADPH oxydase (Courtneidge, 2012; Diaz et al., 2009; Murphy and Courtneidge, 2011). Les ROS sont présentes à l'invadopode et

importantes pour leur formation ainsi que leur activité dégradative (Courtneidge, 2012; Diaz et al., 2009).

Le recrutement et la présence de la cortactine et de Tks5 au niveau de l'invadopode constituent une étape initiatrice et indispensable à la formation et à la maturation de l'invadopode (Oser et al., 2009; Sharma et al., 2013) (voir Figure 16).

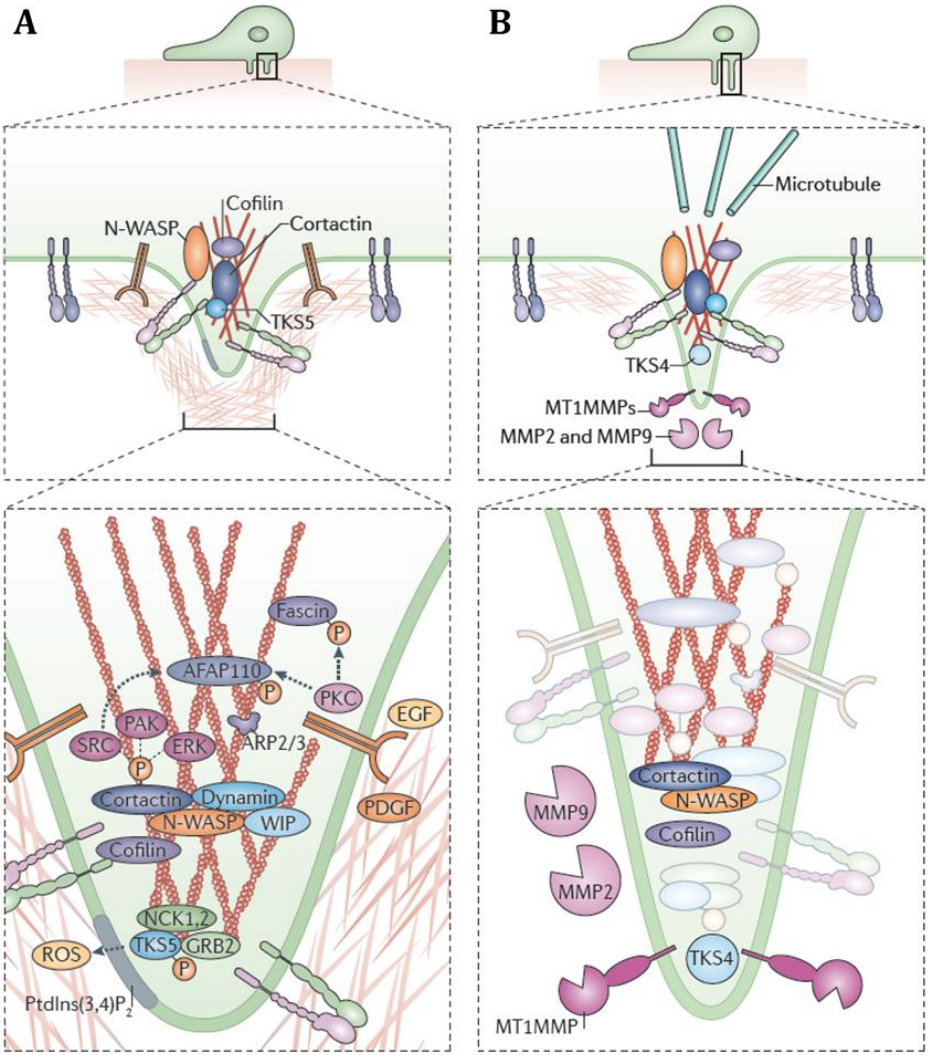

Figure 16 : Localisation au niveau de l'invadopode de la machinerie de polymérisation d'actine et des métalloprotéases matricielles.

(A) La polymérisation de filaments d'actine permet l'assemblage de l'invadopode et le maintien de ces structures. **(B)** La présence de protéases permet la maturation de l'invadopode et lui confère la capacité à dégrader la matrice extracellulaire.

Extrait de Murphy and Courtneidge, "The 'ins' and 'outs' of podosomes and invadopodia: characteristics, formation and function", Nat. Rev. Mol. Cell. Biology (2011) 12, 413-426.

3. Maturation de l'invadopode

La polymérisation de filaments d'actine induite à l'invadopode n'est pas suffisante à elle seule à la maturation de l'invadopode. Ce processus fait appel à un mécanisme conjoint entre la polymérisation de filaments d'actine et l'activité dégradative des cellules. Les filaments d'actine générés à l'invadopode exercent une pression au niveau de la membrane plasmique de l'invadopode, permettant de générer une protrusion. L'activité dégradative des cellules permet de créer un espace extracellulaire permettant l'extension de la protrusion au niveau de la matrice extracellulaire (Artym et al., 2006; Schoumacher et al., 2010) (voir Figure 17 et 18).

La présence de protéases, et notamment MT1-MMP, est indispensable à ce mécanisme (Artym et al., 2006). Il a été montré que l'apport de la protéase à l'invadopode se fait de manière successive à l'apparition et à l'accumulation de cortactine au niveau de la membrane plasmique (Artym et al., 2006) (voir Figure 17). L'accumulation de MT1-MMP confère à l'invadopode une activité protéolytique permettant de dégrader la matrice extracellulaire (Artym et al., 2006) (voir Figure 17 et 18).

Il a récemment été montré que l'activité dégradative de l'invadopode est contrôlée par une régulation locale du pH. De nombreuses protéines impliqués dans la régulation du pH sont présentes à l'invadopode tel que les transporteurs ioniques NaV 1.5 et NHE1 (Beaty et al., 2014; Brisson et al., 2013; Brisson et al., 2012; Busco et al., 2010). Ces transporteurs qui internalisent un ion Na^+ en échange d'un ion H^+ (rapport 1:1) relargué dans le milieu extracellulaire, génèrent un environnement acide au niveau de l'invadopode, favorable notamment à l'activité de certaines protéases comme les cathépsines ou les MMPs.
Il a récemment été montré que la localisation à l'invadopode du transporteur NHE1 est étroitement liée à l'actine (Beaty et al., 2014). La taline, protéine interagissant avec les filaments d'actine, est localisée à la membrane plasmique via sa capacité à interagir avec les intégrines (notamment l'intégrine β1), et permet également la localisation de NHE1 à la membrane plasmique de l'invadopode (Beaty et al., 2014).

Des filaments intermédiaires ainsi que des microtubules ont également été observés au niveau de l'invadopode, possiblement nécessaires à l'apport en protéase vers l'invadopode *via* le trafic intracellulaire (Sakurai-Yageta et al., 2008; Schoumacher et al., 2010; Steffen et al., 2008). Des régulateurs de la stabilité des microtubules tels que HDAC6 (*Histone Deacetylase 6*) sont également impliqués dans la formation et l'activité des invadopodes (Arsenault et al., 2013; Rey et al., 2011).

Les GTPases monomériques apparentées à la protéine oncogénique p21Ras, notamment de la famille des GTPases Rho (Rho, Rac, Cdc42) sont également présentes au niveau de l'invadopode et importante pour sa formation (Murphy and Courtneidge, 2011; Nakahara et al., 2003; Ridley, 2011; Sakurai-Yageta et al., 2008). Cdc42 (Yamaguchi et al., 2005) et ses partenaires tels que CIP4 (*Cdc42-interacting protein 4*) (Hu et al., 2011; Pichot et al., 2010) sont impliqués dans la formation de l'invadopode *via* l'activation de la protéine N-WASP. Cdc42 est également impliqué dans la formation des invadopodes *via* le trafic intracellulaire (Sakurai-Yageta et al., 2008).

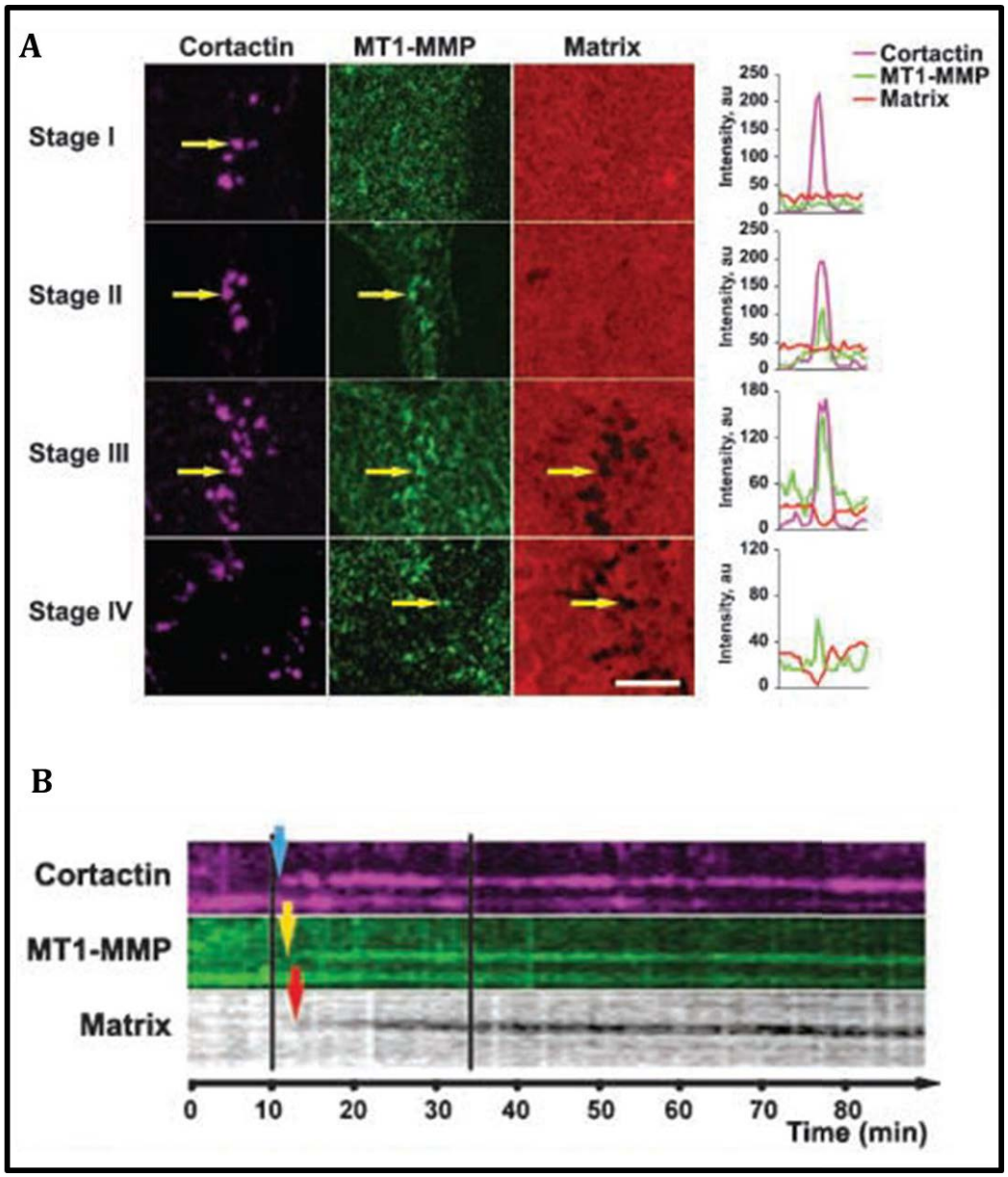

Figure 17 : Maturation de l'invadopode dépendante de la présence de filaments d'actine et de protéases

(A) (Gauche) Des cellules sont cultivées sur du collagène dénaturé (gélatine) couplé à un fluorophore permettant sa visualisation (rouge). La présence de l'invadopode à la membrane plasmique est visualisée par la cortactine (flèche jaune à stage I), s'en suit une accumulation de MT1-MMP (flèche jaune à stage II) qui va permettre la dégradation de la gélatine au niveau de l'invadopode (flèche jaune à stage III, zone noire). **(Droite)** Profil d'intensité de fluorescence de la cortactine (violet), MT1-MMP (vert) et la gélatine (rouge).
(B) Galerie montrant l'évolution au cours du temps de la fluorescence de la cortactine (violet), de MT1-MMP (vert) et de la gélatine (niveaux de gris) au niveau d'un invadopode.

Extrait de Artym et al, "Dynamic Interactions of Cortactin and Membrane Type 1 Matrix Metalloproteinase at Invadopodia: Defining the Stages of Invadopodia Formation and Function", Cancer Res. (2006) 66: (6).

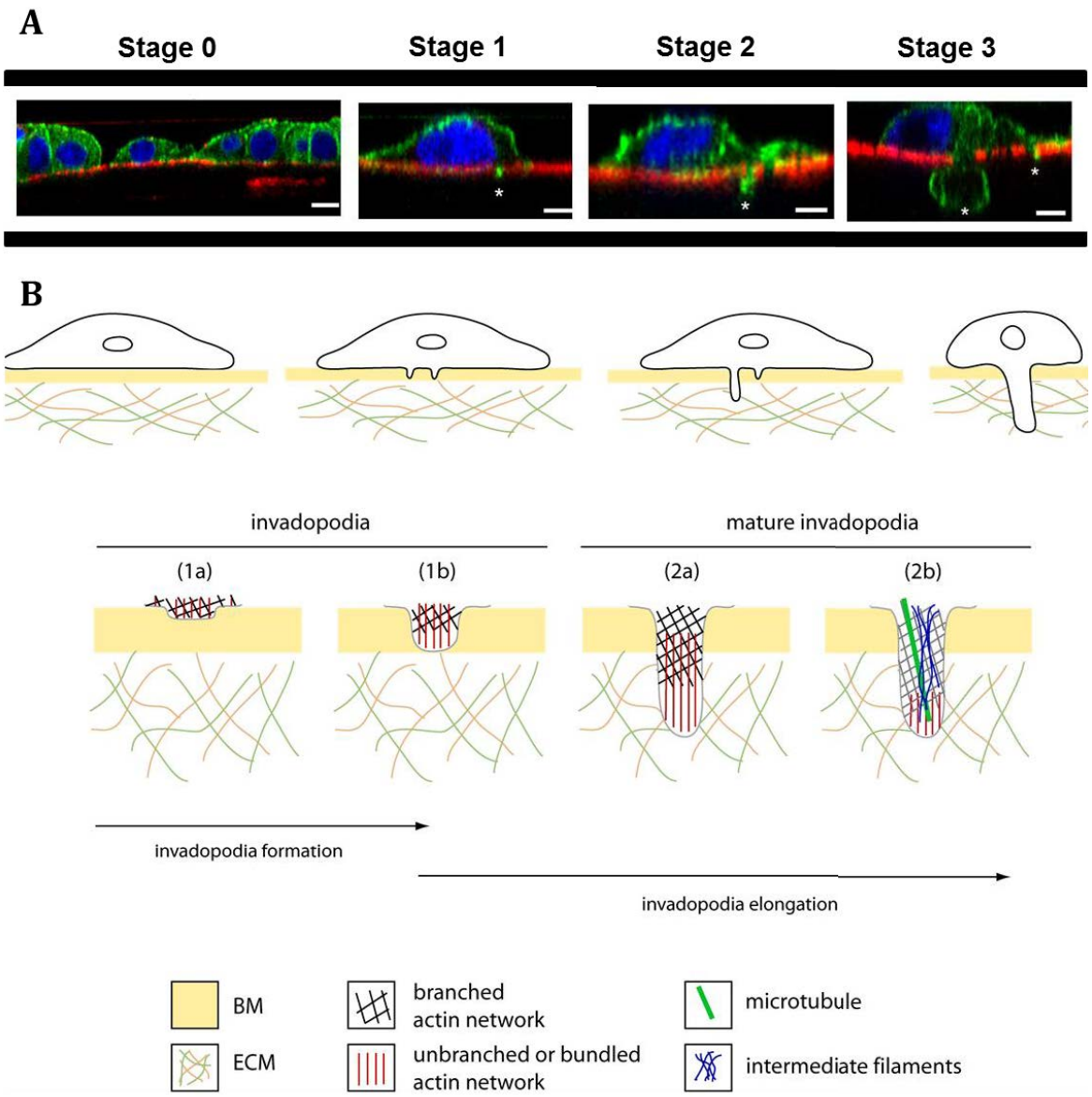

Figure 18 : Evolution de la formation et de la maturation de l'invadopode

(A) Des cellules tumorales invasives sont cultivées au contact d'une membrane basale reconstituée *in vitro* observée par le couplage d'un fluorophore aux laminines permettant leu visualisation (rouge). La cellule est observable par visualisation de son cytosquelette d'actine (vert) et de son noyau (bleu). Les étoiles aux étapes 1, 2 et 3 indiquent la formation et la présence d'invadopodes permettant de traverser la membrane basale. Echelle : stage 0, 10 µm ; stage 1 à 3, 5 µm.
(B) Représentation schématique des observations faites en (A) permettant de mettre en évidence la coopération entre réseaux d'actine (branché et non-branché), microtubules et filaments intermédiaires.

Extrait de Schoumacher et al, "Actin, microtubules, and vimentin intermediate filaments cooperate for elongation of invadopodia", Journal of Cell Biology, (2010) Vol. 189 No. 3 541–556.

IV. Les métalloprotéases matricielles

Les cellules tumorales remodèlent la matrice extracellulaire pour franchir les barrières tissulaires grâce à l'expression de protéases, en particulier les métalloprotéases matricielles (MMP) (Egeblad and Werb, 2002; Kessenbrock et al., 2010; Page-McCaw et al., 2007; Sternlicht and Werb, 2001).

A. Description de la famille des métalloprotéases

Les MMPs sont exprimées de manière constitutive dans les tissus sains où elles jouent un rôle dans des processus physiologiques tels que le développement osseux, l'angiogenèse et la réparation tissulaire (Lu et al., 2011; Ortega et al., 2003; Page-McCaw et al., 2007). Les MMPs sont également impliquées dans les cancers, notamment dans les processus d'invasion tumorale et de formation de métastases (Kessenbrock et al., 2010; Lu et al., 2011).

Par comparaison avec leur niveau basal d'expression dans les tissus sains, certaines MMPs sont surexprimées dans les cellules tumorales de nombreux cancers - notamment de cancer du sein - (Deryugina and Quigley, 2006; Page-McCaw et al., 2007), parmi lesquelles MMP-2 (Polette et al., 1994), MMP-3 (Blavier et al., 2010), MMP-11, MMP-13 et MMP-14 (Kuo et al., 2009), MMP-15 (Tao et al., 2011) ainsi que MMP-9 dont la surexpression est dépendante du facteur de transcription Snail (Jorda et al., 2005) avec lequel la protéase peut également interagir afin d'induire la TEM et jouer ainsi un rôle pro-tumorale (Lin et al., 2011).

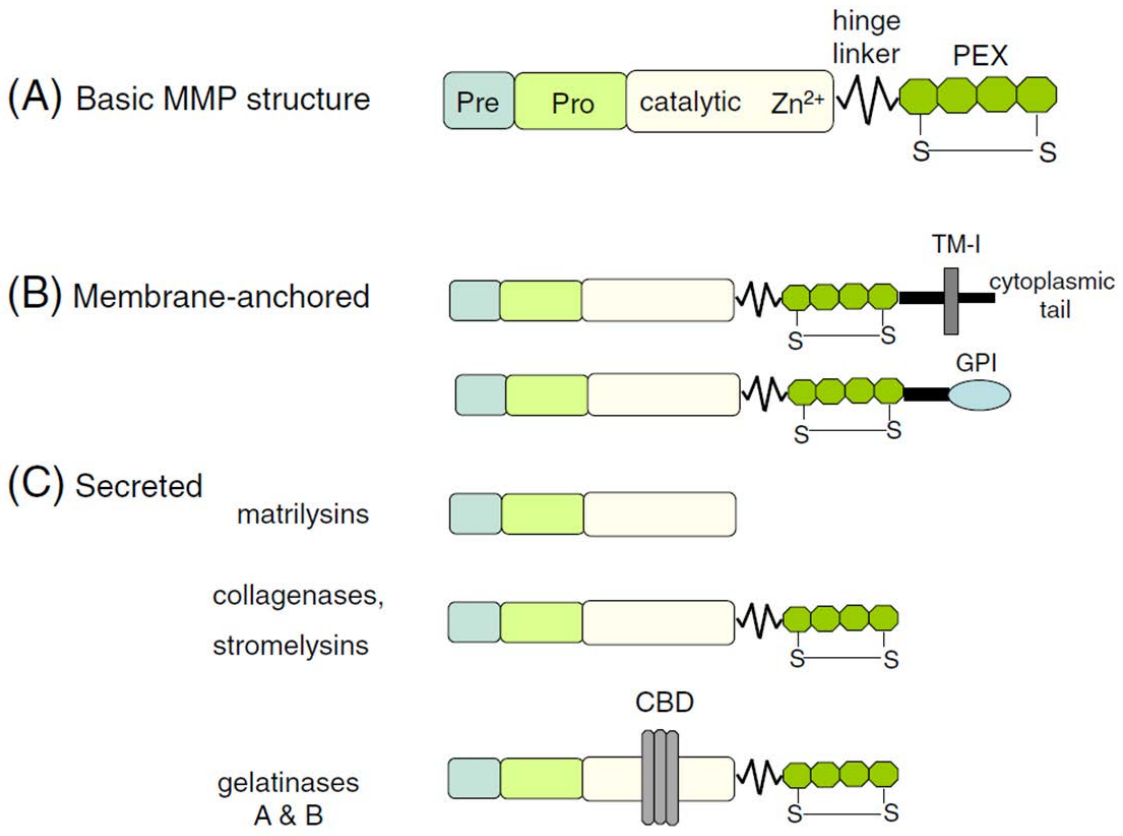

Figure 19 : Structure des métalloprotéases matricielles

(A) Toutes les MMPs possèdent un prédomaine (bleu), un prodomaine (vert clair) et un domaine catalytique (blanc). A l'exception des matrilysines, les MMPs possèdent un domaine hémopexine (vert foncé) relié au domaine catalytique par une région charnière appelée « hinge linker » (noir).
(B) Les MMPs membranaires peuvent être insérée dans la bicouche lipidique de la membrane plasmique via un domaine transmembranaire (TM) suivi d'un domaine cytoplasmique (haut) ou ancré à la membrane plasmique par une ancre GPI (glycosyl-phosphatidylinositol ; bas).
(C) Les MMPs sécrétées ne possèdent pas de domaines pouvant lier la membrane plasmique. Concernant les gelatinases A et B, elles possèdent un domaine CBD (collagen-binding domain) pouvant interagir avec le collagène.

Extrait de Bauvois, "New facets of matrix metalloproteinases MMP-2 and MMP-9 as cell surface transducers: Outside-in signaling and relationship to tumor progression", Biochimica et Biophysica Acta (2012) Vol 1825, Issue 1, Pages 29-36.

Il existe une vingtaine de MMPs classées en deux groupes : les MMPs solubles et les MMPs membranaires (Kessenbrock et al., 2010) (voir Figure 19 et 20).

Structurellement, les MMPs présentent en position N-terminale un peptide signal qui cible la protéase dans les compartiments de la voie de sécrétion. Le peptide signal est suivi du prodomaine – comprenant une centaine d'acides aminés - jouant un rôle auto-inhibiteur de l'activité de la protéase (voir Figure 19). Le prodomaine est suivi du domaine catalytique impliqué dans la dégradation des composants de la matrice extracellulaire (Kessenbrock et al., 2010; Li et al., 2008) ; l'activité catalytique est dépendante de la présence d'un atome de zinc agissant comme co-facteur (Puente et al., 2003). A l'exception de MMP-7 et MMP-26 qui ne présentent que ces trois domaines (peptide signal, pro et catalytique), les autres MMPs possèdent un domaine hémopexine relié au domaine catalytique par une région charnière appelée « *hinge domain* » (voir Figure 19). Ce domaine hémopexine est impliqué dans la reconnaissance du substrat ainsi que dans l'interaction avec d'autres protéines, notamment des MMPs (Cao et al., 2004; Kessenbrock et al., 2010; Li et al., 2008; Suenaga et al., 2005).

En plus de ces domaines, les MT-MMPs (membrane-type MMP ou MMP membranaires) possèdent des domaines permettant leur insertion au niveau de la membrane plasmique: soit un domaine transmembranaire à proximité de l'extrémité C-terminale (MT1-MMP, MT2-MMP, MT3-MMP et MT5-MMP), soit par une ancre lipidique de type GPI (*glycosylphosphatidylinositol*) en position C-terminale (MT4-MMP et MT6-MMP) (Kessenbrock et al., 2010) (voir Figure 19 et 20). L'association des MT-MMPs avec la membrane plasmique rend compte de l'activité protéolytique péricellulaire des cellules tumorales. Contrairement aux MT-MMPs, les MMPs solubles ne possèdent pas de domaines permettant leur insertion à la membrane plasmique et sont sécrétées dans le milieu extracellulaire. Toutefois, les MMPs solubles peuvent se lier indirectement à la membrane plasmique *via* des MT-MMPs ou des récepteurs membranaires de type intégrines ou CD44 (Kessenbrock et al., 2010).

Structure	Membre	Catégorie	Activateurs	Cible de la matrice extracellulaire	Autres cibles
	MMP-1	Collagénase-1	MMP-3, MMP-10, plasmine	Collagène I, II, III, VII et X, gélatine, aggrécane, entactine, tenascine, perlecane,	MMP-2, MMP-9
	MMP-3	Stromélysine-1	Plasmine	Aggrécane, décorine, gélatine, fibronectine, laminine, collagène III, IV, IX et X, tenascine, perlecane,	HB-EGF, pro-TGFβ, E-cadhérine, pro-MMP-1, -7, -8, -9, -13
	MMP-8	Collagénase-2	MMP-3, MMP-10, plasmine	Collagène I, II et III, gélatine, aggrécane	n.d.
	MMP-10	Stromélysine-2	Plasmine	Aggrécane, fibronectine, laminine, collagène III, IV et V	pro-MMP-1, -8, -10
	MMP-11	Stromélysine-3	Furine, plasmine	Aggrécane, gélatine, fibronectine et laminine	IGFBP-1
	MMP-12	Métalloélastase	n.d.	Aggrécane, élastine, fibronectine, laminine, nidogène	Plasminogène
	MMP-13	Collagénase-3	MMP-2, MT1-MMP, plasmine	Collagène I, II, III, IV, IX, X et XIV, aggrécane, fibronectine, tenascine, laminine, perlecane,	pro-TGFβ
	MMP-7	Matrilysine-1	MMP-3, MMP-10, plasmine	Aggrécane, gélatine, fibronectine, laminine, élastine, entactine, collagène IV, ténascine, décorine	β4 intégrine, E-cadhérine, HB-EGF, MMP-1, -2, -9
	MMP-26	Matrilysine-2	n.d.	Gélatine, collagène IV, fibronectine, fibrinogène, vitronectine	pro-MMP-9
CBD	MMP-2	Gélatinase-A	MMP-1, MMP-7, MMP-13, plasmine, MT1-, MT2-, MT3-, MT5-, MT6-MMP	Gélatine, collagène IV, V, VII, X et XI, fibronectine,laminine, élastine, aggrécane	pro-TGFβ, galectine-3, plasminogène
	MMP-9	Gélatinase-B	MMP-2, MMP-3, MMP-10, MMP-13, plasmine	Gélatine, collagène III, IV et V, aggrécane, élastine, entactine, vitronectine	pro-TGFβ, galectine-3, plasminogène, ICAM-1
TM-I	MMP-14	MT1-MMP	Furin	Collagène I, II, III, (IV), gélatine, aggrécane, fibronectine, laminine, fibrine	pro-MMP-2, pro-MMP-13, CD44,
	MMP-15	MT2-MMP	Furin	Aggrécane, fibronectine, laminine, tenascine, nidogène, perlecane	pro-MMP-2
	MMP-16	MT3-MMP	Furin	Collagène III, gélatine, fibronectine	pro-MMP-2
	MMP-24	MT5-MMP	Furin	Gélatine, fibronectine	n.d.
GPI	MMP-17	MT4-MMP	Furin	Fibrine, gélatine	pro-MMP-2
	MMP-25	MT6-MMP	Furin	Gélatine, collagène IV, fibrine, fibronectine, laminine	pro-MMP-2

Figure 20 : Tableau représentant les différentes caractéristiques des MMPs (catégorie, activateurs, cibles)

Ce tableau résume les principales caractéristiques de la famille des MMPs, à savoir leur classification, leurs principales cibles de la matrice extracellulaire ainsi que les autres cibles des MMPs, les protéines activatrices des MMPs. *Tableau adapté de Lu et al, "Extracellular Matrix Degradation and Remodelling in Development and Disease", Cold Spring Harbor Perspectives in Biology (2011) ; 3 :a005058*

Les MMPs sont synthétisées sous forme de proenzyme (zymogen) ; forme inactive de l'enzyme présentant le prodomaine qui intéragit avec le domaine catalytique et l'inhibe. Il existe deux modes d'activation des proMMPs:

- à l'intérieur de la cellule, par des endopeptidase de la famille des sérines protéases, notamment la furine. Cette enzyme clive la métalloprotéase entre le prodomaine et le domaine catalytique, levant l'inhibition et permettant ainsi l'activation de la protéase. C'est le cas de MMP-14 qui est activée par clivage du pro-domaine par la furine au niveau du TGN (Sato et al., 1996; Yana and Weiss, 2000).
- à l'extérieur de la cellule, généralement induit par d'autres MMPs ou par des sérines protéinases (Egeblad and Werb, 2002). pro-MMP-2 et pro-MMP-13 (formes inactives de MMP-2 et MMP-13) ont un mécanisme d'activation particulier qui dépend de MT1-MMP et de TIMP-2 *(tissue inhibitors of matrix metalloproteinase)*, un inhibiteur naturel des MMPs. TIMP-2 s'associe, via le domaine catalytique de MT1-MMP, à une des sous-unités du dimère de MT1-MMP présent au niveau de la face externe de la membrane plasmique de la cellule et inhibe cette sous-unité, formant ainsi un complexe MT1-MMP/TIMP-2 qui sert de récepteur à pro-MMP-2 ou pro-MMP-13. L'activation de pro-MMP-2 et pro-MMP-13 se fait grâce à la sous-unité libre du dimère de MT1-MMP non-associée à TIMP-2 (Itoh et al., 2001; Strongin et al., 1995).

En plus des TIMPs, il existe d'autres inhibiteurs endogènes des MMPs comme l'α2-macroglobulin et la thrombospondin-2 qui forment des complexes à la surface membranaire avec les MT-MMPs activées et permettent leur inactivation en induisant leur internalisation (Egeblad and Werb, 2002). D'autres inhibiteurs, comme la thrombospondin-1, peuvent lier les pro-MMPs au niveau intracellulaire et empêcher leur activation. Ces protéases présentent également des inhibiteurs synthétiques exogènes (Roy et al., 2009).

Les métalloprotéases matricielles sont impliquées dans le clivage et la dégradation de composants de la matrice extracellulaire (voir Figure 20). Chaque MMP possède un répertoire spécifique de substrats au niveau des différents composants de la matrice extracellulaire (Lu et al., 2011; Sternlicht and Werb, 2001) (voir Figure 20). Les MMPs peuvent également cibler des protéines non-matricielles comme d'autres MMPs ou encore certains récepteurs membranaires d'adhésion à la matrice extracellulaire (voir Figure 20).

B. MT1-MMP

La métalloprotéase membranaire de type 1 MT1-MMP (*membrane type 1- matrix metalloproteinase*) est une protéase de la famille des MMPs produit du gène MMP-14 impliquée dans de nombreux processus physiologiques tels que le développement et la régénération osseuse (Holmbeck et al., 2005), l'angiogenèse (Chun et al., 2004) ainsi que le développement de la rétine chez le poisson-zèbre (Janssens et al., 2013). Des souris portant des mutations de MT1-MMP présentent des défauts létaux du développement osseux et de l'angiogenèse (Holmbeck et al., 1999). Un défaut d'activation de MMP-2 par MT1-MMP a également été observé *in vivo* dans ces souris (Zhou et al., 2000).
Dans un contexte pathologique, MT1-MMP a été identifiée comme une enzyme clé du programme tumorale et métastatique (Sabeh et al., 2004). Dans des matrices reconstituées ou bien natives dans des expériences in vitro, MT1-MMP est impliquée dans la dégradation de la membrane basale par les cellules tumorales (Hotary et al., 2006), ainsi que dans l'invasion à travers un environnement tridimensionnel de fibres de collagène de type 1 (Wolf et al., 2013; Wolf et al., 2007).
Dans des modèles animaux, MT1-MMP est essentielle à la croissance tumorale dépendant du remodelage matriciel (Hotary et al., 2003). MT1-MMP est indispensable à la formation des métastases (Perentes et al., 2011). Une autre étude a montré que des souris déficientes en MT1-MMP pouvaient développer des tumeurs primaires sans toutefois former de métastases (Szabova et al., 2008).
Dans les cancers chez l'homme, MT1-MMP est exprimée dans les cellules présentes au front de migration au niveau de mélanomes (Hofmann et al., 2003). Il a été mis en évidence que l'inhibition par anticorps bloquant de MT1-MMP empêche l'angiogenèse, la croissance tumorale et l'invasion tumorale du cancer de l'ovaire (Kaimal et al., 2013).

MT1-MMP est présente à la membrane plasmique et est enrichie au niveau des invadopodes afin de permettre la dégradation de la matrice extracellulaire (Artym et al., 2006; Chen and Wang, 1999; Deryugina et al., 2001; Poincloux et al., 2009; Sakurai-Yageta et al., 2008; Steffen et al., 2008). Il a notamment été montré que l'accumulation de MT1-MMP à l'invadopode succède à la formation de filaments d'actine observés par l'apparition et l'accumulation de la cortactine (Artym et al., 2006). Un immunomarquage de surface de MT1-MMP a permis de mettre en évidence la présence de la protéase en

association avec des zones de dégradation de la matrice extracellulaire (Steffen et al., 2008).

1. Synthèse et structure de MT1-MMP

MT1-MMP, synthétisée sous forme de proenzyme, est activée par clivage du prodomaine au niveau du Trans-Golgi Network (TGN) par la furine avant son ciblage à la membrane plasmique, pour produire une enzyme catalytiquement active à la surface cellulaire (Mazzone et al., 2004; Sato et al., 1996; Yana and Weiss, 2000) (voir Figure 19, 20 et 21).

Structurellement, il a été montré que le domaine transmembranaire (TM) de MT1-MMP est indispensable à sa localisation à la membrane plasmique de la cellule et à son activité (Hotary et al., 2006). MT1-MMP doit être insérée dans la bicouche lipidique de la membrane plasmique pour être active et efficace pour la dégradation de la matrice extracellulaire (Hotary et al., 2006; Li et al., 2008). De plus, ce domaine est spécifique à MT1-MMP (Hotary et al., 2006). Lorsque le domaine TM de MT1-MMP est fusionné aux protéases MMP-2 ou MMP-9 (qui n'ont pas de domaine TM), les protéines chimériques obtenues sont incapables de dégrader la matrice basale (Hotary et al., 2006). De même, lorsque le domaine catalytique de MT1-MMP est remplacé par le domaine catalytique de MMP-1, les cellules ne dégradent pas la membrane basale (Hotary et al., 2006).

Bien que des études aient montré que le domaine cytoplasmique C-terminal de MT1-MMP est dispensable à l'activité catalytique de la protéase (Hotary et al., 2006), il semblerait que ce domaine soit nécessaire à l'activité de MT1-MMP dans la dégradation de la matrice extracellulaire et l'invasion cellulaire (Wu et al., 2005; Yu et al., 2012), notamment en étant la cible de phosphorylations (Moss et al., 2009; Nyalendo et al., 2007; Williams and Coppolino, 2011). Des travaux menés au laboratoire et non-publiés ont confirmé l'importance de ce domaine dans la capacité dégradative *in vitro* des cellules tumorales. Récemment, il a été montré que le domaine cytoplasmique de MT1-MMP permet son interaction avec le cytosquelette d'actine, permettant de maintenir la protéase au niveau des invadopodes, structures riches en filaments d'actine (Yu et al., 2012)

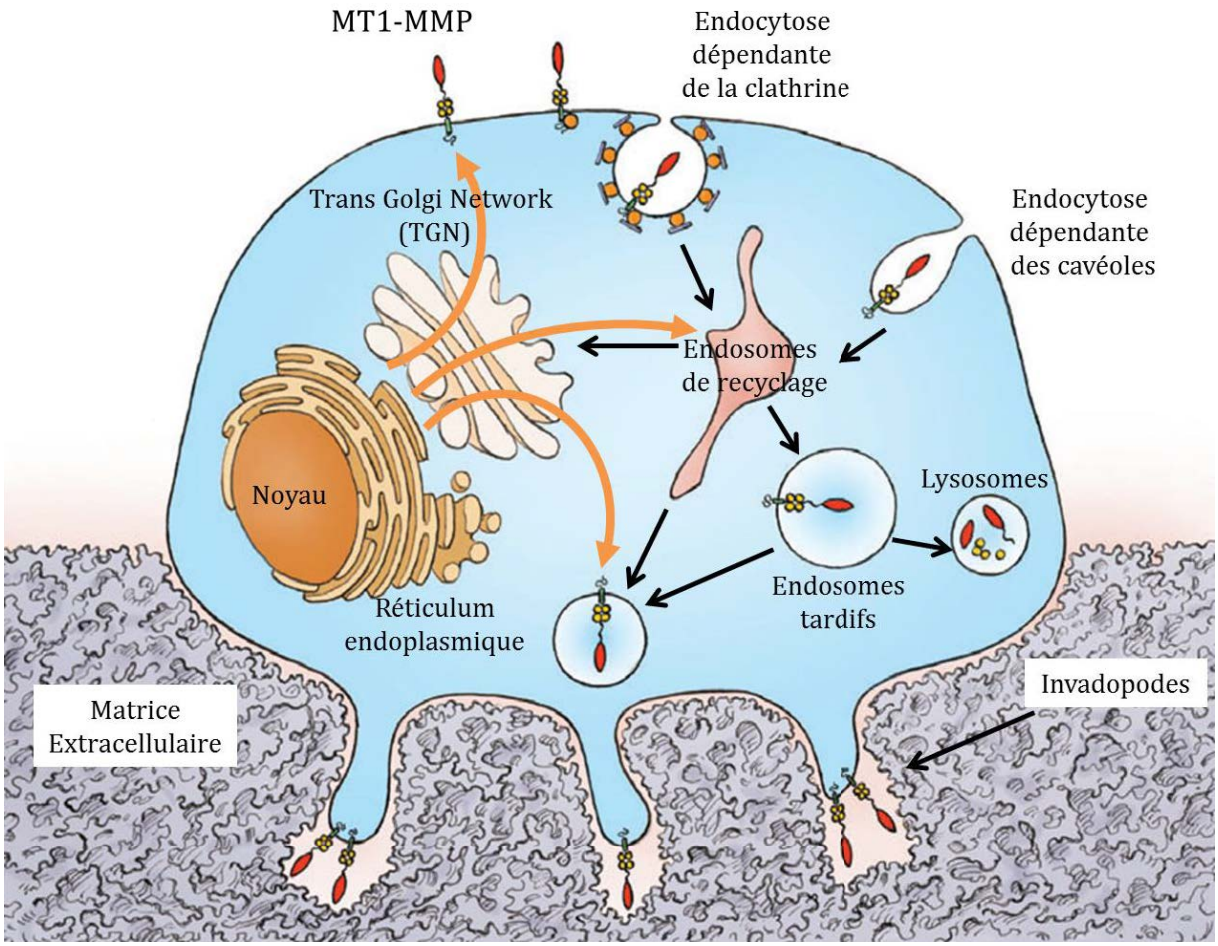

Figure 21 : Synthèse, endocytose et trafic intracellulaire de MT1-MMP

MT1-MMP est adressée à la membrane plasmique de la cellule soit par la voie sécrétoire après synthèse et maturation au niveau du Trans Golgi Network, soit la voie d'endocytose et exocytose, faisant intervenir un trafic intracellulaire de la protéase après endocytose dépendante de la clathrine ou des cavéoles. Une fraction de la protéase est présente dans les endosomes tardifs à partir desquels MT1-MMP est adressée à l'invadopode.

Extrait de Poincloux et al, "Matrix invasion by tumour cells: a focus on MT1-MMP trafficking to invadopodia", Journal of Cell Science 122 (2009) 3015-3024.

2. Activité de MT1-MMP

MT1-MMP s'assemble en homodimères à la membrane plasmique nécessaires à l'activité de dégradation de la matrice extracellulaire (Itoh et al., 2006; Itoh and Seiki, 2006; Tochowicz et al., 2011) et à l'activation d'autres MMPs, notamment MMP-2 (décrit plus haut). Il a d'ailleurs été montré que l'activité de MT1-MMP est corrélée à celle de MMP-2

et de MMP-9 (Al-Raawi et al., 2011). Toutefois, la principale activité de MT1-MMP réside dans la capacité à dégrader de nombreux composants de la matrice extracellulaire comme les collagènes de type 1, 2, 3 et 4 (Atkinson et al., 2001; Gioia et al., 2007; Hotary et al., 2006), les laminines (Bair et al., 2005; Koshikawa et al., 2005; Udayakumar et al., 2003) ainsi que d'autres composants tels que la fibronectine, la vitronectine, les aggrecanes et la fibrine (Overall and Dean, 2006).

Au-delà de son activité de dégradation de la matrice extracellulaire, MT1-MMP est également capable de cliver des récepteurs membranaires tels que l'Ephrine-A2 (Sugiyama et al., 2013), DDR1 (Fu et al., 2013), syndecan-1 et syndecan-4 (Endo et al., 2003; Manon-Jensen et al., 2013; Su et al., 2008), CD44 (Kajita et al., 2001; Kung et al., 2012; Mori et al., 2002; Nakamura et al., 2004; Suenaga et al., 2005; Wiesner et al., 2010), ainsi que des facteurs de croissance comme HB-EGF (Koshikawa et al., 2011) et des protéases de la famille ADAM, tel que ADAM-9 (Chan et al., 2012) et ADAM-12 (Albrechtsen et al., 2013). Il a également été mis en évidence dans des cellules provenant de mélanome que MT1-MMP interagit avec la protéine Notch au niveau de la membrane plasmique, permettant le clivage de Notch avec des conséquence pour la prolifération des cellules (Ma et al., 2014).

3. Endocytose de MT1-MMP

MT1-MMP est transportée le long de la voie de biosynthèse jusqu'à la membrane plasmique, au niveau de laquelle elle est rapidement internalisée principalement par la voie d'endocytose dépendante de la clathrine (Itoh and Seiki, 2006; Jiang et al., 2001; Li et al., 2008; Remacle et al., 2003; Uekita et al., 2001), et potentiellement par une voie dépendante des cavéoles (Annabi et al., 2001; Galvez et al., 2004; Remacle et al., 2003) (voir Figure 21). L'internalisation de MT1-MMP est régulée par la dynamine (Jiang et al., 2001) et par le complexe adaptateur AP-2 qui se lie au niveau d'un motif « LL » présent dans la queue cytoplasmique de MT1-MMP et permet son endocytose (Jiang et al., 2001; Remacle et al., 2003; Uekita et al., 2001).

Il a été montré que l'inhibition de l'endocytose de MT1-MMP favorise la dégradation de la matrice extracellulaire par maintien de la protéase au niveau de la face extracellulaire de la cellule (Jiang et al., 2001; Lafleur et al., 2006; Wu et al., 2005). La protéine CIP-4 (*Cdc42-interacting protein 4*) est un substrat de la protéine Src et est impliquée dans

l'endocytose de MT1-MMP, jouant ainsi un rôle dans la dégradation et l'invasion cellulaire (Hu et al., 2011).
De manière intéressante, il a été montré que l'endocytose de MT1-MMP permet notamment de dissocier le complexe formé par MT1-MMP et TIMP-2 dans l'environnement acide des endosomes (Li et al., 2008; Maquoi et al., 2000; Zucker et al., 2004). Enfin, il a été montré dans les cellules endothéliales que l'intégrine b1 est localisée à la membrane plasmique et s'associe à MT1-MMP. Cette association permet de maintenir MT1-MMP à la surface de la cellule en interférant avec l'endocytose de la protéase (Galvez et al., 2002).

4. Régulation de MT1-MMP par le trafic intracellulaire

A la suite de son internalisation, MT1-MMP s'accumule dans des vésicules intracellulaires (endosomes) à partir desquelles la protéase peut être soit envoyée pour dégradation dans les lysosomes (Takino et al., 2003), soit recyclée à la surface de la cellule (Wang et al., 2004) (voir Figure 21 et 22).
Le trafic intracellulaire des endosomes contenant MT1-MMP est finement régulé par un nombre important de protéines (Frittoli et al., 2011; Poincloux et al., 2009). La maturation et la dynamique des endosomes sont régulées par des GTPases de la famille des Rabs, permettant notamment de déterminer le devenir des endosomes (Barr, 2013; Huotari and Helenius, 2011). Il a été montré que de nombreuses protéines Rab sont impliquées dans la régulation du trafic intracellulaire de MT1-MMP (Wiesner et al., 2013). Différents travaux ont montré que MT1-MMP est localisée dans des endosomes positifs pour Rab-8, Rab-4 et Rab-11 à partir desquelles la protéase peut être recyclée à la surface de la cellule consécutivement à son internalisation (Barcelona et al., 2013; Bravo-Cordero et al., 2007; Jiang et al., 2001; Remacle et al., 2003; Uekita et al., 2001). Une fraction majoritaire de la protéase MT1-MMP est présente dans des compartiments positifs pour Rab-7 (Rosse et al., 2014; Williams and Coppolino, 2011) à partir desquels la protéase est relocalisée à la membrane plasmique.

De nombreuses études ont récemment mis en évidence l'importance de la polymérisation de filaments d'actine à la surface des endosomes dans la régulation de la dynamique des endosomes et dans le recyclage de différents cargos et récepteurs

(Derivery et al., 2009). Une attention particulière sera portée par la suite au complexe WASH, principal acteur de la polymérisation de filaments d'actine à la surface des endosomes.

Au niveau des macrophages, il a été montré que les microtubules jouent un rôle important dans le transport intracellulaire de la protéase, notamment *via* les moteurs moléculaires de type kinésine (Wiesner et al., 2010). Une étude menée au laboratoire a mis en évidence la conservation de ce mécanisme dans des cellules de cancer du sein (Castro-Castro and Chavrier, *en préparation*). Des régulateurs de la stabilité du réseau microtubulaire telles que des protéines modifiant les microtubules comme l'acétyletransférase ATAT-1 (*acetyltransferase 1*) ou la tubuline, comme l'histone déacétylase HDAC6 (*histone deacetylase 6*) influencent également le transport et le ciblage de MT1-MMP à la membrane plasmique (Castro-Castro et al., 2012; Rey et al., 2011).

La machinerie d'exocytose est régulée par un grand nombre de protéines. Certaines protéines SNARE sont impliquées dans la fusion des vésicules avec à la membrane plasmique, permettant l'exocytose du contenu des endosomes dans le milieu extracellulaire (Proux-Gillardeaux et al., 2005). Il a été montré que les protéines SNARE VAMP-7 (*vesicle-associated membrane protein 7*) (Steffen et al., 2008; Williams et al., 2014) et VAMP-3 (*vesicle-associated membrane protein 3*) (Kean et al., 2009) sont présentes à la surface des endosomes contenant MT1-MMP et sont nécessaires à leur avec la membrane plasmique et la dégradation de la matrice extracellulaire en permettant l'exocytose de MT1-MMP (voir Figure 22). Il a d'ailleurs été mis en évidence que VAMP-7 et MT1-MMP co-localisent au niveau des invadopodes en association avec la dégradation de la matrice extracellulaire (Steffen et al., 2008). Des protéines SNARE présentent à la membrane plasmique telles que les syntaxine (-4 et -13), SNAP-23 ainsi que des tétraspanines sont également nécessaires à l'apport de MT1-MMP au niveau de la membrane plasmique (Kean et al., 2009; Schroder et al., 2013; Williams et al., 2014).

Une étude menée au laboratoire a montré que le complexe exocyste, impliqué dans l'arrimage des endosomes avec la membrane plasmique, est nécessaire à la dégradation de la matrice extracellulaire dans des cellules d'adénocarcinomes mammaires (Sakurai-

Yageta et al., 2008), en régulant notamment l'adressage de MT1-MMP à la membrane plasmique, dans un mécanisme impliquant la protéine de polarité IQGAP1, qui interagit avec le complexe exocyste de manière dépendante des GTPases Rho et Cdc42 (Sakurai-Yageta et al., 2008) (voir Figure 22).

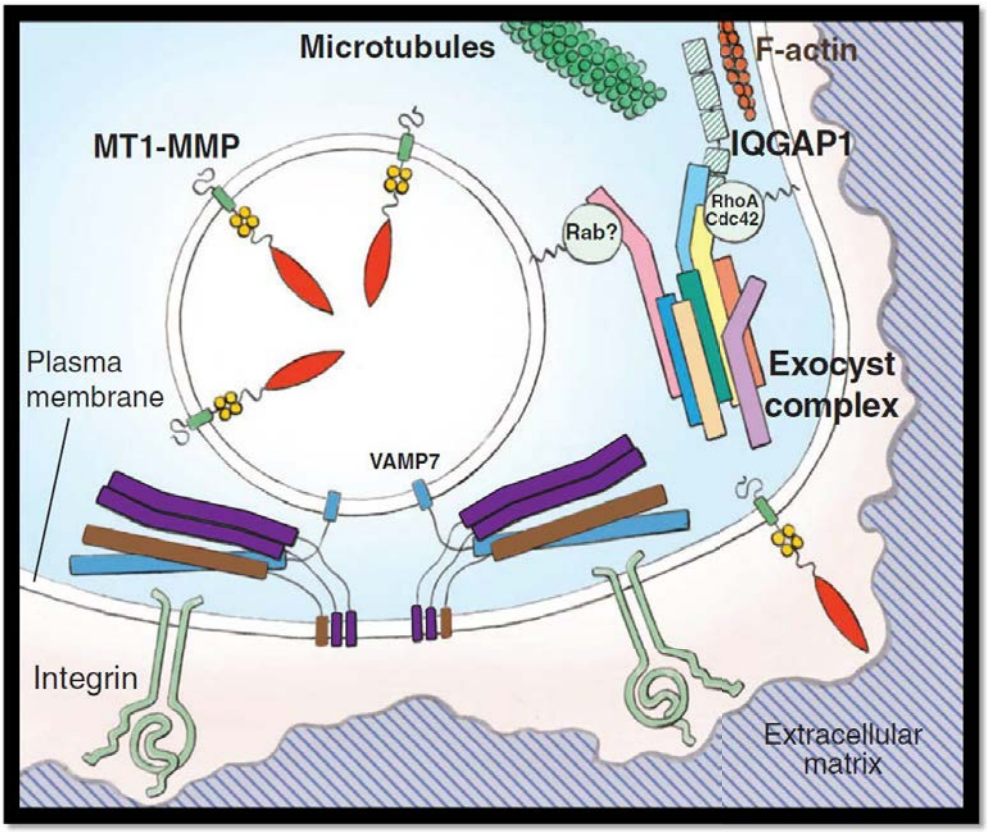

Figure 22 : Adressage de MT1-MMP au niveau de la membrane plasmique de l'invadopode

Les endosomes contenant MT1-MMP sont adressés à la membrane plasmique via un mécanisme impliquant le complexe exocyste et les SNARE, notamment VAMP-7. Ce processus va permettre l'exocytose de MT1-MMP à la membrane plasmique de l'invadopode afin de dégrader la matrice extracellulaire.

Extrait de Poincloux et al, "Matrix invasion by tumour cells: a focus on MT1-MMP trafficking to invadopodia", Journal of Cell Science 122 (2009) 3015-3024.

V. Le complexe exocyste

Le complexe exocyste a été découvert à la fin des années 70 par Peter Novick et Randy Schekman chez *Saccharomyces cerevisiae*, levure bourgeonnante dont la croissance cellulaire se fait par formation et expansion d'un bourgeon à l'extrémité de la cellule. Un des intérêts de ce système cellulaire modèle réside dans le fait que le mécanisme d'exocytose requis pour la croissance de la levure est focalisé à l'extrémité bourgeonnante de cette levure. Les travaux de Novick et Schekman ont mis en évidence une série de protéines impliquées dans le transport et la sécrétion des vésicules au niveau du bourgeon (Novick et al., 1980; Novick and Schekman, 1979; Novick and Schekman, 1983). Des mutations thermosensibles dans ces gènes induisent une accumulation des vésicules intracellulaire incapables de fusionner avec la membrane plasmique, entrainant ainsi un défaut de sécrétion et de croissance cellulaire (Novick et al., 1980; Novick and Schekman, 1979; Novick and Schekman, 1983). L'autre intérêt majeur de ces études qui ont valu un Prix Nobel à R. Schekman, J. Rothman et T. Südhof est qu'elles ont mis en évidence des protéines et des mécanismes conservés chez les eucaryotes supérieurs.

Parmi ces molécules conservées au cours de l'évolution, le complexe exocyste est un complexe octamérique dont la sous-unité Sec15 a été le premier composant mis en évidence en tant qu'effecteur de la protéine Rab Sec4 (Salminen and Novick, 1989) et présente à la membrane plasmique de la levure (Bowser and Novick, 1991). D'abord identifié par ses sous-unités Sec6, Sec8 et Sec15, le complexe exocyste a été complété par Sec3, Sec5, Sec10 et Exo70 (TerBush et al., 1996) ainsi que Exo84 (Guo et al., 1999), pour une masse moléculaire globale avoisinant les 700kDa (Munson and Novick, 2006) (voir Figure 22 et 23).

Le complexe exocyste permet l'arrimage de vésicules intracellulaires au niveau de la membrane plasmique. Des travaux ont mis en évidence la structure du complexe exocyste, identifiant une forme en « Y » dont les deux bras lui permettrait de lier deux bicouches membranaires opposées afin de pouvoir les rapprocher (Hsu et al., 1998; Munson and Novick, 2006) (voir Figure 22 et 23). La sous-unité Exo70 se lie aux

phospholipides, notamment le PI(4,5)P_2, et régule l'adressage du complexe à la membrane plasmique (Fabian et al., 2010; He et al., 2007; Liu et al., 2007; Martin, 2012; Thapa et al., 2012). De par cette interaction avec les lipides, Exo70 et Sec3, sont présents à la membrane plasmique et ont été identifiés comme définissant les sites d'exocytose pour les vésicules intracellulaires (Boyd et al., 2004).
Dans les cellules de mammifères, de nombreux régulateurs du complexe exocyste ont par la suite été identifiés, notamment des GTPase tel que Cdc42 (Sakurai-Yageta et al., 2008; Zhang et al., 2001; Zhang et al., 2008), Arf6 (Prigent et al., 2003), les protéines de la famille Ras, RalA et RalB (Das et al., 2014; Moskalenko et al., 2002; Rosse et al., 2006; Sugihara et al., 2002) ainsi que des membres de la famille des protéines Rab, notamment Rab11 (Neto et al., 2013).

En condition physiologique, le complexe exocyste est impliqué dans la translocation à la membrane plasmique du transporteur du glucose, GLUT-4 (Bao et al., 2008; Chen et al., 2007; Inoue et al., 2003; Inoue et al., 2006). Le complexe exocyste joue également un rôle dans le maintien de la polarité dans les cellules épithéliales, au niveau desquelles le complexe est présent au niveau des jonctions cellulaires (Yeaman et al., 2004) afin de permettre de créer des sites d'exocytose pour le trafic intracellulaire, notamment pour la régulation de la E-cadhérine aux jonctions membranaires (Langevin et al., 2005).
Le complexe exocyste est impliqué dans de nombreux processus dans les cellules de mammifères.

Le complexe exocyste est également impliqué lors de processus pathologiques tel que les cancers (Camonis and White, 2005), notamment dans l'activité dégradative des cellules tumorales. Il a été montré que la perte d'expression de sous-unités du complexe exocyste telles que Sec6, Sec8, Sec10 (Sakurai-Yageta et al., 2008) et Exo70 (Liu et al., 2009a) empêche les cellules d'adénocarcinomes mammaires MDA-MB-231 de dégrader la matrice extracellulaire (Liu et al., 2009a; Sakurai-Yageta et al., 2008), probablement via la régulation de la sécrétion des MMPs (Liu et al., 2009a; Yamamoto et al., 2013).

Le complexe exocyste est associé au cytosquelette de la cellule, notamment *via* le réseau de microtubules (Pathak et al., 2012; Vega and Hsu, 2001) ainsi que le cytosquelette d'actine (Jourdain et al., 2012). Il a été montré chez la levure que la sous-unité Sec3

permet de lier le complexe exocyste aux filaments d'actine (Jourdain et al., 2012). Le complexe interagit également avec le nucléateur de la polymérisation de filaments d'actine, le complexe Arp2/3, *via* la sous-unité Exo70 (Liu et al., 2012; Zuo et al., 2006).

Le complexe exocyste est conservé dans d'autres espèces. Il est notamment présent chez l'amide *Dictyostelium discoideum* (Essid et al., 2012) ainsi que chez C*hlamydomonas reinhardtii* (Komsic-Buchmann et al., 2012) où il joue un rôle dans la contractilité et la décharge de la vacuole intracellulaire.

Le complexe exocyste est un acteur majeur du transport intracellulaire des vésicules, permettant notamment de réguler le mécanisme d'exocytose important pour la communication entre la cellule et son environnement. De par sa capacité à pouvoir interagir avec les lipides membranaires ainsi qu'avec le cytosquelette de la cellule, le complexe exocyste constitue une cible importante dans l'étude et la compréhension des mécanismes d'exocytose.

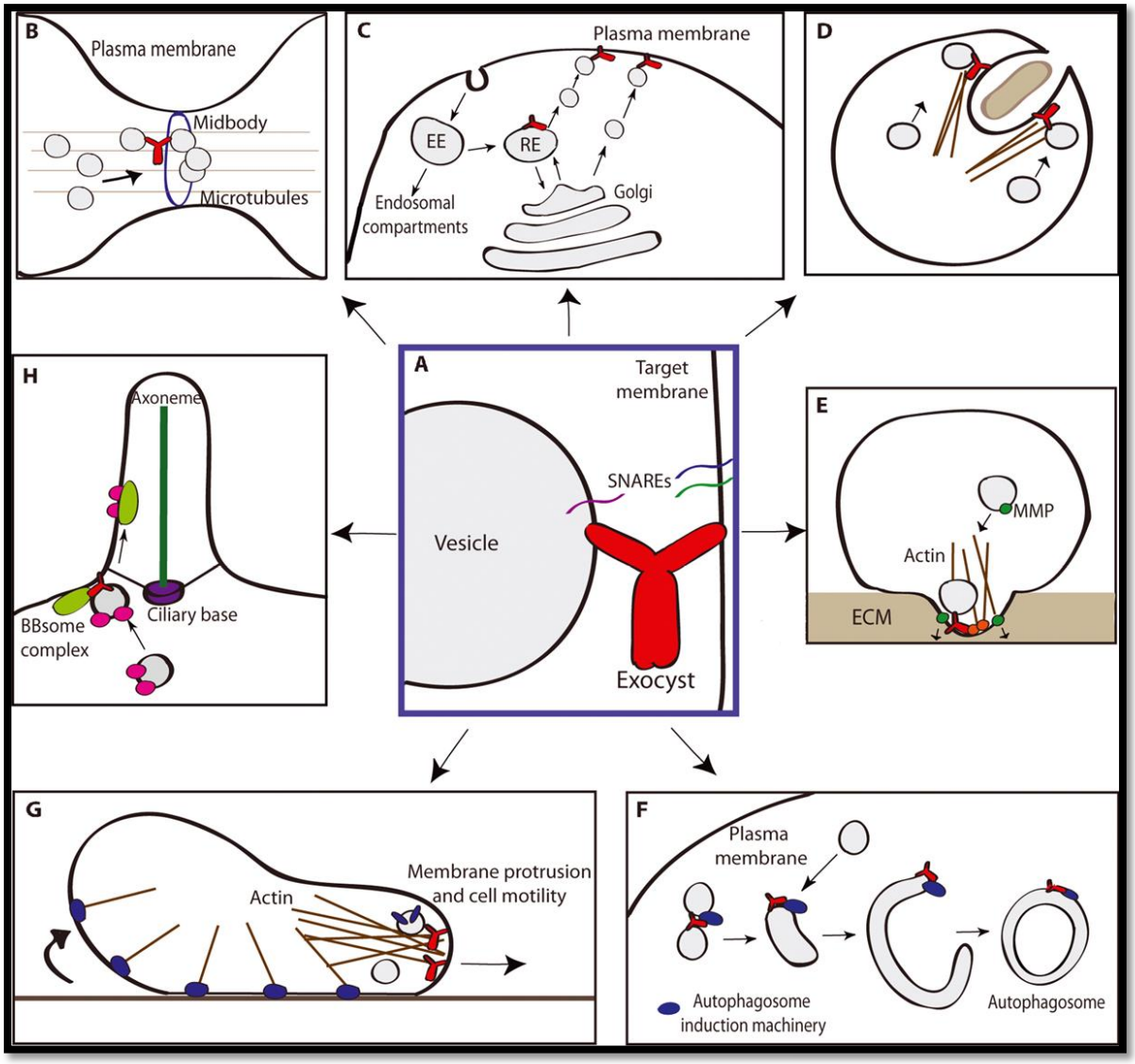

Figure 23 : Le complexe exocyste est impliqué dans de nombreux processus cellulaires

Le complexe exocyste est impliqué dans le rapprochement de deux membranes lipidiques afin de permettre la fusion de ces deux membranes et in fine, l'exocytose du contenu des vésicules **(a)**. Le complexe exocyste est impliqué dans de nombreux mécanismes tel que l'abscision cellulaire lors de la cytocinèse (Gromley et al, 2005 ; Chen et al, 2006) **(b)**, l'exocytose polarisée des vésicules de la voie de sécrétion **(c)**, l'autophagie (Farré et Subramani, 2011 ; Bodemann et al, 2011) **(d)**, la dégradation de la matrice extracellulaire par les cellules tumorales (Sakurai-Yageta et al., 2008) **(e)**, la formation d'autophagosomes **(f)**, la migration cellulaire polarisée (Rossé et al, 2006) **(g)** ainsi que la ciliogénèse (Zuo et al, 2009 ; Das and Guo, 2011) **(h)**.

Extrait de Heider and Munson, "Exorcising the Exocyst Complex" Traffic 2012; 13: 898–907

VI. Le complexe WASH

La protéine WASH (*Wiskott-Aldrich Syndrome Protein and SCAR Homolog*) est un membre de la famille des Wiskott-Aldrich Syndrome Protein (WASP) dont les membres les plus connus sont WASP, N-WASP et WAVE (Campellone and Welch, 2010; Rottner et al., 2010). La protéine WASH est impliquée dans la polymérisation de l'actine sur la face cytosolique de la membrane délimitant les endosomes (Derivery et al., 2009). WASH possède en position C-terminale un domaine VCA (*verprolin homologous or WH2, central hydrophobic, and acidic*) impliqué dans la liaison à l'actine et au complexe Arp2/3 et peut stimuler la nucléation des filaments d'actine en activant le complexe Arp2/3 au niveau des endosomes (Derivery et al., 2009; Duleh and Welch, 2010; Jia et al., 2010; Linardopoulou et al., 2007; Liu et al., 2009b). Ce réseau d'actine est impliqué dans le tri de cargos présents au niveau de l'endosome et permet, par coopération avec le réseau de microtubules, de générer des intermédiaires de transport nécessaires au recyclage de ces cargos. WASH est conservée et interagit avec le complexe Arp2/3 chez la drosophile (Linardopoulou et al., 2007; Liu et al., 2009b).
La protéine WASH fait partie d'un complexe multiprotéique composé de cinq sous-unités: WASH, Strumpellin, SWIP (*strumpellin and wash interacting protein*), FAM-21 et CCDC-53 (Derivery et al., 2009; Gautreau et al., 2014; Jia et al., 2010). Il a également été mis en évidence la présence au sein du complexe WASH de protéines de coiffe, impliquées dans le blocage de la nucléation de filaments d'actine et indispensables à l'activité du complexe WASH (Derivery et al., 2009; Park et al., 2013).

Le complexe WASH est présent au niveau de sous-domaines à la surface des endosomes précoces et tardifs selon le type cellulaire (Derivery et al., 2012; Derivery et al., 2009; Gomez and Billadeau, 2009) ; le nombre de sous-domaines étant corrélé à la taille des endosomes (Gomez and Billadeau, 2009) (voir Figure 24A et 24B). Le complexe WASH interagit avec de nombreux partenaires également présents sur les endosomes parmi lesquels, le complexe retromer (Harbour et al., 2010; Zavodszky et al., 2014a; Zavodszky et al., 2014b). Le retromer est un complexe multiprotéique composé des sous-unités VPS-26, VPS-29 et VPS-35 ainsi que de protéines de la famille des *Sorting NeXin* (SNX) (Seaman, 2012). L'interaction entre le complexe WASH et le complexe retromer permet la localisation du complexe WASH à la surface des endosomes (Freeman et al., 2014;

Harbour et al., 2010) *via* la sous unité FAM-21 du complexe WASH (Jia et al., 2012). Il a été montré qu'une mutation de VPS-35 empêche l'association de WASH à l'endosome et inhibe l'autophagie (Zavodszky et al., 2014a; Zavodszky et al., 2014b).
Il a été montré que des protéines jouant un rôle dans l'ubiquitination (MAGE-L2 et TRIM-27) sont recrutées à la surface des endosomes par le complexe retromer afin de permettre le recyclage de protéine via la régulation du complexe WASH (Hao et al., 2013). Le complexe formé par les protéines MAGE-L2 et TRIM-27 permet l'ubiquitination de la protéine WASH afin d'induire la polymérisation de filaments d'actine nécessaire au recyclage de protéines. Une inhibition de l'ubiquitination de la protéine WASH entraine une tubulation de la membrane des endosomes par un défaut de nucléation de filaments d'actine, entrainant ainsi une perturbation du transport rétrograde (Hao et al., 2013).

La perte du complexe WASH s'accompagne de l'absence de filaments d'actine sur les endosomes et de l'apparition de tubules membranaires émanant de la surface des endosomes (Derivery et al., 2009; Gomez and Billadeau, 2009). Ces changements morphologiques sont accompagnés de perturbation du recyclage de diverses protéines membranaires en transit dans la voie endosomiale comme le récepteur à la transferrine (Derivery et al., 2009), le récepteur β2 adrénergique (Puthenveedu et al., 2010), le transporteur du glucose GLUT-1, le récepteur aux lymphocytes T, TCR (Piotrowski et al., 2013), le récepteur au mannose-6 phosphate (Gomez and Billadeau, 2009; Harbour et al., 2010) et le récepteur à l'EGF (Duleh and Welch, 2010). De plus, la perte d'expression de WASH entraine une accumulation péri-nucléaire des endosomes contenant l'intégrine α5 et un défaut de recyclage des intégrines à la membrane plasmique ainsi qu'une inhibition de la migration cellulaire (Zech et al., 2011).

Au niveau mécanistique, il a été montré que WASH interagit avec la dynamine à la surface des endosomes (Derivery et al., 2009). L'usage d'inhibiteurs de la dynamine induit un identique à celui obtenu par perte d'expression de la protéine WASH (formation de longs tubules émanant de la surface de l'endosome). Dans ces conditions, WASH est présent à la base des tubules (Derivery et al., 2009), renforçant l'idée que le complexe WASH est important pour la fission de tubules membranaires des endosomes à travers la polymérisation d'actine. Ces résultats tendent à mettre en évidence un rôle

de la polymérisation de filaments d'actine induite par WASH à la surface des endosomes dans la formation de vésicules de transport permettant le recyclage de cargos et autres récepteurs.

Chez l'amibe *Dictyostelium discoideum*, la polymérisation de filaments d'actine induite par le complexe WASH est nécessaire à la maturation des lysosomes, notamment en régulant le pH de ces compartiments intracellulaires (Carnell et al., 2011; King et al., 2013). Les filaments d'actine induite par WASH sont importants pour l'élimination de la pompe à protons V-ATPase des lysosomes (Carnell et al., 2011), ainsi que pour le recyclage des protéases (notamment la cathépsineD) présentes au sein de ces lysosomes (King et al., 2013). Ces mécanismes dépendants de WASH permettent une décharge efficace du contenu de ces vésicules.

L'ensemble de ces études soulignent le rôle primordial de la présence de filaments d'actine à la surface des endosomes, nécessaires au bon fonctionnement de ces structures en contrôlant notamment leur dynamique et leur maturation. Ce processus permet de réguler le recyclage intracellulaire de nombreux cargos et semble être un prérequis au bon déroulement des mécanismes d'exocytose.

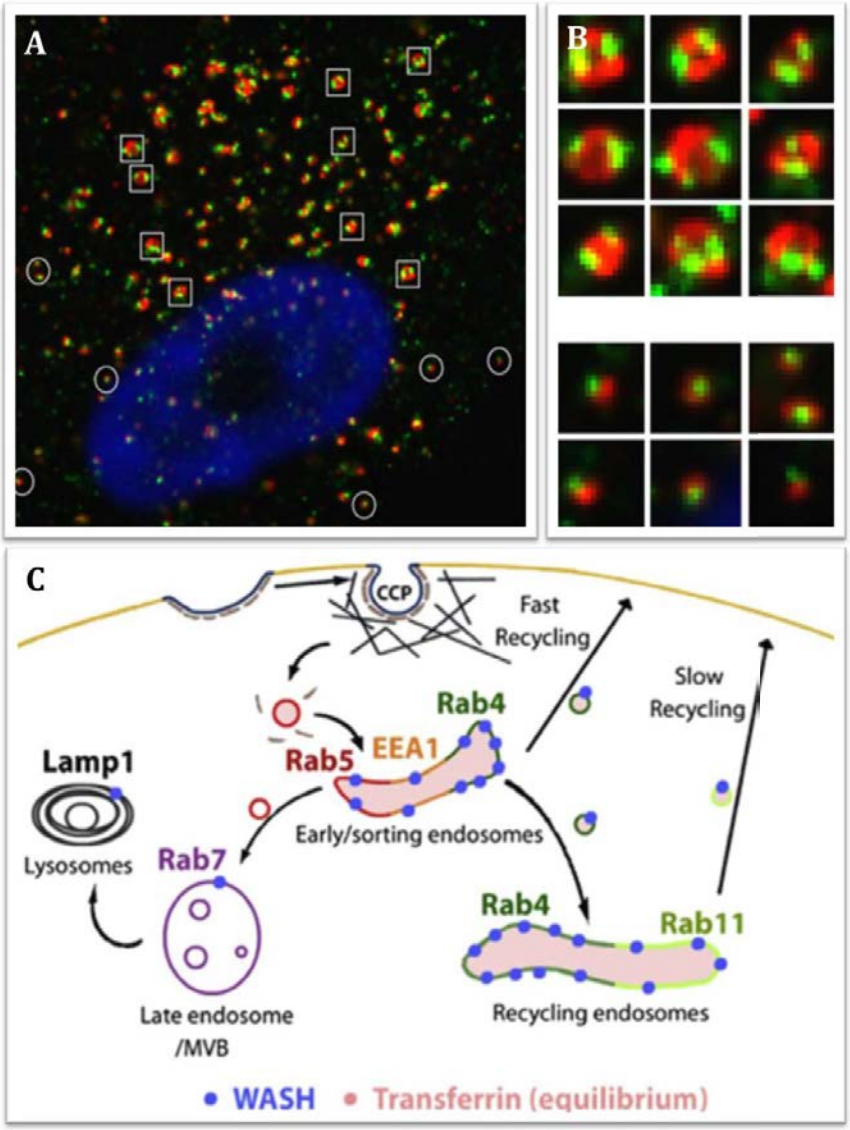

Figure 24: Le complexe WASH localise à la surface des endosomes dont la nature dépend du type cellulaire

(A) WASH (vert) est présent à la surface d'endosomes intracellulaires positifs pour le marqueur des endosomes précoces EEA-1 (rouge). Le noyau est marqué en bleu.
(B) WASH est présent en sous-domaines à la surface des endosomes, dont le nombre dépend de la taille de l'endosome : un seul domaine au niveau d'endosomes de petite taille (bas), plusieurs domaines au niveau d'endosomes de taille plus importante (haut).
Extrait de Gomez and Billadeau, "A FAM21-Containing WASH Complex Regulates Retromer-Dependent Sorting", Dev. Cell (2009) 17, 699–711.

(C) Bien que majoritairement décrit au niveau d'endosomes dits précoces, la nature des endosomes arborant WASH dépend du type cellulaire.
Extrait de Derivery et al, "The Arp2/3 Activator WASH Controls the Fission of Endosomes through a Large Multiprotein Complex", Dev. Cell (2009) 17, 712–723.

Objectifs de mon travail de thèse

Les résultats de nombreux travaux portant sur le trafic intracellulaire de MT1-MMP ont permis de mettre en évidence la contribution de nombreux facteurs nécessaires à l'apport de la protéase au niveau des invadopodes. Cependant, les bases moléculaires de l'exocytose de MT1-MMP à partir des endosomes n'étaient pas élucidées. Compte tenu de l'importance de MT1-MMP au cours de l'invasion tumorale, il nous a semblé essentiel de comprendre comment était régulée l'exocytose de MT1-MMP à partir des compartiments de stockage intracellulaire – les endosomes - et la membrane plasmique de la cellule tumorale au contact avec la matrice extracellulaire.

Parmi les éléments de contrôle du trafic intracellulaire de MT1-MMP, le complexe exocyste est un composant clé en assurant l'arrimage des endosomes avec la membrane plasmique. Ce complexe constituait ainsi une cible intéressante pour l'étude des mécanismes d'adressage de MT1-MMP au niveau des invadopodes.

Afin de comprendre le rôle du complexe exocyste dans les cellules tumorales, des cribles double-hybride ont été effectués chez la levure avec chacune des sous-unités du complexe exocyste afin d'identifier de nouveaux partenaires du complexe qui pourrait nous renseigner sur sa fonction. Ces cribles, menés en collaboration avec Hybrigenics, ont identifié la protéine WASH comme partenaire potentiel des sous-unités Exo84 et Sec3 du complexe exocyste. WASH, une des sous-unités du complexe WASH, induit la polymérisation de l'actine en activant le complexe Arp2/3.

Mon travail de thèse s'est orienté autour de 3 axes :
- la caractérisation *in cellulo* de l'interaction entre les complexes WASH et exocyste
- l'étude du rôle de cette interaction dans le transport intracellulaire de MT1-MMP dans la voie d'endocytose et de recyclage.
- la compréhension du rôle des complexes WASH et exocyste dans l'invasion cellulaire.

Le premier objectif de mon travail de thèse a été de confirmer biochimiquement l'interaction entre les sous-unités Exo84, Sec3 et la protéine WASH par des expériences

d'immunoprécipitation réalisées dans des cellules en culture. Ces résultats ont permis de confirmer les résultats obtenus en double hybride chez la levure et de mettre en évidence que les complexes WASH et exocyste interagissent dans les cellules de mammifère. Dans des cellules en culture, il a été montré que WASH était localisé spécifiquement au niveau des compartiments endosomiaux et que son absence entraînait une tubulation des endosomes ainsi que la perturbation du trafic des récepteurs endocytés (Derivery et al., 2009; Gomez and Billadeau, 2009). Des expériences d'immunofluorescence sur cellules fixées ont permis de mettre en évidence la localisation intracellulaire des sous-unités Exo84 et Sec3 du complexe exocyste ainsi que de la protéine WASH dans les cellules d'adénocarcinome mammaire MDA-MB-231 et d'identifier une potentielle présence et association des complexes WASH et exocyste à la surface des endosomes positifs pour MT1-MMP. De plus, l'utilisation de la technique de « Proximity Ligation Assay » - sorte de co-immunoprécipitation *in situ* – a permis de mettre en évidence une proximité physique (≤40nm) entre les complexes WASH et exocyste.

Au contact avec la matrice extracellulaire, la membrane plasmique de la cellule représente le lieu d'exocytose des endosomes contenant la protéase MT1-MMP et est également impliquée dans la formation des invadopodes. De plus, le complexe exocyste joue un rôle essentiel au niveau de la membrane plasmique dans l'arrimage des vésicules intracellulaires à cette membrane.

Dans un second temps, une large observation de la membrane plasmique a été faite au moyen de la microscopie TIRF (*Total Internal Reflection Fluorescence Microscope*), technique permettant la visualisation des structures à proximité immédiate de la membrane plasmique (zone illuminée de 100-200 nm au-delà de la lamelle de verre). Cette technique constitue un atout majeur à la compréhension des évènements se déroulant au niveau de la membrane plasmique de la cellule. Cette analyse a permis tout d'abord de démontrer que les complexes WASH et exocyste étaient présents à proximité de la membrane plasmique, associés aux endosomes contenant la protéase MT1-MMP en contact avec la membrane plasmique des cellules. Par ailleurs, une approche par perte de fonction des complexes WASH ou exocyste (siRNA) a permis de montrer que ces deux complexes sont nécessaires à la présence ainsi qu'à l'ancrage des endosomes contenant MT1-MMP avec la membrane plasmique, mettant ainsi en évidence une possible

contribution de ces complexes dans l'exocytose de la protéase MT1-MMP, mécanisme indispensable à la dégradation de la matrice extracellulaire.

Finalement, la contribution des complexes WASH et exocyste dans le processus de dégradation de la matrice extracellulaire ainsi qu'au cours de la migration invasive des cellules MDA-MB-231 a été étudiée au travers d'expériences utilisant des environnements tridimensionnel constitué de Matrigel (de composition similaire à la membrane basale, première barrière tissulaire qui s'oppose à l'invasion tumorale dans les carcinomes) ou de collagène de type I (le constituant majeur du stroma tumoral).

L'ensemble de ces analyses a permis de mettre en évidence une possible implication directe des complexes WASH et exocyste dans la capacité des cellules MDA-MB-231 à dégrader la matrice extracellulaire et à migrer dans un environnement matriciel complexe. L'interaction entre les complexes WASH et exocyste ainsi que leur possible localisation au niveau des compartiments endosomiaux où réside MT1-MMP ainsi qu'au niveau de la membrane plasmique confèrent à ces complexes un rôle majeur dans le mécanisme coordonné de transport et d'exocytose localisée de la protéase MT1-MMP au niveau des invadopodes. Ces résultats ont également permis de proposer un nouveau rôle pour WASH dans le tri et/ou le transport de MT1-MMP dans la voie d'endocytose suivant un mécanisme dépendant de la polymérisation de l'actine avec des implications potentielles pour la compréhension des mécanismes cellulaires de l'invasion tumorale.

Article 1

Endosomal WASH and exocyst complexes control exocytosis of MT1-MMP at invadopodia

Pedro Monteiro, Carine Rossé, Antonio Castro-Castro, Marie Irondelle, Emilie Lagoutte, Perrine Paul-Gilloteaux, Claire Desnos, Etienne Formstecher, François Darchen, David Perrais, Alexis Gautreau, Maud Hertzog, and Philippe Chavrier

J. Cell Biol. Vol. 203 No. 6 1063–1079_doi/10.1083/jcb.201306162

La dissémination des cellules cancéreuses et la formation de métastases sont des étapes cruciales dans la progression tumorale et constituent une cause majeure des décès dus au cancer. La métalloprotéase transmembranaire MT1-MMP est un acteur clé impliqué dans le franchissement des barrières tissulaires et le remodelage de la matrice extracellulaire par les cellules cancéreuses. MT1-MMP est présente dans des vésicules intracellulaires, appelées endosomes, à partir desquels elle est adressée à la membrane plasmique afin d'y dégrader la matrice extracellulaire au niveau de protrusions membranaires enrichies en filaments d'actine et en MT1-MMP, appelées invadopodes (Steffen et al., 2008). Une étude menée au laboratoire avait montré que le complexe exocyste est un acteur important pour la formation d'invadopodes dans la lignée d'adénocarcinome mammaire MDA-MB-231 (Sakurai-Yageta et al., 2008). Afin de comprendre le rôle de l'exocyste dans les cellules tumorales, des cribles double-hybride ont été effectués chez la levure avec chacune des sous-unités afin d'identifier des partenaires. La protéine WASH, membre du complexe pentamérique WASH, a été identifiée comme partenaire potentiel des sous-unités Exo84 et Sec3. Afin de confirmer les résultats obtenus en double hybride chez la levure, des expériences d'immunoprécipitation ont montré que la protéine WASH co-immunoprécipite avec Exo84 et Sec3, ainsi qu'avec la sous-unité Sec8 endogène du complexe exocyste, confirmant ainsi l'interaction *in cellulo* entre les complexes WASH et exocyste.

Les complexes WASH et exocyste sont tous deux localisés au niveau de sous-domaines de la surface des endosomes enrichis en MT1-MMP des cellules MDA-MB-231. Ces observations sont en accord avec les résultats princeps identifiant des domaines discrets positifs pour WASH et le complexe Arp2/3 sur la face cytoplasmique des endosomes (Gomez and Billadeau, 2009). De plus nous montrons que les complexes WASH et exocyste contrôlent la polymérisation de l'actine à la surface des endosomes enrichis en MT1-MMP, permettant ainsi de réguler la dynamique de ces compartiments.
Les complexes WASH et exocyste sont nécessaires à la dégradation de la matrice extracellulaire notamment en contrôlant l'apport de la protéase MT1-MMP à la surface de la cellule. Les complexes WASH et exocyste sont présents au niveau de la membrane plasmique à l'interface avec les endosomes positifs pour MT1-MMP ; nos résultats sont en faveur d'un mécansime impliquant la formation de connections entre les endosomes MT1-MMP et la membrane plasmique permettant le transfert de la protéase de la membrane limitante des endosomes à la membrane plasmique au niveau des invadopodes.
Lorsque les cellules MDA-MB-231 sont cultivées sur un substrat composé de fibres de collagène de type I (reconstituant l'environnement du stroma), l'exocytose de MT1-MMP est focalisée au niveau des fibres, au travers d'un mécanisme impliquant les complexes WASH et exocyste qui sont donc impliqués et nécessaires à l'invasion cellulaire par les cellules MDA-MB-231 dans un environnement tridimensionnel.

L'ensemble de ces résultats montrent une implication directe des complexes WASH et exocyste dans la capacité des cellules MDA-MB-231 à dégrader et à envahir la matrice extracellulaire, mettant en évidence une étroite collaboration entre le cytosquelette d'actine et les mécanismes d'exocytose lors des étapes précoces de dégradation de la matrice extracellulaire ainsi que dans l'invasion tumorale.

Contributions article J. Cell Biology :

Le travail que j'ai effectué au cours de ma thèse a été initié au cours de mon stage de Master 2 en novembre 2009 sous la co-supervision de Maud Hertzog et de Philippe Chavrier. Ce travail a abouti en décembre 2013 à une publication dans *The Journal of Cell Biology* et est le fruit d'un travail collectif mené à la fois à l'intérieur et à l'extérieur de l'Institut Curie.

Grâce à des bases solides du travail en laboratoire enseignées et inculquées par **Philippe Chavrier** et **Maud Hertzog**, j'ai pu acquérir de nombreuses compétences en biologie cellulaire - immunofluorescence, immunoprécipitation, microscopie photonique (confocale, TIRF, SIM) - me permettant de mener à bien le projet qui m'a été confié.

Maud Hertzog ayant quitté le labo au début de ma thèse, je suis resté sous l'entière responsabilité de Philippe Chavrier, mon directeur de thèse, présent à toutes les étapes de ce travail. Les expériences présentées dans ce manuscrit sont le résultat d'innombrables échanges, discussions et autres affrontements d'idées entre Philippe et moi dont la finalité quotidienne était de répondre aux questions posées. Ce travail est également le fruit de nombreuses discussions et autres réunions de laboratoires avec les membres du laboratoire de Philippe Chavrier, à savoir notamment **Carine Rossé** et Maud Hertzog.

Le crible ayant identifié la protéine WASH comme potentielle partenaire du complexe exocyste, ce projet a bénéficié de l'aide précieuse d'un spécialiste du complexe WASH, **Alexis Gautreau**, sans qui ce projet aurait été très compliqué à réaliser. Alexis nous a fourni d'inestimables réactifs concernant le complexe WASH (anticorps, plasmides, lignées cellulaires exprimant de manière stable la protéine WASH). Alexis Gautreau a également suivi de près l'avancement de ce travail au cours de certaines réunions de travail en ma présence et celle de mon directeur de thèse, Philippe Chavrier.

L'aide apporté par **Perrine Paul-Gilloteaux** fut de premier ordre dans le développement d'un programme informatique permettant de quantifier - de manière automatisée - l'association des domaines de WASH et de cortactine, ainsi que de WASH

et de Exo84, à la surface des endosomes MT1-MMP. De par l'excellence du savoir-faire de Perrine Paul-Gilloteaux, cette collaboration a été renouvelée et se poursuit actuellement dans le projet en cours que je mène au laboratoire.

Mon travail de thèse m'a également envoyé hors des frontières parisiennes, du côté de Bordeaux, afin de mettre en évidence les continuités établies entre les endosomes contenant MT1-MMP et le milieu extracellulaire. **David Perrais** m'a ainsi accueilli pendant une semaine au sein de son groupe et m'a initié aux expériences de changement de pH du milieu extracellulaire, permettant ainsi de mettre en évidence dans mon système, l'ouverture - pendant un temps assez long de l'ordre de la minute – des endosomes contenant la protéase MT1-MMP et le milieu extracellulaire.

De par leur expertise et expérience dans l'analyse des phénomènes d'exocytose, **François Darchen** et **Claire Desnos** – Université Paris Descartes - ont également contribué à ce travail (voir détail plus loin).

Etienne Formstecher est à l'origine des cribles double-hybride menés chez la levure et permettant d'identifier de nouveaux partenaires au complexe exocyste.

Enfin, les collaborations établies au cours de mon travail se sont également étendues au-delà des frontières françaises et nous ont permis d'interagir avec Laura Machesky et Tobias Zech - à l'époque post-doc chez Laura – mais les aléas de la recherche ont fait que cette collaboration n'a pas apporté les résultats attendus.

Liste détaillée de l'implication de chaque co-auteur dans les résultats présentés dans l'article « Endosomal WASH and exocyst complexes control exocytosis of MT1-MMP at invadopodia »

Figures principales (1 à 9)

Figure1 :

A, B, C, D, F, G : Pedro Monteiro

E: Pedro Monteiro, Perrine Paul-Gilloteaux,

H: Pedro Monteiro, Maud Hertzog

Figure 2:

A, C, D, E, G: Pedro Monteiro

B, F: Pedro Monteiro, Carine Rossé

Figure 3:

A, B, C, D, E, F, G, H, I, J, K: Pedro Monteiro

Figure 4:

A, B, C, D, E, F, G: Pedro Monteiro

Figure 5:

A, C, D, E: Pedro Monteiro

B: Claire Desnos, François Darchen

Figure 6:

A: Pedro Monteiro

B: Carine Rossé

C, D: Antonio Castro-Castro

E, F: Marie Irondelle

Figure 7:

A, B, C, D, E, F, G, H: Pedro Monteiro

Figure 8:

A, B, C, D: Pedro Monteiro

E: Pedro Monteiro, David Perrais

Figure 9:

Pedro Monteiro/Philippe Chavrier

Figures supplémentaires (S1 à S4)

Figure S1: Pedro Monteiro

Figure S2: Pedro Monteiro

Figure S3: Pedro Monteiro

Figure S4: Pedro Monteiro, Carine Rossé, Emilie Lagoutte

Vidéos

Vidéo 1: Pedro Monteiro, Carine Rossé

Vidéo 2: Pedro Monteiro

Vidéo 3: Pedro Monteiro

Vidéo 4: Pedro Monteiro

Vidéo 5: Pedro Monteiro, Carine Rossé

Vidéo 6: Pedro Monteiro

Vidéo 7: Pedro Monteiro, David Perrais

Conception des expériences:	Pedro Monteiro/Philippe Chavrier
Mises en page des figures:	Pedro Monteiro/Philippe Chavrier
Rédaction du manuscrit:	Pedro Monteiro/Philippe Chavrier

Published December 16, 2013

THE JOURNAL OF CELL BIOLOGY

Endosomal WASH and exocyst complexes control exocytosis of MT1-MMP at invadopodia

Pedro Monteiro,[1,2] Carine Rossé,[1,2] Antonio Castro-Castro,[1,2] Marie Irondelle,[1,2] Emilie Lagoutte,[1,2] Perrine Paul-Gilloteaux,[1,3] Claire Desnos,[4,5] Etienne Formstecher,[6] François Darchen,[4,5] David Perrais,[7,8] Alexis Gautreau,[9] Maud Hertzog,[1,2] and Philippe Chavrier[1,2]

[1]Research Center, Institut Curie, 75005 Paris, France
[2]Membrane and Cytoskeleton Dynamics and [3]Cell and Tissue Imaging Facility, Centre National de la Recherche Scientifique UMR 144, 75005 Paris, France
[4]Université Paris Descartes and [5]Centre National de la Recherche Scientifique, UMR8192, 75006 Paris, France
[6]Hybrigenics services SAS, 75014 Paris, France
[7]University of Bordeaux and [8]Centre National de la Recherche Scientifique, Interdisciplinary Institute for Neuroscience, UMR 5297, 33000 Bordeaux, France
[9]Laboratoire d'Enzymologie et Biochimie Structurales, Centre National de la Recherche Scientifique UPR3082, 91198 Gif-sur-Yvette, France

Remodeling of the extracellular matrix by carcinoma cells during metastatic dissemination requires formation of actin-based protrusions of the plasma membrane called invadopodia, where the trans-membrane type 1 matrix metalloproteinase (MT1-MMP) accumulates. Here, we describe an interaction between the exocyst complex and the endosomal Arp2/3 activator Wiskott-Aldrich syndrome protein and Scar homolog (WASH) on MT1-MMP–containing late endosomes in invasive breast carcinoma cells. We found that WASH and exocyst are required for matrix degradation by an exocytic mechanism that involves tubular connections between MT1-MMP–positive late endosomes and the plasma membrane in contact with the matrix. This ensures focal delivery of MT1-MMP and supports pericellular matrix degradation and tumor cell invasion into different pathologically relevant matrix environments. Our data suggest a general mechanism used by tumor cells to breach the basement membrane and for invasive migration through fibrous collagen-enriched tissues surrounding the tumor.

Downloaded from jcb.rupress.org on January 21, 2014

Introduction

The matrix-degrading protrusions of the plasma membrane known as invadopodia are currently thought to form in invasive tumor cells when the extracellular matrix and cues from the tumor microenvironment, such as growth factors, trigger the assembly of F-actin into precursor structures through a signaling cascade involving Cdc42 and Nck1 and the actin regulatory proteins neuronal Wiskott-Aldrich syndrome protein (N-WASP), Arp2/3 complex, cortactin, and cofilin (Lorenz et al., 2004; Yamaguchi et al., 2005; Clark et al., 2007; Ayala et al., 2008; Oser et al., 2009, 2010; Murphy and Courtneidge, 2011). These precursors then mature into functional invadopodia upon accumulation of the trans-membrane type 1 matrix metalloproteinase (MT1-MMP; Artym et al., 2006; Clark et al., 2007; Sakurai-Yageta et al., 2008; Yu et al., 2012).

A significant fraction of MT1-MMP is internalized from the cell surface as a means to regulate its surface level (Jiang et al., 2001; Uekita et al., 2001); In MDA-MB-231 human breast adenocarcinoma cells, we found the majority of intracellular MT1-MMP located in a late endosome compartment (Steffen et al., 2008). We and others reported that an exocytic machinery comprising cortactin, the vesicle-docking exocyst complex, and the SNARE protein vesicle-associated membrane protein 7 (VAMP7) is required for MT1-MMP delivery to invadopodia and invadopodia activity in tumor cells cultured on cross-linked gelatin as a matrix (Artym et al., 2006; Clark et al., 2007; Sakurai-Yageta et al., 2008; Steffen et al., 2008; Liu et al., 2009; Williams and Coppolino, 2011). Based on these findings, we proposed that this cohort of proteins regulates the trafficking and exocytosis of MT1-MMP from late endocytic storage compartments to its invadopodial target plasma membrane (Poincloux et al., 2009). However, the nature of the carriers that mediate plasma membrane

Correspondence to Philippe Chavrier: philippe.chavrier@curie.fr

M. Hertzog's present address is Centre National de la Recherche Scientifique, UMR 5100, Université Paul Sabatier, 31062 Toulouse, France.

Abbreviations used in this paper: CCD, charge-coupled device; MT1-MMP, membrane type 1 matrix metalloproteinase; N-WASP, neuronal Wiskott-Aldrich syndrome protein; SIM, structured illumination microscopy; TIRFM, total interference reflection fluorescence microscope; VAMP7, vesicle-associated membrane protein 7; WASH, Wiskott-Aldrich syndrome protein and Scar homolog.

© 2013 Monteiro et al. This article is distributed under the terms of an Attribution–Noncommercial–Share Alike–No Mirror Sites license for the first six months after the publication date (see http://www.rupress.org/terms). After six months it is available under a Creative Commons License (Attribution–Noncommercial–Share Alike 3.0 Unported license, as described at http://creativecommons.org/licenses/by-nc-sa/3.0/).

Supplemental Material can be found at:
http://jcb.rupress.org/content/suppl/2013/12/15/jcb.201306162.DC1.html
http://jcb.rupress.org/content/suppl/2013/12/23/jcb.201306162.DC2.html
http://jcb.rupress.org/content/suppl/2013/12/23/jcb.201306162.DC3.html

The Rockefeller University Press $30.00
J. Cell Biol. Vol. 203 No. 6 1063–1079
www.jcb.org/cgi/doi/10.1083/jcb.201306162

Published December 16, 2013

delivery of MT1-MMP, the mechanism underlying MT1-MMP exocytosis in the biogenesis of invadopodia, and how exocytosis is possibly influenced by the composition and biophysical properties of the matrix remain poorly understood.

Recent studies have documented an essential role for actin cytoskeleton dynamics in endosome function (Derivery et al., 2009; Gomez and Billadeau, 2009; Morel et al., 2009; Puthenveedu et al., 2010; Carnell et al., 2011; Harrington et al., 2011). The mechanism emerging from these on-going studies indicates that actin–Arp2/3 assemblies organize early endosomal membranes into functional subdomains and contribute to cargo sorting and generation of transport intermediates. Some of these studies also highlighted the essential role of the newly identified Wiskott-Aldrich syndrome protein and Scar homolog (WASH) complex, a member of the WASP (Wiskott–Aldrich syndrome protein) family of Arp2/3 activators associated with the endosomal/lysosomal system and playing a major role in the polymerization of endosomal actin (Derivery et al., 2009; Gomez and Billadeau, 2009; Duleh and Welch, 2010). All together, these data support a critical role for WASH in linking Arp2/3 and F-actin–assisted elongation and fission of endosomal tubules with sorting and trafficking from the endosomal system to the cell surface (Derivery et al., 2009; Gomez and Billadeau, 2009; Puthenveedu et al., 2010; Carnell et al., 2011; Temkin et al., 2011; Zech et al., 2011; Gomez et al., 2012). Here, we describe a novel interaction of WASH with the exocyst complex on MT1-MMP–containing late endosomes in invasive breast tumor cells. Our data support a mechanism of exocytosis of MT1-MMP through late endosome-to-plasma membrane connections occurring at invadopodia and requiring WASH and exocyst complexes for their formation.

Results

WASH and the exocyst complex interact on MT1-MMP–positive endosomes in breast tumor cells

In a series of yeast two-hybrid screens aimed at isolating partners of the eight subunits of the exocyst complex, we identified interactions of both Exo84 and Sec3 exocyst subunits with the amino-terminal region of WASH. Overlapping regions from independent isolated clones defined WASH domains interacting with Sec3 (amino acids 9–109 of WASH) or with Exo84 (amino acids 15–258 of WASH; unpublished data). By using fluorescence microscopy of MDA-MB-231 cells overexpressing GFP-WASH and immunofluorescence microscopy of the endogenous protein and in agreement with the function of WASH as an activator of the Arp2/3 complex (Derivery et al., 2009; Gomez and Billadeau, 2009; Duleh and Welch, 2010), we observed WASH puncta closely associated with punctate accumulations of Arp2/3 complex, F-actin, and the F-actin–binding protein cortactin on MT1-MMP–positive endosomes (Fig. S1 A and Fig. 1, A and B). Exo84 was also detected as puncta closely apposed to and partially overlapping with WASH and cortactin-positive subdomains on MT1-MMP–containing endosomes (Fig. 1, C and D; and Fig. S1 B). Live-cell imaging revealed highly dynamic WASH puncta associated with cortactin (Video 1). The number of WASH-cortactin patches seemed to correlate with endosome size (Fig. 1 B; Gomez and Billadeau, 2009; Derivery et al., 2012). Endosomal puncta of WASH and cortactin were more closely associated (mean distance of ~2 pixels) as compared with WASH and Exo84-positive ones (~5 pixels; Fig. 1 E). Similarly, we observed another component of the WASH complex, FAM21, associated with cortactin domains on MT1-MMP–positive endosomes (Fig. S1 C). WASH was also apposed to punctate structures containing the late endocytic SNARE protein VAMP7 on the limiting membrane of these endosomes (Fig. S1 D), in agreement with the predominant localization of MT1-MMP to late endosomes (Steffen et al., 2008; Williams and Coppolino, 2011). WASH- and cortactin-positive puncta were similarly associated with MT1-MMP–containing endosomes in BT-549 breast cancer cells (Fig. S1 E). To further evaluate association of WASH with cortactin or Exo84 on MT1-MMP–containing endosomes, we performed a Duolink in situ proximity ligation assay (Söderberg et al., 2006). This analysis confirmed a strong association between WASH and cortactin and a weaker one between WASH and Exo84, with most of the Duolink signal coinciding with MT1-MMP–containing endosomes (Fig. 1, F and G). Finally, endogenous WASH protein in HeLa cell extracts coimmunoprecipitated with overexpressed full-length Exo84 and Sec3 and with endogenous Sec8 (Fig. 1 H), thus confirming the two-hybrid results and showing that WASH interacts with the exocyst complex in vivo. Together, these findings reveal the existence of WASH- and Arp2/3–F-actin–cortactin–positive domains on MT1-MMP–containing late endosomes. The exocyst complex is closely apposed to and interacts with WASH-positive subdomains on MT1-MMP–positive endosomes, suggesting a coordinated function of these complexes in breast tumor cells.

WASH and exocyst control actin assembly on MT1-MMP–positive endosomes

To investigate the roles of WASH and the exocyst complex we first looked at the morphology of MT1-MMP–positive endosomes in MDA-MB-231 cells silenced for WASH or Exo84 with two independent siRNAs (Fig. S2, A and B). As previously reported (Steffen et al., 2008), MT1-MMP accumulated in large vacuolar compartments in the central region of the cell as well as in smaller vesicles spread throughout the cytoplasm (Fig. 2 A, class #1). Silencing of WASH resulted in drastic changes in the morphology of the MT1-MMP–containing endosomes: in ~60% of cells they aggregated in the center (Fig. 2, A and B, class #2) and in ~15% of them large clumps of MT1-MMP–positive structures appeared (Fig. 2, A and B, class #3). We observed a similar, albeit less marked, phenomenon in cells silenced for Exo84 (Fig. 2, A and B). Live-cell imaging revealed perinuclear aggregated MT1-MMP–positive endosomes in WASH-depleted cells, some with exaggerated tubular membrane extensions (Fig. 2 C and Video 2). This phenotype is reminiscent of endosome tubulation induced upon depletion of WASH seen in other cell types (Derivery et al., 2009; Gomez and Billadeau, 2009; Gomez et al., 2012). Given the proposed function of WASH-dependent actin/cortactin assembly in regulation of endosomal tubule dynamics, we explored the contribution of WASH and exocyst complex to the formation of Arp2/3–F-actin–cortactin punctate domains on MT1-MMP–positive late endosomes.

Downloaded from jcb.rupress.org on January 21, 2014

Published December 16, 2013

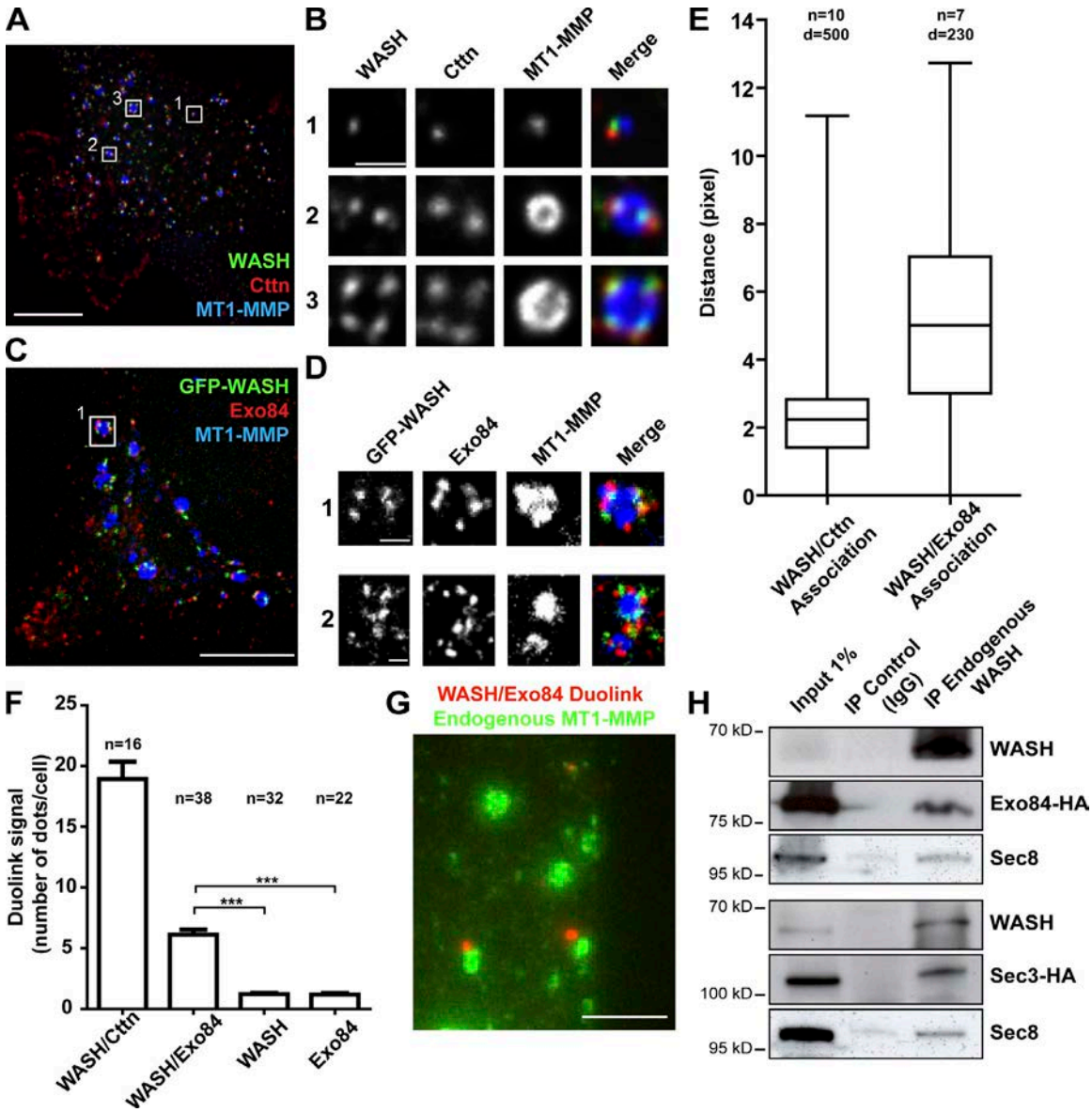

Figure 1. **WASH and exocyst complex associate on adjacent subdomains on MT1-MMP–positive endosomes.** (A) Association of endogenous WASH and cortactin (Cttn) on microdomains on MT1-MMPmCh–positive late endosomes. (B) Zoom of boxed regions in A. Images represent the middle plane of the cells. (C) MDA-MB-231 cells transfected with GFP-WASH were plated on cross-linked gelatin, stained for Exo84 and MT1-MMP, and imaged by 3D deconvolution microscopy. (D) Zoom of boxed region in C (box 1) and from another cell (box 2). Bars: (A and C) 5 µm; (B and D) 1 µm. (E) Box plots of the distance between adjacent puncta of WASH and cortactin or Exo84 on MT1-MMP–positive endosomes (in pixels). Whiskers show 25–75%. Numbers of cells (*n*) and of WASH-cortactin and WASH-Exo84 doublets (d) analyzed from independent experiments are indicated. (F) Quantification of Duolink dots using different antibody pairs as indicated (mean Duolink dots per cell ± SEM; *n* represents the number of cells analyzed for each condition). ***, $P < 0.001$ as compared with WASH-Exo84 combination. (G) Immunolabeling of MT1-MMP (green) was performed after the Duolink reaction between WASH and Exo84 antibodies (red dots). Bar, 5 µm. (H) Coimmunoprecipitation of exocyst subunits with WASH in HeLa cell lysates. Bound proteins were analyzed by immunoblotting with antibodies against WASH, HA-tag, and Sec8. Input lysates (1%) were loaded as control.

Silencing of WASH led to a large reduction of cortactin accumulation on endosomal compartments (Fig. 2, D and E). In contrast, silencing of N-WASP that is required for invadopodial actin assembly (Yamaguchi et al., 2005; Oser et al., 2009, 2010; Yu et al., 2012) had no effect on endosomal cortactin (and WASH)-positive microdomains (Fig. S3 C and Fig. 2, D and E). Interestingly, silencing of Exo84 was accompanied by a limited but significant increase of the size of WASH patches on MT1-MMP–positive endosomes and a marked lengthening of comet-shaped cortactin domains associated with WASH patches (Fig. 2, F and G). Similar observations were obtained upon depletion of Sec8 exocyst subunit (unpublished data). Together, these data indicate that WASH controls actin polymerization on MT1-MMP–positive endosomes and suggest that the exocyst complex associated with WASH may finely tune actin assembly required for regulation of endosomal membrane scission and remodeling (Derivery et al., 2009; Gomez and Billadeau, 2009; Park et al., 2013).

Downloaded from jcb.rupress.org on January 21, 2014

Published December 16, 2013

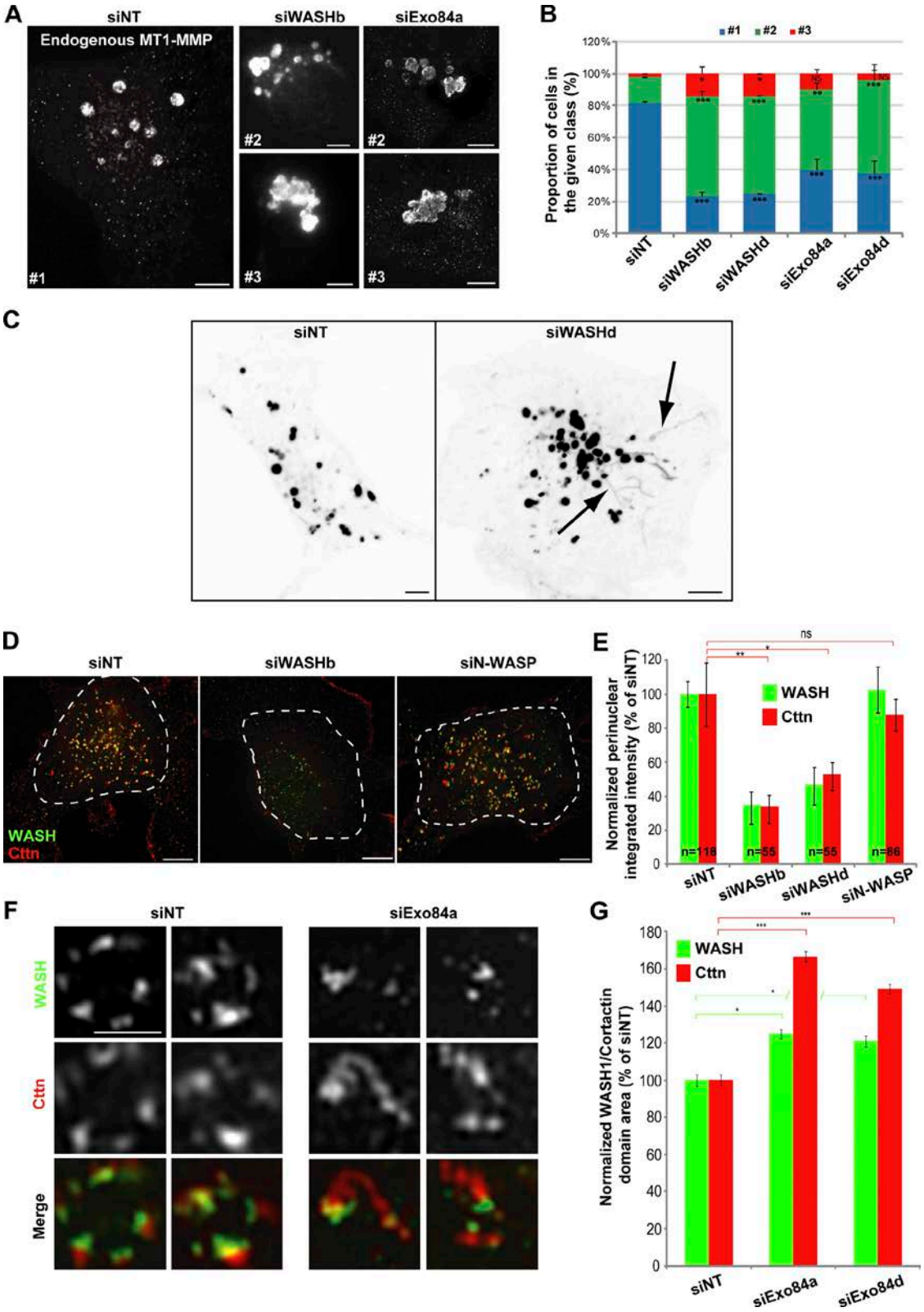

Figure 2. **Regulation of MT1-MMP–positive endosome dynamics by WASH and exocyst complex.** (A and B) MDA-MB-231 cells treated with the indicated siRNAs were plated on cross-linked gelatin and stained for endogenous MT1-MMP. Bars, 5 µm. Cells were scored according to the distribution of MT1-MMP–positive endosomes, i.e., normal distribution (#1, blue boxes in B), clustered endosomes (#2, green box), and aggregated endosomes (#3, red box). Values ploted in B are mean ± SEM of normalized endosome distribution from three independent experiments scoring ~100 cells for each siRNA. *, $P < 0.05$; **, $P < 0.01$; ***, $P < 0.001$ compared with siNT-treated cells (B). (C) MDA-MB-231 cells expressing MT1-MMP-mCh were treated as in A and time series were acquired by spinning-disk microscopy (see Video 2). Still images from the time series are shown. Arrows point to tubular extensions emanating from MT1-MMP–positive endosomes in cells depleted of WASH. Bars, 5 µm. (D) MDA-MB-231 cells treated with the indicated siRNA were processed for immunofluorescence microscopy with antibodies against cortactin (red) and WASH (green). Images were acquired by 3D deconvolution microscopy of the

Downloaded from jcb.rupress.org on January 21, 2014

Published December 16, 2013

WASH is present at docking sites of MT1-MMP–positive endosomes corresponding to invadopodia

Given that MT1-MMP is the key component for pericellular matrix degradation by invadopodia and that the exocyst complex is involved in MT1-MMP delivery to these structures (Sakurai-Yageta et al., 2008; Liu et al., 2009), we investigated whether WASH was also associated with invadopodia. Immunofluorescence microscopy of MDA-MB-231 cells plated on fluorescent gelatin revealed MT1-MMP–positive endosomes flanked by WASH-positive puncta in contact with the plasma membrane, some of which were associated with matrix degradation (Fig. 3, A–C). Observation by total interference reflection fluorescence microscope (TIRFM) of cells plated on a thin layer of cross-linked gelatin coexpressing MT1-MMPmCherry and GFP-tagged WASH or Exo84 showed that puncta of WASH and Exo84 associated with MT1-MMP–positive endosomes were in close contact with the adherent plasma membrane (Fig. 3, D and E). Similarly, WASH-positive puncta associated with MT1-MMP–containing endosomes were visible at the plasma membrane in BT-549 cells by TIRFM (Fig. 3 F). We also observed MT1-MMP–positive endosomes flanked by plasma membrane–apposed puncta containing Arp2/3, FAM21, cortactin, and Exo84 (Fig. 3, G and H; and Fig. S3, A and B). Matrix degradation was strictly confined to and superimposed upon WASH–FAM21–cortactin–Arp2/3–exocyst puncta adjacent to MT1-MMP–containing endosomes (Fig. 3, A, G, and H, arrowheads; and Fig. S3, A and B, arrowheads), strongly suggesting that these structures represent bona fide invadopodia. TIRFM of GFP-cortactin and MT1-MMPmCh documented repeated docking of MT1-MMP–containing endosomes at the level of cortactin-positive invadopodia (Fig. 3, I and J; and Video 3). Interestingly, although all invadopodia were positive for N-WASP, association of WASH with cortactin-positive invadopodia was inversely correlated with the surface of matrix degradation underlying each invadopodium (Fig. 3 K and Fig. S3 C). These results suggest that WASH, associated with MT1-MMP–positive endosomes, interacts transiently with invadopodia and preferentially at an early stage of their lifetime (associated with smaller degradation area) in contrast to N-WASP that is permanently associated with invadopodia.

Invadopodia correspond to late endosome-to-plasma membrane connections

Based on the proposed role of WASH-mediated Arp2/3 activation in the formation of endosomal tubular membrane extensions (Puthenveedu et al., 2010; Gomez et al., 2012; Piotrowski et al., 2013), we hypothesized that WASH puncta, possibly in conjunction with the exocyst complex, may regulate the formation of transient continuities between late endosomes and the invadopodial plasma membrane to allow the delivery of MT1-MMP for matrix degradation. We added a tracer to the extracellular milieu to test whether the endosome lumen was accessible through such connections. MDA-MB-231 cells expressing MT1-MMPmCh were plated on fluorescent gelatin and FITC-dextran was added for a 1-min pulse; then cells were examined immediately after washing out the tracer. A subset of MT1-MMP–positive endosomes were loaded with FITC-dextran during the pulse (Fig. 4 A, arrowheads), some exocytosed their MT1-MMP content while filling up with the dextran (Fig. 4 A, doublehead arrow). Cortactin-rich puncta and foci of matrix degradation were seen adjacent to FITC-dextran pulse-labeled endosomes (Fig. 4, B and C, arrowheads). In addition, after a 1-min pulse, fluorescent dextran–labeled endosomes were positive for Rab7 and VAMP7, arguing that these represent late endosomes making direct connection with the plasma membrane (Fig. 4, D and E). Furthermore, by live-cell TIRFM we observed regurgitation of the luminal FITC-dextran content of endosomes, some occurring through visible thin tubules extending from the endosome (Fig. 4 F). MT1-MMP–containing tubule emanating from plasma membrane–docked endosome was also visible by TIRFM (Fig. 4 G). These observations suggest the existence of tubular connections between MT1-MMP–positive late endosomes and the invadopodial plasma membrane that may mediate MT1-MMP delivery to the surface.

MT1-MMP exocytosis requires WASH and the exocyst complex

We used TIRFM to analyze the effect of silencing of WASH or Exo84 on the density of MT1-MMPmCh–positive endosomes in the zone beneath the plasma membrane. Large numbers of MT1-MMP vesicles were visible at the adherent plasma membrane of MDA-MB-231 cells (Fig. 5 A). Silencing of WASH or Exo84 significantly reduced MT1-MMP–positive endosome density beneath the plasma membrane (Fig. 5, A and B), along with the observed collapse of MT1-MMP–positive endosomes in the cell center (Fig. 2, A and C). All together, these findings indicate that both WASH and the exocyst complex play an important role in polarization and tethering of MT1-MMP–positive endosomes at the plasma membrane. The contribution of WASH and Exo84 to the delivery of MT1-MMP to the invadopodial plasma membrane was assessed by quantifying the surface accumulation of MT1-MMPpHluorin (Lizárraga et al., 2009); fluorescence of this construct is eclipsed in the acidic environment of the late endosome and rises upon exocytosis and exposure to the extracellular pH (Miesenböck, 2012). MT1-MMPpHluorin accumulated at the level of cortactin-positive invadopodia on the ventral cell surface (Fig. 5, C and D). Knockdown of WASH or Exo84 led to a 50% reduction of surface

middle plane of the cells. A region of interest (dashed line) was drawn manually around WASH-cortactin structures for quantification (shown in E). Bars, 5 µm. (E) Quantification of the integrated intensity of perinuclear endosomal cortactin and WASH in cells treated as in D and normalized to the integrated intensity in control cells in two independent experiments. ns, not significant; *, $P < 0.05$; **, $P < 0.01$ compared with control. (F) MDA-MB-231 cells treated with the indicated siRNAs were processed for immunofluorescence microscopy with cortactin and WASH antibodies and analyzed by high-resolution (~100-nm spatial resolution) 3D SIM. Bar, 1 µm. (G) Quantification of the projected surface of WASH and cortactin puncta in cells as described in F, normalized to mean projected surface of the puncta in control cells set to 100 (three independent experiments; $n = 25$ puncta for each condition; *, $P < 0.05$; ***, $P < 0.001$ compared with control).

Downloaded from jcb.rupress.org on January 21, 2014

Published December 16, 2013

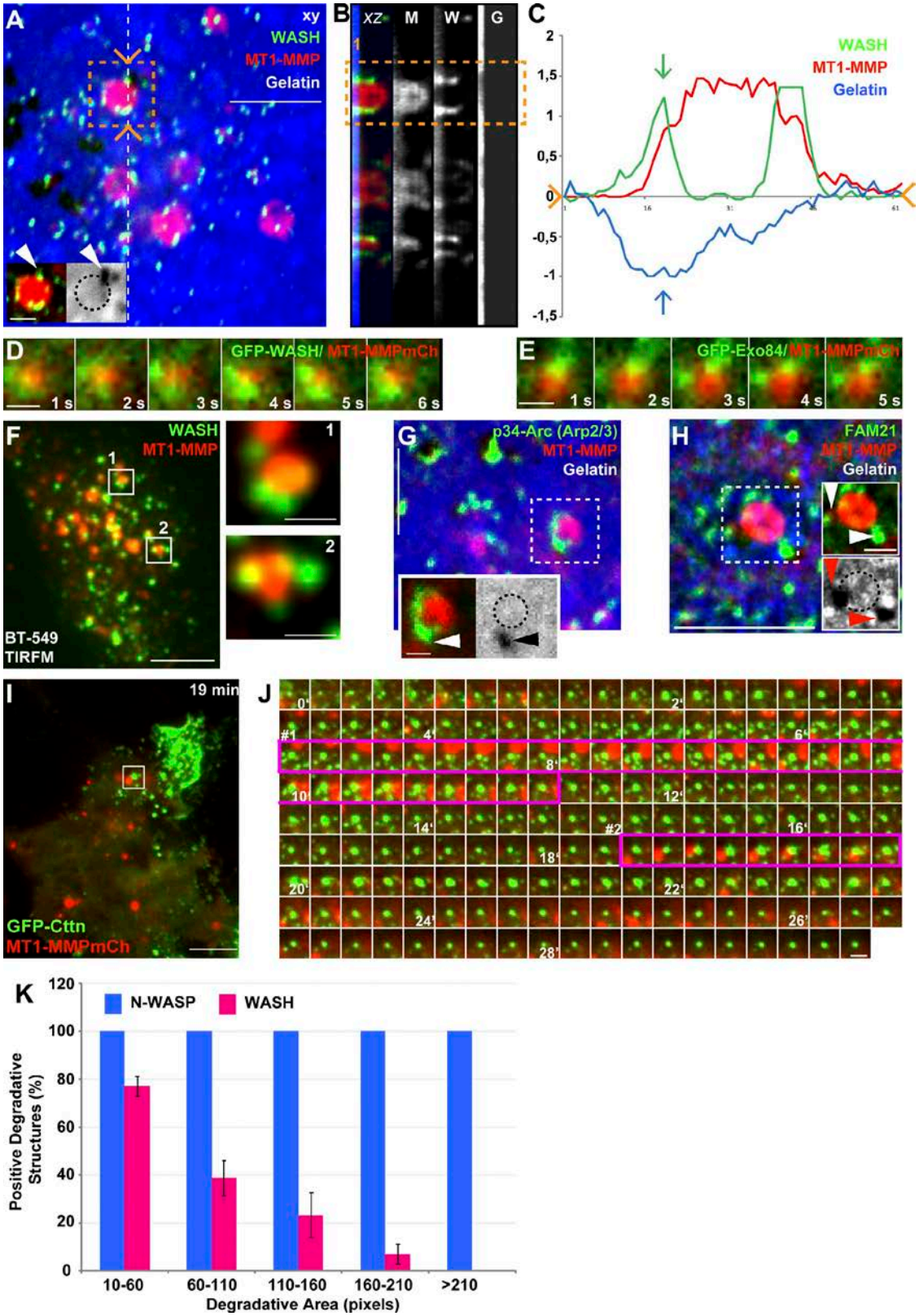

Figure 3. **Association of WASH endosomal puncta with invadopodia.** (A) MDA-MB-231 cells plated on cross-linked FITC-labeled gelatin (blue) were stained with antibodies against MT1-MMP (red) and WASH (green) and imaged by 3D deconvolution microscopy. Image is a single section in the ventral plane of the cell in contact with gelatin. Insets corresponding to the boxed region show split channels with dashed line representing the contour of the MT1-MMP–containing endosome projected on the FITC-gelatin image. Arrowhead points to matrix degradation restricted to WASH puncta adjacent to MT1-MMP–positive endosome. Bars: (main) 5 µm; (inset) 1 µm. (B) Orthogonal section through the dashed line in A. From left to right: merged image, MT1-MMP (M), WASH (W), and FITC-gelatin (G) signals. (C) Fluorescence intensity profile through the dashed line in the boxed region in A (x-axis, in pixels; y-axis, in arbitrary units). (D and E) MDA-MB-231 cells expressing MT1-MMPmCh and GFP-WASH (D) or GFP-Exo84 (E) plated on cross-linked gelatin and

Downloaded from jcb.rupress.org on January 21, 2014

Published December 16, 2013

accumulations of MT1-MMPpHluorin (Fig. 5 E), indicating that WASH and exocyst complex are critical for MT1-MMP exocytosis at invadopodia.

WASH and exocyst complex are required for invasive migration through type I collagen

Silencing of MT1-MMP is known to reduce drastically the ability of MDA-MB-231 cells to degrade a matrix of cross-linked gelatin as a basement membrane mimick (Artym et al., 2006; Sakurai-Yageta et al., 2008; Fig. 6 A). Silencing of WASH diminished the proportion of cells that were able to degrade gelatin and led to a 60–80% reduction in these cells' capacity to do so, similar to the effect of silencing various subunits of the exocyst complex, e.g., Sec6, Sec8, and Sec10 (Sakurai-Yageta et al., 2008) and Exo84 (Fig. 6 A). MT1-MMP levels were unaffected by the various siRNA treatments (Fig. S2 E). By comparison, silencing of N-WASP also led to 60% inhibition of matrix degradation, similar to the effect seen on WASH depletion (Fig. 6 A). Thus, both plasma membrane- and endosome-associated actin nucleation-promoting factors, N-WASP and WASH, are required for invadopodia activity in breast tumor cells. In addition, depletion of WASH or Exo84 led to a significant reduction in the ability of MDA-MB-231 cells to invade through a layer of Matrigel, similar to MT1-MMP knockdown (Fig. 6 B).

Degradation of cross-linked gelatin and Matrigel is representative of carcinoma cells remodeling and breaching the basement membrane. MT1-MMP is also required for dissemination of cancer cells within fibrous type I collagen (Fig. 6 C; Sabeh et al., 2004, 2009; Wolf et al., 2007), thus the question arose whether or not the WASH- and exocyst-dependent mechanism of exocytosis of MT1-MMP–containing late endosomes also operated during remodeling of collagen fibers and invasive migration by tumor cells. We analyzed the capacity of MDA-MB-231 cells to invade the collagen I–filled, cell-free central portion of a 96-well plate over a 2-d culture period. Knockdown of WASH or Exo84 resulted in a strong inhibition of the invasion capacity of the cells in type I collagen similar to the silencing of MT1-MMP (Fig. 6, C and D). In addition, we found that silencing of WASH or Exo84 resulted in a 75–85% inhibition of pericellular collagen I degradation revealed by the Col1-$^{3/4}$C antibody recognizing the cleaved fragment of collagen I dependent on MT1-MMP activity as indicated by the reduction of Col1-$^{3/4}$C signal on MT1-MMP depletion (Fig. 6, E and F; Wolf et al., 2007). Thus these data indicate a general requirement for the exocyst complex and WASH for matrix remodeling and for the invasive potential of breast tumor cells.

Exocytosis of MT1-MMP occurs at contact sites with type I collagen fibers through a WASH- and exocyst-dependent mechanism

We analyzed the organization and dynamics of invadopodia in cells invading through 3D type I collagen environments in relation with WASH- and exocyst-positive MT1-MMP–containing endosomes. Staining of the cells for F-actin and cleaved collagen I fibers (Col1-$^{3/4}$C antibody) revealed the formation of linear accumulations of F-actin on the inner face of the plasma membrane associated with collagen fibers, coincident with regions of collagenolytic activity (Fig. 7 A). These structures have been previously reported and named linear invadopodia (Juin et al., 2012). Similarly to classical dotty-like invadopodia on gelatin (Fig. S3 C), N-WASP colocalized with F-actin in linear invadopodia (Fig. 7 B). Labeling with anti-WASH antibodies showed the typical pattern of endosomal WASH-positive puncta (Fig. 7 C), some of which were closely apposed to linear invadopodia stained for cortactin although WASH did not accumulate in linear invadopodia (Fig. 7, C [inset], D, and E). We used live-cell imaging to analyze the dynamic interactions of WASH- and cortactin-positive puncta with linear invadopodia in cells in a 3D fibrillar collagen environment. Live-cell imaging of MDA-MB-231 cells expressing DsRed-cortactin and GFP-WASH (Video 4 and Fig. 7, D and E) plated on a layer of fluorescent collagen I fibers revealed the dynamic assembly of cortactin-positive linear invadopodia along collagen fibers and their disassembly upon remodeling and relaxation of the underlying fibers (Video 4 and Fig. 7 E). In addition, cortactin- and WASH-positive endosomal puncta interacted highly dynamically with linear invadopodia (Video 4 and Fig. 7, D and E). On examination of the time-lapse sequences there was no obvious transfer of cortactin from endosomal puncta to the linear invadopodia (Fig. 7 E). Analysis of MT1-MMP distribution in fixed cells showed that cortactin puncta were associated with MT1-MMP–positive endosomes (Fig. 7, F and G, arrows) in the vicinity of linear invadopodia positive for cortactin and MT1-MMP (Fig. 7, G and H, arrowheads), in agreement with the collagenolytic activity of these structures. All together, these data suggested that collagen I fibers elicit actin assembly and the formation of N-WASP–positive collagenolytic linear invadopodia and the dynamic recruitment of WASH-cortactin–positive endosomes probably involved in MT1-MMP delivery to these structures.

Exocytic events of MT1-MMP were monitored in live cells cultured on fibrillar collagen using the MT1-MMPpHluorin construct. In cells expressing simultaneously mCherry- and pHluorin-tagged MT1-MMP, dynamic late endosomes (red) were observed in the cytoplasm, with visible green flashes corresponding

analyzed by live-cell dual color TIRFM. Time interval between each image is 1 s. Bars, 1 µm. (F) BT-549 cells plated on cross-linked gelatin were fixed and immunostained for MT1-MMP and WASH and analyzed by TIRFM. Insets are higher magnification views of the boxed regions. (G and H) Cells treated as in A, stained with antibodies against MT1-MMP (red) and p34-Arc subunit of Arp2/3 complex (G, green) or FAM21 (H, green). Arrowheads point to the accumulation of the markers near degradative invadopodia adjacent to MT1-MMP–positive endosomes. Bars: (main) 5 µm; (inset) 1 µm. (I) MDA-MB-231 cells expressing GFP-cortactin and MT1-MMP-mCh plated on cross-linked gelatin and analyzed by dual color TIRFM. A still image from a representative time-lapse series is shown. (J) A series of time-lapse TIRFM images corresponding to the boxed region in panel I. Numbers in the series of time-lapse images represent the time in minutes. Two events of docking of MT1-MMP–containing endosomes (labeled #1 and #2) are boxed in pink. (K) Cells as in A were stained for cortactin and WASH or N-WASP. The graph shows the percentage of WASH- (pink bars) or N-WASP–positive (blue bars) degradative invadopodia positive for cortactin (not depicted) as a function of the surface of matrix degradation (in pixels). Values are means ± SEM scoring 360 invadopodia from 15 WASH-labeled cells and 135 invadopodia from five N-WASP–labeled cells.

Downloaded from jcb.rupress.org on January 21, 2014

Published December 16, 2013

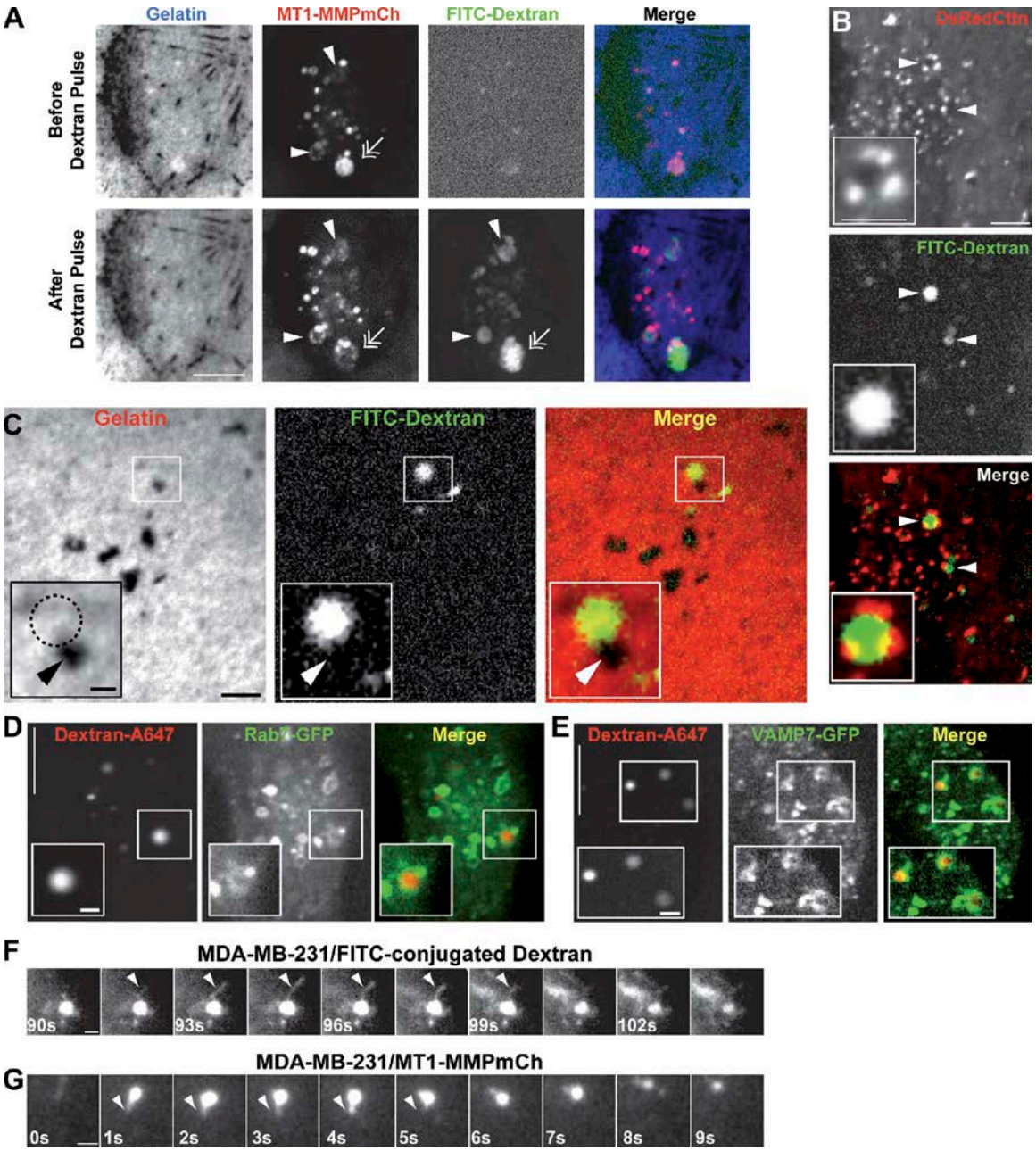

Figure 4. **Tubular connection between MT1-MMP–containing late endosomes and the invadopodial plasma membrane.** (A) MDA-MB-231 cells expressing MT1-MMPmCh were plated on cross-linked gelatin. One optical section was taken in the ventral plane of the cells by confocal spinning disk microscopy (top). A second optical section was taken after a 1-min pulse of FITC-dextran added to the medium (bottom). Arrowheads point to MT1-MMP–positive endosomes filled with FITC-dextran during the pulse. The double-headed arrow points to an endosome that lost its MT1-MMP content and filled up with FITC-dextran. Bar, 5 µm. (B) MDA-MB-231 cells expressing DsRed-cortactin treated as in A and imaged immediately after the FITC-dextran pulse. Arrowheads point to cortactin-positive puncta adjacent to dextran-labeled endosomes. Bars, 5 µm. (C) MDA-MB-231 cells expressing MT1-MMPmCh (not depicted) were plated on cross-linked fluorescent gelatin, pulsed with FITC-dextran, and analyzed by confocal spinning disk microscopy 1–2 min after the pulse. Arrowheads point to focal degradation of the matrix adjacent to a FITC-labeled endosome. Dashed line represents the contour of the FITC-dextran–containing endosome projected on the gelatin image. (D and E) MDA-MB-231 cells expressing Rab7-GFP (D) or VAMP7-GFP (E) were plated on cross-linked gelatin for 5 h. An optical section was taken immediately after a 1-min pulse of A647-dextran added to the medium. Insets are higher magnification views of the boxed regions that point to Rab7- (D) or VAMP7 (E)-positive endosomes filled with A647-dextran during the pulse. Bars: (main) 5 µm; (insets) 1 µm). (F) Live-cell imaging of MDA-MB-231 cells analyzed by TIRFM immediately after the FITC-dextran pulse. The indicated times in the image gallery are seconds after the pulse. Arrowhead points to a tubular extension emanating from the FITC-dextran–labeled endosome during regurgitation of the fluid-phase tracer. Bar, 2 µm. (G) MDA-MB-231 cells expressing MT1-MMPmCh analyzed by TIRFM. The arrowhead points to an MT1-MMP–positive tubule. Bar, 1 µm.

to the de-quenching of pHluorin fluorescence upon exocytosis (Video 5 and Fig. S4). Endosomes scanning portions of the plasma membrane in contact with collagen I fibers were visible (Video 5 and Fig. S4, A and B, $t = 0$ min), which underwent repeated exocytosis in the vicinity of the collagen fibers (Fig. S4, A and B, arrowheads). Live-cell imaging of cells expressing MT1-MMPpHluorin and mCherry-WASH showed that MT1-MMP–containing endosomes undergoing exocytosis were

Downloaded from jcb.rupress.org on January 21, 2014

Published December 16, 2013

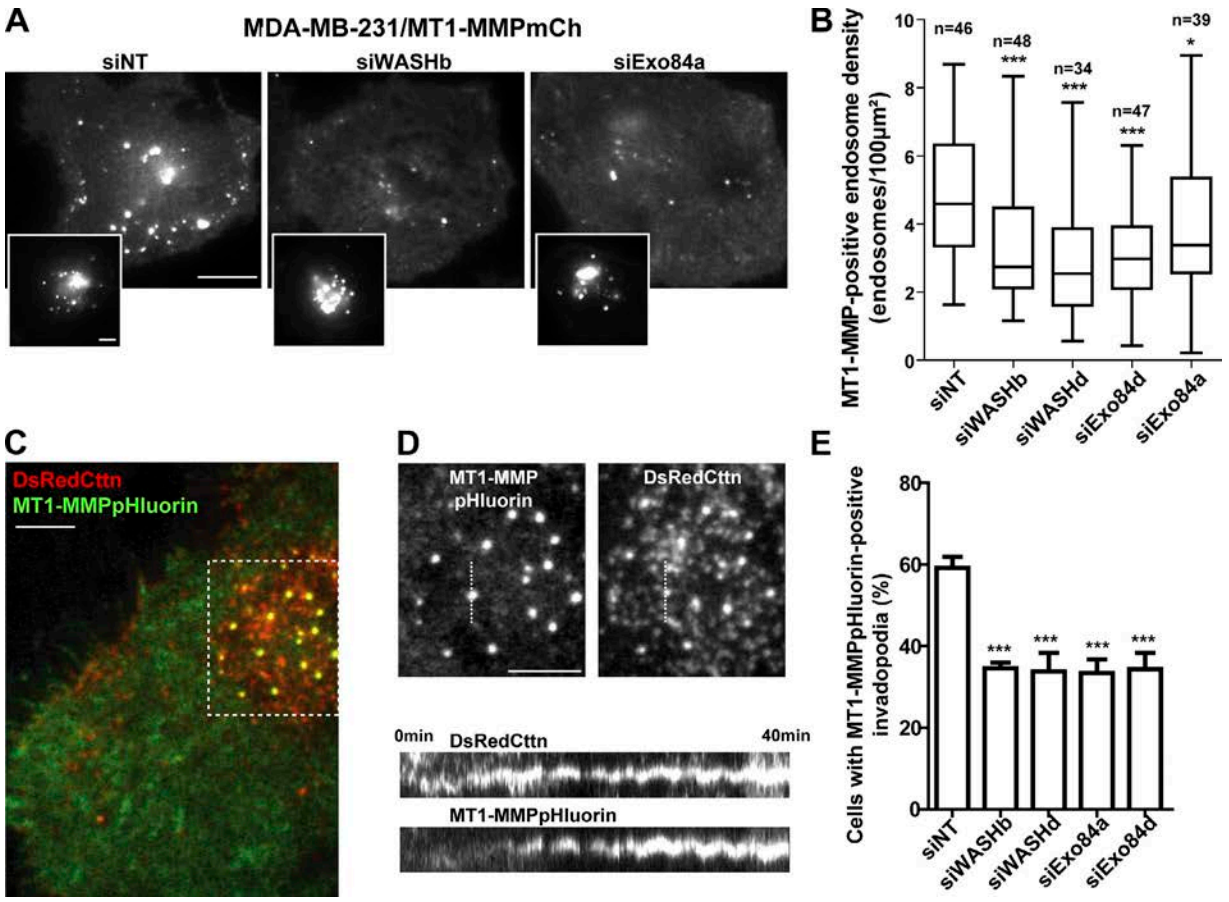

Figure 5. **WASH and exocyst complex are required for invadopodial degradation of the matrix.** (A) Effect of WASH or Exo84 silencing on the density of MT1-MMPmCh–positive vesicles in the subplasma membrane region of MDA-MB-231 cells observed by TIRFM. Insets are the corresponding wide-field images showing similar MT1-MMP expression. Bars, 5 µm. (B) Box plots showing the density of subplasma membrane MT1-MMP vesicles. Number of cells analyzed from four experiments is indicated (*n*). *, $P < 0.05$; ***, $P < 0.001$ (compared with control cells treated with siNT). (C) MDA-MB-231 cells expressing MT1-MMPpHluorin and DsRed-cortactin were plated on cross-linked gelatin for 2–3 h and analyzed by dual color TIRFM. A merged image from a representative time-lapse series is shown. (D, top) Split signals from the boxed region in C showing accumulations of MT1-MMPpHluorin at cortactin-positive invadopodia. Bar, 5 µm. (bottom) Kymograph views of TIRF time series acquired every 10 s. (E) MDA-MB-231 cells expressing MT1-MMPpHluorin were treated with the indicated siRNAs, plated on cross-linked gelatin, and analyzed by TIRFM. Plots show the percentage of cells with MT1-MMPpHluorin–positive invadopodia. Values are means ± SEM from three independent experiments scoring a total of 150–200 cells for each cell population. ***, $P < 0.001$ (compared with cells treated with non-targeting siRNA).

flanked by WASH puncta (Video 6 and Fig. 8, A and B, red arrowheads) and exocytosis preferentially occurred at contact sites with fibers (Video 6 and Fig. 8, A and B, green arrowheads). Multiple exocytic events led to surface accumulation of MT1-MMP along the collagen fibers (at linear invadopodia; Fig. 8 A, white arrowheads) and fiber remodeling (Video 6). Quantitative assessment of MT1-MMPpHluorin flashes revealed a strong inhibition of MT1-MMP exocytic events upon knockdown of WASH or Exo84 (Fig. 8 C), whereas overall MT1-MMP expression was similar in the different cell populations (not depicted).

So far, our observations were compatible with a WASH/Exocyst-dependent mechanism whereby MT1-MMP–positive endosomes exocytose the protease at contact sites with collagen fibers but do not collapse within the plasma membrane bilayer. They also revealed that MT1-MMPpHLuorin flashes lasted for several minutes (Fig. 8 D). In addition, we noticed that although some endosomes with de-quenched MT1-MMPpHluorin were moving along fibers and could possibly detached and reengage with other sites for multiple rounds of MT1-MMP exocytosis, some remained at the same position for several minutes (Videos 5 and 6; Fig. S4; and Fig. 8, A and B). These findings raised the issue of the duration of endosome-to-plasma membrane openings. Using an extracellular pH shifts protocol (Video 7; Perrais et al., 2004), we observed that some endosomes remained opened for several minutes as shown by the fluorescence of pHluorin in the endosomal lumen that was sensitive to the iterative shifts of extracellular pH (at least for 4 min in the example shown in Fig. 8 E and up to 15 min [not depicted]). Of note, similar long-lasting fusion pore openings have been reported during zymogen granule exocytosis in exocrine pancreatic acinar cells (up to 15 min; Perrais et al., 2004; Thorn et al., 2004; Sokac and Bement, 2006). Moreover, the exchange of low and high pH solution within the endosome could take up to 30 s, consistent with the restricted diffusion of solutions through a long tubular connection. Thus, through the functions of WASH and exocyst complex, tumor cells can engage late endocytic MT1-MMP storage compartment in the formation of tubular continuities with the

Downloaded from jcb.rupress.org on January 21, 2014

Published December 16, 2013

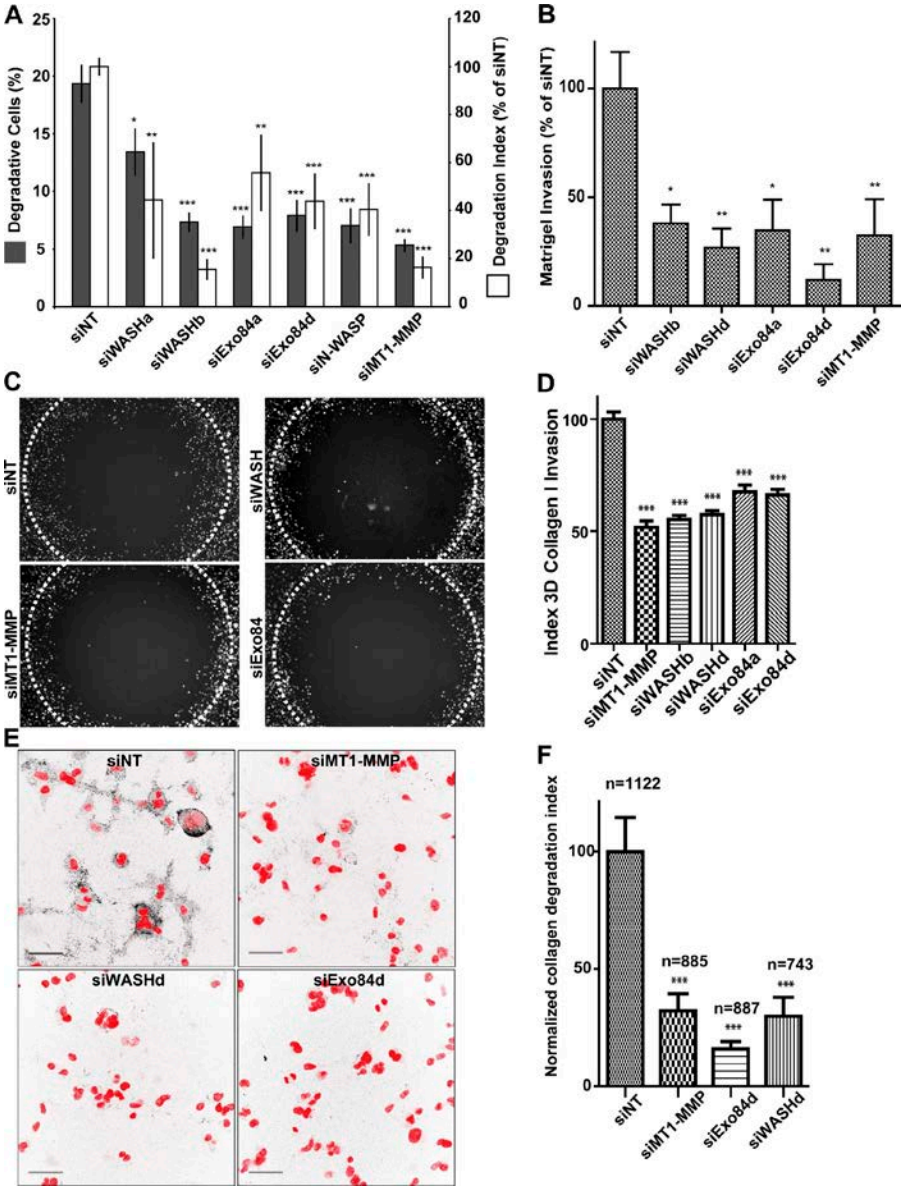

Figure 6. **WASH and exocyst complex are required for matrix remodeling and the invasive potential of breast tumor cells.** (A) MDA-MB-231 cells treated with indicated siRNAs were plated on cross-linked FITC-labeled gelatin and the percentage of degradative cells (gray bars) and the degradation index (white bars) were calculated. Values are means ± SEM from at least three independent experiments scoring a total of 300–400 cells for each siRNA. *, P < 0.05; **, P < 0.01; ***, P < 0.001 (compared with siNT-treated cells). (B) MDA-MB-231 cells treated with indicated siRNAs were quantified on the lower side of the Transwell filter after invasion through Matrigel. Values are mean ± SEM of normalized percentage from two to three independent experiments. *, P < 0.05; **, P < 0.01 (compared with siNT-treated cells). (C) 3D type I collagen circular invasion assay of MDA-MB-231 cells expressing Histone-2B-GFP treated with indicated siRNAs after 48 h. Dashed circles represent the collagen–cell interface at time 0. (D) Values represent mean invasion index ± SEM for the different cell populations from three independent experiments, normalized to cells treated with non-targeting siRNA (***, P < 0.001). (E) MDA-MB-231 cells treated with the indicated siRNAs were embedded in collagen I. Pericellular collagenolysis was detected using anti-Col1-$^{3/4}$C antibodies (in black in the inverted image). Nuclei were stained with DAPI (red). Bars, 50 µm. (F) Quantification of collagenolysis by MDA-MB-231 cells treated with the indicated siRNAs. Values are mean normalized degradation index ± SEM from three (siNT, siExo84d, and siMT1-MMP) or two independent experiments (siWASHd). *n* represents the number of cells analyzed for each cell population. ***, P < 0.001 (as compared with siNT-treated cells).

plasma membrane at contact sites with the extracellular matrix to allow delivery of the protease to the surface and to ensure matrix remodeling required for invasive migration.

Discussion

Our data, which are summarized in a model presented in Fig. 9, support a general mechanism of invadopodia formation whereby the functions of WASH and exocyst complex on closely apposed punctate domains on the cytosolic face of MT1-MMP–positive late endosomes ensure focal delivery of MT1-MMP for pericellular matrix degradation.

We found that loss of WASH function induces disappearance of endosomal F-actin puncta and a collapse of MT1-MMP–positive late endosomal system, which is accompanied by defects in MT1-MMP recycling and delivery to the invadopodial plasma membrane. This is in agreement with an established function of the WASH complex in the recycling route of various plasma membrane proteins in different cell types (Derivery et al., 2009; Gomez and Billadeau, 2009; Zech et al., 2011; Gomez et al., 2012; Piotrowski et al., 2013). In addition, the exocyst complex, which mediates the tethering of exocytic vesicles to the plasma membrane, is also required for the delivery of MT1-MMP to invadopodia (Sakurai-Yageta et al., 2008; Liu et al., 2009; this study). Strikingly, our study reveals that WASH- and F-actin–positive puncta on MT1-MMP endosomes are adjacent to exocyst-positive puncta on this compartment and some components of these two multiprotein complexes (WASH, Exo84, and Sec3 based on two-hybrid data) can interact with each others. The segregation of WASH domains on the cytolic face of the endosomal membrane depends on actin polymerization, which is induced by WASH-mediated activation of the Arp2/3 complex (Derivery et al., 2012). The mechanism underlying the subdomain organization of the exocyst complex at the surface of MT1-MMP–positive endosomes is presently unknown; however, we found that exocyst components can negatively regulate WASH-dependent endosomal actin

Downloaded from jcb.rupress.org on January 21, 2014

Published December 16, 2013

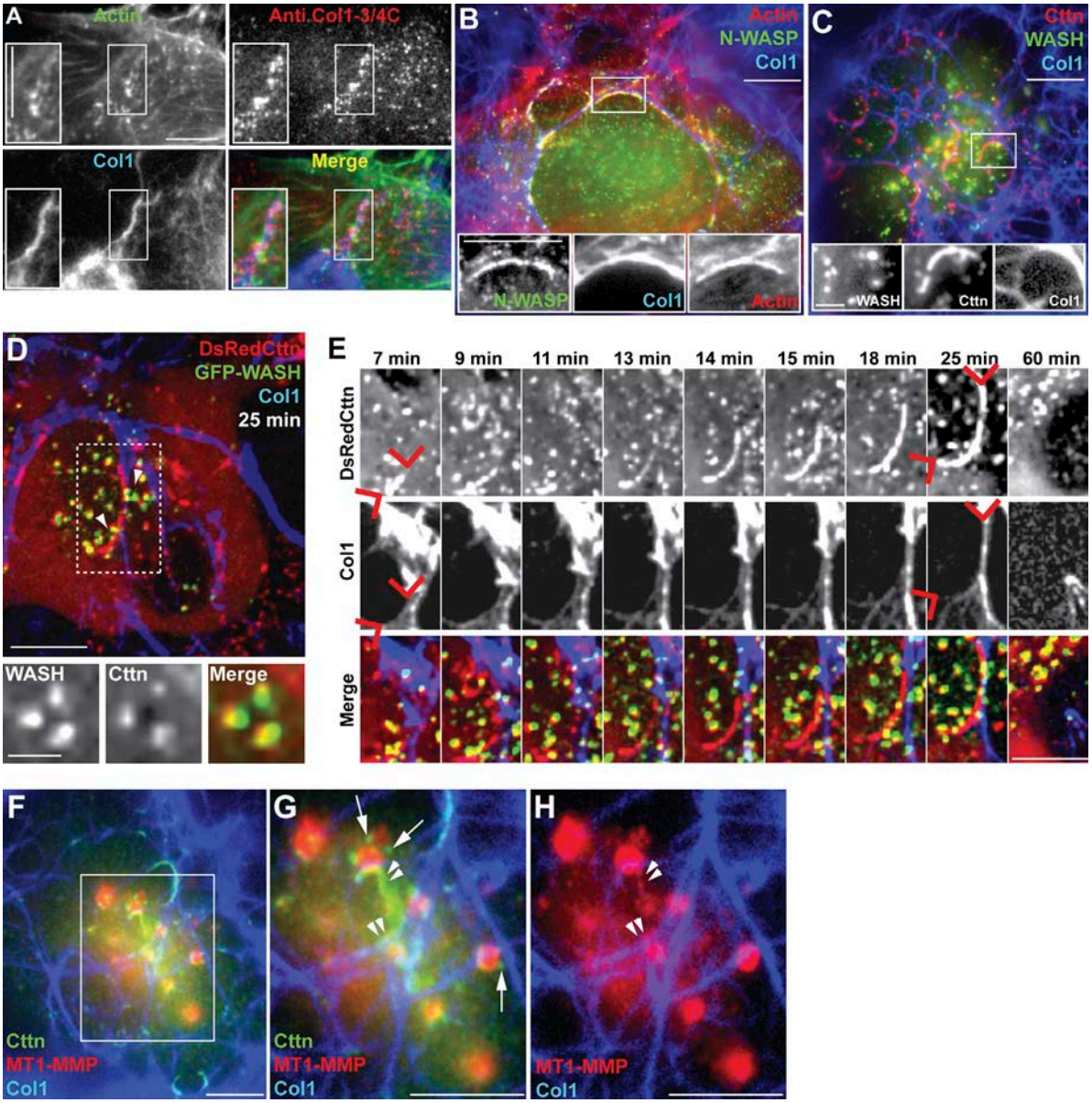

Figure 7. **WASH- and cortactin-positive MT1-MMP–containing endosomes are recruited in the periphery of linear invadopodia in association with collagen fibers.** (A) MDA-MB-231 cells on a layer of collagen I fibers stained with anti-Col1-$^{3/4}$C antibodies recognizing MMP-cleaved collagen I (red) and for F-actin (green) revealing collagenolytic linear invadopodia. Inset is a higher magnification of the boxed region. Bars, 5 µm. (B and C) Cells were plated on a layer of Alexa Fluor 647–conjugated type I collagen (blue) for 30 min and stained for N-WASP (green) and F-actin (red; B) or WASH (green) and cortactin (red; C). Insets are higher magnification of boxed regions. Bars: (main and B [inset]) 5 µm; (C, inset) 1 µm. (D) MDA-MB-231 cells expressing GFP-WASH (green) and DsRed-cortactin (red) were plated on a layer of Alexa Fluor 647–conjugated type I collagen (blue) for 30 min and imaged by confocal spinning disk microscopy. A still image from a representative time-lapse series is shown (t = 25 min). Arrowheads point to WASH- and cortactin-positive puncta (associated with late endosomes) apposed to a cortactin-positive linear invadopodium aligned on collagen fibers. Insets show a higher magnification of WASH and cortactin endosomal puncta. The corresponding time-lapse series is shown in Video 4. Bars: (main) 5 µm; (inset) 1 µm. (E) Higher magnification of the boxed region in D at representative time points. A linear cortactin-positive invadopodium aligned with collagen fibers forms on the inner face of the plasma membrane (13–14 min; red arrowheads); at 60 min, this structure disassembled while collagen I fibers were remodeled. Time is in minutes. Bar, 5 µm. (F–H) Cells on Alexa Fluor 647–conjugated type I collagen (blue) stained for MT1-MMP (red) and cortactin (green). G and H are higher magnification of the boxed region in F. Arrows point to cortactin-positive puncta associated with MT1-MMP–containing endosomes in the vicinity of cortactin- and MT1-MMP–positive linear invadopodia (arrowheads). Bars, 5 µm.

assembly. In this respect, two-hybrid data mapping of the binding site of Exo84 and Sec3 exocyst subunits to the amino-terminal region of WASH suggests a possible competition mechanism because this region of WASH is also required for association with other WASH complex components (Gomez and Billadeau, 2009; Jia et al., 2010). A consequence of exocyst's interaction with WASH could thus be a fine regulation of actin assembly required for late endosome organization and for MT1-MMP recycling to the surface. Therefore, in addition to its well-established function as a tethering factor for exocytic vesicles to the plasma membrane (Heider and Munson, 2012), our findings suggest an unprecedented role for the exocyst in regulating endosomal membrane dynamics.

Remarkably, we found that MT1-MMP–positive endosomes contact and establish connections with the plasma membrane in

Downloaded from jcb.rupress.org on January 21, 2014

Published December 16, 2013

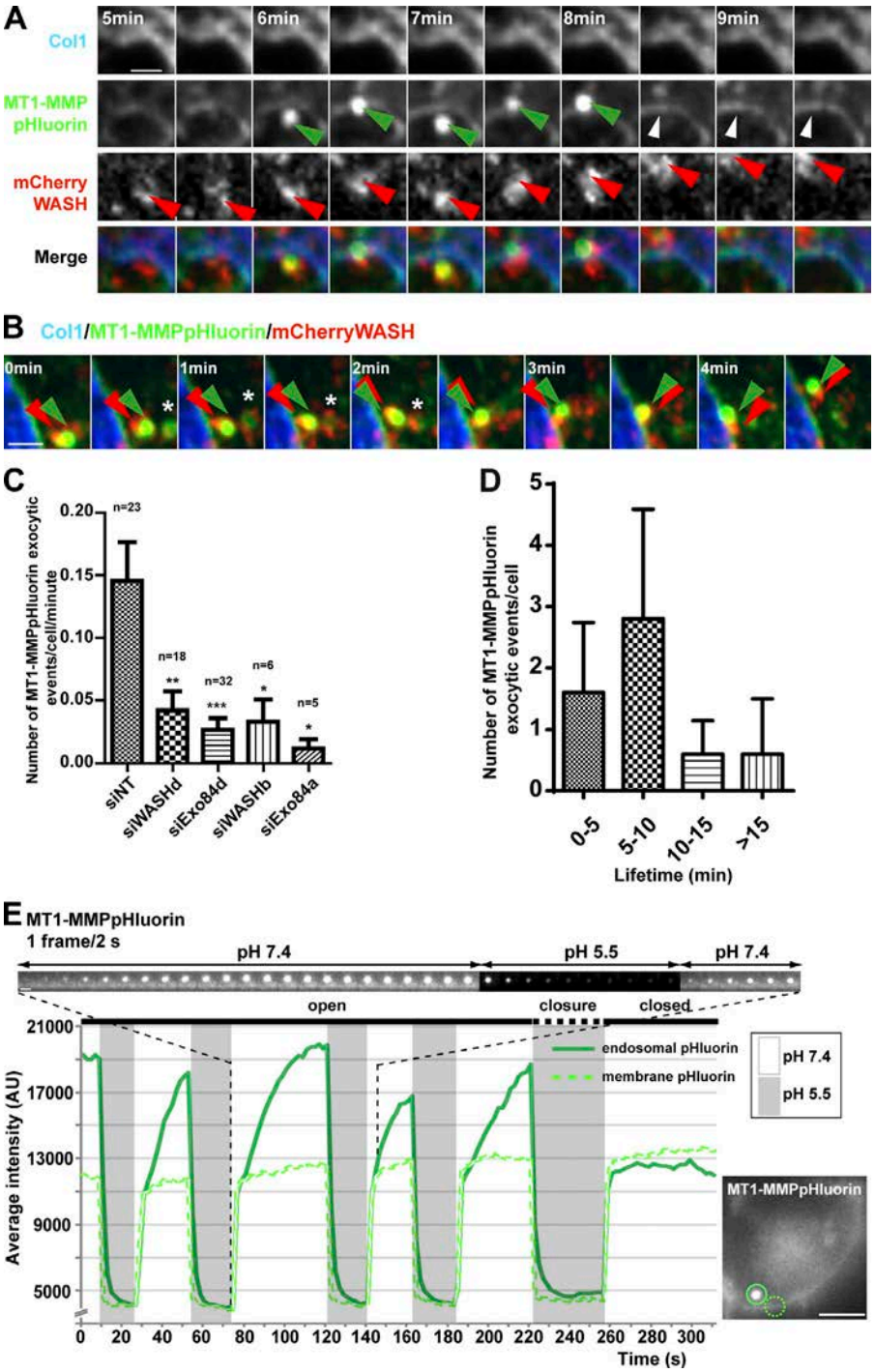

Figure 8. **A WASH- and Exo84-dependent exocytic mechanism of MT1-MMP involved in pericellular collagenolysis.** (A and B) Live-cell imaging of MDA-MB-231 cells expressing MT1-MMPpHluorin (green) and mCherry-WASH (red) constructs, plated on a layer of collagen I for 30 min (see Video 6). The galleries show exocytosis of MT1-MMPpHluorin–positive endosomes (green arrowheads) in the vicinity of a collagen type I fiber (blue). These endosomes harbor WASH-positive patches (red arrowheads). The asterisks in B point the reacidification of a WASH- and MT1-MMPpHluorin–positive endosome. Time is represented in minutes. Bars, 2 µm. (C) MDA-MB-231 cells expressing MT1-MMPmCherry and MT1-MMPpHluorin silenced for the indicated proteins were seeded on a layer of type I collagen fibers and imaged over a 30-min time perios and the frequency of MT1-MMPpHLuorin exocytic events was quantified (box plots of events/cell/min). The number of cells analyzed for each cell population is indicated. *, $P < 0.05$; **, $P < 0.01$; ***, $P < 0.001$ (compared with siNT-treated cells). (D) Lifetime of MT1-MMPpHluorin–positive flashes (in minutes). Data show the number of pHLuorin exocytic flashes per cell for the different lifetimes ± SEM from five cells out of three independent experiments. (E) MDA-MB-231 cells expressing MT1-MMPpHluorin were cultured on a layer of Cy3-labeled type I collagen fibers and subjected to external pH shifts alternating between 7.4 (white zones) and 5.5 (gray zones). The plots represent pHLuorin intensity of a MT1-MMP–positive endosome that underwent exocytosis (circled with a solid line in the inset on the right) and of a region of the plasma membrane (dashed line). The corresponding time-lapse series is shown in Video 7. The gallery above the plot represents a sequence starting with external pH 7.4 corresponding to the circled MT1-MMPpHLuorin–positive endosome (see inset). Bars: (inset) 5 µm; (gallery) 1 µm.

contact with the matrix (basement membrane or fibrous type I collagen) at the level of WASH–F-actin–cortactin– and exocyst-positive puncta. These connections, most likely tubular, that form between late endosomes and the plasma membrane allow exocytosis of MT1-MMP to the surface and they occur at and correspond to bona fide invadopodia. It is currently though that WASH-dependent actin assembly can generate the force to drive the formation of endosomal tubular extensions (Puthenveedu et al., 2010; Derivery et al., 2012; Gomez et al., 2012; Piotrowski et al., 2013). This, together with the capacity of the exocyst complex to mediate membrane tethering and modulate WASH-dependent actin assembly (He and Guo, 2009; Hertzog and Chavrier, 2011; this study), suggests a mechanism whereby WASH and exocyst may work in a coordinated manner to control the formation of endosome-to-plasma membrane connections ensuring MT1-MMP targetting to the invadopodial plasma membrane. In addition, the exocyst complex is known to control SNARE complex assembly and to influence vesicle fusion (Heider and Munson, 2012). Thus, the exocyst could regulate membrane fusion at invadopodial endosome-to-plasma membrane connections. Whether the exocyst can interact and influence the activity of the late endosome SNARE protein VAMP7, which is required for MT1-MMP

Downloaded from jcb.rupress.org on January 21, 2014

Published December 16, 2013

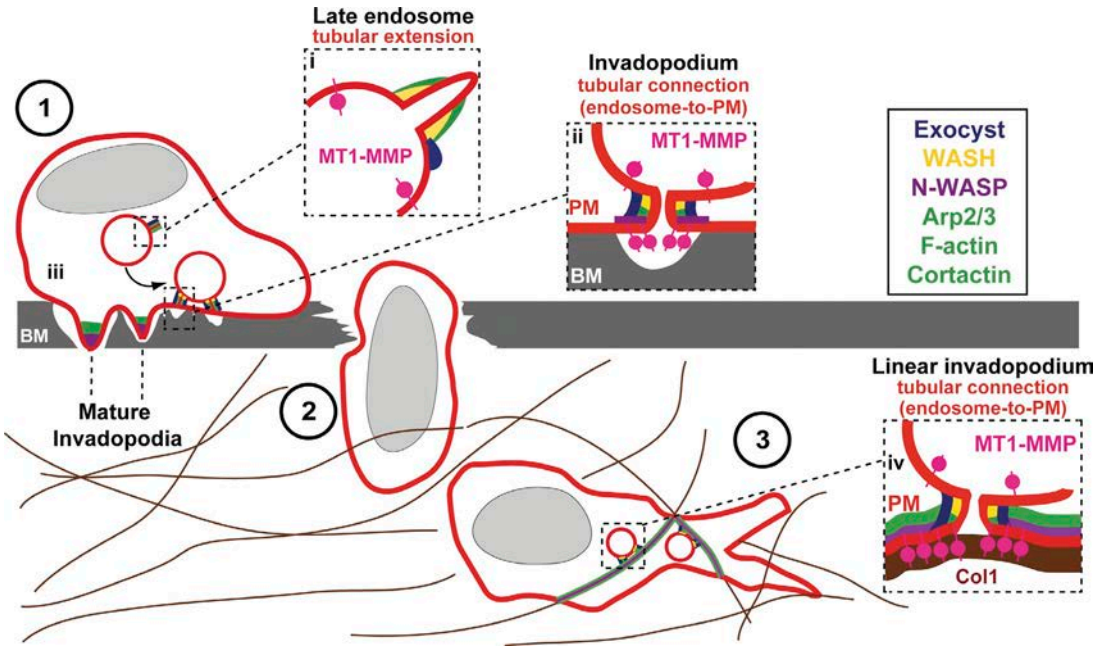

Figure 9. **Schematic model of the general mechanism of exocytosis of MT1-MMP–positive late endosomes at the invadopodial plasma membrane.** WASH-dependent Arp2/3 complex activation and actin/cortactin assembly controls the dynamics of tubular endosomal membrane extensions (inset i) and tubular endosome-to-plasma connections required for transfer and delivery of MT1-MMP from the endosome to the invadopodial plasma membrane (inset ii). The exocyst complex mediates tethering of MT1-MMP–positive late endosomes with the target membrane (ii). Fusion between the endosomal membrane tubule and the invadopodial plasma membrane may necessitate the SNARE protein VAMP7 (not depicted; Steffen et al., 2008; Williams and Coppolino, 2011). Actin and cortactin assembly at invadopodia requires N-WASP and allows membrane protrusion formation and retention of MT1-MMP (insets ii and iii; Yamaguchi et al., 2005; Artym et al., 2006; Oser et al., 2010; Yu et al., 2012). Mature invadopodia are responsible for penetrating and breaching the basement membrane in contact with carcinoma cells (1 and 2; Hotary et al., 2006; Rowe and Weiss, 2008). In the fibrous, collagen-rich extracellular membrane environment surrounding the tumor (3), fibers that oppose cell movement, involving recognition by yet unidentified collagen receptors, trigger the assembly of N-WASP– and F-actin–positive linear invadopodia and the recruitment and exocytosis of MT1-MMP–containing endosomes based on the conserved WASH and exocyst-dependent mechanism (inset iv).

delivery to invadopodia, has to be established (Steffen et al., 2008; Williams and Coppolino, 2011).

Our findings also demonstrate that exocytosis of MT1-MMP does not occur through complete collapse of MT1-MMP–positive endosomes into the plasma membrane, but by a mechanism whereby late endosomes are retrieved apparently intact after fission of endosome-to-plasma membrane connections and can possibly engage in multiple exocytic events. Strikingly, some of these connections remain open for several minutes; however, transfer of MT1-MMP from the storage endosome to the invadopodial plasma membrane is tightly controlled as a large portion of the protease remains associated with the endosome. Thus, the tubular connection forming between the two membrane compartments in a WASH/exocyst-dependent manner may exert different functions; it could stabilize and restrict the extension of the fusion pore between the two membranes and it may also act as a filter to prevent free diffusion of MT1-MMP out of the endosome. Along this line, it was recently shown that N-WASP–dependent invadopodial F-actin can prevent the diffusion of MT1-MMP out of the invadopodia through some interaction of the cytoplasmic domain of the protease with the actin network (Yu et al., 2012). The same type of interactions with WASH-dependent F-actin surrounding the connecting tube would limit diffusion of MT1-MMP out of the endosome and ensure controlled delivery of MT1-MMP to the plasma membrane for controlled remodeling of the basement membrane and collagen fibers.

Finally, this study supports the conclusion that two pools of F-actin–cortactin coexist and cooperate to ensure invadopodia formation and function. One pool is associated with and depends on N-WASP activity, which is associated with the core invadopodia structure forming on the cytoplasmic face of the plasma membrane in association with the matrix. These N-WASP–F-actin–cortactin–positive structures include typical dotty-like invadopodia forming on the adherent plasma membrane in cells on gelatin or basement membrane (Yamaguchi et al., 2005; Artym et al., 2006; Oser et al., 2010; Yu et al., 2012) and linear F-actin–based structures assembling in association with collagen fibers in tumor cells invading through a 3D fibrous environment (Juin et al., 2012; Yu et al., 2012; this study). These different structures represent docking sites for MT1-MMP–containing endosomes and may provide a physical scaffold for plasma membrane protrusion and MT1-MMP retension to penetrate the extracellular matrix and basement membrane. The second pool, with a punctate organization, is associated with and depends on WASH activity on MT1-MMP–positive endosomes and, together with other components including the exocyst complex, contributes to an exocytic mechanism that fuels the invadopodia with the proteolytic activity necessary for pericellular matrix remodelling. The coordinated function of WASH and the exocyst complex in the fundamental biology of invadopodium-mediated proteolysis in different pathologically relevant matrix environments demonstrated here appears a crucial part of the invasive program of carcinoma cells.

Downloaded from jcb.rupress.org on January 21, 2014

Published December 16, 2013

Materials and methods

Antibodies and constructs

Antibodies used in this study are listed in Table S1. Full-length mouse WASH cDNA amino-terminally fused with GFP or mCherry was subcloned in pcDNA3.1 vector (Derivery et al., 2009). Full-length rat cortactin cDNA (provided by M.A. McNiven, Mayo Clinic, Rochester, MI) was subcloned in pDsRed1-N1 and pEGFP-N1 (Takara Bio Inc.) in fusion with carboxy-terminal DsRed or GFP, respectively. Human full-length Exo84 and Sec3 were subcloned in pcDNA3.1 plasmid with amino-terminal GFP or carboxy-terminal HA tags.

Yeast two-hybrid screening

The coding sequence for full-length human Sec3 (GenBank accession no. gi:7023219) and Exo84 (GenBank accession no. gi:58331103) were PCR amplified and cloned into pB27 as carboxy-terminal fusions to LexA. The constructs were checked by sequencing the entire inserts and used as baits to screen at saturation a highly complex human placenta domain library constructed into pP6. pB27 and pP6 derive from the original pBTM116 (Vojtek and Hollenberg, 1995) and pGADGH (Bartel et al., 1993) plasmids, respectively. For Sec3, 96 million clones (10-fold the complexity of the library) were screened using a mating approach with Y187 (matα) and L40ΔGal4 (mata) yeast strains as previously described (Fromont-Racine et al., 1997). 353 His^+ colonies were selected on a medium lacking tryptophan, leucine, and histidine, supplemented with 2 mM 3-aminotriazole. For Exo84, 64 million clones were screened and 164 His^+ colonies were selected using the same protocol. The prey fragments of the positive clones were amplified by PCR and sequenced at their 5′ and 3′ junctions. The resulting sequences were used to identify the corresponding interacting proteins in GenBank using a fully automated procedure. The protein interactions from this publication have been submitted to the IMEx consortium through IntAct (Kerrien et al., 2012) and assigned the identifier IM-17363.

Cell culture, DNA transfection, stable cell lines, and RNAi

The human breast adenocarcinoma cell line MDA-MB-231 (HTB-26; American Type Culture Collection) was maintained in L-15 culture medium (Sigma-Aldrich) with 2 mM glutamine and 15% FCS at 37°C in 1% CO_2. MDA-MB-231 cells stably expressing MT1-MMPmCherry (MT1-MMPmCh) were cultured in the same medium supplemented with 0.5 mg/ml G418 (Sakurai-Yageta et al., 2008). MDA-MB-231 cells stably expressing MT1-MMPpHluorin (Lizárraga et al., 2009), with the GFP-derivative pHluorin tag (super-ecliptic variant [Miesenböck, 2012]) inserted in the extracellular domain, were generated by lentiviral transduction. For transient expression, MDA-MB-231 cells were transfected with plasmid constructs (1 µg) using Lipofectamine LTX (Invitrogen) or Nucleofector (Lonza) according to the manufacturers' instructions. Cells were analyzed 48 h after transfection. BT-549 (HTB-122; American Type Culture Collection) human breast cancer cells were cultured in RPMI medium with 2 mM glutamine and 10% FCS at 37°C in 5% CO_2. siRNA transfection was performed using 50 nM siRNA with Lullaby reagent (OZ Biosciences). Cells were analyzed 72 h after treatment. The siRNA sequences used in this study are shown in Table S2.

Immunoprecipitation

For expression of HA-tagged Exo84 and Sec3 exocyst complex subunits, HeLa cells were transiently transfected using FuGENE (Roche) according to the manufacturer's instructions. 48 h after transfection, cells were lysed in lysis buffer (50 mM Tris-HCl, pH 7.4, 150 mM NaCl, 1% Triton X-100, 1 mM EDTA, and complete Mini Protease Inhibitor Cocktail; Roche), and then centrifuged at 13,000 rpm for 10 min at 4°C. Supernatants (1–2 mg of total protein in 1 ml) were incubated with 1–2 µg of anti-WASH antibodies or control irrelevant IgGs (anti-GST) for 1 h at 4°C, and then protein G–Sepharose 4 Fast Flow (50 µl; GE Healthcare) was added and the incubation was continued for a further 2 h at 4°C. Beads were washed four times in lysis buffer and bound proteins were eluted in SDS sample buffer, separated by SDS-PAGE, and detected by immunoblotting with indicated antibodies using ECL Western Blotting Detection Reagents (GE Healthcare).

Fluorescent gelatin degradation assay

MDA-MB-231 cells were incubated for 5 h on FITC-conjugated cross-linked gelatin (Invitrogen) as described previously (Sakurai-Yageta et al., 2008), and then fixed and stained for F-actin and cortactin. Cells were imaged with the 63× objective of a wide-field microscope (DM6000 B/M; Leica) equipped with a CCD CoolSnap HQ camera (Roper Scientific) and steered by Metamorph (Molecular Devices). For quantification of degradation, the total area of degraded matrix in one field (black pixels) measured with the Threshold command of MetaMorph was divided by the number of phalloidin-labeled cells in the field to define a degradation index, which was normalized to the degradation index of control siNT-treated cells set to 100 as described previously (Sakurai-Yageta et al., 2008).

Indirect immunofluorescence microscopy, 3D deconvolution, and image analysis

MDA-MB-231 cells were cultured on gelatin-coated coverslips. Cells were extracted with 0.5% Triton X-100 in 4% paraformaldehyde and stained for immunofluorescence microscopy. Images were acquired with a wide-field microscope (Eclipse 90i Upright; Nikon) using a 100× Plan Apo VC 1.4 oil objective and a highly sensitive cooled interlined charge-coupled device (CCD) camera (CoolSnap HQ2; Roper Scientific). A z-dimension series of images was taken every 0.2 µm by means of a piezoelectric motor (Physik Instrumente) and the images were deconvoluted (Sibarita, 2005). For quantification of the effect of WASH knockdown on cortactin distribution, a perinuclear region was drawn with the Region Tool of MetaMorph 7 (Molecular Devices) and the integrated intensity was measured with the Region Measurement command. For quantification of the effect of Exo84 knockdown on WASH-cortactin domains, individual WASH and cortactin subdomains were circled with MetaMorph 7 and the integrated intensity was measured with the Region Measurement command.

WASH, Exo84, and cortactin spot detection and codistribution analysis

To detect endosomes, an automatic Otsu threshold is applied to the Gaussian-filtered MT1-MMP–positive endosome image (Σ = 1.5 pixels). Statistics about each endosome are then saved. For each endosome, WASH and Exo84 (or WASH and cortactin) spots are searched for in a neighboring of *x* pixels (manually set by user) in their respective channel. Their number and position are saved per endosome (see the macro in Text file S2 in online supplemental material). From the position of WASH and Exo84 (or WASH and cortactin) spots around each endosomes, each WASH spot is paired with its closest Exo84 (or cortactin) spot neighbor, optimized over all spots around this endosome. This allowed measuring of the distribution of distance between WASH-Exo84 (or WASH-cortactin) spots (see the codistribution analysis Zip file S3 in online supplemental material).

Duolink in situ proximity ligation assay

For Duolink assay (Söderberg et al., 2006), cells grown on coverslips coated with cross-linked gelatin were permeabilized with 0.5% Triton X-100 in 4% paraformaldehyde, fixed in 4% paraformaldehyde, and then incubated with primary antibodies: rabbit polyclonal anti-WASH, goat polyclonal anti-Exo84, and mouse monoclonal anti-cortactin. Secondary antibodies tagged with short DNA oligonucleotides were added. Hybridization, ligation, amplification, and detection were realized according to the manufacturer's protocol (Olink Bioscience). In brief, secondary antibodies were incubated in a preheated humidity chamber for 1 h at 37°C. Ligation was performed with a ligase-containing ligation solution for 30 min at 37°C. Then, the amplification step was performed with a polymerase-containing amplification solution for 1 h and 40 min at 37°C. Finally, coverslips were incubated with Cy3-conjugated IgGs to detect Duolink signal. Coverslips were analyzed by wide-field microscopy and WASH-Exo84 or WASH-cortactin Duolink signal staining was manually counted for each cell and compared with control conditions in which one of the primary antibodies was omitted.

Live-cell spinning disk confocal microscopy and FITC-dextran pulse experiment

MDA-MB-231 cells stably expressing MT1-MMPmCh were plated on glass-bottom dishes (MatTek Corporation) coated with cross-linked gelatin and kept in a humidified atmosphere at 37°C and 1% CO_2. Movement of MT1-MMPmCh–containing vesicles was monitored by acquiring z-stack sequences by confocal spinning disk microscopy (1 z-stack/4 s) with a microscope (Eclipse TE2000-U; Nikon) equipped with a 60× 1.45 NA oil immersion objective, a PIFOC Objective stepper, a CSU22 confocal unit (Yokogawa Corporation of America), and an HQ2 CCD camera steered by Metamorph and a temperature controller.

For dextran pulse experiments, MDA-MB-231 cells expressing MT1-MMPmCh (or transiently expressing Rab7-GFP or VAMP7-GFP) were plated in glass-bottom dishes coated with Alexa Fluor 594–conjugated cross-linked gelatin (or unlabeled gelatin) and a z-stack of images was acquired before adding dextran. FITC- or Alexa Fluor 647–conjugated dextran (10,000 MW) was added to the medium at 2 mg/ml final concentration (from a 20-mg/ml stock solution). After 1 min at 37°C, cells were washed and z-stack sequences were acquired.

Downloaded from jcb.rupress.org on January 21, 2014

Published December 16, 2013

TIRFM

MDA-MB-231 cells transfected with GFP- and mCherry-tagged proteins were plated on glass-bottom dishes coated with cross-linked unlabeled gelatin as previously described. Simultaneous dual color TIRFM sequences were acquired on an inverted microscope (TE2000) equipped with a 100× TIRF objective (1.47 NA), a TIRF arm, an image splitter (DV; Roper Scientific) installed in front of the CCD camera and a temperature controller. GFP and m-Cherry were excited with 491- and 560-nm lasers, respectively (100 mW; Roper Scientific), both controlled for power by an acousto-optic tunable filter. Fluorescent emissions were selected with bandpass and longpass filters (Chroma Technology Corp.) and captured by a QuantEM EMCCD camera (Roper Scientific). The system was driven by Metamorph. To measure the subplasma membrane density of MT1-MMP endosomes, cells stably expressing MT1-MMPmCh and silenced for the protein of interest were plated on a layer of unlabeled gelatin and imaged by TIRFM for an exposure time of 100 ms and with 1 pixel corresponding to 160 nm. The density of MT1-MMPmCh structures was evaluated by thresholding images using using ImageJ software. The threshold was set at 1.3× the cytoplasmic background. The size of the cell footprint was not affected by the siRNAs used.

High-resolution 3D structured illumination microscopy (SIM)

Image acquisition was performed in the 3D SIM mode with a N-SIM microscope (Nikon) equipped with a 100× 1.49 NA oil immersion objective, laser illumination (488 nm at 200 mW and 561 nm at 100 mW) and an EM CCD camera (DU-897; Andor Technology). Image reconstruction was performed using the NIS-Elements software (Nikon; based on Gustafsson et al. [2008]).

Matrigel and collagen I invasion assays

The Transwell Matrigel invasion assay has been previously described (Steffen et al., 2008). Invasive migration in 3D type I collagen was assessed using the Oris Cell Invasion Assay (Platypus Technologies). H2B-EGF–expressing MDA-MB-231 cells were reverse transfected with Lullaby reagent with MT1-MMP, WASH, or Exo84 siRNAs (50 nM). 24 h after transfection, cells were trypsinized and counted and 40,000 cells/well were seeded in the presence of Oris Cell Seeding Stoppers to restrict seeding to the outer annular regions of the wells in a 96-well plate previously coated with a bottom layer of acid-extracted rat tail tendon type I collagen (2.2 mg/ml; BD). Removal of the stoppers reveals a 2-mm diameter unseeded region in the center of each well, into which seeded cells may invade during a 48-h time period, once a collagen I overlay has been applied. H2B-EGFP nuclei images were acquired from each well at the beginning (T0) and 48 h after invasion (T2) using a cooled CCD camera (HQ2) mounted on a microscope (TE2000) equipped with a 4× objective CFI Plan Fluor 0.13 NA, 17.1 WD. Image analysis was performed using Metamorph software. The index of invasion was determined by thresholding the area occupied by H2B-EGFP nuclei in the detection zone of each well after 48 h of invasion. This index is defined by the total area occupied by H2B-EGFP nuclei in unseeded area at the end of the assay (T2) by subtracting the area occupied by H2B-EGFP nuclei at the beginning of the experiment (T0). This area of invasion was normalized and results from three independent experiments are represented.

Live-cell imaging of cells on a layer of fibrous type I collagen

Glass bottom dishes (MatTek Corporation) were layered with 100 µl of a solution of type I collagen mixed with Alexa Fluor 647–conjugated type I collagen (10% final) at a final concentration of 2.2 mg/ml (Sabeh et al., 2004). After gelling for 3 min at 37°C, the collagen layer was washed gently in PBS and 1 ml of the cell suspension in L15 medium with 15% FCS ($1.5–2.5 \times 10^5$ cells/ml) was added. Cells were incubated for 30 min at 37°C in 1% CO_2 before live-cell imaging using multi-color spinning disk confocal microscopy.

Quantification of pericellular collagenolysis

Cells treated with siRNAs against MT1-MMP, WASH, Exo84, or non-targeting siRNA for 48 h (Table S2) were trypsinized and resuspended in 0.2 ml of 2.2 mg/ml collagen I solution (2.5×10^5 cells/ml) loaded on a glass coverslip. After gelling for 30 min at 37°C, complete medium was added and collagen-embedded cells were incubated for 24 h at 37°C in 1% CO_2. After fixation in 4% paraformaldehyde in PBS at 37°C for 30 min, samples were incubated with anti–Col1-$^{3/4}$C antibodies (2.5 µg/ml) for 2 h at 4°C, washed extensively with PBS, and counterstained with Cy3-conjugated anti-rabbit IgG antibodies, DAPI, and Alexa Fluor 488–phalloidin to see the cell shape. Image acquisition was performed with an A1R confocal microscope (Nikon) with a 40× oil objective. Quantification of degradation spots was performed with a homemade ImageJ macro (Zip file S1 in the online supplemental material). Images were preprocessed by a laplacian of Gaussian filter (Sage et al., 2005), with variance reflecting the expected spot size. The spot detection then consists in finding the local minima, sorting them in ascending order of intensity, applying a flood-fill algorithm to each of them using a fixed noise tolerance value set up for all experiments at 10,000, and discarding higher minima whose fill regions touch those of lower minima. Detected spots are then counted and saved for visual verification. No manual correction was done. Degradation index is the number of degradation spots divided by the number of cells present in the field, normalized to the degradation index of control cells set to 100.

MT1-MMPpHluorin exocytosis on collagen type I fibers

MDA-MB-231 cells stably coexpressing MT1-MMPmCherry and MT1-MMPpHluorin constructs were treated with nontargeting, WASH, or Exo84 siRNA for 72 h and plated atop of a drop of polymerized type I collagen. Cells were imaged by confocal spinning disk microscopy (two images/min). The number of exocytic events of MT1-MMPphLuorin (i.e., GFP flashes) was measured per minute and per cell. As a control we measured the mean fluorescence intensity of MT1-MMPmCherry for each cell.

Extracellular pH shifts experiment

MDA-MB-231 cells stably expressing MT1-MMPpHluorin were plated on polymerized type I collagen conjugated with Cy3. Cells were imaged on a microsope (IX71; Olympus) with a 100×, 1.49 NA objective at a frame rate of 0.5 Hz with a QuantEM EMCCD camera. Cells were bathed in a solution containing 140 mM NaCl, 2 mM KCl, 2 mM $MgCl_2$, 2 mM $CaCl_2$, 10 mM Hepes, and 5 mM D-glucose, and adjusted to pH 7.4 and 315 mosm. For the solution at pH 5.5, Hepes was replaced by MES. Solution exchange was performed as described previously (Perrais et al., 2004).

Statistical analyses

Statistical analyses were performed using analysis of variance or Student's *t* test in Prism software.

Online supplemental material

Fig. S1 shows additional data on markers associated with MT1-MMP–positive endosomes in MDA-MB-231 and BT-549 cells. Fig. S2 shows levels of proteins in cells targeted by different siRNAs. Fig. S3 shows additional staining of endosomal and invadopodial markers. Fig. S4 shows a gallery of images taken from a time-lapse sequence of cells expressing MT1-MMPmCh and MT1-MMPpHLuorin. Tables S1 and S2 list antibodies and show sequences of the siRNAs used in this study, respectively. Video 1 shows the dynamics of GFP-WASH– and DsRed-cortactin–positive cytoplasmic puncta in MDA-MB-231 cells. Video 2 shows clustering and tubulation of a MT1-MMP–positive late endosomal system induced upon silencing of WASH in MDA-MB-231 cells. Video 3 dynamically shows contacts of MT1-MMPmCherry–positive endosomes with GFP-cortactin–positive invadopodia on the ventral membrane of MDA-MB-231 cells plated on gelatin. Video 4 documents the existence of two dynamic pools of DsRed-cortactin in MDA-MB-231 cells plated on a layer of collagen fibers; one pool assembles along collagen fibers and correspond to linear invadopodia, and another pool is associated with GFP-WASH–positive puncta on late endosomes. Video 5 shows MDA-MB-231 cells simultaneously expressing mCherry- and pHLuorin-tagged fusion protein of MT1-MMP plated on a layer of collagen fibers. The pH sensitivity of pHLuorin allows the visualization of exocytic events of MT1-MMP–containing endosomes occurring near collagen fibers. Video 6 documents that exocytic MT1-MMPpHLuorin–positive endosomes are positive for mCherry-WASH. Video 7 shows the fluorescence change of MT1-MMPpHLuorin–containing late endosomes according to the pH of the external medium indicative of long-lived late endosome-to-plasma membrane connections. Zip file S1 contains two macros: one for degradation spot detection and one for DAPI-stained nuclei counting, to compute the degradation index of collagen. Text file S2 is the macro used to detect endosomes and aggregated spots. Zip file S3 (codistribution analysis) contains Matlab scripts used to quantify the distance between WASH spots and their closest neighbored cortactin spots (or Exo84 spots) for each endosome. Online supplemental material is available at http://www.jcb.org/cgi/content/full/jcb.201306162/DC1.

The authors wish to thank J. Camonis for initiating the Drosoman yeast two-hybrid joint project between Institut Curie and Hybrigenics SA, A. Savina for help with FITC-dextran experiments, and K. Wolf and P. Friedl for advice and help with experiments using Col1-$^{3/4}$C antibody. We are indebted to V. Fraisier and the staff of the Cell and Tissue Imaging Facility and Nikon Imaging Center at Institut Curie–Centre National de la Recherche Scientifique for help with image acquisition. We thank members of P. Chavrier's laboratory for helpful discussions.

Downloaded from jcb.rupress.org on January 21, 2014

Published December 16, 2013

P. Monteiro was the recipient of a PhD fellowship from Ligue Nationale contre le Cancer. C. Rossé was the recipient of a postdoctoral fellowship from Fondation ARC pour la recherche sur le cancer. Support was provided by grants from the Fondation ARC pour la recherche sur le cancer (SL220100601356) and Agence Nationale pour la Recherche (ANR-08-BLAN-0111) to P. Chavrier, by GenHomme Network (02490-6088) to Hybrigenics SA and to Institut Curie, and by core funding from the Institut Curie and the Centre National de la Recherche Scientifique.

Submitted: 28 June 2013
Accepted: 18 November 2013

References

Artym, V.V., Y. Zhang, F. Seillier-Moiseiwitsch, K.M. Yamada, and S.C. Mueller. 2006. Dynamic interactions of cortactin and membrane type 1 matrix metalloproteinase at invadopodia: defining the stages of invadopodia formation and function. *Cancer Res.* 66:3034–3043. http://dx.doi.org/10.1158/0008-5472.CAN-05-2177

Ayala, I., M. Baldassarre, G. Giacchetti, G. Caldieri, S. Tetè, A. Luini, and R. Buccione. 2008. Multiple regulatory inputs converge on cortactin to control invadopodia biogenesis and extracellular matrix degradation. *J. Cell Sci.* 121:369–378. http://dx.doi.org/10.1242/jcs.008037

Bartel, P.L., C.T. Chien, R. Sternglanz, and S. Fields. 1993. Using the two-hybrid system to detect protein-protein interactions. *In* Cellular Interactions in Development: A Practical Approach, D.A. Hartley, editor. Oxford University Press, Oxford. 153–179.

Carnell, M., T. Zech, S.D. Calaminus, S. Ura, M. Hagedorn, S.A. Johnston, R.C. May, T. Soldati, L.M. Machesky, and R.H. Insall. 2011. Actin polymerization driven by WASH causes V-ATPase retrieval and vesicle neutralization before exocytosis. *J. Cell Biol.* 193:831–839. http://dx.doi.org/10.1083/jcb.201009119

Clark, E.S., A.S. Whigham, W.G. Yarbrough, and A.M. Weaver. 2007. Cortactin is an essential regulator of matrix metalloproteinase secretion and extracellular matrix degradation in invadopodia. *Cancer Res.* 67:4227–4235. http://dx.doi.org/10.1158/0008-5472.CAN-06-3928

Derivery, E., C. Sousa, J.J. Gautier, B. Lombard, D. Loew, and A. Gautreau. 2009. The Arp2/3 activator WASH controls the fission of endosomes through a large multiprotein complex. *Dev. Cell.* 17:712–723. http://dx.doi.org/10.1016/j.devcel.2009.09.010

Derivery, E., E. Helfer, V. Henriot, and A. Gautreau. 2012. Actin polymerization controls the organization of WASH domains at the surface of endosomes. *PLoS ONE.* 7:e39774. http://dx.doi.org/10.1371/journal.pone.0039774

Duleh, S.N., and M.D. Welch. 2010. WASH and the Arp2/3 complex regulate endosome shape and trafficking. *Cytoskeleton (Hoboken).* 67:193–206.

Fromont-Racine, M., J.C. Rain, and P. Legrain. 1997. Toward a functional analysis of the yeast genome through exhaustive two-hybrid screens. *Nat. Genet.* 16:277–282. http://dx.doi.org/10.1038/ng0797-277

Gomez, T.S., and D.D. Billadeau. 2009. A FAM21-containing WASH complex regulates retromer-dependent sorting. *Dev. Cell.* 17:699–711. http://dx.doi.org/10.1016/j.devcel.2009.09.009

Gomez, T.S., J.A. Gorman, A.A. de Narvajas, A.O. Koenig, and D.D. Billadeau. 2012. Trafficking defects in WASH-knockout fibroblasts originate from collapsed endosomal and lysosomal networks. *Mol. Biol. Cell.* 23:3215–3228. http://dx.doi.org/10.1091/mbc.E12-02-0101

Gustafsson, M.G., L. Shao, P.M. Carlton, C.J. Wang, I.N. Golubovskaya, W.Z. Cande, D.A. Agard, and J.W. Sedat. 2008. Three-dimensional resolution doubling in wide-field fluorescence microscopy by structured illumination. *Biophys. J.* 94:4957–4970. http://dx.doi.org/10.1529/biophysj.107.120345

Harrington, A.W., C. St Hillaire, L.S. Zweifel, N.O. Glebova, P. Philippidou, S. Halegoua, and D.D. Ginty. 2011. Recruitment of actin modifiers to TrkA endosomes governs retrograde NGF signaling and survival. *Cell.* 146:421–434. http://dx.doi.org/10.1016/j.cell.2011.07.008

He, B., and W. Guo. 2009. The exocyst complex in polarized exocytosis. *Curr. Opin. Cell Biol.* 21:537–542. http://dx.doi.org/10.1016/j.ceb.2009.04.007

Heider, M.R., and M. Munson. 2012. Exorcising the exocyst complex. *Traffic.* 13:898–907. http://dx.doi.org/10.1111/j.1600-0854.2012.01353.x

Hertzog, M., and P. Chavrier. 2011. Cell polarity during motile processes: keeping on track with the exocyst complex. *Biochem. J.* 433:403–409. http://dx.doi.org/10.1042/BJ20101214

Hotary, K., X.Y. Li, E. Allen, S.L. Stevens, and S.J. Weiss. 2006. A cancer cell metalloprotease triad regulates the basement membrane transmigration program. *Genes Dev.* 20:2673–2686. http://dx.doi.org/10.1101/gad.1451806

Jia, D., T.S. Gomez, Z. Metlagel, J. Umetani, Z. Otwinowski, M.K. Rosen, and D.D. Billadeau. 2010. WASH and WAVE actin regulators of the Wiskott-Aldrich syndrome protein (WASP) family are controlled by analogous structurally related complexes. *Proc. Natl. Acad. Sci. USA.* 107:10442–10447. http://dx.doi.org/10.1073/pnas.0913293107

Jiang, A., K. Lehti, X. Wang, S.J. Weiss, J. Keski-Oja, and D. Pei. 2001. Regulation of membrane-type matrix metalloproteinase 1 activity by dynamin-mediated endocytosis. *Proc. Natl. Acad. Sci. USA.* 98:13693–13698. http://dx.doi.org/10.1073/pnas.241293698

Juin, A., C. Billottet, V. Moreau, O. Destaing, C. Albiges-Rizo, J. Rosenbaum, E. Génot, and F. Saltel. 2012. Physiological type I collagen organization induces the formation of a novel class of linear invadosomes. *Mol. Biol. Cell.* 23:297–309. http://dx.doi.org/10.1091/mbc.E11-07-0594

Kerrien, S., B. Aranda, L. Breuza, A. Bridge, F. Broackes-Carter, C. Chen, M. Duesbury, M. Dumousseau, M. Feuermann, U. Hinz, et al. 2012. The IntAct molecular interaction database in 2012. *Nucleic Acids Res.* 40:D841–D846. http://dx.doi.org/10.1093/nar/gkr1088

Liu, J., P. Yue, V.V. Artym, S.C. Mueller, and W. Guo. 2009. The role of the exocyst in matrix metalloproteinase secretion and actin dynamics during tumor cell invadopodia formation. *Mol. Biol. Cell.* 20:3763–3771. http://dx.doi.org/10.1091/mbc.E08-09-0967

Lizárraga, F., R. Poincloux, M. Romao, G. Montagnac, G. Le Dez, I. Bonne, G. Rigaill, G. Raposo, and P. Chavrier. 2009. Diaphanous-related formins are required for invadopodia formation and invasion of breast tumor cells. *Cancer Res.* 69:2792–2800. http://dx.doi.org/10.1158/0008-5472.CAN-08-3709

Lorenz, M., H. Yamaguchi, Y. Wang, R.H. Singer, and J. Condeelis. 2004. Imaging sites of N-wasp activity in lamellipodia and invadopodia of carcinoma cells. *Curr. Biol.* 14:697–703. http://dx.doi.org/10.1016/j.cub.2004.04.008

Miesenböck, G. 2012. Synapto-pHluorins: genetically encoded reporters of synaptic transmission. *Cold Spring Harb. Protoc.* 2012:213–217. http://dx.doi.org/10.1101/pdb.ip067827

Morel, E., R.G. Parton, and J. Gruenberg. 2009. Annexin A2-dependent polymerization of actin mediates endosome biogenesis. *Dev. Cell.* 16:445–457. http://dx.doi.org/10.1016/j.devcel.2009.01.007

Murphy, D.A., and S.A. Courtneidge. 2011. The 'ins' and 'outs' of podosomes and invadopodia: characteristics, formation and function. *Nat. Rev. Mol. Cell Biol.* 12:413–426. http://dx.doi.org/10.1038/nrm3141

Oser, M., H. Yamaguchi, C.C. Mader, J.J. Bravo-Cordero, M. Arias, X. Chen, V. Desmarais, J. van Rheenen, A.J. Koleske, and J. Condeelis. 2009. Cortactin regulates cofilin and N-WASp activities to control the stages of invadopodium assembly and maturation. *J. Cell Biol.* 186:571–587. http://dx.doi.org/10.1083/jcb.200812176

Oser, M., C.C. Mader, H. Gil-Henn, M. Magalhaes, J.J. Bravo-Cordero, A.J. Koleske, and J. Condeelis. 2010. Specific tyrosine phosphorylation sites on cortactin regulate Nck1-dependent actin polymerization in invadopodia. *J. Cell Sci.* 123:3662–3673. http://dx.doi.org/10.1242/jcs.068163

Park, L., P.A. Thomason, T. Zech, J.S. King, D.M. Veltman, M. Carnell, S. Ura, L.M. Machesky, and R.H. Insall. 2013. Cyclical action of the WASH complex: FAM21 and capping protein drive WASH recycling, not initial recruitment. *Dev. Cell.* 24:169–181. http://dx.doi.org/10.1016/j.devcel.2012.12.014

Perrais, D., I.C. Kleppe, J.W. Taraska, and W. Almers. 2004. Recapture after exocytosis causes differential retention of protein in granules of bovine chromaffin cells. *J. Physiol.* 560:413–428. http://dx.doi.org/10.1113/jphysiol.2004.064410

Piotrowski, J.T., T.S. Gomez, R.A. Schoon, A.K. Mangalam, and D.D. Billadeau. 2013. WASH knockout T cells demonstrate defective receptor trafficking, proliferation, and effector function. *Mol. Cell. Biol.* 33:958–973. http://dx.doi.org/10.1128/MCB.01288-12

Poincloux, R., F. Lizárraga, and P. Chavrier. 2009. Matrix invasion by tumour cells: a focus on MT1-MMP trafficking to invadopodia. *J. Cell Sci.* 122:3015–3024. http://dx.doi.org/10.1242/jcs.034561

Puthenveedu, M.A., B. Lauffer, P. Temkin, R. Vistein, P. Carlton, K. Thorn, J. Taunton, O.D. Weiner, R.G. Parton, and M. von Zastrow. 2010. Sequence-dependent sorting of recycling proteins by actin-stabilized endosomal microdomains. *Cell.* 143:761–773. http://dx.doi.org/10.1016/j.cell.2010.10.003

Rowe, R.G., and S.J. Weiss. 2008. Breaching the basement membrane: who, when and how? *Trends Cell Biol.* 18:560–574. http://dx.doi.org/10.1016/j.tcb.2008.08.007

Sabeh, F., I. Ota, K. Holmbeck, H. Birkedal-Hansen, P. Soloway, M. Balbin, C. Lopez-Otin, S. Shapiro, M. Inada, S. Krane, et al. 2004. Tumor cell traffic through the extracellular matrix is controlled by the membrane-anchored collagenase MT1-MMP. *J. Cell Biol.* 167:769–781. http://dx.doi.org/10.1083/jcb.200408028

Sabeh, F., R. Shimizu-Hirota, and S.J. Weiss. 2009. Protease-dependent versus -independent cancer cell invasion programs: three-dimensional amoeboid movement revisited. *J. Cell Biol.* 185:11–19. http://dx.doi.org/10.1083/jcb.200807195

Sage, D., F.R. Neumann, F. Hediger, S.M. Gasser, and M. Unser. 2005. Automatic tracking of individual fluorescence particles: application to the study of

Downloaded from jcb.rupress.org on January 21, 2014

Published December 16, 2013

chromosome dynamics. *IEEE Trans. Image Process.* 14:1372–1383. http://dx.doi.org/10.1109/TIP.2005.852787

Sakurai-Yageta, M., C. Recchi, G. Le Dez, J.B. Sibarita, L. Daviet, J. Camonis, C. D'Souza-Schorey, and P. Chavrier. 2008. The interaction of IQGAP1 with the exocyst complex is required for tumor cell invasion downstream of Cdc42 and RhoA. *J. Cell Biol.* 181:985–998. http://dx.doi.org/10.1083/jcb.200709076

Sibarita, J.B. 2005. Deconvolution microscopy. *Adv. Biochem. Eng. Biotechnol.* 95:201–243.

Söderberg, O., M. Gullberg, M. Jarvius, K. Ridderstråle, K.J. Leuchowius, J. Jarvius, K. Wester, P. Hydbring, F. Bahram, L.G. Larsson, and U. Landegren. 2006. Direct observation of individual endogenous protein complexes in situ by proximity ligation. *Nat. Methods*. 3:995–1000. http://dx.doi.org/10.1038/nmeth947

Sokac, A.M., and W.M. Bement. 2006. Kiss-and-coat and compartment mixing: coupling exocytosis to signal generation and local actin assembly. *Mol. Biol. Cell*. 17:1495–1502. http://dx.doi.org/10.1091/mbc.E05-10-0908

Steffen, A., G. Le Dez, R. Poincloux, C. Recchi, P. Nassoy, K. Rottner, T. Galli, and P. Chavrier. 2008. MT1-MMP-dependent invasion is regulated by TI-VAMP/VAMP7. *Curr. Biol.* 18:926–931. http://dx.doi.org/10.1016/j.cub.2008.05.044

Temkin, P., B. Lauffer, S. Jäger, P. Cimermancic, N.J. Krogan, and M. von Zastrow. 2011. SNX27 mediates retromer tubule entry and endosome-to-plasma membrane trafficking of signalling receptors. *Nat. Cell Biol.* 13:715–721. http://dx.doi.org/10.1038/ncb2252

Thorn, P., K.E. Fogarty, and I. Parker. 2004. Zymogen granule exocytosis is characterized by long fusion pore openings and preservation of vesicle lipid identity. *Proc. Natl. Acad. Sci. USA*. 101:6774–6779. http://dx.doi.org/10.1073/pnas.0400336101

Uekita, T., Y. Itoh, I. Yana, H. Ohno, and M. Seiki. 2001. Cytoplasmic tail–dependent internalization of membrane-type 1 matrix metalloproteinase is important for its invasion-promoting activity. *J. Cell Biol.* 155:1345–1356. http://dx.doi.org/10.1083/jcb.200108112

Vojtek, A.B., and S.M. Hollenberg. 1995. Ras-Raf interaction: two-hybrid analysis. *Methods Enzymol.* 255:331–342.

Williams, K.C., and M.G. Coppolino. 2011. Phosphorylation of membrane type 1-matrix metalloproteinase (MT1-MMP) and its vesicle-associated membrane protein 7 (VAMP7)-dependent trafficking facilitate cell invasion and migration. *J. Biol. Chem.* 286:43405–43416. http://dx.doi.org/10.1074/jbc.M111.297069

Wolf, K., Y.I. Wu, Y. Liu, J. Geiger, E. Tam, C. Overall, M.S. Stack, and P. Friedl. 2007. Multi-step pericellular proteolysis controls the transition from individual to collective cancer cell invasion. *Nat. Cell Biol.* 9:893–904. http://dx.doi.org/10.1038/ncb1616

Yamaguchi, H., M. Lorenz, S. Kempiak, C. Sarmiento, S. Coniglio, M. Symons, J. Segall, R. Eddy, H. Miki, T. Takenawa, and J. Condeelis. 2005. Molecular mechanisms of invadopodium formation: the role of the N-WASP–Arp2/3 complex pathway and cofilin. *J. Cell Biol.* 168:441–452. http://dx.doi.org/10.1083/jcb.200407076

Yu, X., T. Zech, L. McDonald, E.G. Gonzalez, A. Li, I. Macpherson, J.P. Schwarz, H. Spence, K. Futó, P. Timpson, et al. 2012. N-WASP coordinates the delivery and F-actin–mediated capture of MT1-MMP at invasive pseudopods. *J. Cell Biol.* 199:527–544. http://dx.doi.org/10.1083/jcb.201203025

Zech, T., S.D. Calaminus, P. Caswell, H.J. Spence, M. Carnell, R.H. Insall, J. Norman, and L.M. Machesky. 2011. The Arp2/3 activator WASH regulates α5β1-integrin-mediated invasive migration. *J. Cell Sci.* 124:3753–3759. http://dx.doi.org/10.1242/jcs.080986

Downloaded from jcb.rupress.org on January 21, 2014

Monteiro et al., http://www.jcb.org/cgi/content/full/jcb.201306162/DC1

THE JOURNAL OF CELL BIOLOGY

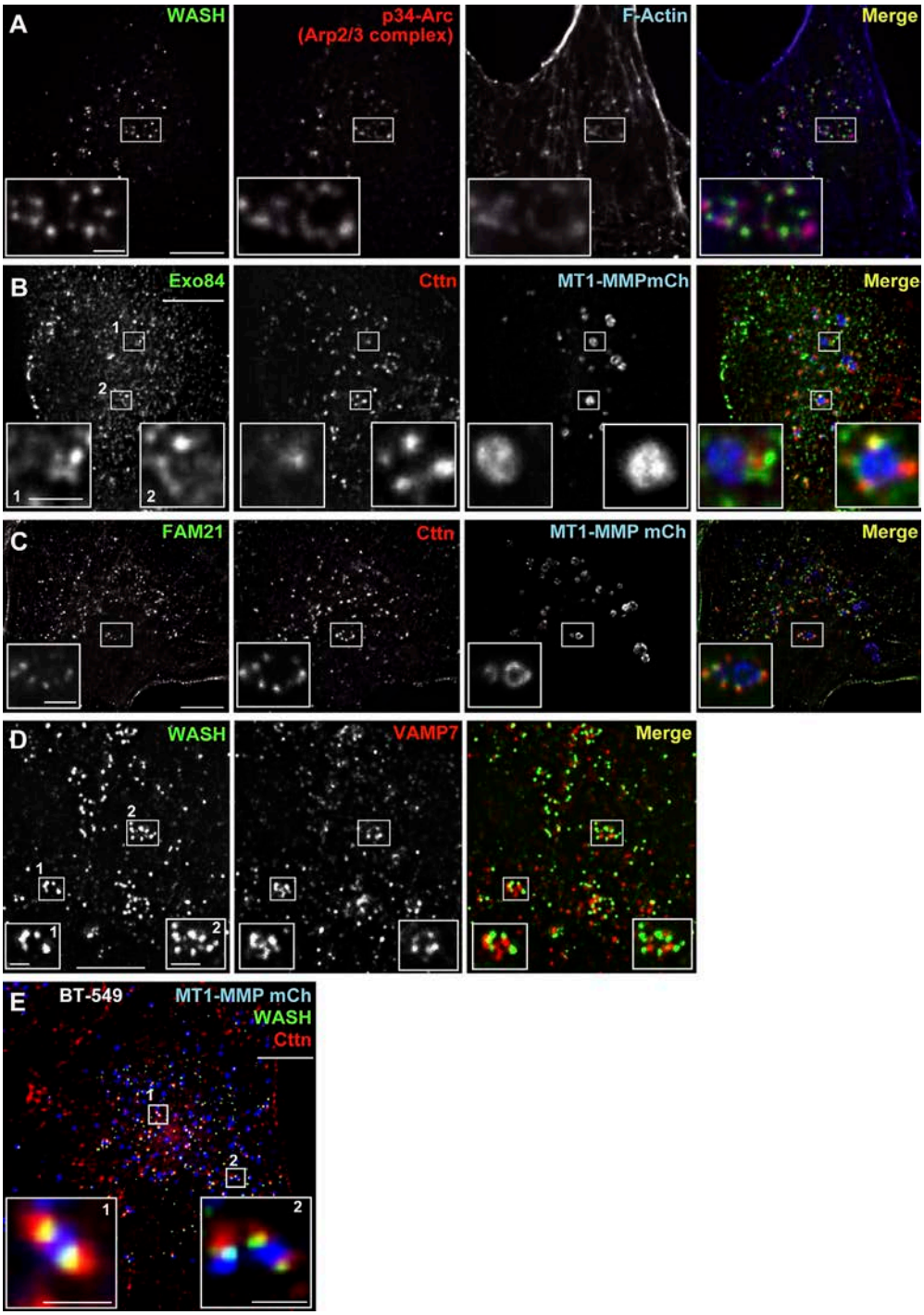

Figure S1. **3D deconvolution microscopy analysis of WASH and exocyst microdomains on MT1-MMP–positive endosomes.** (A) MDA-MB-231 cells on cross-linked gelatin were stained with antibodies against WASH, the p34-Arc subunit of the Arp2/3 complex, and fluorescent phalloidin to stain F-actin structures, revealing WASH microdomains adjacent to Arp2/3 complex–F-actin microdomains. (B) MDA-MB-231 cells stably expressing MT1-MMPmCh plated on cross-linked gelatin were processed for immunofluorescence microscopy with antibodies against Exo84 and cortactin. (C) MDA-MB-231 cells stably expressing MT1-MMPmCh were counterstained for the endogenous FAM21 subunit of the WASH complex and for cortactin. (D) MDA-MB-231 cells were analyzed by immunofluorescence microscopy with antibodies against WASH and VAMP7. (E) BT-549 breast cancer cells stably expressing MT1-MMPmCh were plated on cross-linked gelatin and stained with antibodies against WASH and cortactin. Each deconvoluted image corresponds to a projection of three or four planes in the middle of the cells. Bars: (main) 5 µm; (inset) 1 µm.

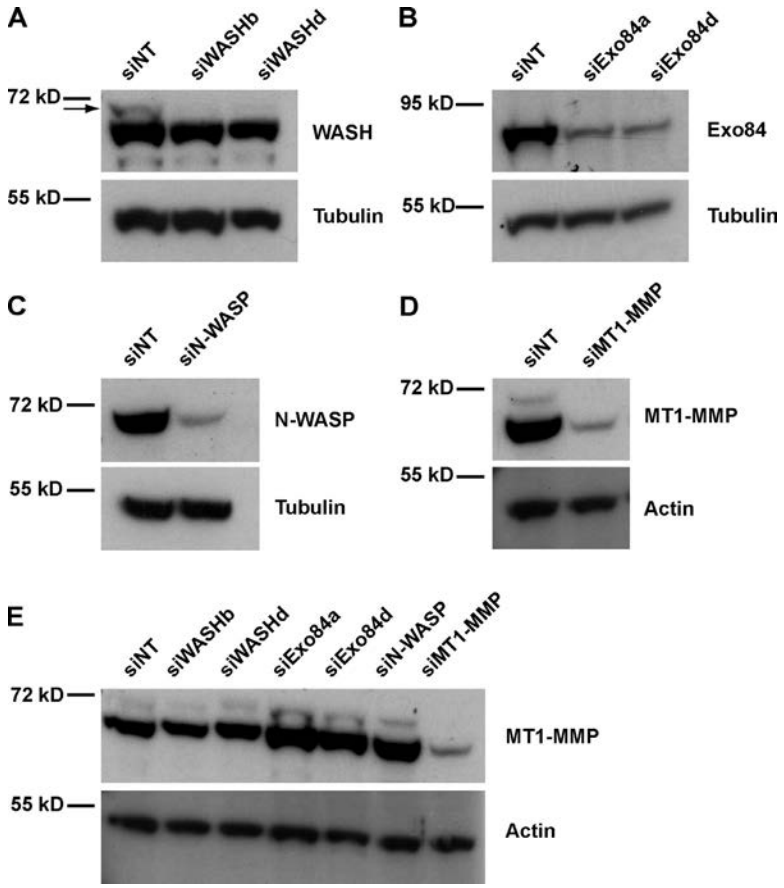

Figure S2. **Immunoblotting analysis of siRNA-treated cells.** (A–E) Immunoblotting analysis of MDA-MB-231 cells treated for 72 h with the indicated siRNAs. Immunoblotting with anti-tubulin was used as a loading control. Antibody specificity is indicated on the right.

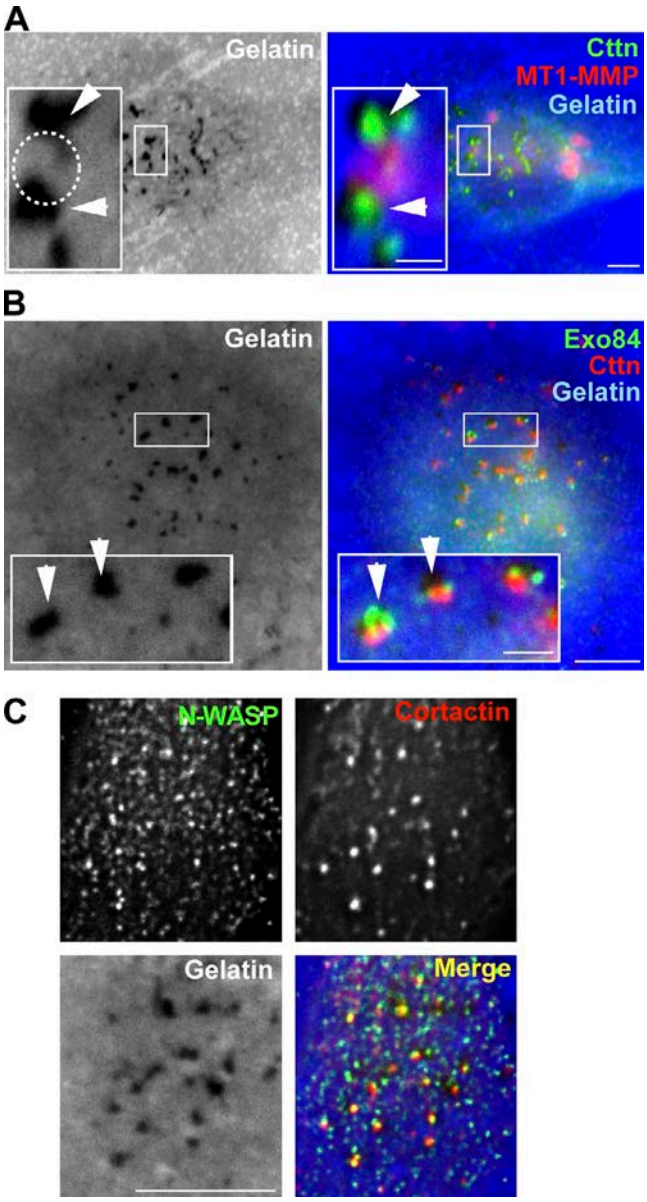

Figure S3. **Docking of MT1-MMP–positive endosomes at the invadopodial plasma membrane.** (A and B) MDA-MB-231 cells plated for 5 h on cross-linked FITC-labeled gelatin (blue) were processed for immunofluorescence microscopy with antibodies against cortactin and MT1-MMP (A) or cortactin and Exo84 (B). The images represent a single section in the ventral plane of the cells in contact with gelatin. Insets are higher magnification views of the boxed regions. Dashed line in A represents the contour of the MT1-MMP–containing endosome projected on the gelatin image. Arrowheads point to matrix degradation restricted to cortactin-positive invadopodia adjacent to MT1-MMP–positive endosomes. (C) Cells treated as in A were stained with antibodies against N-WASP (green) and cortactin (red). Bars, 5 μm.

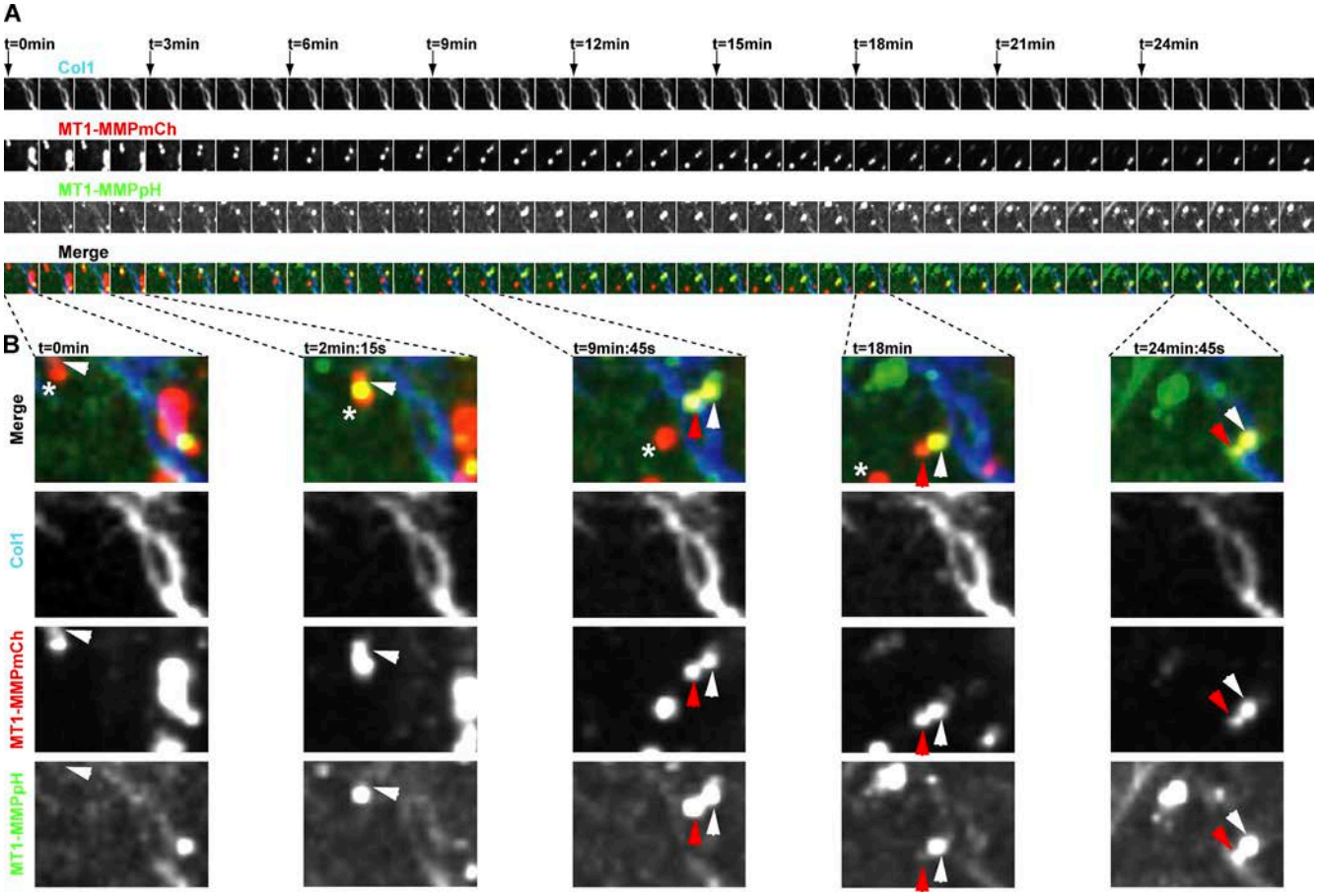

Figure S4. **Kiss-and-run exocytosis of MT1-MMPpHluorin at contact sites with collagen fibers.** (A) MDA-MB-231 cells stably expressing MT1-MMPmCh (red) and MT1-MMPpHluorin (green, after exocytosis) were plated on a glass bottom dish layered with Alexa Fluor 647–conjugated collagen I (blue) for 30 min and imaged by confocal spinning disk microscopy. A gallery of consecutive images from a representative time-lapse series (see corresponding Video 5) is shown with separated channels and merged images (bottom). (B) High magnification of selected frames from the time series in A. At the beginning of the time lapse (t0), a group of three MT1-MMP–positive endosomes (red) is visible. At $t = 2$ min, 15 s, one endosome undergoes exocytosis in the vicinity of collagen fibers and turns green (white arrowhead). This endosomes remains green until the end of the time series, indicating that it does not reacidify. A second endosome undergoes exocytosis at the contact site with a collagen fiber (red arrowhead; $t = 9$ min, 55 s). This endosome reacidifies its lumen (turns back red; $t = 18$ min), and undergoes a second round of exocytosis ($t = 24$ min, 45 s). During this sequence of events, these two endosomes scan a region aligned along collagen fibers. A third endosome moves away and does not undergo exocytosis (asterisk).

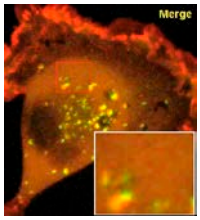

Video 1. **WASH- and cortactin-positive puncta are closely apposed on vesicular structures in MDA-MB-231 cells.** MDA-MB-231 cells expressing EGFP-cortactin (green) and DsRed-cortactin (red) were plated for 5 h on cross-linked gelatin and analyzed by confocal spinning disk fluorescence microscopy (inverted Ti-E; Nikon). The boxed region is shown at higher magnification in the inset. Images were taken every 3 s for 140 s (indicated time is in min:s). Bar, 5 µm.

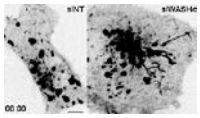

Video 2. **WASH knockdown induces tubulation of MT1-MMP–positive endosomes.** MDA-MB-231 cells expressing MT1-MMPmCh were treated with a siRNA specific for WASH (right) or with a control nontargeting (siNT; left) siRNA for 72 h and then plated on cross-linked gelatin and analyzed by confocal spinning disk fluorescence microscopy (inverted Ti-E; Nikon). Images were taken every 5 s for 284 s (indicated time is in min:s). Bar, 5 µm.

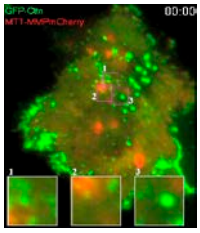

Video 3. **Repeated contacts of MT1-MMP–positive endosomes with invadopodia.** MDA-MB-231 cells expressing GFP-cortactin (green) and MT1-MMP-mCh (red) were plated on cross-linked gelatin for 5 h and analyzed by dual color TIRFM (inverted Ti-E; Nikon). Insets correspond to the boxed regions. Asterisks point to MT1-MMP–positive endosomes interacting with cortactin-positive invadopodia. Images were taken every 10 s for 30 min (indicated time is in min:s). Bar, 5 µm.

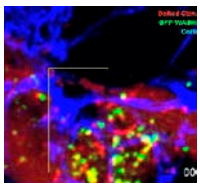

Video 4. **Dynamics of WASH-cortactin–positive endosomal puncta and of linear invadopodia in cells cultured on a layer of fibrillar collagen.** MDA-MB-231 cells expressing GFP-WASH (green) and DsRed-cortactin (red) were plated on a layer of Alexa Fluor 647–conjugated collagen I fibers (blue) for 30 min and imaged by confocal spinning disk microscopy (inverted Ti-E; Nikon). Bottom panels show split channels corresponding to the boxed region. Arrows point to WASH- and cortactin-positive puncta associated to dynamic endosomes interacting with region of the cell in contact with type I collagen fibers. Images were taken every minute for 60 min. Bar, 5 µm.

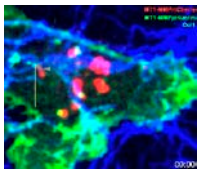

Video 5. **Flashes of MT1-MMPpHluorin define exocytic events at contact sites with collagen fibers.** MDA-MB-231 cells expressing MT1-MMPmCherry and MT1-MMPpHluorin were plated on a layer of Alexa Fluor 647–conjugated collagen I fibers (blue) for 30 min and imaged by confocal spinning disk microscopy (inverted Ti-E; Nikon). Botton panels show split channels corresponding to the boxed region. White arrowheads point to MT1-MMPpHluorin exocytic events (green flashes). Gray arrowheads correspond to eclipsed MT1-MMPpHluorin (red endosomes). Images were taken every 45 s for 27 min (indicated time is in min:s).

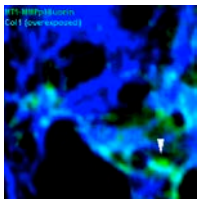

Video 6. **WASH-positive puncta are associated with MT1-MMP–containing endosomes undergoing exocytosis at contact sites with collagen fibers.** MDA-MB-231 cells expressing MT1-MMPpHluorin (green) and mCherry-WASH (red) were plated on a layer of Alexa Fluor 647–conjugated collagen I fibers (blue) for 30 min and imaged by confocal spinning disk microscopy (inverted Ti-E; Nikon). Left panel is a merge of the three channels and right panel shows only MT1-MMPpHluorin and collagen I fluorescence. White arrowheads point to MT1-MMPpHluorin exocytic events (green flashes). Gray arrowheads correspond to eclipsed MT1-MMPpHluorin (in acid pH endosomes). Images were taken every 30 s for 23 min (indicated time is in min:s).

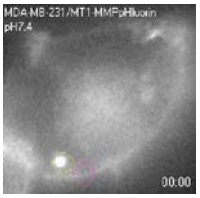

Video 7. **Long-lasting fusion pore opening during exocytosis of a MT1-MMP–containing endosome.** MDA-MB-231 cells expressing MT1-MMPpHLuorin were cultured on a layer of Cy3-labeled type I collagen fibers and subjected to a shift of the external pH alternating between 7.4 and 5.5. A MT1-MMP–positive endosome that undergoes exocytosis is circled in yellow. An adjacent region of the plasma membrane is circled in purple. Cells were imaged by wide-field videomicroscopy (IX71; Olympus). Images were taken every 2 s for 292 s (indicated time is in min:s).

Table S1. **Antibodies**

Antigen	Type (species)	Source
WASH	Polyclonal (rabbit)	Derivery et al., 2009
Exo84 (EXOC8)	Polyclonal (rabbit)	C. Yeaman (University of Iowa, Iowa City, IA)
Exo84 (EXOC8)	Polyclonal (goat)	Santa Cruz Biotechnology, Inc.
FAM21	Polyclonal (rabbit)	Santa Cruz Biotechnology, Inc.
Cortactin	Polyclonal (rabbit)	Sigma-Aldrich
Cortactin	Monoclonal (mouse)	EMD Millipore
p34-Arc (ARPC2)	Polyclonal (rabbit)	EMD Millipore
p34-Arc (ARPC2)	Monoclonal (mouse)	T. Stradal (University of Münster, Münster, Germany)
MT1-MMP	Monoclonal (mouse)	EMD Millipore
Sec8 (EXOC4)	Monoclonal (mouse)	BD
N-WASP	Polyclonal (rabbit)	Cell Signaling Technology
Rab7	Monoclonal (rabbit)	Cell Signaling Technology
VAMP7	Monoclonal (mouse)	T. Galli (Centre National de la Recherche Scientifique, Institut Jacques Monod, Paris, France)
HA epitope	Monoclonal (rat)	Roche
Col1-$^{3/4}$C	Polyclonal (rabbit)	ImmunoGlobe GmbH
Alexa Fluor–conjugated phalloidin		Invitrogen
Secondary antibodies		Jackson ImmunoResearch Laboratories, Inc.

Table S2. **siRNAs used in RNAi experiments**

Gene	Sense	Company
WASH #a	5′-GCAGCGUGAAGGAGCGAAA-3′	Thermo Fisher Scientific
WASH #b	5′- UGUCGGAUCUCUUCAACAA-3′	Thermo Fisher Scientific
WASH #d	5′- CCUACAAGAUGGGGUACUA-3′	Thermo Fisher Scientific
Exo84 #a	5′-AAGGCGGTTATAATTTGTCTT-3′	QIAGEN
Exo84 #d	5′-CACGGCTTTCTCATGAACGAT-3′	QIAGEN
MT1-MMP	5′-GGAUGGACACGGAGAAUUU-3′ 5′-GGAAACAAGUACUACCGUU-3′ 5′-GGUCUCAAAUGGCAACAUA-3′ 5′-GAUCAAGGCCAAUGUUCGA-3′	Thermo Fisher Scientific
N-WASP	5′-CAGCAGAUCGGAACUGUAU-3′ 5′-UAGAGAGGGUGCUCAGCUA-3′ 5′-GGUGUUGCUUGUCUUGUUA-3′ 5′-CCAGAAAUCACAACAAAUA-3′	Thermo Fisher Scientific
Non-targeting		Thermo Fisher Scientific
Cortactin	5′-CACCAGGAGCATATCAACATA-3′	QIAGEN
Cortactin	5′-ATGCAACTTATTGTATCTGAA-3′	QIAGEN

Reference

Derivery, E., C. Sousa, J.J. Gautier, B. Lombard, D. Loew, and A. Gautreau. 2009. The Arp2/3 activator WASH controls the fission of endosomes through a large multiprotein complex. *Dev. Cell*. 17:712–723. http://dx.doi.org/10.1016/j.devcel.2009.09.010

Provided online are two zip files and one macro.

Zip file S1 contains two macros: one for degradation spot detection and one for DAPI-stained nuclei counting, to compute the degradation index of collagen.

Text file S2 is the macro used to detect endosomes and aggregated spots.

Zip file S3 contains Matlab scripts used to quantify the distance between WASH spots and their closest neighbored cortactin spots (or Exo84 spots) for each endosome.

Discussion générale

I. Le réseau d'actine présent à la surface de l'endosome est finement régulé et indispensable au fonctionnement de l'endosome.

Les endosomes sont les principaux acteurs du trafic intracellulaire, notamment impliqués dans deux grands processus cellulaires que sont l'endocytose et l'exocytose, afin de permettre à la cellule d'interagir et de communiquer avec son environnement dans le but de maintenir l'homéostasie de la cellule et de participer à l'adhésion et à la migration cellulaire (Huotari and Helenius, 2011). Les endosomes représentent un carrefour entre voie de biosynthèse des protéines et voie d'endocytose. Les cargos et autres récepteurs présents à la surface de la cellule sont endocytés grâce à des vésicules d'endocytose qui une fois formées, fusionnent avec les structures endosomiales et notamment les endosomes dits précoces. Les protéines présentent au niveau de ces endosomes peuvent avoir plusieurs destinées : soit être recyclées à la membrane plasmique afin de permettre leur réutilisation, soit être envoyées vers l'appareil de Golgi, soit être envoyées en voie de dégradation (Grant and Donaldson, 2009). Pour cela, il est nécessaire une machinerie capable de reconnaitre les protéines présentes au niveau de la membrane de l'endosome afin de les ségréger et de les regrouper en domaines membranaires spécifiques et enfin, générer des intermédiaires de transport dans le but de délivrer ces protéines vers leur emplacement exacte (Seaman, 2008). De nombreux facteurs sont présents au niveau de la face cytosolique de la membrane des endosomes afin de permettre le tri des protéines ainsi que la formation d'intermédiaires de transport. Parmi ces facteurs, la superfamille des petites protéines G, notamment la famille des Rab, est indispensable à ces processus. Au-delà de définir une identité à l'endosome (précoce, tardif,…), les protéines Rab contrôlent plusieurs étapes essentielles du trafic vésiculaire incluant la formation de la vésicule, le transport, l'ancrage et la fusion de la vésicule avec la membrane receveuse (Stenmark and Olkkonen, 2001). Les membres les mieux connus et caractérisés sont Rab5 (présente au niveau de la face externe des endosomes précoces), Rab4 (voie de recyclage rapide),

Rab11 (voie de recyclage lente) ainsi que Rab7 et Rab9 (endosomes tardifs et voie de dégradation) (Barr, 2013; Galvez et al., 2012; Stenmark, 2009).

Les mécanismes de tri des protéines présentes au niveau de la membrane de l'endosome sont dépendants à la fois de la présence de filaments d'actine et du complexe retromer (Seaman, 2012). Le complexe retromer est composé des protéines Vps35, Vps26 et Vps29 (VPS : *vacuolar protein sorting*) formant un sous-complexe, ainsi que des membres de la famille des *sorting nexin* protéines (SNX) formant un second sous-complexe (Seaman, 2012). Les protéines SNX possèdent des domaines BAR (Bin–Amphiphysin–Rvs) qui se lient aux lipides et permettent d'induire des déformations et des courbures au niveau de la membrane de l'endosome tandis que les protéines Vps sont responsables de la reconnaissance des protéines et cargos à transporter (Attar and Cullen, 2010; Brankatschk et al., 2011; Cullen, 2008; McMahon and Gallop, 2005; Pons et al., 2012). Le complexe retromer est notamment impliqué dans le transport rétrograde du récepteur mannose 6 phosphate vers le golgi (Bonifacino and Hurley, 2008; Seaman, 2012) ainsi que dans le recyclage à la membrane plasmique du récepteur beta2 adrénergique ou encore du transporteur du glucose GLUT1 (!!! INVALID CITATION !!!; Seaman et al., 2013; Steinberg et al., 2013; Temkin et al., 2011)

L'actine joue un rôle important dans divers processus cellulaires physiologiques (motilité, endocytose, exocytose, phagocytose) et pathologiques (invasion, formation des invadopodes). Au cours de ces dernières années, de nombreuses études ont mis en évidence la présence d'une machinerie de polymérisation de l'actine à la surface des endosomes – aussi bien endosomes précoces, endosomes de recyclage et compartiments tardifs de type endosome multivésiculaires/lysosomes. Cette machinerie, incluant le complexe Arp2/3 et son complexe activateur WASH, est localisée au niveau de la face cytosolique de la membrane limitante des endosomes et permet de polymériser un réseau d'actine à la surface des endosomes (Derivery et al., 2009; Gautreau et al., 2014).
Il a par ailleurs été montre que la polymérisation de filaments d'actine à la surface des endosomes dépendante du complexe Arp2/3 peut être modulée par d'autres protéines tel que les annexines (annexine-A2) ainsi que Spire1 (Morel et al., 2009).

La polymérisation de filaments d'actine à la surface de l'endosome permet d'assister la formation d'extensions de membrane. Ce réseau d'actine a été impliqué dans la formation et la fission d'intermédiaires de transport nécessaires au recyclage de nombreux récepteurs et autres cargos, à partir des endosomes vers d'autres compartiments tel que le Trans Golgi Network (TGN) lors du transport rétrograde de cargos ou vers la membrane plasmique (Carnell et al., 2011; Derivery et al., 2009; Gomez and Billadeau, 2009; Monteiro et al., 2013; Puthenveedu et al., 2010; Zech et al., 2011). Ce processus implique la formation de tubules membranaires, générés par des déformations membranaires induites par l'association avec le réseau d'actine et les microtubules et impliquant des moteurs moléculaire (Gautreau et al., 2014) (voir Figure 25). De plus, il a été montré que ce réseau de filaments d'actine peut également interagir avec les cargos présents au niveau de la membrane de l'endosome et permettre un regroupement membranaire de ces protéines nécessaire à leur tri (Puthenveedu et al., 2010).

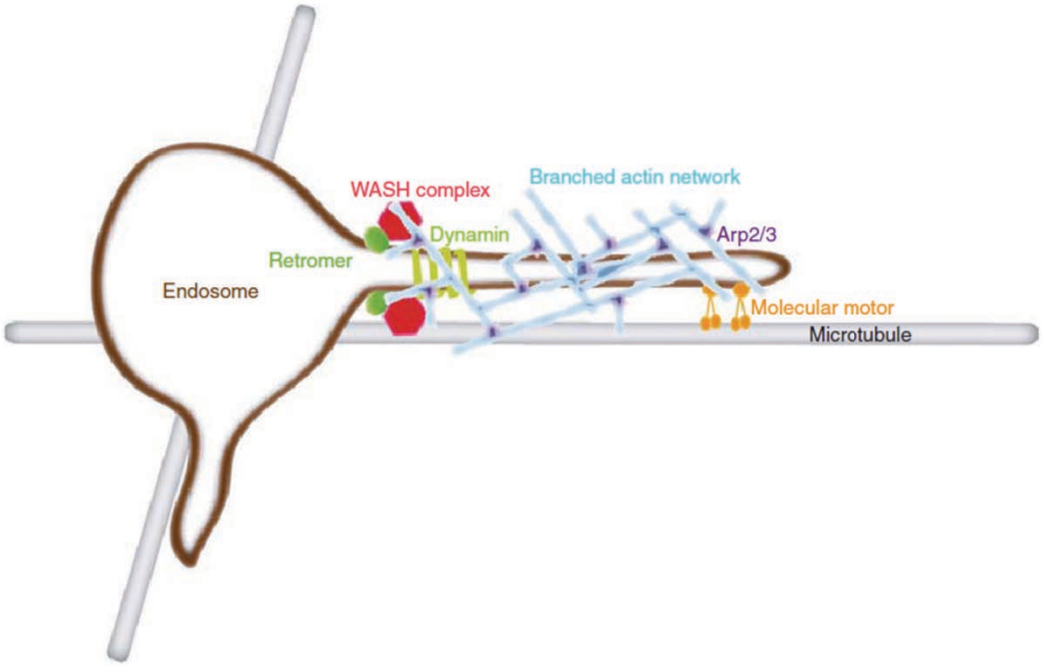

Figure 25: Le complexe WASH permet d'induire la polymérisation de filaments d'actine à la surface d'endosomes

Le complexe WASH présent à la surface des endosomes est responsable de la polymérisation de filaments d'actine, responsables, de concert avec les microtubules, de la formation de vésicules de transport permettant de recycler des protéines présentes au niveau de ces endosomes.

Extrait de Gautreau et al, "Function and Regulation of the Endosomal Fusion and Fission Machineries", Cold Spring Harb Perspect Biol, 2014 ; 6:a016832

De nombreuses protéines sont recrutées à la surface des endosomes tel que la dynamine (Derivery et al., 2009; Rosse et al., 2014), la cortactine (Monteiro et al., 2013; Rosse et al., 2014), le complexe exocyste (Monteiro et al., 2013) ainsi que des protéines à activité sérine/thréonine kinase telles que les protéines PKC atypiques (aPKC) (Rosse et al., 2014). Ces protéines ont été identifiées comme étant importantes dans le trafic intracellulaire de nombreux cargos, notamment MT1-MMP, ainsi que dans leur recyclage et leur adressage à la membrane plasmique via une régulation du réseau de filaments d'actine à la surface des endosomes.

Le complexe exocyste a été identifié comme un nouveau partenaire du complexe WASH (Monteiro et al., 2013). Nous avons montré que dans les cellules d'adénocarcinomes mammaires MDA-MB-231, les complexes WASH et exocyste interagissent et sont localisés en sous-domaines à la surface des endosomes contenant la protéase MT1-MMP. Ces complexes sont requis pour l'adressage des endosomes au niveau de la membrane plasmique de la cellule afin de permettre l'exocytose focalisée de MT1-MMP. Ce processus requiert la formation de tubules membranaires qui émanent de l'endosome et créent une connexion entre l'endosome et le milieu extracellulaire afin de permettre le passage de la protéase de l'endosome vers la membrane plasmique de la cellule et le milieu extracellulaire.

De manière intéressante, nos résultats et les données de la littérature suggèrent l'existence de deux réseaux branchés d'actine, d'orientation opposée et coopérant à l'interface entre les endosomes et la membrane plasmique au niveau de l'invadopode pour assurer l'arrimage des endosomes, la formation des connections endosomes/membrane plasmique et l'exocytose de MT1-MMP (voir Figure 26). Le premier réseau branché d'actine est présent au niveau de l'invadopode et sa polymérisation est dépendante du complexe Arp2/3 et de sa protéine activatrice N-WASP (Lorenz et al., 2004; Oser et al., 2009; Yamaguchi et al., 2005) (voir Figure 26). La première fonction de ce réseau branché d'actine est de générer la force requise à la protrusion membranaire au niveau de l'invadopode. Couplée à la dégradation de la matrice extracellulaire, la protrusion membranaire permet à la cellule tumorale de remodeler et de s'enfoncer activement à travers la matrice comme par exemple lors du passage de la membrane basale. Ce réseau membranaire d'actine pourrait également

constituer un site de reconnaissance pour l'endosome à la membrane plasmique afin de permettre l'arrimage et la fusion de l'endosome à la membrane plasmique et de faciliter un mécanisme dépendant respectivement du complexe exocyste et de la protéine SNARE VAMP7 (Sakurai-Yageta et al., 2008; Steffen et al., 2008). Enfin, ce réseau d'actine semble également impliqué dans la rétention de la protéase MT1-MMP au niveau de l'invadopode. Dans des cellules tumorales cultivées dans un réseau de collagène fibrillaire, il a été montré que la présence de filaments d'actine dont la polymérisation est dépendante de N-WASP participe au recrutement et à la localisation de la protéase MT1-MMP au niveau de la protrusion de la cellule (Yu et al., 2012). Cette étude a montré que la protéase MT1-MMP interagit avec l'actine par le motif LLY de son domaine C-terminal (Yu et al., 2012), également défini comme un motif essentiel pour l'endocytose de MT1-MMP via l'interaction avec le complexe adapteur AP-2 (Uekita et al., 2001).

Le second réseau branché d'actine, faisant face au premier est présent à la surface des endosomes contenant MT1-MMP ; sa polymérisation est dépendante du complexe Arp2/3 et du complexe activateur WASH (voir Figure 25 et Figure 26).
Il a été reporté que ces patchs d'actine sont nécessaire au tri et au recyclage de cargos présents au niveau des endosomes (Puthenveedu et al., 2010). Certains cargos participent au mécanisme de leur propre tri au niveau de la membrane de l'endosome, notamment par interaction avec le réseau d'actine. Il a été montré que le récepteur β2-adrénergique interagit avec les filaments d'actine présents à la surface de l'endosome. Cette interaction permet le tri du récepteur au niveau de tubules membranaires nécessaire à son recyclage au niveau de la membrane plasmique (Puthenveedu et al., 2010). De par sa capacité à lier l'actine (Yu et al., 2012), MT1-MMP pourrait être impliqué dans son propre tri en interagissant à la surface de l'endosome avec le réseau d'actine induit par WASH.

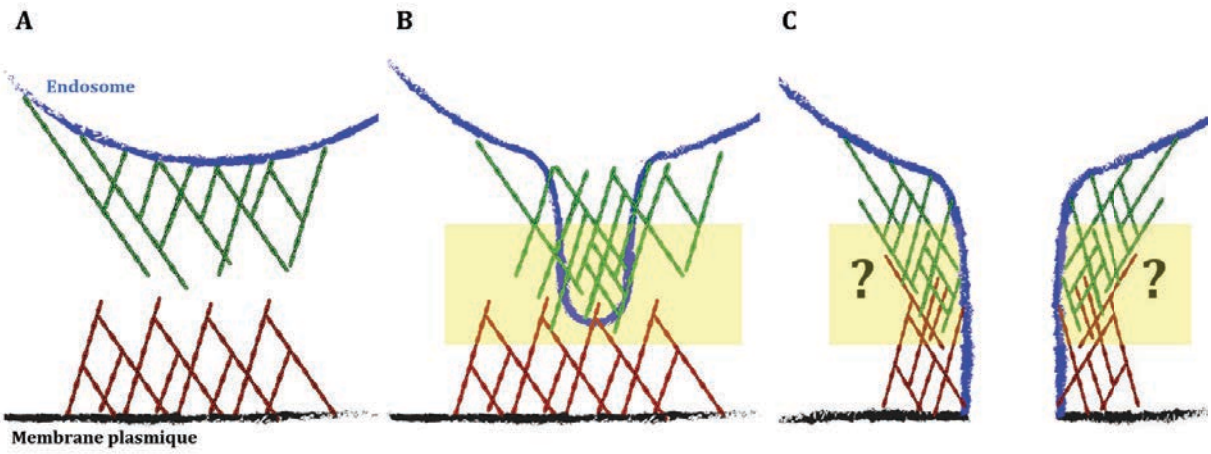

Figure 26: Mise en relation de deux réseaux branchés d'actine de polarité opposée

Le complexe WASH est responsable de la polymérisation d'un réseau de filaments d'actine à la surface des endosomes (en vert) tandis que N-WASP est nécessaire à la polymérisation d'un réseau de filaments d'actine à la membrane plasmique de la cellule (en rouge). L'interface entre ces deux réseaux (en jaune) définie le lieu de polymérisation et de rencontre des deux réseaux de filaments d'actine.

Il serait particulièrement intéressant de comprendre comment ces deux réseaux d'actine de polarité inverse coopèrent entre eux et pourraient s'imbriquer pour avoir un rôle physique dans l'arrimage de l'endosome au niveau des invadopodes qui, comme nous l'avons montré, peut durer plusieurs minutes. Il est également envisageable que ces réseaux d'actine soient importants afin d'empêcher la coalescence de l'endosome dans la membrane plasmique. Il a été montré chez l'amibe *dictyostelium discoideum* que la perte du manteau de filaments d'actine présent à la surface des vacuoles intracellulaire entraîne une importante agglomération de ces vacuoles entre elles (Drengk et al., 2003). Lors de l'exocytose des endosomes contenant MT1-MMP au niveau de l'invadopode, ces deux réseaux d'actine peuvent possiblement empêcher la fusion totale de l'endosome avec la membrane plasmique de la cellule, expliquant en partie le mécanisme de type « kiss-and-run » (avec un « run » très lent – en fait je proposerais le concept de « French kiss » pour désigner ce mécanisme au cours duquel l'endosome et la membrane restent en contact intime pendant plusieurs minutes) observé au niveau de l'invadopode des cellules tumorales (Monteiro et al., 2013).

Un autre aspect intéressant soulevé par mon travail concerne le rôle de l'interaction entre le complexe WASH et le complexe exocyste au-delà de leur coopération dans le

mécanisme d'arrimage et de formation de la connexion physique entre l'endosome et l'invadopode. Les renseignements obtenus lors des cribles double-hybride chez la levure ont permis de définir les domaines minimaux d'interactions entre WASH et Exo84 (ainsi que WASH et Sec3) (voir Figure 27).

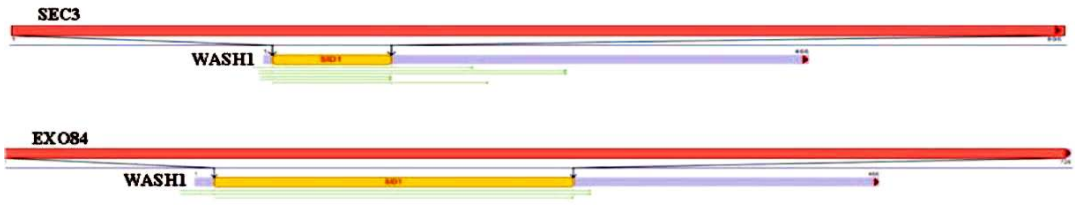

Figure 27 : Carte des domaines d'interaction de Sec3 et Exo84 avec WASH obtenus par cribles double hybride.

Les séquences complètes de Sec3 et Exo84 (rouge) ont été utilisées comme proie lors de cribles double hybride chez la levure. Des clones isolés de WASH (vert) ont permis de définir les domaines minimum d'interaction (jaune) au niveau de la région N-terminale de WASH, précédemment identifiée comme impliquée dans l'interaction avec le reste du complexe WASH. *Collaboration Hybrigenics*

Il serait intéressant de savoir si l'interaction entre le complexe WASH et le complexe exocyste intervient dans le recrutement d'un ou de ces complexes à la surface de l'endosome. Nous avons montré que la perte d'expression des sous-unités Exo84 (et Sec8, non publié) du complexe exocyste n'affectait pas le recrutement de WASH à la surface de l'endosome (Monteiro et al., 2013). Par contre nous n'avons pas déterminé si le complexe WASH influence le recrutement de l'exocyste sur l'endosome.

Par ailleurs, il serait intéressant de savoir si l'interaction de la protéine WASH avec le complexe exocyste est compétitive avec d'autres interactions impliquant la protéine WASH ; en premier lieu, avec les autres sous-unités du complexe WASH (WASH, Strumpellin, SWIP, FAM-21 et CCDC-53). En interférant avec l'interaction de WASH avec les autres sous-unités du complexe, Sec3 et Exo84 pourraient influencer l'activité de WASH dans le mécanisme d'activation du complexe Arp2/3 et l'assemblage de l'actine sur l'endosome. En accord avec cette hypothèse, nous avons observé une augmentation de la présence de la cortactine associée aux domaines de WASH dans les cellules déplétées pour Exo84 (Monteiro et al., 2013). Etant une protéine pouvant lier l'actine, cette accumulation de cortactine traduit une présence accrue de filaments d'actine sans doute corrélée à une polymérisation exacerbée de l'actine. La perte d'expression de la sous-unité Exo84 du complexe exocyste peut ainsi avoir plusieurs effets :

- l'absence de la sous-unité Exo84 peut induire une activité plus importante du complexe WASH, favorisant une activité accrue dans le mécanisme de polymérisation d'actine. Ce résultat indique que la sous-unité Exo84 (ou plus généralement le complexe exocyste) inhiberait l'activité de polymérisation d'actine médiée par WASH lorsque qu'elle interagit avec le complexe WASH.
- l'absence de la sous-unité Exo84 perturberait la dynamique des filaments d'actine présents à la surface de l'endosome. Exo84 pourrait permettre le recrutement de protéines régulatrices de l'actine tel que la cofiline afin de coopérer avec ces protéines et permettre de scinder les filaments existant et permettre le renouvellement du réseau.

Par ailleurs, des études menées par le groupe de Wei Guo ont mis en évidence l'implication du complexe exocyste dans les mécanismes de polymérisation de filaments d'actine dépendante du complexe Arp2/3 et de sa protéine activatrice WAVE (Liu et al., 2012; Zuo et al., 2006). Ces études ont montré que la sous-unité Exo70 du complexe exocyste interagit directement avec le complexe Arp2/3 et est impliquée dans la formation de protrusions dépendante de la polymérisation d'actine (Zuo et al., 2006). Par la suite, des études plus approfondies ont permis de montrer que l'interaction entre la sous-unité Exo70 du complexe exocyste et le complexe Arp2/3 favorisait l'interaction entre le complexe Arp2/3 et sa protéine activatrice WAVE2, permettant ainsi d'augmenter l'efficacité de nucléation d'un réseau branché de filaments d'actine au cours d'expériences de polymérisation d'actine *in vitro* (Liu et al., 2012). L'interaction entre le complexe exocyste - via la sous-unité Exo70 - et le complexe Arp2/3 au niveau de la membrane plasmique de la cellule favoriserait la polymérisation de filaments d'actine nécessaire à la formation d'un lamellipode requis à la migration cellulaire.

Ces travaux, ainsi que mon travail de thèse, montrent que le complexe exocyste est impliqué à la polymérisation de filaments d'actine à la fois au niveau de la membrane plasmique de la cellule qu'à la surface de l'endosome. Le complexe exocyste pourrait donc moduler la polymérisation d'actine à la fois en interagissant avec le complexe Arp2/3 ou avec les protéines activatrices telles que WASH.

Par ailleurs, il a été montré, principalement par des expériences de co-immunoprécipiation *in cellulo*, que la protéine WASH interagit entre autres avec la tubuline (Gomez and Billadeau, 2009), le complexe retromer (Gomez and Billadeau, 2009; Harbour et al., 2010; Seaman, 2012), la dynamine (Derivery et al., 2009) ainsi

qu'avec le complexe Arp2/3 (Derivery et al., 2009; Pollard, 2007) au niveau de la face cytosolique des endosomes. L'interaction du complexe exocyste avec le complexe WASH est-elle dépendante d'une autre interaction ? Est-elle compétitive avec une interaction impliquant le complexe WASH ? Des expériences de co-immunoprecipitation dans des conditions de perte d'expression et/ou de fonction de protéines impliquées dans ces interactions (sous-unités des complexes Arp2/3 et retromer, dynamine, cortactine) pourront permettre de répondre à ces questions.

Un autre travail mené au laboratoire auquel j'ai contribué (voir annexe) suggère que la polymérisation d'actine à la surface des endosomes est contrôlée par les protéines de polarité PKC atypiques (aPKC) (Rosse et al., 2014). Nous avons montré que les aPKCs sont présentes à la surface des endosomes contenant MT1-MMP et phosphorylent la cortactine, ce qui régule l'interaction de la cortactine avec la dynamine et le recrutement de la dynamine sur les endosomes. De par son rôle dans la fission membranaire décrit dans la littérature dans des processus tel que l'endocytose, la dynamine permet la scission d'intermédiaires de transports formés à partir des endosomes (Derivery et al., 2009; Rosse et al., 2014). Dans les cellules MDA-MB-231, ce mécanisme permet le recyclage de la protéase MT1-MMP à la surface de la cellule et contribue au mécanisme de dégradation de la matrice extracellulaire par les cellules tumorales (Rosse et al., 2014). Des expériences d'immunohistochimie sur des coupes de tumeurs mammaires nous ont permis de mettre en évidence une co-surexpression de la protéase MT1-MMP et de aPKC dans certains sous-types de cancers du sein, correspondant à des formes agressives. Ce travail a été réalisé en collaboration avec des cliniciens de l'hôpital Curie (programme incitatif et coopératif coordonné par Anne-Vincent Salomon et Philippe Chavrier).

Au-delà de leur rôle dans la génération d'intermédiaires de transports à la surface d'endosome, les aPKCs peuvent possiblement être impliquées - via la phosphorylation de la cortactine – dans le recrutement de la dynamine au niveau des zones d'exocytose de MT1-MMP, afin de scinder les tubules membranaires et ainsi mettre fin au contact entre l'endosome et l'invadopode (voir Figure 28).

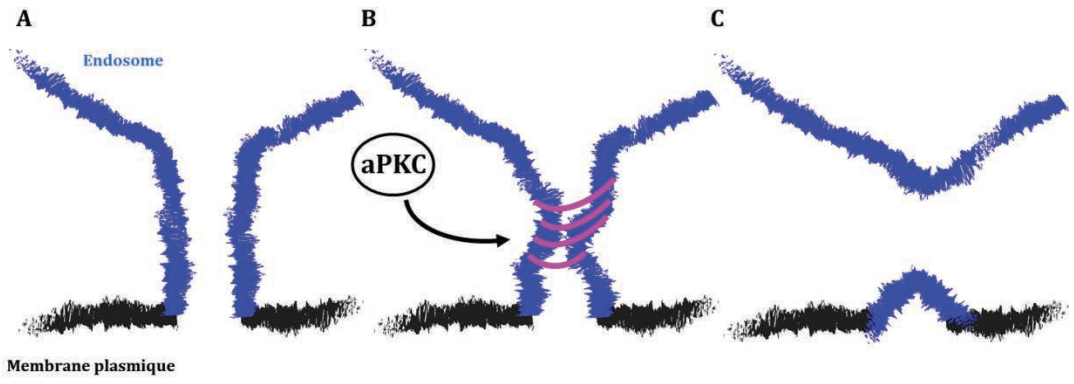

Figure 28 : Mécanisme impliquant les aPKC et la dynamine lors de l'exocytose des endosomes contenant MT1-MMP.

La dynamine est représentée en rose et pourrait permettre de scinder les tubules présents entre l'endosome et la membrane plasmique.

L'ensemble de ces travaux montre que les protéines WASH, cortactine, dynamine, aPKC et Exo84 sont présentes à la surface d'endosomes contenant MT1-MMP et permettent de réguler la polymérisation de filaments d'actine nécessaire au recyclage de la protéase au niveau de la membrane plasmique.

II. Contrôle de l'exocytose de MT1-MMP dans un environnement tridimensionnel

Mon travail de thèse a mis en évidence le mécanisme d'exocytose de la protéase MT1-MMP dépendant de l'actine – via le complexe WASH - et du complexe exocyste au niveau des invadopodes, nécessaire à l'activité dégradative de la matrice extracellulaire par la cellule tumorale. Ce travail a contribué à montrer le rôle de MT1-MMP dans les processus dégradatifs et invasifs, à la fois sur un substrat matriciel bidimensionnel (couche de gélatine) et dans un environnement tridimensionnel.

Cependant, certaines études ont montré que sous certaines conditions, la migration des cellules tumorales à travers des matrices extracellulaires reconstituées *in vitro* pouvait être indépendante de l'activité protéolytique des cellules (Sabeh et al., 2009; Wolf et al., 2013). Comme décrit dans le chapitre introductif, l'invasion cellulaire dans un réseau

fibrillaire dense nécessite l'activité dégradative des cellules tandis que l'invasion dans un réseau fibrillaire large (ou présentant des défauts de cross-linking dus au mode préparatoire du collagène) est indépendante des protéases (voir Figure 29A). Il semblerait donc que la cellule soit capable d'adapter son mode de migration à son environnement par des mécanismes permettant à la cellule d'intégrer les signaux envoyés par l'environnement (nature de la matrice, porosité,…) et de les traduire de manière intracellulaire de façon à permettre à la cellule de modifier son processus migratoire.

Les études précédemment citées ont également mis en évidence l'importance du noyau dans l'invasion de la cellule tumorale à travers un environnement tridimensionnel, aboutissant à la notion que le noyau est un élément limitant au cours du processus invasif. Le noyau cellulaire constitue l'organelle le plus volumineux de la cellule et également le plus rigide et le moins déformable (Harada et al., 2014; Wolf et al., 2013; Wolf et al., 2007) (voir Figure 29B). Des pores suffisamment larges doivent être crées au sein du réseau fibrillaire afin de laisser passer le noyau.

Lorsque des cellules tumorales sont traitées par un inhibiteur pharmacologique des MMPs (GM6001) et sont cultivées dans un réseau de collagène fibrillaire non-permissifs – c'est-à-dire présentant des pores étroits ne laissant pas diffuser les cellules - la migration des cellules au sein de ce réseau est freinée. Dans ces conditions, le noyau des cellules en présence de l'inhibiteur présentent une morphologie particulière (Wolf et al., 2013; Wolf et al., 2007) (voir Figure 29B). Les fibres de collagène n'étant pas dégradées par les cellules, elles constituent un obstacle au mouvement cellulaire et nucléaire : la cellule essaye de passer mais son noyau se retrouve coincé au niveau des pores interfibrillaires étriqués, créant ainsi des constrictions au niveau du noyau. Ces travaux mettent en évidence l'implication de l'activité dégradative de la cellule dans la relaxation des fibres de collagène nécessaire au passage du noyau de la cellule.

La cellule est donc capable de sentir son environnement et de mettre en place une réponse adaptée aux signaux envoyés par l'extérieur. Une hypothèse intéressante réside dans le fait que l'intégration des signaux externes à la cellule fasse intervenir directement le noyau de la cellule (voir Figure 29C). Au travers de son noyau, la cellule serait capable d'assimiler le fait que la matrice est permissive ou non à son déplacement, déclenchant une réponse appropriée : exocytose de MT1-MMP ou pas (voir Figure 29C).

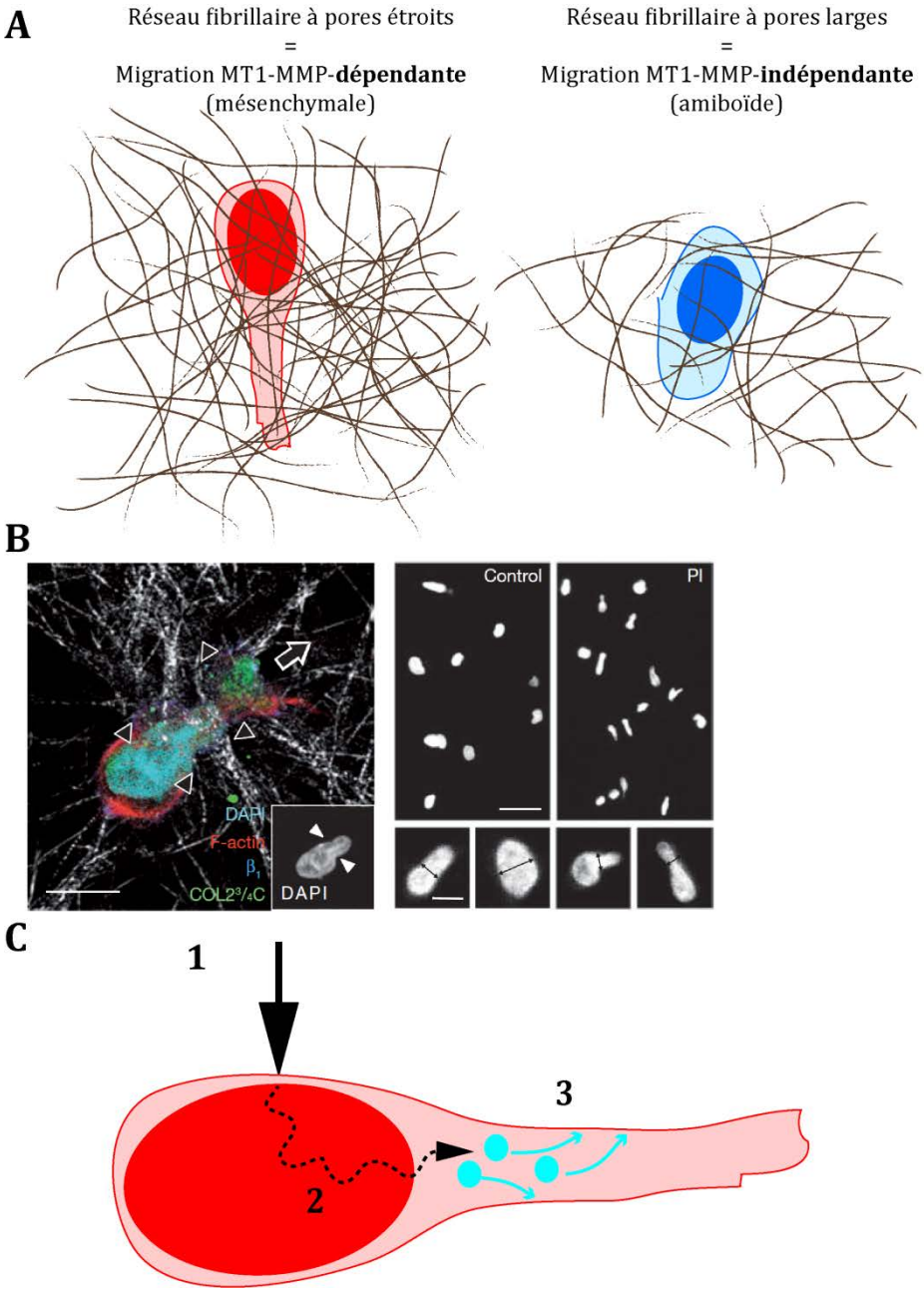

Figure 29 : Rôle du noyau cellulaire dans la migration à travers un réseau de collagène fibrillaire

(A) Selon la nature du réseau de collagène, la cellule va adopter un mode de migration dépendant ou non de l'activité protéolytique de MT1-MMP. **(B)** Observation d'une cellule tumorale traitée par un inhibiteur de protéases et cultivée au sein d'un réseau de collagène fibrillaire. Ne pouvant plus dégrader les fibres de collagène, la cellule est coincée au sein de ce réseau et le noyau présente des déformations (encart et milieu). Echelle : 10µm image de gauche et encart de l'image de droite ; 50µm image de droite en haut, condition control. *Extrait de Wolf et al, "Multi-step pericellular proteolysis controls the transition from individual to collective cancer cell invasion", Nat. Cell. Biology, (2007) 9:8 893-904.* **(C)** Représentation schématique de l'hypothèse selon laquelle le noyau cellulaire est capable de sentir une contrainte externe à la cellule (1 ; flèche noire) et de traduire le signal imposé par cette contrainte de manière intracellulaire (2 ; flèche pointillé) afin de moduler son activité dégradative via le contrôle de l'exocytose des endosomes contenant MT1-MMP (3 ; bleu).

Le noyau peut éventuellement agir sur l'activité dégradative de la cellule tumorale de différentes façons :
-soit en contrôlant la transcription de gènes codant pour des protéines impliquées dans les processus invasifs. Une étude transcriptomique de l'expression de certaines protéines impliquées notamment dans la formation des invadopodes (Cortactine, N-WASP, Tks5,…), dans le mécanisme d'exocytose de MT1-MMP (WASH, complexe exocyste, VAMP7,…) ainsi que sur le niveau d'expression des protéases elle-mêmes (MT1-MMP, MMP-2, MMP-9) permettrait de mettre en évidence cette hypothèse.

- soit en modulant la machinerie d'exocytose.

Un projet en cours au laboratoire tente de mettre en évidence le rôle et l'influence de la matrice extracellulaire dans les mécanismes d'exocytose de MT1-MMP au sein d'un réseau de collagène fibrillaire. Des résultats préliminaires ont montré que lorsque la rigidité des fibres de collagène était augmentée (par différents types de traitements incluant le traitement par la lysyl-oxydase, LOX, qui est surexprimée dans certains cancers (Kirschmann et al., 2002)), les cellules au contact de ces fibres présentaient un nombre élevé d'évènements d'exocytose comparé aux cellules au contact de fibres dont la rigidité n'est pas modifiée. Ces résultats montrent que l'application d'une contrainte plus importante (fibres plus rigides) au niveau de la cellule a pour effet de stimuler le mécanisme d'exocytose de la protéase MT1-MMP.

Des travaux en cours au laboratoire auxquels je contribue suggèrent que la stimulation de l'exocytose de MT1-MMP passe par une coopération entre le noyau cellulaire et les endosomes intracellulaire contenant la protéase.

Pour cela, nous utilisons la lignée cellulaire d'adénocarcinomes mammaires MDA-MB-231 et nous observons leur comportement dans un environnement tridimensionnel de collagène fibrillaire. Dans ces conditions de culture, les cellules arborent une longue et unique protrusion cellulaire précédent le noyau (voir Figure 30). De manière fort intéressante, nous avons observé que les endosomes contenant la protéase MT1-MMP sont présents et exocytent leur contenu à l'avant du noyau (voir Figure 30A). Lorsque ces cellules sont traitées par le GM6001 (inhibiteurs à large spectre des MMPs), l'activité

dégradative de la cellule est inhibée et la protéase s'accumule au niveau des fibres de collagène sans toutefois les dégrader et les relaxer (voir Figure 30B). Le noyau se retrouve progressivement coincé dans le réseau fibrillaire et présente des déformations (voir Figure 30B). De manière intéressante, nous avons également observé que les endosomes sont associés à la constriction du noyau imposée par les fibres de collagène (voir Figure 30B), laissant penser que la constriction nucléaire pourrait être un signal de recrutement et d'exocytose des endosomes pour permettre la relaxation de la contrainte imposée par les fibres de collagène sur le noyau.

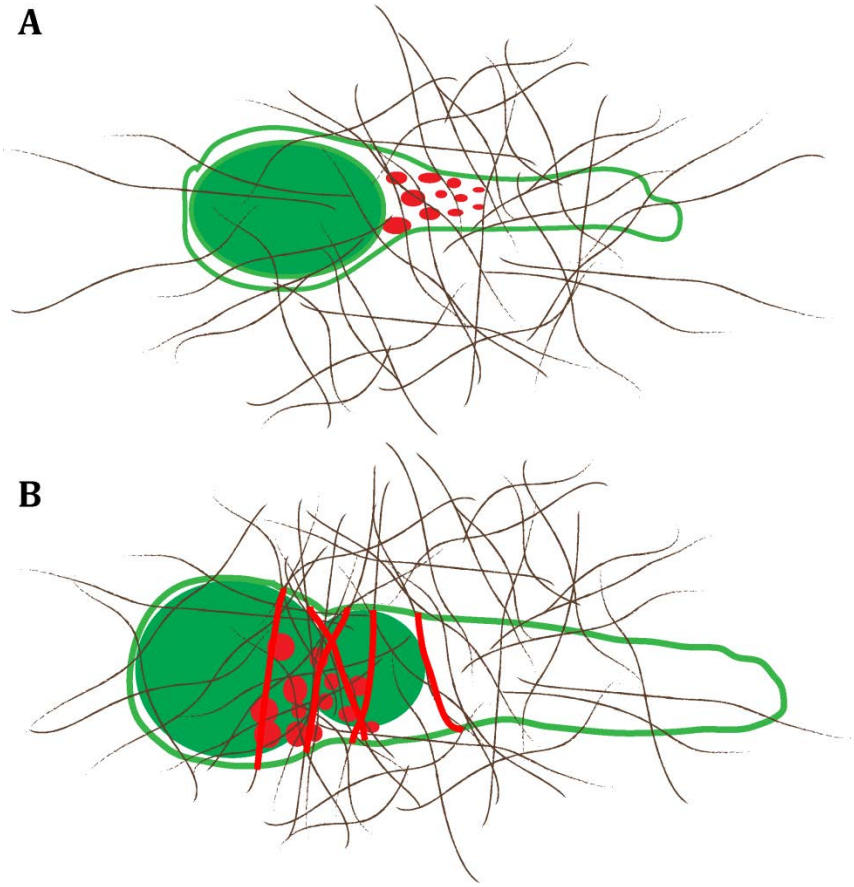

Figure 30 : Effet de l'inhibition de l'activité catalytique de MT1-MMP sur des cellules tumorales MDA-MB-231 cultivées dans un réseau de collagène fibrillaire.

(A) Dans une cellule tumorale envahissant un réseau de collagène fibrillaire, les endosomes contenant la protéase MT1-MMP (rouge) sont présents à l'avant du noyau (vert). **(B)** Lorsque les cellules sont traitées par l'inhibiteur de protéases GM6001, l'activité dégradative de MT1-MMP est inhibée. La protéase d'accumule alors au niveau des fibres de collagènes (traits rouge) qui ne sont pas relaxées et imposent une contrainte au niveau du noyau qui se retrouve coincé et exhibe des déformations. Les endosomes contenant MT1-MMP s'accumule au niveau des constrictions nucléaires (rouge).

Afin de confirmer l'hypothèse faisant état d'une stimulation de l'exocytose de MT1-MMP par une coopération entre le noyau cellulaire et les endosomes intracellulaire contenant la protéase, il est tout d'abord essentiel de mettre en évidence un possible lien entre les endosomes et l'enveloppe nucléaire.

Les endosomes sont des vésicules intracellulaires associées au réseau de microtubules et dont le trafic intracellulaire est dépendant des microtubules (Grant and Donaldson, 2009). Les microtubules sont polymérisés au niveau du MTOC de la cellule (*Microtubules organizing center*). De nombreux liens ont été mis en évidence entre le MTOC et le noyau cellulaire, notamment via l'association des microtubules aux nesprines, protéines insérées dans l'enveloppe nucléaire et permettant d'associer le noyau au cytosquelette d'actine et aux microtubules (Gundersen and Worman, 2013; Isermann and Lammerding, 2013). Certaines études ont montré que dans des conditions perte d'expression des nesprines, le MTOC se trouvait à une distance plus importante du noyau par rapport aux conditions contrôle (Schneider et al., 2011).
Il serait intéressant d'observer le comportement des endosomes contenant MT1-MMP dans des conditions de perte d'expression et/ou de fonction des nesprines dans les cellules tumorales MDA-MB-231 cultivées dans un réseau de collagène fibrillaire. Il serait également intéressant de comprendre si la perte de fonction des nesprines rompt un possible lien entre les endosomes positifs pour MT1-MMP et le noyau cellulaire et par conséquent, perturbe l'activité dégradative de la cellule en entraînant un défaut d'exocytose de la protéase. Ces observations pourraient permettre de mettre en évidence l'impact du noyau dans le contrôle de l'exocytose de MT1-MMP.

Dans un second temps, une étude de la rigidité nucléaire pourrait apporter des précisions quant à l'influence du noyau dans le mécanisme d'exocytose de MT1-MMP dans un réseau de fibres de collagène. Les lamines sont des protéines associées à l'enveloppe interne du noyau et impliquées dans la rigidité du noyau (Swift and Discher, 2014). Il a été montré que plus le niveau d'expression protéique des lamines est élevé, plus l'invasion dans un environnement tridimensionnel est freinée, mettant en évidence le fait que la rigidité nucléaire constitue une contrainte à la migration cellulaire à travers un réseau fibrillaire (Harada et al., 2014; Wolf et al., 2013). Il serait intéressant de comprendre comment les cellules réagissent à une perte d'expression des lamines et

notamment, observer si dans ces conditions, l'activité dégradative de la cellule est requise ou non. Ces résultats pourront mettre en évidence le fait que le noyau cellulaire puisse contrôler son propre passage à travers le réseau de collagène fibrillaire via un contrôle de la machinerie d'exocytose de MT1-MMP.

En parallèle de son rôle dans la dégradation des tissus environnants par les cellules tumorales, la protéase MT1-MMP - enzyme clé du programme métastatique – semble être importante dans la translocation du noyau cellulaire à travers les fibres de collagène constituants les tissus adjacents à la tumeur. La cellule – via son noyau - serait capable de sentir son environnement et de répondre à ces signaux en modulant son activité dégradative notamment en contrôlant la machinerie d'exocytose de la protéase MT1-MMP.

Remerciements

Une thèse étant avant tout une aventure collective, je tiens à remercier les nombreuses personnes qui, de près ou de loin, ont participé à cette histoire.

Je tiens tout d'abord à remercier chaleureusement le Professeur Joëlle Sobczak-Thépot, le Professeur Thierry Soldati, le Dr. Corinne Albigès-Rizo ainsi que le Dr. Ana-Maria Lennon-Duménil d'avoir accepté de faire partie de mon jury de thèse et d'avoir apporté leur regard et expertise à l'évaluation de mon travail de thèse.

Viens le tour de l'inévitable directeur de thèse, le Dr Philippe Chavrier. Voilà maintenant quelques années que je suis entré dans le laboratoire de Philippe afin d'y effectuer mon stage de Master 1. De l'élève timide et peu confiant, il ne reste pas grand-chose. Philippe a fait preuve d'une exigence contagieuse qui m'a permis de surmonter mes angoisses, de m'affirmer et de m'épanouir jour après jour, afin de devenir le 'scientifique' (sur ce point, seul l'avenir nous le dira) que je suis aujourd'hui. Je suis fier et content du travail accompli sous sa supervision. Je lui suis, et serai, toujours reconnaissant…

Un grand merci à « la garde rapprochée® » : Maud Hertzog, Carine Rossé, Guillaume Montagnac et Mathieu Boissan. Maud m'a permis d'effectuer mon stage de Master 1 dans le laboratoire de Philippe, c'est en quelque sorte elle qui m'a ouvert les portes de ce laboratoire. Elle a été précieuse à mes débuts et je lui dois un énorme merci. Carine a en quelque sorte « pris le relai » et a été très importante dans l'apprentissage de la vie de laboratoire, présente au quotidien par son aide et les nombreuses discussions enrichissantes. Je ne sais pas comment j'aurais survécu dans le laboratoire sans Guillaume et nos innombrables discussions sportives, interrompues par ci par là de quelques remarques scientifiques, bien évidement. Enfin, Mathieu Boissan (MCU-PH… je n'ai jamais su si c'était son deuxième nom de famille…), avec qui j'ai appris que 'rigueur' et 'travail' sont des maîtres mots dans la réussite d'un projet et surtout, que « chaque mot doit être à sa place ».

Un grand merci aux autres membres du laboratoire, ô combien importants dans la vie quotidienne du laboratoire: Valentina Marchesin, Emilie Lagoutte, Catalina Lodillinsky, Marie Irondelle, Antonio Castro-Castro, Elvira Infante, Alan Guichard, Joanna Cyrta, Michèle Colineau ainsi que ceux de la première heure, Gaëlle le Dez, Floria Lizarraga et Mercedes Rey-Rey.

Merci à Jean Salamero et aux membres de son équipe, Vincent Fraisier, Lucie Sengmanivong, François Waharte, Ludovic Leconte, Perrine Paul-Gilloteaux, Jérôme Boulanger et Charles Geudry, pour leur aide dans l'apprentissage et l'utilisation des différentes techniques de microscopie de pointe dont jouit l'Institut Curie ainsi que dans la compréhension et l'analyse d'image.

Un grand merci à nos proches collaborateurs pour leur aide ainsi que les nombreuses discussions ayant permis d'aboutir à une belle histoire : Alexis Gautreau, Claire Desnos, Francois Darchen et David Perrais. Merci également aux membres de mon comité de thèse, le Dr. Ana Maria Lennon-Duménil et le Dr. Alexandre Benmerah, d'avoir suivi et évalué l'évolution de mon travail au cours de ses années.

Un grand merci à tous les collaborateurs de Curie avec qui j'ai pu discuter, échanger, apprendre au quotidien, très souvent de manière informelle mais toujours constructive.

Merci à Jean-Baptiste, à Davide, à Alex et aux autres membres de la « team » pour tous ces bons moments de sports, de joie et de peine, mais avant tout, de partage et d'amitié.

Pour finir, merci à ceux de l'ombre, ceux avec qui nous profitons des bons moments et qui surtout, supportent les nombreux moments de peine et de frustration. Merci aux amis de tous âges et de toutes nationalités. Un grand merci à celle qui partage ma vie et qui, par sa positivité et sa générosité sans borne, m'a énormément aidé et soutenu dans les moments les plus difficiles... Por fim, um grande obrigado aos meus pais e minha irmã pela paciência que tiveram e ajuda que me deram ao longo destes anos todos. *Afinal, houve estrelas no céu a dourar 'este' caminho…*

Références

Abram, C.L., D.F. Seals, I. Pass, D. Salinsky, L. Maurer, T.M. Roth, and S.A. Courtneidge. 2003. The adaptor protein fish associates with members of the ADAMs family and localizes to podosomes of Src-transformed cells. *The Journal of biological chemistry*. 278:16844-16851.

Ahmed, N., S. Maines-Bandiera, M.A. Quinn, W.G. Unger, S. Dedhar, and N. Auersperg. 2006. Molecular pathways regulating EGF-induced epithelio-mesenchymal transition in human ovarian surface epithelium. *American journal of physiology. Cell physiology*. 290:C1532-1542.

Al-Raawi, D., H. Abu-El-Zahab, M. El-Shinawi, and M.M. Mohamed. 2011. Membrane type-1 matrix metalloproteinase (MT1-MMP) correlates with the expression and activation of matrix metalloproteinase-2 (MMP-2) in inflammatory breast cancer. *International journal of clinical and experimental medicine*. 4:265-275.

Albiges-Rizo, C., O. Destaing, B. Fourcade, E. Planus, and M.R. Block. 2009. Actin machinery and mechanosensitivity in invadopodia, podosomes and focal adhesions. *Journal of cell science*. 122:3037-3049.

Albrechtsen, R., M. Kveiborg, D. Stautz, J. Vikesa, J.B. Noer, A. Kotzsh, F.C. Nielsen, U.M. Wewer, and C. Frohlich. 2013. ADAM12 redistributes and activates MMP-14, resulting in gelatin degradation, reduced apoptosis and increased tumor growth. *Journal of cell science*. 126:4707-4720.

Albrechtsen, R., D. Stautz, A. Sanjay, M. Kveiborg, and U.M. Wewer. 2011. Extracellular engagement of ADAM12 induces clusters of invadopodia with localized ectodomain shedding activity. *Experimental cell research*. 317:195-209.

Alexander, S., G.E. Koehl, M. Hirschberg, E.K. Geissler, and P. Friedl. 2008. Dynamic imaging of cancer growth and invasion: a modified skin-fold chamber model. *Histochemistry and cell biology*. 130:1147-1154.

Annabi, B., M. Lachambre, N. Bousquet-Gagnon, M. Page, D. Gingras, and R. Beliveau. 2001. Localization of membrane-type 1 matrix metalloproteinase in caveolae membrane domains. *The Biochemical journal*. 353:547-553.

Arsenault, D., K. Brochu-Gaudreau, M. Charbonneau, and C.M. Dubois. 2013. HDAC6 deacetylase activity is required for hypoxia-induced invadopodia formation and cell invasion. *PloS one*. 8:e55529.

Artym, V.V., K. Matsumoto, S.C. Mueller, and K.M. Yamada. 2011. Dynamic membrane remodeling at invadopodia differentiates invadopodia from podosomes. *European journal of cell biology*. 90:172-180.

Artym, V.V., Y. Zhang, F. Seillier-Moiseiwitsch, K.M. Yamada, and S.C. Mueller. 2006. Dynamic interactions of cortactin and membrane type 1 matrix metalloproteinase at invadopodia: defining the stages of invadopodia formation and function. *Cancer research*. 66:3034-3043.

Atkinson, S.J., M.L. Patterson, M.J. Butler, and G. Murphy. 2001. Membrane type 1 matrix metalloproteinase and gelatinase A synergistically degrade type 1 collagen in a cell model. *FEBS letters*. 491:222-226.

Attar, N., and P.J. Cullen. 2010. The retromer complex. *Advances in enzyme regulation*. 50:216-236.

Aumailley, M., L. Bruckner-Tuderman, W.G. Carter, R. Deutzmann, D. Edgar, P. Ekblom, J. Engel, E. Engvall, E. Hohenester, J.C. Jones, H.K. Kleinman, M.P. Marinkovich, G.R. Martin, U. Mayer, G. Meneguzzi, J.H. Miner, K. Miyazaki, M. Patarroyo, M. Paulsson, V. Quaranta, J.R. Sanes, T. Sasaki, K. Sekiguchi, L.M. Sorokin, J.F. Talts, K. Tryggvason, J. Uitto, I. Virtanen, K. von der Mark, U.M. Wewer, Y. Yamada, and P.D. Yurchenco. 2005. A simplified laminin nomenclature. *Matrix biology : journal of the International Society for Matrix Biology*. 24:326-332.

Ayala, I., M. Baldassarre, G. Giacchetti, G. Caldieri, S. Tete, A. Luini, and R. Buccione. 2008. Multiple regulatory inputs converge on cortactin to control invadopodia biogenesis and extracellular matrix degradation. *Journal of cell science*. 121:369-378.

Bair, E.L., M.L. Chen, K. McDaniel, K. Sekiguchi, A.E. Cress, R.B. Nagle, and G.T. Bowden. 2005. Membrane type 1 matrix metalloprotease cleaves laminin-10 and promotes prostate cancer cell migration. *Neoplasia*. 7:380-389.

Baldassarre, M., A. Pompeo, G. Beznoussenko, C. Castaldi, S. Cortellino, M.A. McNiven, A. Luini, and R. Buccione. 2003. Dynamin participates in focal extracellular matrix degradation by invasive cells. *Molecular biology of the cell*. 14:1074-1084.

Bao, Y., J.A. Lopez, D.E. James, and W. Hunziker. 2008. Snapin interacts with the Exo70 subunit of the exocyst and modulates GLUT4 trafficking. *The Journal of biological chemistry*. 283:324-331.

Barcelona, P.F., J.R. Jaldin-Fincati, M.C. Sanchez, and G.A. Chiabrando. 2013. Activated alpha2-macroglobulin induces Muller glial cell migration by regulating MT1-MMP activity through LRP1. *FASEB journal : official publication of the Federation of American Societies for Experimental Biology*. 27:3181-3197.

Barr, F.A. 2013. Review series: Rab GTPases and membrane identity: causal or inconsequential? *The Journal of cell biology*. 202:191-199.

Beaty, B.T., V.P. Sharma, J.J. Bravo-Cordero, M.A. Simpson, R.J. Eddy, A.J. Koleske, and J. Condeelis. 2013. beta1 integrin regulates Arg to promote invadopodial maturation and matrix degradation. *Molecular biology of the cell*. 24:1661-1675, S1661-1611.

Beaty, B.T., Y. Wang, J.J. Bravo-Cordero, V.P. Sharma, V. Miskolci, L. Hodgson, and J. Condeelis. 2014. Talin regulates moesin-NHE-1 recruitment to invadopodia and promotes mammary tumor metastasis. *The Journal of cell biology*. 205:737-751.

Berrier, A.L., and K.M. Yamada. 2007. Cell-matrix adhesion. *Journal of cellular physiology*. 213:565-573.

Billottet, C., M. Tuefferd, D. Gentien, A. Rapinat, J.P. Thiery, P. Broet, and J. Jouanneau. 2008. Modulation of several waves of gene expression during FGF-1 induced epithelial-mesenchymal transition of carcinoma cells. *Journal of cellular biochemistry*. 104:826-839.

Blavier, L., A. Lazaryev, X.H. Shi, F.J. Dorey, G.M. Shackleford, and Y.A. DeClerck. 2010. Stromelysin-1 (MMP-3) is a target and a regulator of Wnt1-induced epithelial-mesenchymal transition (EMT). *Cancer biology & therapy*. 10:198-208.

Bonifacino, J.S., and J.H. Hurley. 2008. Retromer. *Current opinion in cell biology*. 20:427-436.

Bowden, E.T., M. Barth, D. Thomas, R.I. Glazer, and S.C. Mueller. 1999. An invasion-related complex of cortactin, paxillin and PKCmu associates with invadopodia at sites of extracellular matrix degradation. *Oncogene*. 18:4440-4449.

Bowden, E.T., E. Onikoyi, R. Slack, A. Myoui, T. Yoneda, K.M. Yamada, and S.C. Mueller. 2006. Co-localization of cortactin and phosphotyrosine identifies active invadopodia in human breast cancer cells. *Experimental cell research*. 312:1240-1253.

Bowser, R., and P. Novick. 1991. Sec15 protein, an essential component of the exocytotic apparatus, is associated with the plasma membrane and with a soluble 19.5S particle. *The Journal of cell biology*. 112:1117-1131.

Boyd, C., T. Hughes, M. Pypaert, and P. Novick. 2004. Vesicles carry most exocyst subunits to exocytic sites marked by the remaining two subunits, Sec3p and Exo70p. *The Journal of cell biology*. 167:889-901.

Brankatschk, B., V. Pons, R.G. Parton, and J. Gruenberg. 2011. Role of SNX16 in the dynamics of tubulo-cisternal membrane domains of late endosomes. *PloS one*. 6:e21771.

Bravo-Cordero, J.J., R. Marrero-Diaz, D. Megias, L. Genis, A. Garcia-Grande, M.A. Garcia, A.G. Arroyo, and M.C. Montoya. 2007. MT1-MMP proinvasive activity is regulated by a novel Rab8-dependent exocytic pathway. *The EMBO journal*. 26:1499-1510.

Bravo-Cordero, J.J., M. Oser, X. Chen, R. Eddy, L. Hodgson, and J. Condeelis. 2011. A novel spatiotemporal RhoC activation pathway locally regulates cofilin activity at invadopodia. *Current biology : CB*. 21:635-644.

Brisson, L., V. Driffort, L. Benoist, M. Poet, L. Counillon, E. Antelmi, R. Rubino, P. Besson, F. Labbal, S. Chevalier, S.J. Reshkin, J. Gore, and S. Roger. 2013. NaV1.5 Na(+) channels allosterically regulate the NHE-1 exchanger and promote the activity of breast cancer cell invadopodia. *Journal of cell science*. 126:4835-4842.

Brisson, L., L. Gillet, S. Calaghan, P. Besson, J.Y. Le Guennec, S. Roger, and J. Gore. 2011. Na(V)1.5 enhances breast cancer cell invasiveness by increasing NHE1-dependent H(+) efflux in caveolae. *Oncogene*. 30:2070-2076.

Brisson, L., S.J. Reshkin, J. Gore, and S. Roger. 2012. pH regulators in invadosomal functioning: proton delivery for matrix tasting. *European journal of cell biology*. 91:847-860.

Buccione, R., G. Caldieri, and I. Ayala. 2009. Invadopodia: specialized tumor cell structures for the focal degradation of the extracellular matrix. *Cancer metastasis reviews*. 28:137-149.

Burger, K.L., B.S. Learman, A.K. Boucherle, S.J. Sirintrapun, S. Isom, B. Diaz, S.A. Courtneidge, and D.F. Seals. 2014. Src-dependent Tks5 phosphorylation regulates invadopodia-associated invasion in prostate cancer cells. *The Prostate*. 74:134-148.

Buschman, M.D., P.A. Bromann, P. Cejudo-Martin, F. Wen, I. Pass, and S.A. Courtneidge. 2009. The novel adaptor protein Tks4 (SH3PXD2B) is required for functional podosome formation. *Molecular biology of the cell*. 20:1302-1311.

Busco, G., R.A. Cardone, M.R. Greco, A. Bellizzi, M. Colella, E. Antelmi, M.T. Mancini, M.E. Dell'Aquila, V. Casavola, A. Paradiso, and S.J. Reshkin. 2010. NHE1 promotes invadopodial ECM proteolysis through acidification of the peri-invadopodial space. *FASEB journal : official publication of the Federation of American Societies for Experimental Biology*. 24:3903-3915.

Caldieri, G., G. Giacchetti, G. Beznoussenko, F. Attanasio, I. Ayala, and R. Buccione. 2009. Invadopodia biogenesis is regulated by caveolin-mediated modulation of membrane cholesterol levels. *Journal of cellular and molecular medicine*. 13:1728-1740.

Camonis, J.H., and M.A. White. 2005. Ral GTPases: corrupting the exocyst in cancer cells. *Trends in cell biology*. 15:327-332.

Campellone, K.G., and M.D. Welch. 2010. A nucleator arms race: cellular control of actin assembly. *Nature reviews. Molecular cell biology*. 11:237-251.

Candiello, J., M. Balasubramani, E.M. Schreiber, G.J. Cole, U. Mayer, W. Halfter, and H. Lin. 2007. Biomechanical properties of native basement membranes. *The FEBS journal*. 274:2897-2908.

Cao, J., P. Kozarekar, M. Pavlaki, C. Chiarelli, W.F. Bahou, and S. Zucker. 2004. Distinct roles for the catalytic and hemopexin domains of membrane type 1-matrix metalloproteinase in substrate degradation and cell migration. *The Journal of biological chemistry*. 279:14129-14139.

Carnell, M., T. Zech, S.D. Calaminus, S. Ura, M. Hagedorn, S.A. Johnston, R.C. May, T. Soldati, L.M. Machesky, and R.H. Insall. 2011. Actin polymerization driven by WASH causes V-ATPase retrieval and vesicle neutralization before exocytosis. *The Journal of cell biology*. 193:831-839.

Castro-Castro, A., C. Janke, G. Montagnac, P. Paul-Gilloteaux, and P. Chavrier. 2012. ATAT1/MEC-17 acetyltransferase and HDAC6 deacetylase control a balance of acetylation of alpha-tubulin and cortactin and regulate MT1-MMP trafficking and breast tumor cell invasion. *European journal of cell biology*. 91:950-960.

Chan, K.M., H.L. Wong, G. Jin, B. Liu, R. Cao, Y. Cao, K. Lehti, K. Tryggvason, and Z. Zhou. 2012. MT1-MMP inactivates ADAM9 to regulate FGFR2 signaling and calvarial osteogenesis. *Developmental cell*. 22:1176-1190.

Charras, G., and E. Paluch. 2008. Blebs lead the way: how to migrate without lamellipodia. *Nature reviews. Molecular cell biology*. 9:730-736.

Chau, D.Y., R.J. Collighan, E.A. Verderio, V.L. Addy, and M. Griffin. 2005. The cellular response to transglutaminase-cross-linked collagen. *Biomaterials*. 26:6518-6529.

Chen, W.T. 1989. Proteolytic activity of specialized surface protrusions formed at rosette contact sites of transformed cells. *The Journal of experimental zoology*. 251:167-185.

Chen, W.T. 1996. Proteases associated with invadopodia, and their role in degradation of extracellular matrix. *Enzyme & protein*. 49:59-71.

Chen, W.T., J.M. Chen, S.J. Parsons, and J.T. Parsons. 1985. Local degradation of fibronectin at sites of expression of the transforming gene product pp60src. *Nature*. 316:156-158.

Chen, W.T., and J.Y. Wang. 1999. Specialized surface protrusions of invasive cells, invadopodia and lamellipodia, have differential MT1-MMP, MMP-2, and TIMP-2 localization. *Annals of the New York Academy of Sciences*. 878:361-371.

Chen, X.W., D. Leto, S.H. Chiang, Q. Wang, and A.R. Saltiel. 2007. Activation of RalA is required for insulin-stimulated Glut4 trafficking to the plasma membrane via the exocyst and the motor protein Myo1c. *Developmental cell*. 13:391-404.

Chun, T.H., F. Sabeh, I. Ota, H. Murphy, K.T. McDonagh, K. Holmbeck, H. Birkedal-Hansen, E.D. Allen, and S.J. Weiss. 2004. MT1-MMP-dependent neovessel formation within the confines of the three-dimensional extracellular matrix. *The Journal of cell biology*. 167:757-767.

Clark, E.S., A.S. Whigham, W.G. Yarbrough, and A.M. Weaver. 2007. Cortactin is an essential regulator of matrix metalloproteinase secretion and extracellular matrix degradation in invadopodia. *Cancer research*. 67:4227-4235.

Courtneidge, S.A. 2012. Cell migration and invasion in human disease: the Tks adaptor proteins. *Biochemical Society transactions*. 40:129-132.

Cox, T.R., D. Bird, A.M. Baker, H.E. Barker, M.W. Ho, G. Lang, and J.T. Erler. 2013. LOX-mediated collagen crosslinking is responsible for fibrosis-enhanced metastasis. *Cancer research*. 73:1721-1732.

Crimaldi, L., S.A. Courtneidge, and M. Gimona. 2009. Tks5 recruits AFAP-110, p190RhoGAP, and cortactin for podosome formation. *Experimental cell research*. 315:2581-2592.

Cullen, P.J. 2008. Endosomal sorting and signalling: an emerging role for sorting nexins. *Nature reviews. Molecular cell biology*. 9:574-582.

Das, A., S. Gajendra, K. Falenta, M.J. Oudin, P. Peschard, S. Feng, B. Wu, C.J. Marshall, P. Doherty, W. Guo, and G. Lalli. 2014. RalA promotes a direct exocyst-Par6 interaction to regulate polarity in neuronal development. *Journal of cell science*. 127:686-699.

David-Pfeuty, T., and S.J. Singer. 1980. Altered distributions of the cytoskeletal proteins vinculin and alpha-actinin in cultured fibroblasts transformed by Rous sarcoma virus. *Proceedings of the National Academy of Sciences of the United States of America*. 77:6687-6691.

De Craene, B., and G. Berx. 2013. Regulatory networks defining EMT during cancer initiation and progression. *Nature reviews. Cancer*. 13:97-110.

Dejica, V.M., J.S. Mort, S. Laverty, M.D. Percival, J. Antoniou, D.J. Zukor, and A.R. Poole. 2008. Cleavage of type II collagen by cathepsin K in human osteoarthritic cartilage. *The American journal of pathology*. 173:161-169.

Derivery, E., E. Helfer, V. Henriot, and A. Gautreau. 2012. Actin polymerization controls the organization of WASH domains at the surface of endosomes. *PloS one*. 7:e39774.

Derivery, E., C. Sousa, J.J. Gautier, B. Lombard, D. Loew, and A. Gautreau. 2009. The Arp2/3 activator WASH controls the fission of endosomes through a large multiprotein complex. *Developmental cell*. 17:712-723.

Deryugina, E.I., and J.P. Quigley. 2006. Matrix metalloproteinases and tumor metastasis. *Cancer metastasis reviews*. 25:9-34.

Deryugina, E.I., B. Ratnikov, E. Monosov, T.I. Postnova, R. DiScipio, J.W. Smith, and A.Y. Strongin. 2001. MT1-MMP initiates activation of pro-MMP-2 and integrin alphavbeta3 promotes maturation of MMP-2 in breast carcinoma cells. *Experimental cell research*. 263:209-223.

Desmarais, V., H. Yamaguchi, M. Oser, L. Soon, G. Mouneimne, C. Sarmiento, R. Eddy, and J. Condeelis. 2009. N-WASP and cortactin are involved in invadopodium-dependent chemotaxis to EGF in breast tumor cells. *Cell motility and the cytoskeleton*. 66:303-316.

Destaing, O., E. Planus, D. Bouvard, C. Oddou, C. Badowski, V. Bossy, A. Raducanu, B. Fourcade, C. Albiges-Rizo, and M.R. Block. 2010. beta1A integrin is a master regulator of invadosome organization and function. *Molecular biology of the cell*. 21:4108-4119.

Di Paolo, G., and P. De Camilli. 2006. Phosphoinositides in cell regulation and membrane dynamics. *Nature*. 443:651-657.

Diaz, B., G. Shani, I. Pass, D. Anderson, M. Quintavalle, and S.A. Courtneidge. 2009. Tks5-dependent, nox-mediated generation of reactive oxygen species is necessary for invadopodia formation. *Science signaling*. 2:ra53.

Diaz, B., A. Yuen, S. Iizuka, S. Higashiyama, and S.A. Courtneidge. 2013. Notch increases the shedding of HB-EGF by ADAM12 to potentiate invadopodia formation in hypoxia. *The Journal of cell biology*. 201:279-292.

Docherty, N.G., O.E. O'Sullivan, D.A. Healy, M. Murphy, J. O'Neill A, J.M. Fitzpatrick, and R.W. Watson. 2006. TGF-beta1-induced EMT can occur independently of its proapoptotic effects and is aided by EGF receptor activation. *American journal of physiology. Renal physiology*. 290:F1202-1212.

Drengk, A., J. Fritsch, C. Schmauch, H. Ruhling, and M. Maniak. 2003. A coat of filamentous actin prevents clustering of late-endosomal vacuoles in vivo. *Current biology : CB*. 13:1814-1819.

Duleh, S.N., and M.D. Welch. 2010. WASH and the Arp2/3 complex regulate endosome shape and trafficking. *Cytoskeleton*. 67:193-206.

Eckert, M.A., T.M. Lwin, A.T. Chang, J. Kim, E. Danis, L. Ohno-Machado, and J. Yang. 2011. Twist1-induced invadopodia formation promotes tumor metastasis. *Cancer cell*. 19:372-386.

Egeblad, M., and Z. Werb. 2002. New functions for the matrix metalloproteinases in cancer progression. *Nature reviews. Cancer*. 2:161-174.

Ellenbroek, S.I., S. Iden, and J.G. Collard. 2012. Cell polarity proteins and cancer. *Seminars in cancer biology*. 22:208-215.

Endo, K., T. Takino, H. Miyamori, H. Kinsen, T. Yoshizaki, M. Furukawa, and H. Sato. 2003. Cleavage of syndecan-1 by membrane type matrix metalloproteinase-1 stimulates cell migration. *The Journal of biological chemistry*. 278:40764-40770.

Engl, W., B. Arasi, L.L. Yap, J.P. Thiery, and V. Viasnoff. 2014. Actin dynamics modulate mechanosensitive immobilization of E-cadherin at adherens junctions. *Nature cell biology*. 16:587-594.

Essid, M., N. Gopaldass, K. Yoshida, C. Merrifield, and T. Soldati. 2012. Rab8a regulates the exocyst-mediated kiss-and-run discharge of the Dictyostelium contractile vacuole. *Molecular biology of the cell*. 23:1267-1282.

Evans, J.V., A.G. Ammer, J.E. Jett, C.A. Bolcato, J.C. Breaux, K.H. Martin, M.V. Culp, P.M. Gannett, and S.A. Weed. 2012. Src binds cortactin through an SH2 domain cystine-mediated linkage. *Journal of cell science*. 125:6185-6197.

Fabian, L., H.C. Wei, J. Rollins, T. Noguchi, J.T. Blankenship, K. Bellamkonda, G. Polevoy, L. Gervais, A. Guichet, M.T. Fuller, and J.A. Brill. 2010. Phosphatidylinositol 4,5-bisphosphate directs spermatid cell polarity and exocyst localization in Drosophila. *Molecular biology of the cell*. 21:1546-1555.

Farrell, J., C. Kelly, J. Rauch, K. Kida, A. Garcia-Munoz, N. Monsefi, B. Turriziani, C. Doherty, J.P. Mehta, D. Matallanas, J.C. Simpson, W. Kolch, and A. von Kriegsheim. 2014. HGF induces epithelial-to-mesenchymal transition by modulating the mammalian hippo/MST2 and ISG15 pathways. *Journal of proteome research*. 13:2874-2886.

Fekete, A., G. Bogel, S. Pesti, Z. Peterfi, M. Geiszt, and L. Buday. 2013. EGF regulates tyrosine phosphorylation and membrane-translocation of the scaffold protein Tks5. *Journal of molecular signaling*. 8:8.

Freeman, C.L., G. Hesketh, and M.N. Seaman. 2014. RME-8 coordinates the activity of the WASH complex with the function of the retromer SNX dimer to control endosomal tubulation. *Journal of cell science*. 127:2053-2070.

Friedl, P., and S. Alexander. 2011. Cancer invasion and the microenvironment: plasticity and reciprocity. *Cell*. 147:992-1009.

Friedl, P., and D. Gilmour. 2009. Collective cell migration in morphogenesis, regeneration and cancer. *Nature reviews. Molecular cell biology*. 10:445-457.

Friedl, P., and K. Wolf. 2003. Proteolytic and non-proteolytic migration of tumour cells and leucocytes. *Biochemical Society symposium*:277-285.

Friedl, P., and K. Wolf. 2009. Proteolytic interstitial cell migration: a five-step process. *Cancer metastasis reviews*. 28:129-135.

Friedl, P., K. Wolf, and J. Lammerding. 2011. Nuclear mechanics during cell migration. *Current opinion in cell biology*. 23:55-64.

Frittoli, E., A. Palamidessi, A. Disanza, and G. Scita. 2011. Secretory and endo/exocytic trafficking in invadopodia formation: the MT1-MMP paradigm. *European journal of cell biology*. 90:108-114.

Fu, H.L., A. Sohail, R.R. Valiathan, B.D. Wasinski, M. Kumarasiri, K.V. Mahasenan, M.M. Bernardo, D. Tokmina-Roszyk, G.B. Fields, S. Mobashery, and R. Fridman. 2013. Shedding of discoidin domain receptor 1 by membrane-type matrix metalloproteinases. *The Journal of biological chemistry*. 288:12114-12129.

Gaggioli, C. 2008. Collective invasion of carcinoma cells: when the fibroblasts take the lead. *Cell adhesion & migration*. 2:45-47.

Gaggioli, C., S. Hooper, C. Hidalgo-Carcedo, R. Grosse, J.F. Marshall, K. Harrington, and E. Sahai. 2007. Fibroblast-led collective invasion of carcinoma cells with differing roles for RhoGTPases in leading and following cells. *Nature cell biology*. 9:1392-1400.

Galvez, B.G., S. Matias-Roman, M. Yanez-Mo, F. Sanchez-Madrid, and A.G. Arroyo. 2002. ECM regulates MT1-MMP localization with beta1 or alphavbeta3 integrins at distinct cell compartments modulating its internalization and activity on human endothelial cells. *The Journal of cell biology*. 159:509-521.

Galvez, B.G., S. Matias-Roman, M. Yanez-Mo, M. Vicente-Manzanares, F. Sanchez-Madrid, and A.G. Arroyo. 2004. Caveolae are a novel pathway for membrane-type 1 matrix metalloproteinase traffic in human endothelial cells. *Molecular biology of the cell*. 15:678-687.

Galvez, T., J. Gilleron, M. Zerial, and G.A. O'Sullivan. 2012. SnapShot: Mammalian Rab proteins in endocytic trafficking. *Cell*. 151:234-234 e232.

Gautreau, A., K. Oguievetskaia, and C. Ungermann. 2014. Function and regulation of the endosomal fusion and fission machineries. *Cold Spring Harbor perspectives in biology*. 6.

Ghersi, G., Q. Zhao, M. Salamone, Y. Yeh, S. Zucker, and W.T. Chen. 2006. The protease complex consisting of dipeptidyl peptidase IV and seprase plays a role in the migration and invasion of human endothelial cells in collagenous matrices. *Cancer research*. 66:4652-4661.

Gillet, L., S. Roger, P. Besson, F. Lecaille, J. Gore, P. Bougnoux, G. Lalmanach, and J.Y. Le Guennec. 2009. Voltage-gated Sodium Channel Activity Promotes Cysteine Cathepsin-dependent Invasiveness and Colony Growth of Human Cancer Cells. *The Journal of biological chemistry*. 284:8680-8691.

Gimona, M., R. Buccione, S.A. Courtneidge, and S. Linder. 2008. Assembly and biological role of podosomes and invadopodia. *Current opinion in cell biology*. 20:235-241.

Gioia, M., S. Monaco, G.F. Fasciglione, A. Coletti, A. Modesti, S. Marini, and M. Coletta. 2007. Characterization of the mechanisms by which gelatinase A, neutrophil collagenase, and membrane-type metalloproteinase MMP-14 recognize collagen I and enzymatically process the two alpha-chains. *Journal of molecular biology*. 368:1101-1113.

Gomez, T.S., and D.D. Billadeau. 2009. A FAM21-containing WASH complex regulates retromer-dependent sorting. *Developmental cell*. 17:699-711.

Grant, B.D., and J.G. Donaldson. 2009. Pathways and mechanisms of endocytic recycling. *Nature reviews. Molecular cell biology*. 10:597-608.

Green, K.J., S. Getsios, S. Troyanovsky, and L.M. Godsel. 2010. Intercellular junction assembly, dynamics, and homeostasis. *Cold Spring Harbor perspectives in biology*. 2:a000125.

Guinebretiere, J.M., E. Menet, A. Tardivon, P. Cherel, and D. Vanel. 2005. Normal and pathological breast, the histological basis. *European journal of radiology*. 54:6-14.

Gunasinghe, N.P., A. Wells, E.W. Thompson, and H.J. Hugo. 2012. Mesenchymal-epithelial transition (MET) as a mechanism for metastatic colonisation in breast cancer. *Cancer metastasis reviews*. 31:469-478.

Gundersen, G.G., and H.J. Worman. 2013. Nuclear positioning. *Cell*. 152:1376-1389.

Guo, W., A. Grant, and P. Novick. 1999. Exo84p is an exocyst protein essential for secretion. *The Journal of biological chemistry*. 274:23558-23564.

Gupta, G.P., and J. Massague. 2006. Cancer metastasis: building a framework. *Cell*. 127:679-695.

Haaksma, C.J., R.J. Schwartz, and J.J. Tomasek. 2011. Myoepithelial cell contraction and milk ejection are impaired in mammary glands of mice lacking smooth muscle alpha-actin. *Biology of reproduction*. 85:13-21.

Han, J., T. Luo, Y. Gu, G. Li, W. Jia, and M. Luo. 2009. Cathepsin K regulates adipocyte differentiation: possible involvement of type I collagen degradation. *Endocrine journal*. 56:55-63.

Hanahan, D., and R.A. Weinberg. 2000. The hallmarks of cancer. *Cell*. 100:57-70.

Hanahan, D., and R.A. Weinberg. 2011. Hallmarks of cancer: the next generation. *Cell*. 144:646-674.

Hao, Y.H., J.M. Doyle, S. Ramanathan, T.S. Gomez, D. Jia, M. Xu, Z.J. Chen, D.D. Billadeau, M.K. Rosen, and P.R. Potts. 2013. Regulation of WASH-dependent actin polymerization and protein trafficking by ubiquitination. *Cell*. 152:1051-1064.

Harada, T., J. Swift, J. Irianto, J.W. Shin, K.R. Spinler, A. Athirasala, R. Diegmiller, P.C. Dingal, I.L. Ivanovska, and D.E. Discher. 2014. Nuclear lamin stiffness is a barrier to 3D migration, but softness can limit survival. *The Journal of cell biology*. 204:669-682.

Harbour, M.E., S.Y. Breusegem, R. Antrobus, C. Freeman, E. Reid, and M.N. Seaman. 2010. The cargo-selective retromer complex is a recruiting hub for protein complexes that regulate endosomal tubule dynamics. *Journal of cell science*. 123:3703-3717.

Hardy, K.M., B.W. Booth, M.J. Hendrix, D.S. Salomon, and L. Strizzi. 2010. ErbB/EGF signaling and EMT in mammary development and breast cancer. *Journal of mammary gland biology and neoplasia*. 15:191-199.

Hauck, C.R., D.A. Hsia, D. Ilic, and D.D. Schlaepfer. 2002. v-Src SH3-enhanced interaction with focal adhesion kinase at beta 1 integrin-containing invadopodia promotes cell invasion. *The Journal of biological chemistry*. 277:12487-12490.

He, B., F. Xi, X. Zhang, J. Zhang, and W. Guo. 2007. Exo70 interacts with phospholipids and mediates the targeting of the exocyst to the plasma membrane. *The EMBO journal*. 26:4053-4065.

Hofmann, U.B., A.A. Eggert, K. Blass, E.B. Brocker, and J.C. Becker. 2003. Expression of matrix metalloproteinases in the microenvironment of spontaneous and experimental melanoma metastases reflects the requirements for tumor formation. *Cancer research*. 63:8221-8225.

Holmbeck, K., P. Bianco, J. Caterina, S. Yamada, M. Kromer, S.A. Kuznetsov, M. Mankani, P.G. Robey, A.R. Poole, I. Pidoux, J.M. Ward, and H. Birkedal-Hansen. 1999. MT1-MMP-deficient mice develop dwarfism, osteopenia, arthritis, and connective tissue disease due to inadequate collagen turnover. *Cell*. 99:81-92.

Holmbeck, K., P. Bianco, I. Pidoux, S. Inoue, R.C. Billinghurst, W. Wu, K. Chrysovergis, S. Yamada, H. Birkedal-Hansen, and A.R. Poole. 2005. The metalloproteinase MT1-MMP is required for normal development and maintenance of osteocyte processes in bone. *Journal of cell science*. 118:147-156.

Horikoshi, Y., A. Suzuki, T. Yamanaka, K. Sasaki, K. Mizuno, H. Sawada, S. Yonemura, and S. Ohno. 2009. Interaction between PAR-3 and the aPKC-PAR-6 complex is indispensable for apical domain development of epithelial cells. *Journal of cell science*. 122:1595-1606.

Hoshino, D., K.M. Branch, and A.M. Weaver. 2013. Signaling inputs to invadopodia and podosomes. *Journal of cell science*. 126:2979-2989.

Hotary, K., X.Y. Li, E. Allen, S.L. Stevens, and S.J. Weiss. 2006. A cancer cell metalloprotease triad regulates the basement membrane transmigration program. *Genes & development*. 20:2673-2686.

Hotary, K.B., E.D. Allen, P.C. Brooks, N.S. Datta, M.W. Long, and S.J. Weiss. 2003. Membrane type I matrix metalloproteinase usurps tumor growth control imposed by the three-dimensional extracellular matrix. *Cell*. 114:33-45.

Hsu, S.C., C.D. Hazuka, R. Roth, D.L. Foletti, J. Heuser, and R.H. Scheller. 1998. Subunit composition, protein interactions, and structures of the mammalian brain sec6/8 complex and septin filaments. *Neuron*. 20:1111-1122.

Hu, J., A. Mukhopadhyay, P. Truesdell, H. Chander, U.K. Mukhopadhyay, A.S. Mak, and A.W. Craig. 2011. Cdc42-interacting protein 4 is a Src substrate that regulates invadopodia and invasiveness of breast tumors by promoting MT1-MMP endocytosis. *Journal of cell science*. 124:1739-1751.

Hui, R., J.R. Ball, R.D. Macmillan, F.S. Kenny, O.W. Prall, D.H. Campbell, A.L. Cornish, R.A. McClelland, R.J. Daly, J.F. Forbes, R.W. Blamey, E.A. Musgrove, J.F. Robertson, R.I. Nicholson, and R.L. Sutherland. 1998. EMS1 gene expression in primary breast cancer: relationship to cyclin D1 and oestrogen receptor expression and patient survival. *Oncogene*. 17:1053-1059.

Huotari, J., and A. Helenius. 2011. Endosome maturation. *The EMBO journal*. 30:3481-3500.

Illman, S.A., K. Lehti, J. Keski-Oja, and J. Lohi. 2006. Epilysin (MMP-28) induces TGF-beta mediated epithelial to mesenchymal transition in lung carcinoma cells. *Journal of cell science*. 119:3856-3865.

Inoue, M., L. Chang, J. Hwang, S.H. Chiang, and A.R. Saltiel. 2003. The exocyst complex is required for targeting of Glut4 to the plasma membrane by insulin. *Nature*. 422:629-633.

Inoue, M., S.H. Chiang, L. Chang, X.W. Chen, and A.R. Saltiel. 2006. Compartmentalization of the exocyst complex in lipid rafts controls Glut4 vesicle tethering. *Molecular biology of the cell*. 17:2303-2311.

Isermann, P., and J. Lammerding. 2013. Nuclear mechanics and mechanotransduction in health and disease. *Current biology : CB*. 23:R1113-1121.

Itoh, Y., N. Ito, H. Nagase, R.D. Evans, S.A. Bird, and M. Seiki. 2006. Cell surface collagenolysis requires homodimerization of the membrane-bound collagenase MT1-MMP. *Molecular biology of the cell*. 17:5390-5399.

Itoh, Y., and M. Seiki. 2006. MT1-MMP: a potent modifier of pericellular microenvironment. *Journal of cellular physiology*. 206:1-8.

Itoh, Y., A. Takamura, N. Ito, Y. Maru, H. Sato, N. Suenaga, T. Aoki, and M. Seiki. 2001. Homophilic complex formation of MT1-MMP facilitates proMMP-2 activation on the cell surface and promotes tumor cell invasion. *The EMBO journal*. 20:4782-4793.

Janssens, E., D. Gaublomme, L. De Groef, V.M. Darras, L. Arckens, N. Delorme, F. Claes, I. Van Hove, and L. Moons. 2013. Matrix metalloproteinase 14 in the zebrafish: an eye on retinal and retinotectal development. *PloS one*. 8:e52915.

Jelassi, B., A. Chantome, F. Alcaraz-Perez, A. Baroja-Mazo, M.L. Cayuela, P. Pelegrin, A. Surprenant, and S. Roger. 2011. P2X(7) receptor activation enhances SK3 channels- and cystein cathepsin-dependent cancer cells invasiveness. *Oncogene*. 30:2108-2122.

Jia, D., T.S. Gomez, D.D. Billadeau, and M.K. Rosen. 2012. Multiple repeat elements within the FAM21 tail link the WASH actin regulatory complex to the retromer. *Molecular biology of the cell*. 23:2352-2361.

Jia, D., T.S. Gomez, Z. Metlagel, J. Umetani, Z. Otwinowski, M.K. Rosen, and D.D. Billadeau. 2010. WASH and WAVE actin regulators of the Wiskott-Aldrich syndrome protein (WASP) family are controlled by analogous structurally related complexes. *Proceedings of the National Academy of Sciences of the United States of America*. 107:10442-10447.

Jiang, A., K. Lehti, X. Wang, S.J. Weiss, J. Keski-Oja, and D. Pei. 2001. Regulation of membrane-type matrix metalloproteinase 1 activity by dynamin-mediated endocytosis. *Proceedings of the National Academy of Sciences of the United States of America*. 98:13693-13698.

Jiang, W.G., G. Davies, T.A. Martin, C. Parr, G. Watkins, M.D. Mason, and R.E. Mansel. 2006. Expression of membrane type-1 matrix metalloproteinase, MT1-MMP in human breast cancer and its impact on invasiveness of breast cancer cells. *International journal of molecular medicine*. 17:583-590.

Jorda, M., D. Olmeda, A. Vinyals, E. Valero, E. Cubillo, A. Llorens, A. Cano, and A. Fabra. 2005. Upregulation of MMP-9 in MDCK epithelial cell line in response to expression of the Snail transcription factor. *Journal of cell science*. 118:3371-3385.

Jourdain, I., H.C. Dooley, and T. Toda. 2012. Fission yeast sec3 bridges the exocyst complex to the actin cytoskeleton. *Traffic*. 13:1481-1495.

Kadler, K.E., A. Hill, and E.G. Canty-Laird. 2008. Collagen fibrillogenesis: fibronectin, integrins, and minor collagens as organizers and nucleators. *Current opinion in cell biology*. 20:495-501.

Kaimal, R., R. Aljumaily, S.L. Tressel, R.V. Pradhan, L. Covic, A. Kuliopulos, C. Zarwan, Y.B. Kim, S. Sharifi, and A. Agarwal. 2013. Selective blockade of matrix metalloprotease-14 with a monoclonal antibody abrogates invasion, angiogenesis, and tumor growth in ovarian cancer. *Cancer research*. 73:2457-2467.

Kajita, M., Y. Itoh, T. Chiba, H. Mori, A. Okada, H. Kinoh, and M. Seiki. 2001. Membrane-type 1 matrix metalloproteinase cleaves CD44 and promotes cell migration. *The Journal of cell biology*. 153:893-904.

Kalluri, R. 2003. Basement membranes: structure, assembly and role in tumour angiogenesis. *Nature reviews. Cancer*. 3:422-433.

Kalluri, R., and R.A. Weinberg. 2009. The basics of epithelial-mesenchymal transition. *The Journal of clinical investigation*. 119:1420-1428.

Kean, M.J., K.C. Williams, M. Skalski, D. Myers, A. Burtnik, D. Foster, and M.G. Coppolino. 2009. VAMP3, syntaxin-13 and SNAP23 are involved in secretion of matrix metalloproteinases, degradation of the extracellular matrix and cell invasion. *Journal of cell science*. 122:4089-4098.

Kempiak, S.J., H. Yamaguchi, C. Sarmiento, M. Sidani, M. Ghosh, R.J. Eddy, V. Desmarais, M. Way, J. Condeelis, and J.E. Segall. 2005. A neural Wiskott-Aldrich Syndrome protein-mediated pathway for localized activation of actin polymerization that is regulated by cortactin. *The Journal of biological chemistry*. 280:5836-5842.

Kessenbrock, K., V. Plaks, and Z. Werb. 2010. Matrix metalloproteinases: regulators of the tumor microenvironment. *Cell*. 141:52-67.

Khursheed, M., and M.D. Bashyam. 2014. Apico-basal polarity complex and cancer. *Journal of biosciences*. 39:145-155.

Kindzelskii, A.L., I. Amhad, D. Keller, M.J. Zhou, R.P. Haugland, B.A. Garni-Wagner, M.R. Gyetko, R.F. Todd, 3rd, and H.R. Petty. 2004. Pericellular proteolysis by leukocytes and tumor cells on substrates: focal activation and the role of urokinase-type plasminogen activator. *Histochemistry and cell biology*. 121:299-310.

King, J.S., A. Gueho, M. Hagedorn, N. Gopaldass, F. Leuba, T. Soldati, and R.H. Insall. 2013. WASH is required for lysosomal recycling and efficient autophagic and phagocytic digestion. *Molecular biology of the cell*. 24:2714-2726.

Kirschmann, D.A., E.A. Seftor, S.F. Fong, D.R. Nieva, C.M. Sullivan, E.M. Edwards, P. Sommer, K. Csiszar, and M.J. Hendrix. 2002. A molecular role for lysyl oxidase in breast cancer invasion. *Cancer research*. 62:4478-4483.

Kleinman, H.K., and G.R. Martin. 2005. Matrigel: basement membrane matrix with biological activity. *Seminars in cancer biology*. 15:378-386.

Kollmar, M., D. Lbik, and S. Enge. 2012. Evolution of the eukaryotic ARP2/3 activators of the WASP family: WASP, WAVE, WASH, and WHAMM, and the proposed new family members WAWH and WAML. *BMC research notes*. 5:88.

Komsic-Buchmann, K., L.M. Stephan, and B. Becker. 2012. The SEC6 protein is required for contractile vacuole function in Chlamydomonas reinhardtii. *Journal of cell science*. 125:2885-2895.

Koshikawa, N., T. Minegishi, A. Sharabi, V. Quaranta, and M. Seiki. 2005. Membrane-type matrix metalloproteinase-1 (MT1-MMP) is a processing enzyme for human laminin gamma 2 chain. *The Journal of biological chemistry*. 280:88-93.

Koshikawa, N., H. Mizushima, T. Minegishi, F. Eguchi, F. Yotsumoto, K. Nabeshima, S. Miyamoto, E. Mekada, and M. Seiki. 2011. Proteolytic activation of heparin-binding EGF-like growth factor by membrane-type matrix metalloproteinase-1 in ovarian carcinoma cells. *Cancer science*. 102:111-116.

Kung, C.I., C.Y. Chen, C.C. Yang, C.Y. Lin, T.H. Chen, and H.S. Wang. 2012. Enhanced membrane-type 1 matrix metalloproteinase expression by hyaluronan oligosaccharides in breast cancer cells facilitates CD44 cleavage and tumor cell migration. *Oncology reports*. 28:1808-1814.

Kuo, P.T., T.P. Lin, L.C. Liu, C.H. Huang, J.K. Lin, J.Y. Kao, and T.D. Way. 2009. Penta-O-galloyl-beta-D-glucose suppresses prostate cancer bone metastasis by transcriptionally repressing EGF-induced MMP-9 expression. *Journal of agricultural and food chemistry*. 57:3331-3339.

Kusuma, N., D. Denoyer, J.A. Eble, R.P. Redvers, B.S. Parker, R. Pelzer, R.L. Anderson, and N. Pouliot. 2012. Integrin-dependent response to laminin-511 regulates breast tumor cell invasion and metastasis. *International journal of cancer. Journal international du cancer*. 130:555-566.

Lafleur, M.A., F.A. Mercuri, N. Ruangpanit, M. Seiki, H. Sato, and E.W. Thompson. 2006. Type I collagen abrogates the clathrin-mediated internalization of membrane type 1 matrix metalloproteinase (MT1-MMP) via the MT1-MMP hemopexin domain. *The Journal of biological chemistry*. 281:6826-6840.

Lammermann, T., and M. Sixt. 2009. Mechanical modes of 'amoeboid' cell migration. *Current opinion in cell biology*. 21:636-644.

Langevin, J., M.J. Morgan, J.B. Sibarita, S. Aresta, M. Murthy, T. Schwarz, J. Camonis, and Y. Bellaiche. 2005. Drosophila exocyst components Sec5, Sec6, and Sec15 regulate DE-Cadherin trafficking from recycling endosomes to the plasma membrane. *Developmental cell*. 9:365-376.

Li, A., J.C. Dawson, M. Forero-Vargas, H.J. Spence, X. Yu, I. Konig, K. Anderson, and L.M. Machesky. 2010. The actin-bundling protein fascin stabilizes actin in invadopodia and potentiates protrusive invasion. *Current biology : CB*. 20:339-345.

Li, X.Y., I. Ota, I. Yana, F. Sabeh, and S.J. Weiss. 2008. Molecular dissection of the structural machinery underlying the tissue-invasive activity of membrane type-1 matrix metalloproteinase. *Molecular biology of the cell*. 19:3221-3233.

Li, Y., M. Tondravi, J. Liu, E. Smith, C.C. Haudenschild, M. Kaczmarek, and X. Zhan. 2001. Cortactin potentiates bone metastasis of breast cancer cells. *Cancer research*. 61:6906-6911.

Lin, C.Y., P.H. Tsai, C.C. Kandaswami, P.P. Lee, C.J. Huang, J.J. Hwang, and M.T. Lee. 2011. Matrix metalloproteinase-9 cooperates with transcription factor Snail to induce epithelial-mesenchymal transition. *Cancer science*. 102:815-827.

Linardopoulou, E.V., S.S. Parghi, C. Friedman, G.E. Osborn, S.M. Parkhurst, and B.J. Trask. 2007. Human subtelomeric WASH genes encode a new subclass of the WASP family. *PLoS genetics*. 3:e237.

Linder, S. 2007. The matrix corroded: podosomes and invadopodia in extracellular matrix degradation. *Trends in cell biology*. 17:107-117.

Linder, S., C. Wiesner, and M. Himmel. 2011. Degrading devices: invadosomes in proteolytic cell invasion. *Annual review of cell and developmental biology*. 27:185-211.

Liu, J., P. Yue, V.V. Artym, S.C. Mueller, and W. Guo. 2009a. The role of the exocyst in matrix metalloproteinase secretion and actin dynamics during tumor cell invadopodia formation. *Molecular biology of the cell*. 20:3763-3771.

Liu, J., Y. Zhao, Y. Sun, B. He, C. Yang, T. Svitkina, Y.E. Goldman, and W. Guo. 2012. Exo70 stimulates the Arp2/3 complex for lamellipodia formation and directional cell migration. *Current biology : CB*. 22:1510-1515.

Liu, J., X. Zuo, P. Yue, and W. Guo. 2007. Phosphatidylinositol 4,5-bisphosphate mediates the targeting of the exocyst to the plasma membrane for exocytosis in mammalian cells. *Molecular biology of the cell*. 18:4483-4492.

Liu, R., M.T. Abreu-Blanco, K.C. Barry, E.V. Linardopoulou, G.E. Osborn, and S.M. Parkhurst. 2009b. Wash functions downstream of Rho and links linear and branched actin nucleation factors. *Development*. 136:2849-2860.

Lopez-Castejon, G., J. Theaker, P. Pelegrin, A.D. Clifton, M. Braddock, and A. Surprenant. 2010. P2X(7) receptor-mediated release of cathepsins from macrophages is a cytokine-independent mechanism potentially involved in joint diseases. *Journal of immunology*. 185:2611-2619.

Lorenz, M., H. Yamaguchi, Y. Wang, R.H. Singer, and J. Condeelis. 2004. Imaging sites of N-wasp activity in lamellipodia and invadopodia of carcinoma cells. *Current biology : CB*. 14:697-703.

Lu, P., K. Takai, V.M. Weaver, and Z. Werb. 2011. Extracellular matrix degradation and remodeling in development and disease. *Cold Spring Harbor perspectives in biology*. 3.

Lucas, J.T., Jr., B.P. Salimath, M.G. Slomiany, and S.A. Rosenzweig. 2010. Regulation of invasive behavior by vascular endothelial growth factor is HEF1-dependent. *Oncogene*. 29:4449-4459.

Lv, Z.D., B. Kong, J.G. Li, H.L. Qu, X.G. Wang, W.H. Cao, X.Y. Liu, Y. Wang, Z.C. Yang, H.M. Xu, and H.B. Wang. 2013. Transforming growth factor-beta 1 enhances the invasiveness of breast cancer cells by inducing a Smad2-dependent epithelial-to-mesenchymal transition. *Oncology reports*. 29:219-225.

Ma, J., X. Tang, P. Wong, B. Jacobs, E.C. Borden, and B. Bedogni. 2014. Noncanonical activation of Notch1 protein by membrane type 1 matrix metalloproteinase (MT1-MMP) controls melanoma cell proliferation. *The Journal of biological chemistry*. 289:8442-8449.

Mader, C.C., M. Oser, M.A. Magalhaes, J.J. Bravo-Cordero, J. Condeelis, A.J. Koleske, and H. Gil-Henn. 2011. An EGFR-Src-Arg-cortactin pathway mediates functional maturation of invadopodia and breast cancer cell invasion. *Cancer research*. 71:1730-1741.

Mandal, S., K.R. Johnson, and M.J. Wheelock. 2008. TGF-beta induces formation of F-actin cores and matrix degradation in human breast cancer cells via distinct signaling pathways. *Experimental cell research*. 314:3478-3493.

Manon-Jensen, T., H.A. Multhaupt, and J.R. Couchman. 2013. Mapping of matrix metalloproteinase cleavage sites on syndecan-1 and syndecan-4 ectodomains. *The FEBS journal*. 280:2320-2331.

Maquoi, E., F. Frankenne, E. Baramova, C. Munaut, N.E. Sounni, A. Remacle, A. Noel, G. Murphy, and J.M. Foidart. 2000. Membrane type 1 matrix metalloproteinase-associated degradation of tissue inhibitor of metalloproteinase 2 in human tumor cell lines. *The Journal of biological chemistry*. 275:11368-11378.

Martin, T.F. 2012. Role of PI(4,5)P(2) in Vesicle Exocytosis and Membrane Fusion. *Sub-cellular biochemistry*. 59:111-130.

Martinez-Quiles, N., H.Y. Ho, M.W. Kirschner, N. Ramesh, and R.S. Geha. 2004. Erk/Src phosphorylation of cortactin acts as a switch on-switch off mechanism that controls its ability to activate N-WASP. *Molecular and cellular biology*. 24:5269-5280.

Mazzone, M., M. Baldassarre, G. Beznoussenko, G. Giacchetti, J. Cao, S. Zucker, A. Luini, and R. Buccione. 2004. Intracellular processing and activation of membrane type 1 matrix metalloprotease depends on its partitioning into lipid domains. *Journal of cell science*. 117:6275-6287.

McCaffrey, L.M., J. Montalbano, C. Mihai, and I.G. Macara. 2012. Loss of the Par3 polarity protein promotes breast tumorigenesis and metastasis. *Cancer cell*. 22:601-614.

McMahon, H.T., and J.L. Gallop. 2005. Membrane curvature and mechanisms of dynamic cell membrane remodelling. *Nature*. 438:590-596.

McNiven, M.A., L. Kim, E.W. Krueger, J.D. Orth, H. Cao, and T.W. Wong. 2000. Regulated interactions between dynamin and the actin-binding protein cortactin modulate cell shape. *The Journal of cell biology*. 151:187-198.

Meng, W., and M. Takeichi. 2009. Adherens junction: molecular architecture and regulation. *Cold Spring Harbor perspectives in biology*. 1:a002899.

Monteiro, P., C. Rosse, A. Castro-Castro, M. Irondelle, E. Lagoutte, P. Paul-Gilloteaux, C. Desnos, E. Formstecher, F. Darchen, D. Perrais, A. Gautreau, M. Hertzog, and P. Chavrier. 2013. Endosomal WASH and exocyst complexes control exocytosis of MT1-MMP at invadopodia. *The Journal of cell biology*. 203:1063-1079.

Morel, E., R.G. Parton, and J. Gruenberg. 2009. Annexin A2-dependent polymerization of actin mediates endosome biogenesis. *Developmental cell*. 16:445-457.

Mori, H., T. Tomari, N. Koshikawa, M. Kajita, Y. Itoh, H. Sato, H. Tojo, I. Yana, and M. Seiki. 2002. CD44 directs membrane-type 1 matrix metalloproteinase to lamellipodia by associating with its hemopexin-like domain. *The EMBO journal*. 21:3949-3959.

Moskalenko, S., D.O. Henry, C. Rosse, G. Mirey, J.H. Camonis, and M.A. White. 2002. The exocyst is a Ral effector complex. *Nature cell biology*. 4:66-72.

Moss, N.M., Y.I. Wu, Y. Liu, H.G. Munshi, and M.S. Stack. 2009. Modulation of the membrane type 1 matrix metalloproteinase cytoplasmic tail enhances tumor cell invasion and proliferation in three-dimensional collagen matrices. *The Journal of biological chemistry*. 284:19791-19799.

Moumen, M., A. Chiche, S. Cagnet, V. Petit, K. Raymond, M.M. Faraldo, M.A. Deugnier, and M.A. Glukhova. 2011. The mammary myoepithelial cell. *The International journal of developmental biology*. 55:763-771.

Mueller, S.C., and W.T. Chen. 1991. Cellular invasion into matrix beads: localization of beta 1 integrins and fibronectin to the invadopodia. *Journal of cell science*. 99 (Pt 2):213-225.

Mueller, S.C., Y. Yeh, and W.T. Chen. 1992. Tyrosine phosphorylation of membrane proteins mediates cellular invasion by transformed cells. *The Journal of cell biology*. 119:1309-1325.

Munson, M., and P. Novick. 2006. The exocyst defrocked, a framework of rods revealed. *Nature structural & molecular biology*. 13:577-581.

Murphy, D.A., and S.A. Courtneidge. 2011. The 'ins' and 'outs' of podosomes and invadopodia: characteristics, formation and function. *Nature reviews. Molecular cell biology*. 12:413-426.

Nakahara, H., T. Otani, T. Sasaki, Y. Miura, Y. Takai, and M. Kogo. 2003. Involvement of Cdc42 and Rac small G proteins in invadopodia formation of RPMI7951 cells. *Genes to cells : devoted to molecular & cellular mechanisms*. 8:1019-1027.

Nakamura, H., N. Suenaga, K. Taniwaki, H. Matsuki, K. Yonezawa, M. Fujii, Y. Okada, and M. Seiki. 2004. Constitutive and induced CD44 shedding by ADAM-like proteases and membrane-type 1 matrix metalloproteinase. *Cancer research*. 64:876-882.

Neto, H., G. Balmer, and G. Gould. 2013. Exocyst proteins in cytokinesis: Regulation by Rab11. *Communicative & integrative biology*. 6:e27635.

Novick, P., C. Field, and R. Schekman. 1980. Identification of 23 complementation groups required for post-translational events in the yeast secretory pathway. *Cell*. 21:205-215.

Novick, P., and R. Schekman. 1979. Secretion and cell-surface growth are blocked in a temperature-sensitive mutant of Saccharomyces cerevisiae. *Proceedings of the National Academy of Sciences of the United States of America*. 76:1858-1862.

Novick, P., and R. Schekman. 1983. Export of major cell surface proteins is blocked in yeast secretory mutants. *The Journal of cell biology*. 96:541-547.

Nurnberg, A., T. Kitzing, and R. Grosse. 2011. Nucleating actin for invasion. *Nature reviews. Cancer*. 11:177-187.

Nyalendo, C., M. Michaud, E. Beaulieu, C. Roghi, G. Murphy, D. Gingras, and R. Beliveau. 2007. Src-dependent phosphorylation of membrane type I matrix metalloproteinase on cytoplasmic tyrosine 573: role in endothelial and tumor cell migration. *The Journal of biological chemistry*. 282:15690-15699.

O'Brien, P., and B.F. O'Connor. 2008. Seprase: an overview of an important matrix serine protease. *Biochimica et biophysica acta*. 1784:1130-1145.

Oikawa, T., T. Itoh, and T. Takenawa. 2008. Sequential signals toward podosome formation in NIH-src cells. *The Journal of cell biology*. 182:157-169.

Oikawa, T., and T. Takenawa. 2009. PtdIns(3,4)P2 instigates focal adhesions to generate podosomes. *Cell adhesion & migration*. 3:195-197.

Ortega, N., D. Behonick, D. Stickens, and Z. Werb. 2003. How proteases regulate bone morphogenesis. *Annals of the New York Academy of Sciences*. 995:109-116.

Oser, M., and J. Condeelis. 2009. The cofilin activity cycle in lamellipodia and invadopodia. *Journal of cellular biochemistry*. 108:1252-1262.

Oser, M., H. Yamaguchi, C.C. Mader, J.J. Bravo-Cordero, M. Arias, X. Chen, V. Desmarais, J. van Rheenen, A.J. Koleske, and J. Condeelis. 2009. Cortactin regulates cofilin and N-WASp activities to control the stages of invadopodium assembly and maturation. *The Journal of cell biology*. 186:571-587.

Overall, C.M., and R.A. Dean. 2006. Degradomics: systems biology of the protease web. Pleiotropic roles of MMPs in cancer. *Cancer metastasis reviews*. 25:69-75.

Page-McCaw, A., A.J. Ewald, and Z. Werb. 2007. Matrix metalloproteinases and the regulation of tissue remodelling. *Nature reviews. Molecular cell biology*. 8:221-233.

Papageorgis, P., A.W. Lambert, S. Ozturk, F. Gao, H. Pan, U. Manne, Y.O. Alekseyev, A. Thiagalingam, H.M. Abdolmaleky, M. Lenburg, and S. Thiagalingam. 2010. Smad signaling is required to maintain epigenetic silencing during breast cancer progression. *Cancer research*. 70:968-978.

Park, L., P.A. Thomason, T. Zech, J.S. King, D.M. Veltman, M. Carnell, S. Ura, L.M. Machesky, and R.H. Insall. 2013. Cyclical action of the WASH complex: FAM21 and capping protein drive WASH recycling, not initial recruitment. *Developmental cell*. 24:169-181.

Pathak, R., V.D. Delorme-Walker, M.C. Howell, A.N. Anselmo, M.A. White, G.M. Bokoch, and C. Dermardirossian. 2012. The microtubule-associated Rho activating factor GEF-H1 interacts with exocyst complex to regulate vesicle traffic. *Developmental cell*. 23:397-411.

Peinado, H., D. Olmeda, and A. Cano. 2007. Snail, Zeb and bHLH factors in tumour progression: an alliance against the epithelial phenotype? *Nature reviews. Cancer*. 7:415-428.

Perentes, J.Y., N.D. Kirkpatrick, S. Nagano, E.Y. Smith, C.M. Shaver, D. Sgroi, I. Garkavtsev, L.L. Munn, R.K. Jain, and Y. Boucher. 2011. Cancer cell-associated MT1-MMP promotes blood vessel invasion and distant metastasis in triple-negative mammary tumors. *Cancer research*. 71:4527-4538.

Pichot, C.S., C. Arvanitis, S.M. Hartig, S.A. Jensen, J. Bechill, S. Marzouk, J. Yu, J.A. Frost, and S.J. Corey. 2010. Cdc42-interacting protein 4 promotes breast cancer cell invasion and formation of invadopodia through activation of N-WASp. *Cancer research*. 70:8347-8356.

Pignatelli, J., D.A. Tumbarello, R.P. Schmidt, and C.E. Turner. 2012. Hic-5 promotes invadopodia formation and invasion during TGF-beta-induced epithelial-mesenchymal transition. *The Journal of cell biology*. 197:421-437.

Piotrowski, J.T., T.S. Gomez, R.A. Schoon, A.K. Mangalam, and D.D. Billadeau. 2013. WASH knockout T cells demonstrate defective receptor trafficking, proliferation, and effector function. *Molecular and cellular biology*. 33:958-973.

Poincloux, R., F. Lizarraga, and P. Chavrier. 2009. Matrix invasion by tumour cells: a focus on MT1-MMP trafficking to invadopodia. *Journal of cell science*. 122:3015-3024.

Polette, M., N. Gilbert, I. Stas, B. Nawrocki, A. Noel, A. Remacle, W.G. Stetler-Stevenson, P. Birembaut, and M. Foidart. 1994. Gelatinase A expression and localization in human breast cancers. An in situ hybridization study and immunohistochemical detection using confocal microscopy. *Virchows Archiv : an international journal of pathology*. 424:641-645.

Pollard, T.D. 2007. Regulation of actin filament assembly by Arp2/3 complex and formins. *Annual review of biophysics and biomolecular structure*. 36:451-477.

Pollard, T.D., and G.G. Borisy. 2003. Cellular motility driven by assembly and disassembly of actin filaments. *Cell*. 112:453-465.

Pons, V., C. Ustunel, C. Rolland, E. Torti, R.G. Parton, and J. Gruenberg. 2012. SNX12 role in endosome membrane transport. *PloS one*. 7:e38949.

Prigent, M., T. Dubois, G. Raposo, V. Derrien, D. Tenza, C. Rosse, J. Camonis, and P. Chavrier. 2003. ARF6 controls post-endocytic recycling through its downstream exocyst complex effector. *The Journal of cell biology*. 163:1111-1121.

Proux-Gillardeaux, V., R. Rudge, and T. Galli. 2005. The tetanus neurotoxin-sensitive and insensitive routes to and from the plasma membrane: fast and slow pathways? *Traffic*. 6:366-373.

Puente, X.S., L.M. Sanchez, C.M. Overall, and C. Lopez-Otin. 2003. Human and mouse proteases: a comparative genomic approach. *Nature reviews. Genetics*. 4:544-558.

Puthenveedu, M.A., B. Lauffer, P. Temkin, R. Vistein, P. Carlton, K. Thorn, J. Taunton, O.D. Weiner, R.G. Parton, and M. von Zastrow. 2010. Sequence-dependent sorting of recycling proteins by actin-stabilized endosomal microdomains. *Cell*. 143:761-773.

Rajadurai, C.V., S. Havrylov, K. Zaoui, R. Vaillancourt, M. Stuible, M. Naujokas, D. Zuo, M.L. Tremblay, and M. Park. 2012. Met receptor tyrosine kinase signals through a cortactin-Gab1 scaffold complex, to mediate invadopodia. *Journal of cell science*. 125:2940-2953.

Remacle, A., G. Murphy, and C. Roghi. 2003. Membrane type I-matrix metalloproteinase (MT1-MMP) is internalised by two different pathways and is recycled to the cell surface. *Journal of cell science*. 116:3905-3916.

Rey, M., M. Irondelle, F. Waharte, F. Lizarraga, and P. Chavrier. 2011. HDAC6 is required for invadopodia activity and invasion by breast tumor cells. *European journal of cell biology*. 90:128-135.

Ricard-Blum, S. 2011. The collagen family. *Cold Spring Harbor perspectives in biology*. 3:a004978.

Ridley, A.J. 2011. Life at the leading edge. *Cell*. 145:1012-1022.

Ridley, A.J., M.A. Schwartz, K. Burridge, R.A. Firtel, M.H. Ginsberg, G. Borisy, J.T. Parsons, and A.R. Horwitz. 2003. Cell migration: integrating signals from front to back. *Science*. 302:1704-1709.

Rivera, G.M., D. Vasilescu, V. Papayannopoulos, W.A. Lim, and B.J. Mayer. 2009. A reciprocal interdependence between Nck and PI(4,5)P(2) promotes localized N-WASp-mediated actin polymerization in living cells. *Molecular cell*. 36:525-535.

Rodriguez-Boulan, E., and I.G. Macara. 2014. Organization and execution of the epithelial polarity programme. *Nature reviews. Molecular cell biology*. 15:225-242.

Rosse, C., A. Hatzoglou, M.C. Parrini, M.A. White, P. Chavrier, and J. Camonis. 2006. RalB mobilizes the exocyst to drive cell migration. *Molecular and cellular biology*. 26:727-734.

Rosse, C., C. Lodillinsky, L. Fuhrmann, M. Nourieh, P. Monteiro, M. Irondelle, E. Lagoutte, S. Vacher, F. Waharte, P. Paul-Gilloteaux, M. Romao, L. Sengmanivong, M. Linch, J. van Lint, G. Raposo, A. Vincent-Salomon, I. Bieche, P.J. Parker, and P. Chavrier. 2014. Control of MT1-MMP transport by atypical PKC during breast-cancer progression. *Proceedings of the National Academy of Sciences of the United States of America*. 111:E1872-1879.

Rottner, K., J. Hanisch, and K.G. Campellone. 2010. WASH, WHAMM and JMY: regulation of Arp2/3 complex and beyond. *Trends in cell biology*. 20:650-661.

Rotty, J.D., C. Wu, and J.E. Bear. 2013. New insights into the regulation and cellular functions of the ARP2/3 complex. *Nature reviews. Molecular cell biology*. 14:7-12.

Rowe, R.G., and S.J. Weiss. 2008. Breaching the basement membrane: who, when and how? *Trends in cell biology*. 18:560-574.

Rowe, R.G., and S.J. Weiss. 2009. Navigating ECM barriers at the invasive front: the cancer cell-stroma interface. *Annual review of cell and developmental biology*. 25:567-595.

Roy, R., J. Yang, and M.A. Moses. 2009. Matrix metalloproteinases as novel biomarkers and potential therapeutic targets in human cancer. *Journal of clinical oncology : official journal of the American Society of Clinical Oncology*. 27:5287-5297.

Sabeh, F., I. Ota, K. Holmbeck, H. Birkedal-Hansen, P. Soloway, M. Balbin, C. Lopez-Otin, S. Shapiro, M. Inada, S. Krane, E. Allen, D. Chung, and S.J. Weiss. 2004. Tumor cell traffic through the extracellular matrix is controlled by the membrane-anchored collagenase MT1-MMP. *The Journal of cell biology*. 167:769-781.

Sabeh, F., R. Shimizu-Hirota, and S.J. Weiss. 2009. Protease-dependent versus -independent cancer cell invasion programs: three-dimensional amoeboid movement revisited. *The Journal of cell biology*. 185:11-19.

Saengsawang, W., K.L. Taylor, D.C. Lumbard, K. Mitok, A. Price, L. Pietila, T.M. Gomez, and E.W. Dent. 2013. CIP4 coordinates with phospholipids and actin-associated proteins to localize to the protruding edge and produce actin ribs and veils. *Journal of cell science*. 126:2411-2423.

Sage, J., E. Leblanc-Noblesse, C. Nizard, T. Sasaki, S. Schnebert, E. Perrier, R. Kurfurst, D. Bromme, G. Lalmanach, and F. Lecaille. 2012. Cleavage of nidogen-1 by cathepsin S impairs its binding to basement membrane partners. *PloS one*. 7:e43494.

Sakurai-Yageta, M., C. Recchi, G. Le Dez, J.B. Sibarita, L. Daviet, J. Camonis, C. D'Souza-Schorey, and P. Chavrier. 2008. The interaction of IQGAP1 with the exocyst complex is required for tumor cell invasion downstream of Cdc42 and RhoA. *The Journal of cell biology*. 181:985-998.

Salminen, A., and P.J. Novick. 1989. The Sec15 protein responds to the function of the GTP binding protein, Sec4, to control vesicular traffic in yeast. *The Journal of cell biology*. 109:1023-1036.

Sanchez-Bailon, M.P., A. Calcabrini, D. Gomez-Dominguez, B. Morte, E. Martin-Forero, G. Gomez-Lopez, A. Molinari, K.U. Wagner, and J. Martin-Perez. 2012. Src kinases catalytic activity regulates proliferation, migration and invasiveness of MDA-MB-231 breast cancer cells. *Cellular signalling*. 24:1276-1286.

Sanz-Moreno, V., and C.J. Marshall. 2010. The plasticity of cytoskeletal dynamics underlying neoplastic cell migration. *Current opinion in cell biology*. 22:690-696.

Sato, H., T. Kinoshita, T. Takino, K. Nakayama, and M. Seiki. 1996. Activation of a recombinant membrane type 1-matrix metalloproteinase (MT1-MMP) by furin and its interaction with tissue inhibitor of metalloproteinases (TIMP)-2. *FEBS letters*. 393:101-104.

Schneider, M., W. Lu, S. Neumann, A. Brachner, J. Gotzmann, A.A. Noegel, and I. Karakesisoglou. 2011. Molecular mechanisms of centrosome and cytoskeleton anchorage at the nuclear envelope. *Cellular and molecular life sciences : CMLS*. 68:1593-1610.

Schoumacher, M., R.D. Goldman, D. Louvard, and D.M. Vignjevic. 2010. Actin, microtubules, and vimentin intermediate filaments cooperate for elongation of invadopodia. *The Journal of cell biology*. 189:541-556.

Schroder, H.M., S.C. Hoffmann, M. Hecker, T. Korff, and T. Ludwig. 2013. The tetraspanin network modulates MT1-MMP cell surface trafficking. *The international journal of biochemistry & cell biology*. 45:1133-1144.

Seals, D.F., E.F. Azucena, Jr., I. Pass, L. Tesfay, R. Gordon, M. Woodrow, J.H. Resau, and S.A. Courtneidge. 2005. The adaptor protein Tks5/Fish is required for podosome formation and function, and for the protease-driven invasion of cancer cells. *Cancer cell*. 7:155-165.

Seals, D.F., and S.A. Courtneidge. 2003. The ADAMs family of metalloproteases: multidomain proteins with multiple functions. *Genes & development*. 17:7-30.

Seaman, M.N. 2008. Endosome protein sorting: motifs and machinery. *Cellular and molecular life sciences : CMLS*. 65:2842-2858.

Seaman, M.N. 2012. The retromer complex - endosomal protein recycling and beyond. *Journal of cell science*. 125:4693-4702.

Seaman, M.N., A. Gautreau, and D.D. Billadeau. 2013. Retromer-mediated endosomal protein sorting: all WASHed up! *Trends in cell biology*. 23:522-528.

Shahbazi, M.N., D. Megias, C. Epifano, A. Akhmanova, G.G. Gundersen, E. Fuchs, and M. Perez-Moreno. 2013. CLASP2 interacts with p120-catenin and governs microtubule dynamics at adherens junctions. *The Journal of cell biology*. 203:1043-1061.

Sharma, V.P., R. Eddy, D. Entenberg, M. Kai, F.B. Gertler, and J. Condeelis. 2013. Tks5 and SHIP2 regulate invadopodium maturation, but not initiation, in breast carcinoma cells. *Current biology : CB*. 23:2079-2089.

Shin, J.W., K.R. Spinler, J. Swift, J.A. Chasis, N. Mohandas, and D.E. Discher. 2013. Lamins regulate cell trafficking and lineage maturation of adult human hematopoietic cells. *Proceedings of the National Academy of Sciences of the United States of America*. 110:18892-18897.

Smith-Pearson, P.S., E.K. Greuber, G. Yogalingam, and A.M. Pendergast. 2010. Abl kinases are required for invadopodia formation and chemokine-induced invasion. *The Journal of biological chemistry*. 285:40201-40211.

Soofi, S.S., J.A. Last, S.J. Liliensiek, P.F. Nealey, and C.J. Murphy. 2009. The elastic modulus of Matrigel as determined by atomic force microscopy. *Journal of structural biology*. 167:216-219.

Srinivasan, D., and R. Plattner. 2006. Activation of Abl tyrosine kinases promotes invasion of aggressive breast cancer cells. *Cancer research*. 66:5648-5655.

Stautz, D., A. Sanjay, M.T. Hansen, R. Albrechtsen, U.M. Wewer, and M. Kveiborg. 2010. ADAM12 localizes with c-Src to actin-rich structures at the cell periphery and regulates Src kinase activity. *Experimental cell research*. 316:55-67.

Steffen, A., G. Le Dez, R. Poincloux, C. Recchi, P. Nassoy, K. Rottner, T. Galli, and P. Chavrier. 2008. MT1-MMP-dependent invasion is regulated by TI-VAMP/VAMP7. *Current biology : CB*. 18:926-931.

Steinberg, F., M. Gallon, M. Winfield, E.C. Thomas, A.J. Bell, K.J. Heesom, J.M. Tavare, and P.J. Cullen. 2013. A global analysis of SNX27-retromer assembly and cargo specificity reveals a function in glucose and metal ion transport. *Nature cell biology*. 15:461-471.

Stenmark, H. 2009. Rab GTPases as coordinators of vesicle traffic. *Nature reviews. Molecular cell biology*. 10:513-525.

Stenmark, H., and V.M. Olkkonen. 2001. The Rab GTPase family. *Genome biology*. 2:REVIEWS3007.

Sternlicht, M.D., and Z. Werb. 2001. How matrix metalloproteinases regulate cell behavior. *Annual review of cell and developmental biology*. 17:463-516.

Strongin, A.Y., I. Collier, G. Bannikov, B.L. Marmer, G.A. Grant, and G.I. Goldberg. 1995. Mechanism of cell surface activation of 72-kDa type IV collagenase. Isolation of the activated form of the membrane metalloprotease. *The Journal of biological chemistry*. 270:5331-5338.

Stylli, S.S., T.T. Stacey, A.M. Verhagen, S.S. Xu, I. Pass, S.A. Courtneidge, and P. Lock. 2009. Nck adaptor proteins link Tks5 to invadopodia actin regulation and ECM degradation. *Journal of cell science*. 122:2727-2740.

Su, G., S.A. Blaine, D. Qiao, and A. Friedl. 2008. Membrane type 1 matrix metalloproteinase-mediated stromal syndecan-1 shedding stimulates breast carcinoma cell proliferation. *Cancer research*. 68:9558-9565.

Suenaga, N., H. Mori, Y. Itoh, and M. Seiki. 2005. CD44 binding through the hemopexin-like domain is critical for its shedding by membrane-type 1 matrix metalloproteinase. *Oncogene*. 24:859-868.

Sugihara, K., S. Asano, K. Tanaka, A. Iwamatsu, K. Okawa, and Y. Ohta. 2002. The exocyst complex binds the small GTPase RalA to mediate filopodia formation. *Nature cell biology*. 4:73-78.

Sugiyama, N., E. Gucciardo, O. Tatti, M. Varjosalo, M. Hyytiainen, M. Gstaiger, and K. Lehti. 2013. EphA2 cleavage by MT1-MMP triggers single cancer cell invasion via homotypic cell repulsion. *The Journal of cell biology*. 201:467-484.

Summy, J.M., and G.E. Gallick. 2003. Src family kinases in tumor progression and metastasis. *Cancer metastasis reviews*. 22:337-358.

Svitkina, T.M., and G.G. Borisy. 1999. Arp2/3 complex and actin depolymerizing factor/cofilin in dendritic organization and treadmilling of actin filament array in lamellipodia. *The Journal of cell biology*. 145:1009-1026.

Swift, J., and D.E. Discher. 2014. The nuclear lamina is mechano-responsive to ECM elasticity in mature tissue. *Journal of cell science*. 127:3005-3015.

Swift, J., I.L. Ivanovska, A. Buxboim, T. Harada, P.C. Dingal, J. Pinter, J.D. Pajerowski, K.R. Spinler, J.W. Shin, M. Tewari, F. Rehfeldt, D.W. Speicher, and D.E. Discher. 2013. Nuclear lamin-A scales with tissue stiffness and enhances matrix-directed differentiation. *Science*. 341:1240104.

Szabova, L., K. Chrysovergis, S.S. Yamada, and K. Holmbeck. 2008. MT1-MMP is required for efficient tumor dissemination in experimental metastatic disease. *Oncogene*. 27:3274-3281.

Takenawa, T., and T. Itoh. 2001. Phosphoinositides, key molecules for regulation of actin cytoskeletal organization and membrane traffic from the plasma membrane. *Biochimica et biophysica acta*. 1533:190-206.

Takino, T., H. Miyamori, N. Kawaguchi, T. Uekita, M. Seiki, and H. Sato. 2003. Tetraspanin CD63 promotes targeting and lysosomal proteolysis of membrane-type 1 matrix metalloproteinase. *Biochemical and biophysical research communications*. 304:160-166.

Tao, G., A.K. Levay, T. Gridley, and J. Lincoln. 2011. Mmp15 is a direct target of Snai1 during endothelial to mesenchymal transformation and endocardial cushion development. *Developmental biology*. 359:209-221.

Tarone, G., D. Cirillo, F.G. Giancotti, P.M. Comoglio, and P.C. Marchisio. 1985. Rous sarcoma virus-transformed fibroblasts adhere primarily at discrete protrusions of the ventral membrane called podosomes. *Experimental cell research*. 159:141-157.

Temkin, P., B. Lauffer, S. Jager, P. Cimermancic, N.J. Krogan, and M. von Zastrow. 2011. SNX27 mediates retromer tubule entry and endosome-to-plasma membrane trafficking of signalling receptors. *Nature cell biology*. 13:715-721.

TerBush, D.R., T. Maurice, D. Roth, and P. Novick. 1996. The Exocyst is a multiprotein complex required for exocytosis in Saccharomyces cerevisiae. *The EMBO journal*. 15:6483-6494.

Thapa, N., Y. Sun, M. Schramp, S. Choi, K. Ling, and R.A. Anderson. 2012. Phosphoinositide signaling regulates the exocyst complex and polarized integrin trafficking in directionally migrating cells. *Developmental cell*. 22:116-130.

Thiery, J.P. 2002. Epithelial-mesenchymal transitions in tumour progression. *Nature reviews. Cancer*. 2:442-454.

Thiery, J.P., H. Acloque, R.Y. Huang, and M.A. Nieto. 2009. Epithelial-mesenchymal transitions in development and disease. *Cell*. 139:871-890.

Tochowicz, A., P. Goettig, R. Evans, R. Visse, Y. Shitomi, R. Palmisano, N. Ito, K. Richter, K. Maskos, D. Franke, D. Svergun, H. Nagase, W. Bode, and Y. Itoh. 2011. The dimer interface of the membrane type 1 matrix metalloproteinase hemopexin domain: crystal structure and biological functions. *The Journal of biological chemistry*. 286:7587-7600.

Tu, C., C.F. Ortega-Cava, G. Chen, N.D. Fernandes, D. Cavallo-Medved, B.F. Sloane, V. Band, and H. Band. 2008. Lysosomal cathepsin B participates in the podosome-mediated extracellular matrix degradation and invasion via secreted lysosomes in v-Src fibroblasts. *Cancer research*. 68:9147-9156.

Udayakumar, T.S., M.L. Chen, E.L. Bair, D.C. Von Bredow, A.E. Cress, R.B. Nagle, and G.T. Bowden. 2003. Membrane type-1-matrix metalloproteinase expressed by prostate carcinoma cells cleaves human laminin-5 beta3 chain and induces cell migration. *Cancer research*. 63:2292-2299.

Uekita, T., Y. Itoh, I. Yana, H. Ohno, and M. Seiki. 2001. Cytoplasmic tail-dependent internalization of membrane-type 1 matrix metalloproteinase is important for its invasion-promoting activity. *The Journal of cell biology*. 155:1345-1356.

Uruno, T., J. Liu, P. Zhang, Y. Fan, C. Egile, R. Li, S.C. Mueller, and X. Zhan. 2001. Activation of Arp2/3 complex-mediated actin polymerization by cortactin. *Nature cell biology*. 3:259-266.

Vaananen, H.K., and T. Laitala-Leinonen. 2008. Osteoclast lineage and function. *Archives of biochemistry and biophysics*. 473:132-138.

Vega, I.E., and S.C. Hsu. 2001. The exocyst complex associates with microtubules to mediate vesicle targeting and neurite outgrowth. *The Journal of neuroscience : the official journal of the Society for Neuroscience*. 21:3839-3848.

Veltman, D.M., and R.H. Insall. 2010. WASP family proteins: their evolution and its physiological implications. *Molecular biology of the cell*. 21:2880-2893.

Wang, S., Y. Yuan, L. Liao, S.Q. Kuang, J.C. Tien, B.W. O'Malley, and J. Xu. 2009. Disruption of the SRC-1 gene in mice suppresses breast cancer metastasis without affecting primary tumor formation. *Proceedings of the National Academy of Sciences of the United States of America*. 106:151-156.

Wang, X., D. Ma, J. Keski-Oja, and D. Pei. 2004. Co-recycling of MT1-MMP and MT3-MMP through the trans-Golgi network. Identification of DKV582 as a recycling signal. *The Journal of biological chemistry*. 279:9331-9336.

Weaver, A.M., J.E. Heuser, A.V. Karginov, W.L. Lee, J.T. Parsons, and J.A. Cooper. 2002. Interaction of cortactin and N-WASp with Arp2/3 complex. *Current biology : CB*. 12:1270-1278.

Weaver, A.M., A.V. Karginov, A.W. Kinley, S.A. Weed, Y. Li, J.T. Parsons, and J.A. Cooper. 2001. Cortactin promotes and stabilizes Arp2/3-induced actin filament network formation. *Current biology : CB*. 11:370-374.

Weijer, C.J. 2009. Collective cell migration in development. *Journal of cell science*. 122:3215-3223.

Wiesner, C., K. El Azzouzi, and S. Linder. 2013. A specific subset of RabGTPases controls cell surface exposure of MT1-MMP, extracellular matrix degradation and three-dimensional invasion of macrophages. *Journal of cell science*. 126:2820-2833.

Wiesner, C., J. Faix, M. Himmel, F. Bentzien, and S. Linder. 2010. KIF5B and KIF3A/KIF3B kinesins drive MT1-MMP surface exposure, CD44 shedding, and extracellular matrix degradation in primary macrophages. *Blood*. 116:1559-1569.

Williams, K.C., and M.G. Coppolino. 2011. Phosphorylation of membrane type 1-matrix metalloproteinase (MT1-MMP) and its vesicle-associated membrane protein 7 (VAMP7)-dependent trafficking facilitate cell invasion and migration. *The Journal of biological chemistry*. 286:43405-43416.

Williams, K.C., R.E. McNeilly, and M.G. Coppolino. 2014. SNAP23, Syntaxin4, and vesicle-associated membrane protein 7 (VAMP7) mediate trafficking of membrane type 1-matrix metalloproteinase (MT1-MMP) during invadopodium formation and tumor cell invasion. *Molecular biology of the cell*. 25:2061-2070.

Willis, A.L., F. Sabeh, X.Y. Li, and S.J. Weiss. 2013. Extracellular matrix determinants and the regulation of cancer cell invasion stratagems. *Journal of microscopy*. 251:250-260.

Wolf, K., I. Mazo, H. Leung, K. Engelke, U.H. von Andrian, E.I. Deryugina, A.Y. Strongin, E.B. Brocker, and P. Friedl. 2003a. Compensation mechanism in tumor cell migration: mesenchymal-amoeboid transition after blocking of pericellular proteolysis. *The Journal of cell biology*. 160:267-277.

Wolf, K., R. Muller, S. Borgmann, E.B. Brocker, and P. Friedl. 2003b. Amoeboid shape change and contact guidance: T-lymphocyte crawling through fibrillar collagen is independent of matrix remodeling by MMPs and other proteases. *Blood*. 102:3262-3269.

Wolf, K., M. Te Lindert, M. Krause, S. Alexander, J. Te Riet, A.L. Willis, R.M. Hoffman, C.G. Figdor, S.J. Weiss, and P. Friedl. 2013. Physical limits of cell migration: control by ECM space and nuclear deformation and tuning by proteolysis and traction force. *The Journal of cell biology*. 201:1069-1084.

Wolf, K., Y.I. Wu, Y. Liu, J. Geiger, E. Tam, C. Overall, M.S. Stack, and P. Friedl. 2007. Multi-step pericellular proteolysis controls the transition from individual to collective cancer cell invasion. *Nature cell biology*. 9:893-904.

Wu, X., B. Gan, Y. Yoo, and J.L. Guan. 2005. FAK-mediated src phosphorylation of endophilin A2 inhibits endocytosis of MT1-MMP and promotes ECM degradation. *Developmental cell*. 9:185-196.

Xue, B., K. Krishnamurthy, D.C. Allred, and S.K. Muthuswamy. 2013. Loss of Par3 promotes breast cancer metastasis by compromising cell-cell cohesion. *Nature cell biology*. 15:189-200.

Yamaguchi, H., and J. Condeelis. 2007. Regulation of the actin cytoskeleton in cancer cell migration and invasion. *Biochimica et biophysica acta*. 1773:642-652.

Yamaguchi, H., M. Lorenz, S. Kempiak, C. Sarmiento, S. Coniglio, M. Symons, J. Segall, R. Eddy, H. Miki, T. Takenawa, and J. Condeelis. 2005. Molecular mechanisms of invadopodium formation: the role of the N-WASP-Arp2/3 complex pathway and cofilin. *The Journal of cell biology*. 168:441-452.

Yamaguchi, H., and T. Oikawa. 2010. Membrane lipids in invadopodia and podosomes: key structures for cancer invasion and metastasis. *Oncotarget*. 1:320-328.

Yamaguchi, H., Y. Takeo, S. Yoshida, Z. Kouchi, Y. Nakamura, and K. Fukami. 2009. Lipid rafts and caveolin-1 are required for invadopodia formation and extracellular matrix degradation by human breast cancer cells. *Cancer research*. 69:8594-8602.

Yamaguchi, H., S. Yoshida, E. Muroi, M. Kawamura, Z. Kouchi, Y. Nakamura, R. Sakai, and K. Fukami. 2010. Phosphatidylinositol 4,5-bisphosphate and PIP5-kinase Ialpha are required for invadopodia formation in human breast cancer cells. *Cancer science*. 101:1632-1638.

Yamamoto, A., A. Kasamatsu, S. Ishige, K. Koike, K. Saito, Y. Kouzu, H. Koike, Y. Sakamoto, K. Ogawara, M. Shiiba, H. Tanzawa, and K. Uzawa. 2013. Exocyst complex component Sec8: a presumed component in the progression of human oral squamous-cell carcinoma by secretion of matrix metalloproteinases. *Journal of cancer research and clinical oncology*. 139:533-542.

Yana, I., and S.J. Weiss. 2000. Regulation of membrane type-1 matrix metalloproteinase activation by proprotein convertases. *Molecular biology of the cell*. 11:2387-2401.

Yang, J., and R.A. Weinberg. 2008. Epithelial-mesenchymal transition: at the crossroads of development and tumor metastasis. *Developmental cell*. 14:818-829.

Yeaman, C., K.K. Grindstaff, and W.J. Nelson. 2004. Mechanism of recruiting Sec6/8 (exocyst) complex to the apical junctional complex during polarization of epithelial cells. *Journal of cell science*. 117:559-570.

Yilmaz, M., and G. Christofori. 2009. EMT, the cytoskeleton, and cancer cell invasion. *Cancer metastasis reviews*. 28:15-33.

Yokoyama, K., N. Kamata, R. Fujimoto, S. Tsutsumi, M. Tomonari, M. Taki, H. Hosokawa, and M. Nagayama. 2003. Increased invasion and matrix metalloproteinase-2 expression by Snail-induced mesenchymal transition in squamous cell carcinomas. *International journal of oncology*. 22:891-898.

Yu, X., T. Zech, L. McDonald, E.G. Gonzalez, A. Li, I. Macpherson, J.P. Schwarz, H. Spence, K. Futo, P. Timpson, C. Nixon, Y. Ma, I.M. Anton, B. Visegrady, R.H. Insall, K. Oien, K. Blyth, J.C. Norman, and L.M. Machesky. 2012. N-WASP coordinates the delivery and F-actin-mediated capture of MT1-MMP at invasive pseudopods. *The Journal of cell biology*. 199:527-544.

Yurchenco, P.D. 2011. Basement membranes: cell scaffoldings and signaling platforms. *Cold Spring Harbor perspectives in biology*. 3.

Zarzynska, J.M. 2014. Two FACes of TGF-beta1 in breast cancer. *Mediators of inflammation*. 2014:141747.

Zavodszky, E., M.N. Seaman, K. Moreau, M. Jimenez-Sanchez, S.Y. Breusegem, M.E. Harbour, and D.C. Rubinsztein. 2014a. Mutation in VPS35 associated with Parkinson's disease impairs WASH complex association and inhibits autophagy. *Nature communications*. 5:3828.

Zavodszky, E., M.N. Seaman, and D.C. Rubinsztein. 2014b. VPS35 Parkinson mutation impairs autophagy via WASH. *Cell cycle*. 13.

Zech, T., S.D. Calaminus, P. Caswell, H.J. Spence, M. Carnell, R.H. Insall, J. Norman, and L.M. Machesky. 2011. The Arp2/3 activator WASH regulates alpha5beta1-integrin-mediated invasive migration. *Journal of cell science*. 124:3753-3759.

Zhang, X., E. Bi, P. Novick, L. Du, K.G. Kozminski, J.H. Lipschutz, and W. Guo. 2001. Cdc42 interacts with the exocyst and regulates polarized secretion. *The Journal of biological chemistry*. 276:46745-46750.

Zhang, X., K. Orlando, B. He, F. Xi, J. Zhang, A. Zajac, and W. Guo. 2008. Membrane association and functional regulation of Sec3 by phospholipids and Cdc42. *The Journal of cell biology*. 180:145-158.

Zhou, Z., S.S. Apte, R. Soininen, R. Cao, G.Y. Baaklini, R.W. Rauser, J. Wang, Y. Cao, and K. Tryggvason. 2000. Impaired endochondral ossification and angiogenesis in mice deficient in membrane-type matrix metalloproteinase I. *Proceedings of the National Academy of Sciences of the United States of America*. 97:4052-4057.

Zucker, S., M. Hymowitz, C. Conner, Y. DeClerck, and J. Cao. 2004. TIMP-2 is released as an intact molecule following binding to MT1-MMP on the cell surface. *Experimental cell research*. 293:164-174.

Zuo, X., J. Zhang, Y. Zhang, S.C. Hsu, D. Zhou, and W. Guo. 2006. Exo70 interacts with the Arp2/3 complex and regulates cell migration. *Nature cell biology*. 8:1383-1388.

Annexes

Article 2

Control of MT1-MMP transport by atypical PKC during breast-cancer progression

Carine Rossé, Catalina Lodillinsky, Laetitia Fuhrmann, Maya Nourieh, **Pedro Monteiro**, Marie Irondelle, Emilie Lagoutte, Sophie Vacher, François Waharte, Perrine Paul-Gilloteaux, Maryse Romao, Lucie Sengmanivong, Mark Linch, Johan van Lint, Graça Raposo, Anne Vincent-Salomon, Ivan Bièche, Peter J. Parker and Philippe Chavrier

Proc Natl Acad Sci U S A. (2014) 6;111(18):E1872-9 doi: 10.1073/pnas.1400749111

Contribution article PNAS :

J'ai apporté ma contribution à cette étude en identifiant l'implication des protéines aPKC (zeta et iota) dans la formation d'invadopodes dans les cellules tumorales. J'ai observé le comportement de cellules MDA-MB-231 co-exprimant la cortactine ainsi que la protéase MT1-MMP – couplée à une étiquette pHluorin – cultivées sur un susbtrat de collagène dénaturé (Figure 3F). Contrairement aux cellules contrôle (traitement par siRNA non relevant), les cellules dont l'expression de aPKC (zeta et iota) est éteinte par traitement siRNA ne sont plus capables de former des invadopodes positifs pour la cortactine ainsi que MT1-MMP (Figure 3G).

Figure 3F et 3G : mise en place de l'expérience, quantification et panel de la figure.

J'ai par ailleurs également apporté ma contribution à la mise en page des Figures 4 et S3.

Control of MT1-MMP transport by atypical PKC during breast-cancer progression

Carine Rossé[a,b,1], Catalina Lodillinsky[a,b], Laetitia Fuhrmann[a], Maya Nourieh[a], Pedro Monteiro[a,b,c], Marie Irondelle[a,b], Emilie Lagoutte[a,b], Sophie Vacher[d], François Waharte[a,e], Perrine Paul-Gilloteaux[a,e], Maryse Romao[a,f], Lucie Sengmanivong[a,e,g], Mark Linch[h], Johan van Lint[i], Graça Raposo[a,f], Anne Vincent-Salomon[a,j,k], Ivan Bièche[d], Peter J. Parker[h,l], and Philippe Chavrier[a,b,1]

[a]Research Center, Institut Curie, 75005 Paris, France; [b]Membrane and Cytoskeleton Dynamics, Centre National de la Recherche Scientifique, Unité Mixte de Recherche 144, 75005 Paris, France; [c]Sorbonne Universités, Université Pierre et Marie Curie, University of Paris VI, Institut de Formation Doctorale, 75252 Paris Cedex 5, France; [d]Department of Genetics, Institut Curie, 75005 Paris, France; [e]Cell and Tissue Imaging Facility, Centre National de la Recherche Scientifique, Unité Mixte de Recherche 144, 75005 Paris, France; [f]Structure and Membrane Compartments, Centre National de la Recherche Scientifique, Unité Mixte de Recherche 144, 75005 Paris, France; [g]Nikon Imaging Centre, Institut Curie, Centre National de la Recherche Scientifique, 75005 Paris, France; [h]Protein Phosphorylation Laboratory, Cancer Research UK London Research Institute, London WC2A 3LY, United Kingdom; [i]Department of Molecular Cell Biology, Faculty of Medicine, Katholieke Universiteit Leuven, 3000 Leuven, Belgium; [j]Department of Tumor Biology, Institut Curie, 75005 Paris, France; [k]Institut National de la Santé et de la Recherche Médicale U830, 75005 Paris, France; and [l]Division of Cancer Studies, King's College London, Guy's Campus, London WC2A 3LY, United Kingdom

Edited by Mina J. Bissell, E. O. Lawrence Berkeley National Laboratory, Berkeley, CA, and approved March 27, 2014 (received for review January 14, 2014)

Dissemination of carcinoma cells requires the pericellular degradation of the extracellular matrix, which is mediated by membrane type 1-matrix metalloproteinase (MT1-MMP). In this article, we report a co–up-regulation and colocalization of MT1-MMP and atypical protein kinase C iota (aPKCι) in hormone receptor-negative breast tumors in association with a higher risk of metastasis. Silencing of aPKC in invasive breast-tumor cell lines impaired the delivery of MT1-MMP from late endocytic storage compartments to the surface and inhibited matrix degradation and invasion. We provide evidence that aPKCι, in association with MT1-MMP–containing endosomes, phosphorylates cortactin, which is present in F-actin–rich puncta on MT1-MMP–positive endosomes and regulates cortactin association with the membrane scission protein dynamin-2. Thus, cell line-based observations and clinical data reveal the concerted activity of aPKC, cortactin, and dynamin-2, which control the trafficking of MT1-MMP from late endosome to the plasma membrane and play an important role in the invasive potential of breast-cancer cells.

membrane traffic | actin cytoskeleton | multi-vesicular body | MMP14

Metastasis—the process by which cells from a primary tumor invade local tissues and disseminate to distant sites—marks the transition from a benign tumor to a lethal, malignant cancer. One intrinsic property of metastatic tumor cells that allows them to breach tissue barriers is their ability to degrade the proteins of the extracellular matrix (ECM). This remodeling of the ECM by cancer cells depends on matrix-degrading proteases, including matrix metalloproteinases (MMPs) (1, 2). Although secreted MMPs have been implicated in cancer for several decades, it is more recently that a subgroup of membrane-anchored MMPs, including membrane type 1 (MT1)-MMP, have been recognized as important proteases involved in dissemination of tumor cells and cancer progression (3–7).

Membrane type 1-matrix metalloproteinase (MT1-MMP) is up-regulated in human cancers, including breast cancers, and it is enriched at the front of invasive lesions (8, 9). In tumor-derived cells cultured on a flat ECM substratum, such as gelatin or type I collagen, MT1-MMP accumulates in specialized matrix-degrading plasma-membrane domains called invadopodia (10). The current view is that interaction of matrix receptors on the tumor-cell surface with components of the ECM leads to assembly of nascent invadopodia containing F-actin and cortactin, which mature into matrix-degrading invadopodia when they accumulate MT1-MMP (11).

Little is known about how invadopodia form in metastatic cells and how they are endowed with proteolytic activity. In MDA-MB-231 human breast adenocarcinoma cells, newly synthesized MT1-MMP passes through the secretory pathway to reach the plasma membrane where it is then endocytosed (12). The majority of internalized MT1-MMP is located in a late endocytic compartment from where a fraction recycles to plasma-membrane invadopodia (13). Various studies, including our own, have identified several components of the exocytic machinery that are required for delivery of MT1-MMP to invadopodia, including cortactin (a regulator of actin dynamics), the exocyst complex (required for docking of transport vesicles), and vesicle-associated membrane protein 7 (VAMP7) (a late endosome v-SNARE protein involved in vesicle fusion) (10, 13–16). Although these findings provide important insights into how MT1-MMP is delivered to the invadopodial plasma membrane, the mechanisms underlying the formation of MT1-MMP transport intermediates from late endocytic compartments remain largely unexplored.

Atypical protein kinase C (aPKC) comprises a branch of the serine/threonine PKC superfamily consisting of two isoforms, aPKCς and aPKCι, that are distinct from the typical, diacylglycerol-regulated isoforms (17). aPKCζ/ι are activated mainly by components of the PAR complex, Cdc42 and Par-3, and play a critical role in the formation of epithelial cell–cell junctions and the development of apico-basal polarity in mammalian epithelial cells (18). Previously, we reported the role of an aPKCζ/ι–exocyst complex in signaling at the leading edge of

Significance

We characterize a mechanism through which the polarity protein atypical PKCι controls invasion and matrix remodeling by tumor cells by regulating endosome-to-plasma membrane traffic of the membrane type 1-matrix metalloproteinase (MT1-MMP) in breast-cancer cells. Further analysis shows that atypical PKCι and MT1-MMP are co–up-regulated in hormone receptor-negative breast tumors in association with higher risk of metastasis. These findings provide previously unidentified avenues for the design of therapeutic interventions.

Author contributions: C.R. and P.C. designed research; C.R., L.F., P.M., M.I., S.V., M.R., and L.S. performed research; E.L., P.P.-G., M.L., and J.v.L. contributed new reagents/analytic tools; C.R., C.L., M.N., P.M., M.I., S.V., F.W., P.P.-G., G.R., A.V.-S., I.B., P.J.P., and P.C. analyzed data; and C.R. and P.C. wrote the paper.

The authors declare no conflict of interest.

This article is a PNAS Direct Submission.

[1]To whom correspondence may be addressed. E-mail: philippe.chavrier@curie.fr or carine.rosse@curie.fr.

This article contains supporting information online at www.pnas.org/lookup/suppl/doi:10.1073/pnas.1400749111/-/DCSupplemental.

migrating cells, so controlling paxillin phosphorylation and regulating focal adhesion dynamics (19). In addition, several lines of evidence implicate aPKCζ/ι in cancer: aPKCζ is required for epidermal growth factor-induced chemotaxis of human breast-cancer cells (20), and aPKCζ/ι promotes matrix degradation by Src-transformed mouse NIH 3T3 fibroblasts (21). Moreover, aPKCι expression is up-regulated in various cancers, including breast cancer, and correlates with poor prognosis (22, 23). The ability of aPKCζ/ι to control both cell polarity and the migration of cells makes it a prime candidate for a role in tumor progression and metastasis although the specific functions of aPKCζ/ι in metastatic cells are currently only poorly understood.

Here, we report an up-regulation and relocalization of MT1-MMP and aPKCι in breast-tumor samples associated with a high risk of metastasis. We found that silencing of aPKCζ/ι in human breast adenocarcinoma cell lines impairs ECM degradation and invasion of the cells into different reconstituted 3D matrix environments. These functional effects of aPKCζ/ι silencing correlate with defects in cortactin phosphorylation and distribution and dynamin-2 (dyn-2) recruitment and function on MT1-MMP–containing endosomes, resulting in impaired delivery of MT1-MMP to the invadopodial plasma membrane. This study thus identifies a previous unidentified coordinated function for aPKCζ/ι, cortactin, and dyn-2 in the control of MT1-MMP trafficking from late endosomes to the plasma membrane during breast-tumor cell invasion, providing a rationale for the design of therapeutic interventions.

Results

Co–Up-Regulation of MT1-MMP and aPKCι mRNAs Is Associated with Adverse Clinical Outcomes in Breast Cancer. In previous studies, we implicated the exocyst complex in MT1-MMP trafficking to invadopodia in MDA-MB-231 breast-tumor cells (15) and identified a coordinated function of the exocyst complex and aPKCζ/ι in migrating cells (19). MT1-MMP and aPKCι are overexpressed in various cancers, including breast cancers, and up-regulation is associated with poor prognosis (8, 9, 22, 24). These data suggested the possible interplay between MT1-MMP and aPKCζ/ι in the invasive program of breast-tumor cells. Expression of MT1-MMP and 11 aPKCζ/ι family members was investigated by qRT-PCR analysis in breast-tumor samples from 458 patients with unilateral invasive breast tumors and known long-term outcome (Table S1). MT1-MMP expression correlated most with aPKCι mRNA ($r = +0.556$, $P < 10^{-7}$) (Table 1). We looked for correlations between aPKCι and MT1-MMP mRNA status and standard clinicopathological and biological factors in this cohort. About one third of breast tumors tested (153/458) showed aPKCι mRNA overexpression (a greater than threefold increase compared with normal tissues), and 23.3% (107/458) showed MT1-MMP mRNA overexpression (Table S1). In the tumor group that overexpressed both aPKCι and MT1-MMP, we saw a statistically significant association with histopathological grade III ($P = 0.0041$), estrogen receptor (ER)-negative ($P = 0.0014$), and progesterone receptor (PR)-negative ($P = 0.001$) status, as well as with the molecular subtype ($P = 0.003$) (Table S1). Of note, 24.6% (17/69) of triple-negative breast cancers (ER^- PR^- $HER2^-$), a type of aggressive and highly proliferative tumors, overexpressed MT1-MMP and aPKCι vs. 12.8% (50/389) for the other subtypes ($P = 0.011$). Furthermore, by combining aPKCι and MT1-MMP mRNA expression status, we identified four distinct prognostic groups with significantly different metastasis-free survival (MFS) curves ($P = 0.008$) (Fig. 1*A*). The patients with the poorest prognosis had both aPKCι and MT1-MMP mRNA overexpression whereas those with the best prognosis had normal aPKCι and MT1-MMP mRNA levels.

Table 1. Correlation using the Spearman's rank correlation test between 11 genes of the PKC family and MT1-MMP mRNA expression in human breast cancer

Gene (protein)	Spearman correlation coefficient	*P**
PRKCA (PKCα)	0.233	**0.0000021**
PRKCE (PKCε)	0.045	0.34 (NS)
PRKCH (PKCη)	0.157	**0.0009**
PKN2 (PKN2)	0.061	0.19 (NS)
PRKCZ (PKCζ)	0.10	0.82 (NS)
PRKCD (PKCδ)	0.016	0.74 (NS)
PRKCQ (PKCθ)	−0.054	0.24 (NS)
PRKCI (PKCι)	0.556	**< 0.0000001**
PRKCB (PKCβ)	0.389	**< 0.0000001**
PKN1 (PKN1)	0.199	**0.000038**

Expression of genes encoding PKCs and MT1-MMP was analyzed by reverse transcriptase-quantitative polymerase chain reaction (RT-qPCR) of 458 mRNA tumor samples. Very low levels of mRNA encoding PKCγ were detectable but not reliably quantifiable by RT-qPCR assays using the fluorescence SYBR green methodology (cycle threshold > 35). NS, not significant.
**P* value of Spearman rank correlation test. In bold type, significant *P* values.

MT1-MMP and aPKCι Colocalize in Cytoplasmic Granules and at Cell–Cell Contacts in Hormone Receptor-Negative Breast-Carcinoma Cells. To investigate changes in protein levels and localization of MT1-MMP and aPKCι during breast-tumor progression, a human tissue microarray (TMA) of 68 breast tumors representative of the four main molecular subtypes (*Experimental Procedures*) was analyzed by immunohistocytochemistry (IHC), on consecutive sections (25) (Dataset S1 and Fig. 1 *B* and *C*). Compared with epithelial cells in surrounding nonneoplastic tissues, aPKCι was overexpressed in cancer cells in all subtypes whereas expression of MT1-MMP was significantly up-regulated in hormone receptor-negative tumors (ER^- PR^- $HER2^+$ and ER^- PR^- $HER2^-$) (Dataset S1, Fig. S1 *A* and *B*, and Fig. 1*D*). These data demonstrate a positive correlation between aPKCι and MT1-MMP expression in hormone receptor-negative subtypes of breast carcinomas at both the mRNA and protein levels.

aPKCι staining was restricted to the apical surface of normal breast epithelial cells lining the lumen of the duct whereas, in tumor cells, overexpressed aPKCι lost its apical localization (Fig. 1*B* and Fig. S1*C*) and showed a predominant unpolarized distribution at cell–cell contacts and cytoplasmic granules in the majority of the tumors (Fig. 1*B* and Fig. S1 *D* and *E*). There was little or no aPKCι staining in the stroma. MT1-MMP was laterally localized in luminal epithelial cells in normal tissues and also expressed in myoepithelial cells (Fig. 1*C* and Fig. S1*C*). MT1-MMP distribution was predominantly unpolarized in cancer cells in overexpressing tumors (Fig. 1*C* and Fig. S1*C*), with both a strong cell–cell contact association and a granular cytoplasmic distribution (Fig. 1*C* and Fig. S1 *D* and *E*). Thus, in contrast to their distinct localization at separate plasma-membrane domains of normal luminal breast epithelial cells, aPKCι and MT1-MMP significantly codistributed at cell–cell contacts and cytoplasmic granules, including in hormone receptor-negative tumors. These findings correlating up-regulation of aPKCι and MT1-MMP during breast-tumor progression indicate a poor prognosis for these combined markers.

aPKCζ/ι Is Required for MT1-MMP–Dependent Matrix Degradation and Breast-Tumor Cell Invasion. The functional interplay between MT1-MMP and aPKCι in tumor-cell invasion was investigated in MDA-MB-231 and BT-549 cells, two cell lines that can be classified as triple-negative breast cancer (26). Silencing of MT1-MMP expression strongly diminished invadopodial degradation of gelatin (Fig. 2 *A* and *B*) (10, 15). We investigated whether

aPKCζ/ι played a role in MT1-MMP–dependent matrix proteolysis by silencing both aPKCζ and aPKCι in these cell lines using two independent pairs of siRNAs (Fig. 2 *A* and *B*, *Insets*, immunoblots and Fig. S2 *A* and *B*) and then quantifying matrix degradation. Compared with cells treated with an irrelevant siRNA (luciferase, siLuc), these cells showed a 60–70% reduction of their degradative capacity (Fig. 2 *A* and *B* and Fig. S2 *C* and *D*). This inhibition of matrix degradation in the absence of aPKCζ/ι was not due to alteration of MT1-MMP levels in the cells (Fig. 2 *A* and *B*, *Insets*, immunoblots and Fig. S2 *A* and *B*). Furthermore, overexpression of MT1-MMP overcompensated the adverse effect of aPKCζ/ι silencing on gelatin degradation (Fig. 2*C*, compare red bars and black bars). These data indicate

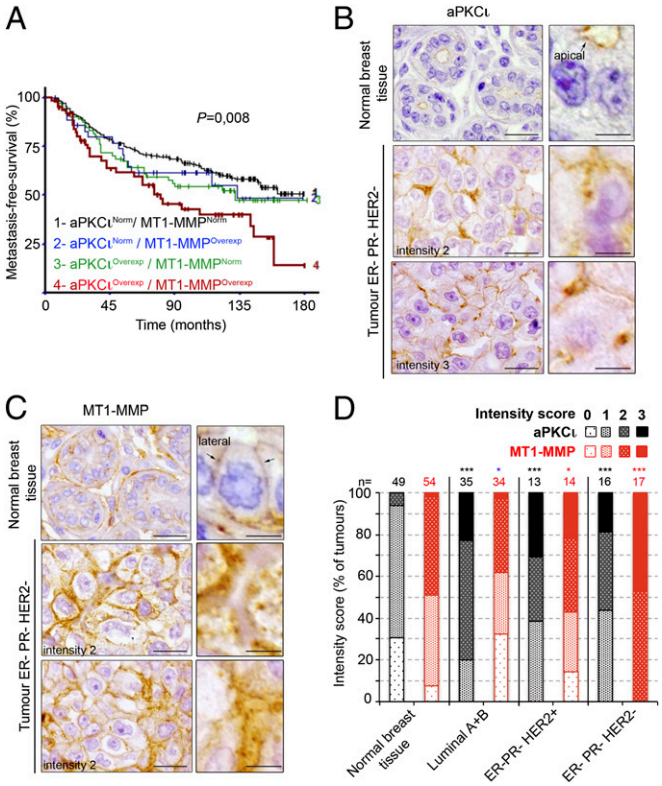

Fig. 1. Co–up-regulation and colocalization of MT1-MMP and aPKCι in hormone receptor-negative breast tumors correlate with poor prognosis. (*A*) Metastasis-free survival (MFS) curves for breast-tumor patients with normal (Norm) or overexpressed (Overexp, >3) aPKCι and MT1-MMP mRNA levels (Spearman rank). (*B* and *C*) aPKCι (*B*) and MT1-MMP (*C*) immunohistochemistry staining on consecutive sections of human breast tumor TMAs showing adjacent nonneoplastic tissue and representative ER^- PR^- $HER2^-$/triple-negative tumors. Note that adjacent nonneoplastic tissue shown in *Top* panels correspond to tumor sample shown in *Middle* panels. *Right* panels show higher magnification. [Scale bars: 20 μm (*Left*) and 5 μm (*Right*).] (D) Intensity scoring of aPKCι (black bars) and MT1-MMP (red bars) immunohistochemistry staining (on a 0-to-3 scale as documented in Fig. S1 *A* and *B*) of a tissue microarray of human breast tumors representative of the different molecular subtypes and adjacent nonneoplastic areas (Normal breast tissue). Breast molecular subtypes were defined as follows: luminal A+B according to ref. 52 [luminal A, estrogen receptor (ER) ≥ 10%, progesterone receptor (PR) ≥ 20%, Ki67 < 14%; luminal B, ER ≥ 10%, PR < 20%, Ki67 ≥ 14%]; ER− PR− HER2+, ER < 10%, PR < 10%, HER2 2+ amplified or 3+ according to ref. 53; ER− PR− HER2− (triple-negative), ER < 10%, PR < 10%, HER2 0/1+ or 2+ nonamplified according to ASCO guidelines (53). n, the number of tumors analyzed. $*P < 0.05$; $***P < 0.001$; ns, non significant compared with normal adjacent tissues (χ^2 test). Note that intensity scores of MT1-MMP expression in luminal A+B tumors are inferior to normal tissues.

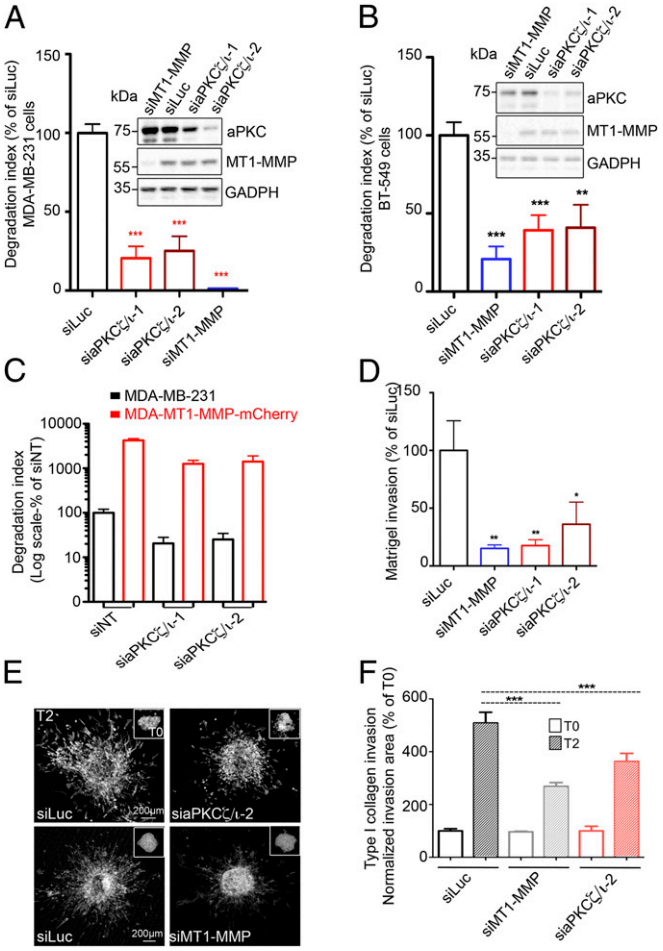

Fig. 2. Atypical PKCζ/ι regulate MT1-MMP–dependent matrix degradation and invasion. (*A* and *B*) Quantification of FITC–gelatin degradation by MDA-MB-231 (*A*) and BT-549 cells (*B*) treated with indicated siRNAs. Values are means ± SEM of the normalized degradation area from at least three independent experiments. (*Insets*) Immunoblotting with antibodies against aPKCζ/ι and MT1-MMP of cells treated with the indicated siRNAs. Immunoblotting with antibodies against GAPDH served as a control for loading. (*C*) Quantification of FITC–gelatin degradation by MDA-MB-231 stably expressing MT1-MMP–mCherry treated with the indicated siRNAs (red bars) compared with untransfected MDA-MB-231 cells (black bars). Note the logarithmic scale. (*D*) MDA-MB-231 cells treated with indicated siRNAs were tested for their ability to invade through Matrigel. Values are means ± SEM normalized to the mean for siLuc-treated cells. $*P < 0.05$; $**P < 0.01$. (*E*) Multicellular spheroids of MDA-MB-231 cells treated with siRNAs against luciferase or aPKCζ/ι (siaPKCζ/ι-2) were embedded in 3D acid-extracted type I collagen (T0) and further incubated for 2 d (T2). Images show phalloidin-labeled spheroids collected at T2 (*Insets* correspond to spheroids at T0). (Scale bars: 200 μm.) (*F*) Data are mean invasion area in type I collagen at T2 normalized to the mean invasion area at T0 ± SEM ($n = 3$ independent experiments; 15–20 spheroids were analyzed for each cell population). $***P < 0.001$.

that aPKCζ/ι is required for matrix proteolysis by breast-tumor cells through the control of MT1-MMP function.

We further assessed the effect of aPKCζ/ι silencing on MDA-MB-231 cell invasion across a thick layer of Matrigel and on invasive migration through fibrous type I collagen because MT1-MMP is required for invasion in these environments (13, 27). Double silencing of aPKCζ and aPKCι impaired invasion in Matrigel to a similar extent to silencing of MT1-MMP itself (Fig. 2*D*). Similarly, silencing of both aPKCζ and -ι inhibited the dissemination of MDA-MB-231 cells from multicellular spheroids into the surrounding 3D gel of type I collagen (Fig. 2 *E* and

F). These data indicate that aPKCζ/ι is required for MT1-MMP–dependent invasion of MDA-MB-231 cells in two different reconstituted matrices that mimic the 3D environment of cancer cells in vivo.

Atypical PKCζ/ι Control MT1-MMP–Containing Endosome Distribution and MT1-MMP Exocytosis. Immunoelectron microscopy of MDA-MB-231 cells stably expressing MT1-MMP–mCherry revealed association of MT1-MMP with the limiting membrane and internal luminal vesicles of vesicular compartments, with morphology typical of multivesicular bodies (Fig. 3*A*). These observations are consistent with the predominant association of MT1-MMP with VAMP7- and Rab7-positive late endocytic compartments in MDA-MB-231 cells (13, 16). Imaging of live cells expressing GFP–aPKCι revealed an association of this protein with ∼32% of MT1-MMP–mCherry–positive vesicles (Fig. 3*B* and Fig. S2*E*), reminiscent of the colocalization of aPKCι and MT1-MMP on cytoplasmic granular compartments in hormone receptor-negative breast carcinoma (Fig. 1*C* and Fig. S1*E*).

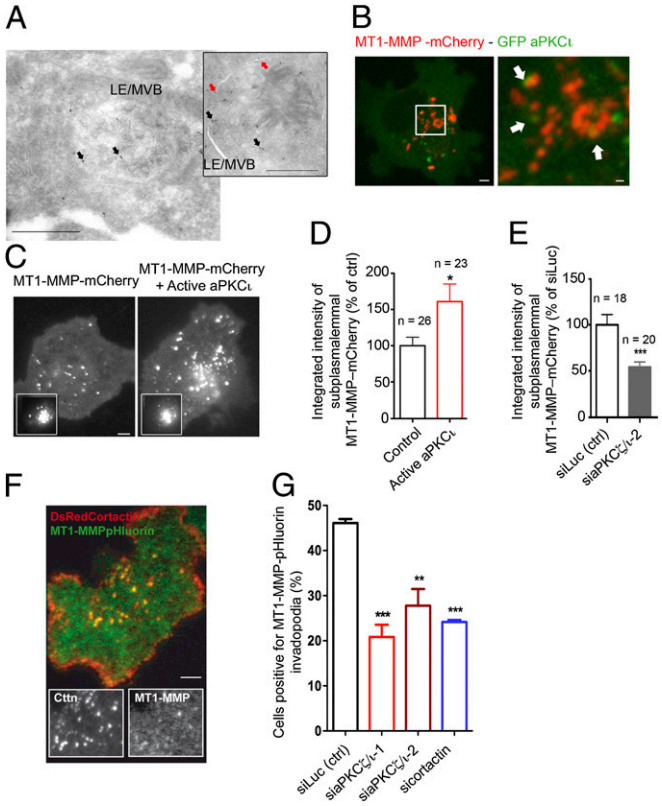

Fig. 3. aPKCζ/ι regulate MT1-MMP trafficking to plasma membrane invadopodia. (*A*) Ultrathin cryosection of MDA-MB-231 cells expressing MT1-MMP–mCherry labeled with MT1-MMP antibody followed by protein A-gold. Red arrows, MT1-MMP in the limiting membrane; black arrows, MT1-MMP associated with intraluminal vesicles of late endosomes/multivesicular bodies (LE/MVB). (Scale bars: 500 nm.) (*B*) Confocal spinning-disk microscopy image of an MDA-MB-231 cell expressing GFP–aPKCι and MT1-MMP–mCherry. [Scale bars: 5 μm (*Left*) and 1 μm (*Right*, boxed region at higher magnification). (*C*) MDA-MB-231 expressing MT1-MMP–mCherry alone or together with constitutively active aPKCι were imaged by TIRFM. (*Insets*) Corresponding wide-field images showing equal MT1-MMP expression. (Scale bar: 5 μm.) (*D* and *E*) Integrated intensity of MT1-MMP–mCherry signal per unit membrane area measured from TIRFM images. Values represent mean percentage of membrane MT1-MMP normalized to cells expressing only MT1-MMP–mCherry (*D*) or siLuc-treated cells (*E*) ± SEM. $*P < 0.05$; $***P < 0.001$. (*F*) MDA-MB-231 cells expressing MT1-MMP–pHluorin and DsRed-cortactin plated on cross-linked gelatin and analyzed by dual color TIRFM. (*Insets*) Split signals from the boxed region. (Scale bar: 5 μm.) (*G*) Plots show the percentage of cells with MT1-MMP–pHluorin–positive invadopodia. Efficiency of cortactin knockdown is shown in Fig. 4*G*. Values are means ± SEM from three independent experiments scoring a total of 150–200 cells for each cell population. $**P < 0.01$; $***P < 0.001$ (compared with cells treated with siLuc siRNA).

We investigated whether aPKCζ/ι may be required for MT1-MMP trafficking to the plasma membrane. Expression of a constitutively active allele of aPKCι resulted in an ∼1.5-fold increase of the density of MT1-MMP–containing vesicles in the vicinity of the plasma membrane visualized by total interference reflection fluorescence microscopy (TIRFM) (Fig. 3 *C* and *D* and Fig. S2*F*). On the contrary, aPKCζ/ι depletion induced a twofold reduction in MT1-MMP–positive endosomes at the plasma membrane (Fig. 3*E* and Fig. S2*G*). The contribution of aPKCζ/ι to MT1-MMP delivery to the invadopodial plasma membrane was assessed by quantifying surface accumulation of MT1-MMP–pHluorin (28); fluorescence of this construct is eclipsed in the acidic environment of the late endosome and rises immediately upon exocytosis and exposure to the extracellular pH (29). As expected, MT1-MMP–pHluorin accumulated at the level of cortactin-positive invadopodia on the ventral cell surface (Fig. 3*F*). Knockdown of aPKCζ/ι led to a 40–60% reduction of plasma-membrane accumulation of MT1-MMP–pHluorin, similar to the effect of cortactin siRNA, which is required for MT1-MMP delivery to invadopodia (10, 14) (Fig. 3*G*). All together, these data reveal that aPKCζ/ι controls the polarization of MT1-MMP–positive endosomes to the cell surface and MT1-MMP exocytosis and regulates pericellular matrix remodeling.

Dynamin-2 Associates with Cortactin on MT1-MMP–Positive Endosomes in an aPKCζ/ι-Dependent Manner and Is Required for MT1-MMP Trafficking and Matrix Degradation. Analysis of the subcellular distribution of cortactin by indirect immunofluorescence in MDA-MB-231 cells revealed that, in addition to its invadopodial location (Fig. 3*F* and Fig. S2 *C* and *D*) (10, 14), cortactin also accumulated in the central region of the cell and was dynamically associated with MT1-MMP–containing endosomes (more than 95% of MT1-MMP–positive endosomes harbored at least one cortactin-rich puncta) (Fig. 4*A* and Movie S1). In addition, F-actin and the p34-Arc subunit of Arp2/3 complex, which are components of the cytoskeleton and partner proteins of cortactin, colocalized with cortactin patches on MT1-MMP–containing endosomes in MDA-MB-231 and BT-549 cells (Fig. S3 *A*–*C*). High-resolution structured illumination microscopy revealed the presence of distinct submicrometer-sized cortactin domains associated with MT1-MMP–positive endosomes (Fig. S3*D*). Knockdown of aPKCζ/ι induced coalescence of the cortactin domains on MT1-MMP–containing endosomes (Fig. 4*A* and Fig. S3*D*) and a dramatic ∼80% increase of cortactin on MT1-MMP–positive endosomes (Fig. 4*B*). These data demonstrate that cortactin associates with F-actin assemblies on MT1-MMP–positive endosomes in an aPKCζ/ι-regulated manner.

The endosomal actin and cortactin cytoskeleton is known to regulate the formation and fission of tubulovesicular transport carriers involved in the recycling of surface proteins within the endocytic pathway (30, 31). We looked at the dynamic distribution of the late endocytic marker GFP–Rab7, which is associated with MT1-MMP–positive endosomes and colocalizes with endosomal cortactin (Fig. S3*E*) (32). By live-cell imaging, we observed the formation of GFP–Rab7-positive tubules emanating from MT1-MMP–containing endosomes and the fission of these tubules (Fig. S3*F*, *Upper*). Silencing of aPKCζ/ι, by contrast, was accompanied by more persistent Rab7– and MT1-MMP–containing tubular extensions (Fig. S3 *E*, *Right* and *F*, *Lower*), suggesting that aPKCζ/ι controls MT1-MMP–containing late endosome membrane remodeling.

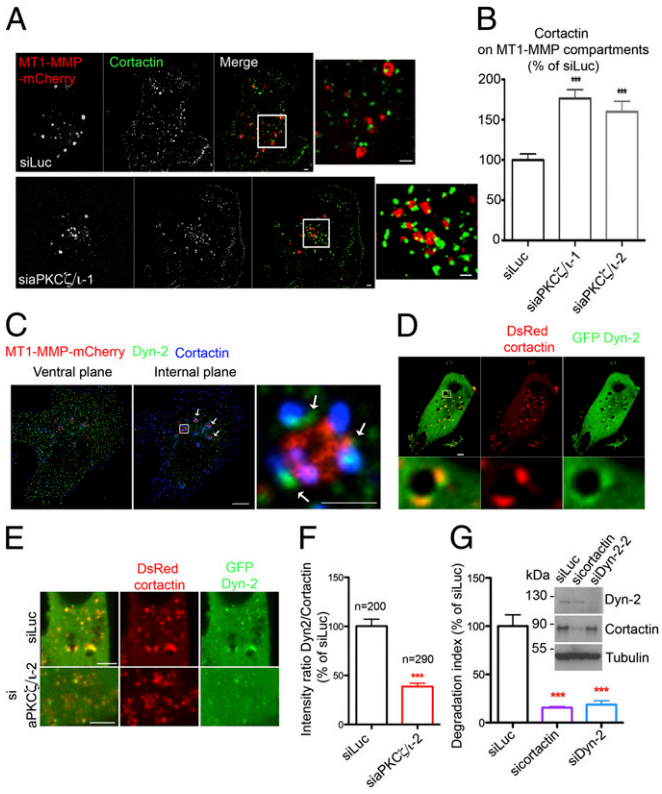

Fig. 4. aPKCζ/ι regulates cortactin and dynamin-2 recruitment on MT1-MMP–positive endosomes. (*A*) MDA-MB-231 cells stably expressing MT1-MMP–mCherry (red) were treated with indicated siRNAs, plated on gelatin, and immunolabeled with an antibody against cortactin (in green). [Scale bars: 5 μm (entire cell) and 1 μm (boxed region at higher magnification, *Right* panel of each row).] (*B*) Quantification of cortactin on MT1-MMP–mCherry–containing vesicles in deconvoluted image stacks of MDA-MD-231 cells as in *A*. The *x* axis indicates mean cortactin intensity associated with MT1-MMP–mCherry–containing endosomes normalized to the value in control siLuc-treated cells (in percentage) ± SEM (from 50 cells from each cell population). $***P < 0.001$. (*C*) MDA-MB-231 cells expressing MT1-MMP–mCherry (red) were immunolabeled for cortactin (blue) and dyn-2 (green). (*Left*) The distribution of dyn-2 on the ventral plane of the cell in clathrin-coated pits with partial association with cortactin. (*Center*) Documents dyn-2's association with cortactin-positive puncta on MT1-MMP–mCherry vesicles (arrows). (*Right*) A higher magnification of the boxed region. [Scale bars: 5 μm (*Left* and *Center*) and 1 μm (*Right*)]. (*D*) Confocal spinning-disk microscopy image of MDA-MB-231 cells expressing GFP–dyn2 and DsRed–cortactin (Movie S2). [Scale bars: 5 μm (*Upper*) and 1 μm (*Lower*). (*E*) Dual-color confocal spinning-disk microscopy of MDA-MB-231 cells expressing DsRed–cortactin and GFP–dyn-2 and treated with indicated siRNAs. (Scale bars: 5 μm.) (*F*) The ratio of signal intensities from GFP–dyn-2 and DsRed–cortactin was measured for 200 and 290 endosomal cortactin patches in cells treated with siRNAs against luciferase or aPKC, respectively. $***P < 0.001$. (*G*) Quantification of gelatin degradation by MDA-MB-231 cells treated with indicated siRNAs. Values are means ± SEM of the normalized degradation area from three independent experiments. (*Inset*) Immunoblotting with indicated antibodies using tubulin as a control for loading.

Cortactin regulates membrane dynamics through its interaction with dyn-2, which is involved in membrane scission and is required for the formation and function of invadopodia (33, 34). We therefore analyzed the location of endogenous dyn-2 and cortactin by immunolabeling MDA-MB-231 cells stably expressing MT1-MMP–mCherry. This immunolabeling revealed a close apposition of dyn-2 patches with cortactin puncta on ∼90% of MT1-MMP–positive endosomes (Fig. 4*C*, internal plane). Note that, as expected, dyn-2 associated with clathrin-coated pits on the plasma membrane with partial colocalization with cortactin (Fig. 4*C*, ventral plane). When coexpressed with DsRed–cortactin, GFP–dyn-2 colocalized with cortactin domains on vesicular structures in the central-cell region (Fig. 4*D* and Movie S2). In addition, deletion of the proline-rich domain (ΔPRD) of dyn-2, which mediates its interaction with the SH3 domain of cortactin (33), abolished dyn-2 association with MT1-MMP–containing vesicles (Fig. S4*A*). Reciprocally, expression of a DsRed–cortactin protein lacking the SH3 domain (cortactinΔSH3) resulted in a diffuse cytosolic distribution of GFP–dyn-2 (Fig. S4*B* and quantification in Fig. 5*C*). These data demonstrate that dyn-2 colocalizes with cortactin on MT1-MMP–containing endosomes and indicate a cortactin-dependent, possibly transient association of dyn-2 with these endosomes.

The observation that loss of aPKCζ/ι activity triggered accumulation of Rab7– and MT1-MMP–positive membrane tubules (Fig. S3 *E* and *F*) prompted us to investigate whether accumulation of cortactin on MT1-MMP–containing endosomes in aPKCζ/ι-depleted cells affected dyn-2 recruitment and consequently tubule fission. To do so, we silenced aPKCζ/ι in MDA-MB-231 cells and observed a reduction of GFP–Dyn-2 recruitment associated with DsRed–cortactin patches along with increased endosomal cortactin accumulation (Fig. 4*E* and Fig. S4*C*, internal plane). Analysis of the intensity ratio of the fluorescence signals from GFP–dyn-2 and DsRed–cortactin in endosomal patches showed that the intensity ratio in aPKCζ/ι-depleted cells was reduced by 60% compared with the control—siLuc-treated—cells (Fig. 4*F*). In contrast, aPKCζ/ι knockdown did not affect the association of Dyn-2 with clathrin-coated pits at the plasma membrane (Fig. S4*C*, ventral plane). Thus, we conclude that accumulation of cortactin in the absence of aPKCζ/ι function interferes specifically with Dyn-2 recruitment on MT1-MMP–containing late endosomes. In addition, in agreement with previous findings (34), silencing of dyn-2 in MDA-MB-231 cells correlated with a substantial loss of their ability to degrade the matrix similar to the effect of cortactin knockdown (Fig. 4*G*). Accumulation of MT1-MMP–positive vesicles and tubules connected to and extending from MT1-MMP–containing endosomes was visible in Dyn-2–depleted cells (Fig. S4 *D* and *E* and Movie S3). Collectively, these data indicate that dyn-2 acts downstream of cortactin and that aPKCζ/ι is required for the formation and function of cortactin–dyn-2 assemblies on multivesicular bodies/late endosomes, suggesting a mechanism involved in the formation and fission of tubulovesicular carriers from these endosomes.

aPKCζ/ι-Dependent Phosphorylation of Cortactin Controls Its Association with dyn-2. We then addressed how aPKCζ/ι controls cortactin and dyn-2 association on MT1-MMP–containing endosomes. We tested whether cortactin was a direct substrate for aPKCζ/ι by incubating purified GST-tagged human cortactin in the presence of recombinant human aPKCι. Phosphorylation was detected with antibodies raised against cortactin phospho-Ser298, which was recently identified as a phosphorylation site for aPKCζ/ι-related PKD (35, 36). In higher metazoans, mRNA splicing generates cortactin variants with four, five, or six conserved tandem actin-binding repeats in which repeats 5 and 6 are the most conserved (37). The cortactin variant used for this study contains five tandem repeats; Ser261 in repeat 5 is highly conserved and equivalent to Ser298 in repeat 6. Recombinant aPKCι induced phosphorylation of recombinant human cortactin (Fig. 5*A*). In addition, coexpression of the five repeat-containing cortactin variant (33) with aPKCι in MDA-MB-231 cells similarly resulted in phosphorylation of cortactin (Fig. 5*B*). Thus, our data suggest that Ser261 is directly phosphorylated by aPKCι.

Next, we investigated the consequences of substitution of serine 261 to alanine (nonphosphorylable mutation) or to aspartate (phosphomimetic mutation) on gelatin degradation.

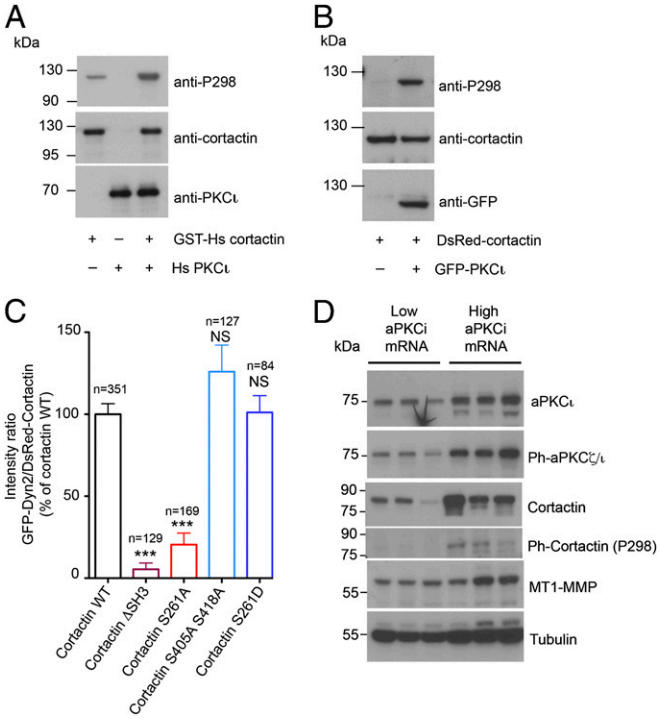

Fig. 5. Phosphorylation of cortactin by aPKCι controls dyn-2 association with cytoplasmic cortactin-positive puncta. (*A*) Purified GST-tagged human cortactin (2 μg) was incubated in the presence (0.5 μg) or absence of recombinant human aPKCι for 20 min at 37 °C. Cortactin phosphorylation was analyzed by immunoblotting with antibodies against cortactin pSer298 phosphopeptide (anti-P298). (*B*) Lysates of MDA-MB-231 cells expressing DsRed–cortactin alone or together with GFP–aPKCι were analyzed by immunoblotting with antibodies against pSer298 (anti-P298), total cortactin, or GFP. (*C*) Quantification of dyn-2 on cortactin patches from confocal dual-color spinning-disk images of MDA-MD-231 cells overexpressing GFP–dyn-2 together with DsRed-tagged wild-type cortactin or variants as indicated. The ratios of the signal intensities from dyn-2 and cortactin were measured from *n* endosome patches. ***$P < 0.001$; NS, not significant. (*D*) Whole-cell extracts from breast tumors underexpressing (low) or overexpressing (high) aPKCι mRNA were analyzed by immunoblotting with the indicated antibodies. Tubulin was used as a control for equal loading.

Overexpression of cortactin S261A in BT-549 cells led to an ~50% reduction in matrix degradation whereas cortactin S261D had the opposite stimulatory effect (Fig. S4*F*). In addition, similar to the loss of aPKCζ/ι (Fig. 4 *E* and *F*), expression of cortactin-S261A caused drastic and specific depletion of dyn-2 from endosomal patches (Fig. 5*C* and Fig. S4*G*). By contrast, mutation of the extracellular signal-regulated serine/threonine kinase (ERK1/2) phosphorylation sites S405 and S418 of cortactin into alanine did not affect dyn-2 association with endosomes (Fig. 5*C*). Overexpression of the phosphomimetic cortactin S261D variant did not affect significantly dyn-2 recruitment on MT1-MMP–containing endosomes (Fig. 5*C*), suggesting that aPKCζ/ι-mediated phosphorylation of cortactin may also affect the dynamics of dyn-2 association to MT1-MMP–positive late endosomes. Finally, we observed that, in breast tumors, increased total phosphorylated aPKCι correlated with high cortactin expression and phosphorylation at the aPKCι-specific site in the actin-binding repeats (Fig. 5*D*). Together, our data indicate that aPKCι-mediated phosphorylation of cortactin regulates endosomal accumulation of cortactin and its association with dyn-2 to control MT1-MMP–positive endosome dynamics during the invasive program of breast-tumor cells.

Discussion

In this study, we report an unprecedented function for aPKCζ/ι in the invasion of breast-tumor cells. Our data show that aPKCζ/ι silencing in two breast-adenocarcinoma cell lines representative of triple-negative breast cancers inhibits MT1-MMP–dependent matrix degradation and tumor-cell invasion, while having no effect on MT1-MMP expression. Instead, aPKCζ/ι controls the trafficking and plasma-membrane targeting of MT1-MMP to invadopodia. In MDA-MB-231 and BT-549 cells, aPKCζ/ι associates partially with cortactin and its binding partners, F-actin and dyn-2, in patches on late endosomes that contain an intracellular reservoir of the transmembrane metalloproteinase MT1-MMP. aPKCζ/ι phosphorylates cortactin directly, and depletion of the kinase interferes with cortactin-dependent recruitment of the membrane scission protein dyn-2, correlating with tubulation of endosomal membranes and impaired trafficking and exocytosis of MT1-MMP to the cell surface. Thus, we conclude that aPKCζ/ι promotes the formation of transport vesicles carrying MT1-MMP (and possibly other proteins involved in invasion such as integrins) (38) from its intracellular reservoir in late endosomes to the cell surface, where it contributes to preparing the extracellular matrix for the invasion of the tumor cells. Consistent with this mechanism, our analysis of breast-tumor biopsies shows overexpression of both aPKCι and MT1-MMP in the most aggressive hormone receptor-negative $HER2^+$ and triple-negative subtypes. These proteins are found at cell–cell contacts and in intracellular vesicles in carcinoma cells, contrasting with their distinct locations on the apical and lateral plasma membranes, respectively, in healthy breast epithelial cells. The positive correlation between MT1-MMP and aPKCι mRNA expression in clinical samples was associated with poor prognosis, underscoring the functional importance of the kinase in progress of the disease.

The direct phosphorylation of cortactin residue S261 by aPKCι, as well as the association of aPKCι with cortactin-enriched domains on MT1-MMP–containing intracellular compartments, suggests that aPKCι phosphorylates cortactin on MT1-MMP–containing late endosomes. The accumulation of hypophosphorylated cortactin in aPKCζ/ι-depleted cells or in the Ser261Ala mutant inhibited association of dyn-2 with cortactin-positive patches on MT1-MMP–containing endosomes, and it decreased matrix degradation. Based on the known function of dyn-2 in membrane scission on various compartments, including late endosomes (39), impaired dyn-2 recruitment onto MT1-MMP–positive late endosomes is probably responsible for the endosomal membrane tubulation we see, with adverse consequences for MT1-MMP delivery to the surface. Thus, our data reveal a role for aPKCζ/ι on late endocytic compartments and a previously unidentified mechanism of late endosome membrane remodeling based on cortactin phosphorylation by aPKC to control dyn-2 recruitment. Phosphorylation of S405 and S418 of cortactin by ERK1/2 also stimulates invadopodia formation and matrix degradation. In addition, phosphorylation of cortactin by ERK is involved in a recycling mechanism of internalized ECM components from late endosomes/lysosomes to promote cell motility (32). However, our data indicate that ERK phosphorylation sites do not contribute to dyn-2 recruitment to cortactin-positive patches, thus suggesting different mechanisms of action for aPKCζ/ι and ERK-dependent phosphorylation sites for cortactin function during tumor-cell invasion.

Recent studies have documented an essential role for actin cytoskeleton dynamics in endosome function (30, 31, 40). The mechanism emerging from these studies indicates that actin–Arp2/3 assemblies organize early endosomal membranes into functional subdomains and contribute to cargo sorting and generation of transport intermediates. Our observation that dynamic cortactin–Arp2/3–actin subdomains of MT1-MMP–containing multivesicular

bodies coincide with sites of emergence and scission of tubulovesicular MT1-MMP carriers suggests a similar key role for actin in generating transport intermediates from multivesicular bodies/late endosomes. These mechanistic insights from cells in culture are consistent with our analysis of breast-tumor samples showing up-regulation of both aPKCι and MT1-MMP associated with hormone receptor-negative aggressive breast tumors and with poor prognosis; patients whose tumors overexpressed both aPKCι and MT1-MMP had a significantly higher risk of metastasis. When taken together with the known implication of cortactin in cancer (41, 42) and the reported up-regulation of dyn-2 expression in human metastatic tumors (43), our findings identify a key role for aPKCι, cortactin, dyn-2, and MT1-MMP in aggressive epithelial breast carcinomas and emphasize the role of polarity defects and endosomal transport in breast carcinogenesis, opening new avenues for innovative therapeutic strategies in aggressive forms of breast cancers.

The redistribution of aPKCι and MT1-MMP from the apical and lateral surfaces of epithelial cells, respectively, in normal mammary ducts to cell–cell contacts and vesicles—probably endosomes—in carcinoma cells correlates with the loss of epithelial-cell polarity observed in breast tumors. This redistribution seems particularly relevant in the context of tumor progression (see also ref. 44). Apical–basal polarity requires the activity of several proteins, including the apically located PAR complex, which contains aPKCζ/ι as well as CDC42, Par3, and Par6 (18). Moreover, components of the PAR complex regulate vesicle transport in the endocytic pathway and play a critical role in the uptake and recycling of components required for epithelial integrity (45, 46). Thus, our data suggest that a mechanism of endocytic recycling of specific cargoes based on aPKCζ/ι/cortactin/dyn-2 may operate in normal epithelial cells and may be required for maintenance of apicobasolateral polarity. Like aPKCι, Par6 is up-regulated in breast tumors (47) whereas loss of Par3 promotes breast-cancer metastasis (48, 49). Collectively, these data suggest that deregulation of PAR complex components in breast carcinomas contributes to tumor progression via deregulation of cell polarity and that one major consequence of aPKCζ/ι overexpression and mislocalization in tumors is the recycling and exocytosis of MT1-MMP, promoting metastasis of carcinoma cells in most aggressive breast tumors.

Experimental Procedures

Antibodies and Plasmid Constructs. For antibodies and plasmid constructs, see *SI Experimental Procedures*.

Cell Culture, Transfection, Stable Cell Lines, and Knockdown. For cell culture, transfection, stable cell lines, and knockdown, see *SI Experimental Procedures*.

Fluorescent Gelatin Degradation Assay and Invasion Assays. Assays of fluorescent gelatin degradation were performed and quantified as previously described (15). About 250–300 cells from at least three independent experiments were analyzed for each condition. Assays to measure cell invasion into Matrigel and to measure the invasion of cells from multicellular spheroids into native type I collagen assays were performed as described previously (13, 50). The latter assays were quantified by estimating the diameter of spheroids at T0 and T2 as described (50).

Indirect Immunofluorescence Microscopy, 3D Deconvolution, and Image Analysis. MDA-MB-231 cells were cultured on gelatin-coated coverslips and processed for immunofluorescence microscopy as previously described (13). Image acquisition and analysis are described in *SI Experimental Procedures*.

Live-Cell Imaging and Analysis of MT1-MMP–Containing Endosome Movement. For live-cell imaging and analysis of MT1-MMP–containing endosome movement, see *SI Experimental Procedures*.

Total Interference Reflection Fluorescence Microscopy. Cells expressing MT1-MMP–mCherry and depleted of the proteins of interest (cortactin, aPKCζ/ι, dyn-2) by means of siRNAs were plated on cross-linked gelatin-coated glass-bottom dishes (MatTek) for 2 h before imaging. TIRFM imaging was performed on a custom setup as described previously with a penetration depth of 150–300 nm (51). MT1-MMP–mCherry at the cell surface was quantified by using integrated intensity measurement in Metamorph software.

Structured Illumination Microscopy. For structured illumination microscopy, see *SI Experimental Procedures*.

Electron Microscopy. For electron microscopy, see *SI Experimental Procedures*.

Human Samples and Clinical and Tissue Microarray Data. Our series of cases was composed of 68 cases of invasive ductal carcinoma representative of each molecular subtype of breast cancer: i.e., luminal A, luminal B, ER^- PR^- $HER2^+$, and ER^- PR^- $HER2^-$ (triple-negative). Clinicopathological parameters of breast-cancer cases examined are described in Dataset S1. Breast molecular subtypes were defined as follows: luminal A+B according to ref. 52 [luminal A, estrogen receptor (ER) ≥ 10%, progesterone receptor (PR) ≥ 20%, Ki67 < 14%; luminal B, ER ≥ 10%, PR < 20%, Ki67 ≥ 14%]; ER^- PR^- $HER2^+$, ER < 10%, PR < 10%, HER2 2+ amplified or 3+ according to ref. 53; ER^- PR^- $HER2^-$ (triple-negative), ER < 10%, PR < 10%, HER2 0/1+ or 2+ nonamplified according to American Society of Clinical Oncology (ASCO) guidelines (53). MT1-MMP and aPKCι expression and association with clinicopathological features of breast cancer were assessed by IHC analysis of a breast-cancer tissue microarray (TMA) of invasive ductal carcinoma. TMA consisted of replicate tumor cores (1-mm diameter) selected from whole-tumor tissue section in the most representative tumor areas (high tumor-cell density) of each tumor sample and a matched tissue core from adjacent nontumoral breast epithelium (referred to as normal breast tissue). Immunohistocytochemistry staining was performed according to previously published protocols (54).

Analyses were performed in accordance with the French Bioethics Law 2004–800 and the French National Institute of Cancer (INCa) Ethics Charter and after approval by the Institut Curie review board and ethics committee (Comité de Pilotage du Groupe Sein), which waived the need for written informed consent from the participants. Women were informed of the research use of their tissues and did not declare any opposition for such research. Data were analyzed anonymously.

RNA Extraction and Real-Time PCR Analysis. For RNA extraction and real-time PCR analysis, see *SI Experimental Procedures*.

Statistical Analyses. Relationships between mRNA levels of various target genes and comparison of target-gene mRNA levels with clinical parameters were estimated by using the χ^2 test (for links between two qualitative parameters) and the Spearman rank correlation test (for links between two quantitative parameters). Differences between the two populations were judged significant at confidence levels greater than 95% ($P < 0.05$). Metastasis-free survival (MFS) was determined as the interval between diagnosis and detection of the first metastasis. Survival distributions were estimated by the Kaplan–Meier method, and the significance of differences between survival rates was ascertained using a log-rank test. Relationships between protein expression and distribution in tumors vs. normal adjacent tissues were estimated using the Kruskal–Wallis test (for links between qualitative and quantitative parameters). Other statistical analyses were performed using the ANOVA or Student *t* test (link between one qualitative parameter and one quantitative parameter) in Prism software.

ACKNOWLEDGMENTS. We thank Drs. M. Arpin, T. Galli, and M. A. McNiven for providing reagents. We acknowledge the Breast Cancer Study Group of Institut Curie headed by Drs. B. Sigal-Zafrani and T. Dubois (Transfer Department, Institut Curie) and the patients for the breast-tumor samples. C.R. and P.M. were supported by a fellowship from the Fondation ARC pour la Recherche sur le Cancer (ARC). L.F. and M.N. were supported by the Incentive and Cooperative Research Programme "Breast Cancer: Cell Invasion and Motility" of Institut Curie. Funding for this work was provided by ARC Grant SL220100601356, by Agence Nationale pour la Recherche Grant ANR-08-BLAN-0111 and Institut National du Cancer Grant 2012-1-PL BIO-02-IC-1 (to P.C.), and by core funding from Institut Curie and the Centre National pour la Recherche Scientifique. We acknowledge France-BioImaging infrastructure supported by the French National Research Agency (ANR-10-INSB-04, Investments for the future).

1. Egeblad M, Werb Z (2002) New functions for the matrix metalloproteinases in cancer progression. *Nat Rev Cancer* 2(3):161–174.
2. Kessenbrock K, Plaks V, Werb Z (2010) Matrix metalloproteinases: Regulators of the tumor microenvironment. *Cell* 141(1):52–67.
3. Sato H, et al. (1994) A matrix metalloproteinase expressed on the surface of invasive tumour cells. *Nature* 370(6484):61–65.
4. Strongin AY, et al. (1995) Mechanism of cell surface activation of 72-kDa type IV collagenase: Isolation of the activated form of the membrane metalloprotease. *J Biol Chem* 270(10):5331–5338.
5. Hotary KB, et al. (2003) Membrane type I matrix metalloproteinase usurps tumor growth control imposed by the three-dimensional extracellular matrix. *Cell* 114(1): 33–45.
6. Hotary K, Li XY, Allen E, Stevens SL, Weiss SJ (2006) A cancer cell metalloprotease triad regulates the basement membrane transmigration program. *Genes Dev* 20(19): 2673–2686.
7. Wolf K, et al. (2007) Multi-step pericellular proteolysis controls the transition from individual to collective cancer cell invasion. *Nat Cell Biol* 9(8):893–904.
8. Jiang WG, et al. (2006) Expression of membrane type-1 matrix metalloproteinase, MT1-MMP in human breast cancer and its impact on invasiveness of breast cancer cells. *Int J Mol Med* 17(4):583–590.
9. Perentes JY, et al. (2011) Cancer cell-associated MT1-MMP promotes blood vessel invasion and distant metastasis in triple-negative mammary tumors. *Cancer Res* 71(13):4527–4538.
10. Artym VV, Zhang Y, Seillier-Moiseiwitsch F, Yamada KM, Mueller SC (2006) Dynamic interactions of cortactin and membrane type 1 matrix metalloproteinase at invadopodia: Defining the stages of invadopodia formation and function. *Cancer Res* 66(6):3034–3043.
11. Murphy DA, Courtneidge SA (2011) The 'ins' and 'outs' of podosomes and invadopodia: characteristics, formation and function. *Nat Rev Mol Cell Biol* 12(7): 413–426.
12. Poincloux R, Lizárraga F, Chavrier P (2009) Matrix invasion by tumour cells: A focus on MT1-MMP trafficking to invadopodia. *J Cell Sci* 122(Pt 17):3015–3024.
13. Steffen A, et al. (2008) MT1-MMP-dependent invasion is regulated by TI-VAMP/VAMP7. *Curr Biol* 18(12):926–931.
14. Clark ES, Whigham AS, Yarbrough WG, Weaver AM (2007) Cortactin is an essential regulator of matrix metalloproteinase secretion and extracellular matrix degradation in invadopodia. *Cancer Res* 67(9):4227–4235.
15. Sakurai-Yageta M, et al. (2008) The interaction of IQGAP1 with the exocyst complex is required for tumor cell invasion downstream of Cdc42 and RhoA. *J Cell Biol* 181(6): 985–998.
16. Williams KC, Coppolino MG (2011) Phosphorylation of membrane type 1-matrix metalloproteinase (MT1-MMP) and its vesicle-associated membrane protein 7 (VAMP7)-dependent trafficking facilitate cell invasion and migration. *J Biol Chem* 286(50):43405–43416.
17. Mellor H, Parker PJ (1998) The extended protein kinase C superfamily. *Biochem J* 332(Pt 2):281–292.
18. McCaffrey LM, Macara IG (2011) Epithelial organization, cell polarity and tumorigenesis. *Trends Cell Biol* 21(12):727–735.
19. Rosse C, et al. (2009) An aPKC-exocyst complex controls paxillin phosphorylation and migration through localised JNK1 activation. *PLoS Biol* 7(11):e1000235.
20. Sun R, et al. (2005) Protein kinase C zeta is required for epidermal growth factor-induced chemotaxis of human breast cancer cells. *Cancer Res* 65(4):1433–1441.
21. Rodriguez EM, Dunham EE, Martin GS (2009) Atypical protein kinase C activity is required for extracellular matrix degradation and invasion by Src-transformed cells. *J Cell Physiol* 221(1):171–182.
22. Kojima Y, et al. (2008) The overexpression and altered localization of the atypical protein kinase C lambda/iota in breast cancer correlates with the pathologic type of these tumors. *Hum Pathol* 39(6):824–831.
23. Awadelkarim KD, et al. (2012) Quantification of PKC family genes in sporadic breast cancer by qRT-PCR: Evidence that PKCι/λ overexpression is an independent prognostic factor. *Int J Cancer* 131(12):2852–2862.
24. Regala RP, et al. (2005) Atypical protein kinase C iota is an oncogene in human non-small cell lung cancer. *Cancer Res* 65(19):8905–8911.
25. Sørlie T, et al. (2001) Gene expression patterns of breast carcinomas distinguish tumor subclasses with clinical implications. *Proc Natl Acad Sci USA* 98(19):10869–10874.
26. Neve RM, et al. (2006) A collection of breast cancer cell lines for the study of functionally distinct cancer subtypes. *Cancer Cell* 10(6):515–527.
27. Sabeh F, Shimizu-Hirota R, Weiss SJ (2009) Protease-dependent versus -independent cancer cell invasion programs: Three-dimensional amoeboid movement revisited. *J Cell Biol* 185(1):11–19.
28. Lizárraga F, et al. (2009) Diaphanous-related formins are required for invadopodia formation and invasion of breast tumor cells. *Cancer Res* 69(7):2792–2800.
29. Miesenbock G (2012) Synapto-pHluorins: Genetically encoded reporters of synaptic transmission. *Cold Spring Harb Protoc* 2012(2):213–217.
30. Derivery E, et al. (2009) The Arp2/3 activator WASH controls the fission of endosomes through a large multiprotein complex. *Dev Cell* 17(5):712–723.
31. Puthenveedu MA, et al. (2010) Sequence-dependent sorting of recycling proteins by actin-stabilized endosomal microdomains. *Cell* 143(5):761–773.
32. Sung BH, Zhu X, Kaverina I, Weaver AM (2011) Cortactin controls cell motility and lamellipodial dynamics by regulating ECM secretion. *Curr Biol* 21(17):1460–1469.
33. McNiven MA, et al. (2000) Regulated interactions between dynamin and the actin-binding protein cortactin modulate cell shape. *J Cell Biol* 151(1):187–198.
34. Baldassarre M, et al. (2003) Dynamin participates in focal extracellular matrix degradation by invasive cells. *Mol Biol Cell* 14(3):1074–1084.
35. Eiseler T, Hausser A, De Kimpe L, Van Lint J, Pfizenmaier K (2010) Protein kinase D controls actin polymerization and cell motility through phosphorylation of cortactin. *J Biol Chem* 285(24):18672–18683.
36. Rozengurt E (2011) Protein kinase D signaling: Multiple biological functions in health and disease. *Physiology (Bethesda)* 26(1):23–33.
37. van Rossum AG, Schuuring-Scholtes E, van Buuren-van Seggelen V, Kluin PM, Schuuring E (2005) Comparative genome analysis of cortactin and HS1: The significance of the F-actin binding repeat domain. *BMC Genomics* 6:15.
38. Dozynkiewicz MA, et al. (2012) Rab25 and CLIC3 collaborate to promote integrin recycling from late endosomes/lysosomes and drive cancer progression. *Dev Cell* 22(1): 131–145.
39. Schroeder B, Weller SG, Chen J, Billadeau D, McNiven MA (2010) A Dyn2-CIN85 complex mediates degradative traffic of the EGFR by regulation of late endosomal budding. *EMBO J* 29(18):3039–3053.
40. Harrington AW, et al. (2011) Recruitment of actin modifiers to TrkA endosomes governs retrograde NGF signaling and survival. *Cell* 146(3):421–434.
41. Luo ML, et al. (2006) Amplification and overexpression of CTTN (EMS1) contribute to the metastasis of esophageal squamous cell carcinoma by promoting cell migration and anoikis resistance. *Cancer Res* 66(24):11690–11699.
42. Clark ES, et al. (2009) Aggressiveness of HNSCC tumors depends on expression levels of cortactin, a gene in the 11q13 amplicon. *Oncogene* 28(3):431–444.
43. Eppinga RD, et al. (2012) Increased expression of the large GTPase dynamin 2 potentiates metastatic migration and invasion of pancreatic ductal carcinoma. *Oncogene* 31(10):1228–1241.
44. Huang L, Muthuswamy SK (2010) Polarity protein alterations in carcinoma: A focus on emerging roles for polarity regulators. *Curr Opin Genet Dev* 20(1):41–50.
45. Leibfried A, Fricke R, Morgan MJ, Bogdan S, Bellaiche Y (2008) Drosophila Cip4 and WASp define a branch of the Cdc42-Par6-aPKC pathway regulating E-cadherin endocytosis. *Curr Biol* 18(21):1639–1648.
46. Winter JF, et al. (2012) Caenorhabditis elegans screen reveals role of PAR-5 in RAB-11-recycling endosome positioning and apicobasal cell polarity. *Nat Cell Biol* 14(7): 666–676.
47. Nolan ME, et al. (2008) The polarity protein Par6 induces cell proliferation and is overexpressed in breast cancer. *Cancer Res* 68(20):8201–8209.
48. McCaffrey LM, Montalbano J, Mihai C, Macara IG (2012) Loss of the Par3 polarity protein promotes breast tumorigenesis and metastasis. *Cancer Cell* 22(5):601–614.
49. Xue B, Krishnamurthy K, Allred DC, Muthuswamy SK (2013) Loss of Par3 promotes breast cancer metastasis by compromising cell-cell cohesion. *Nat Cell Biol* 15(2): 189–200.
50. Rey M, Irondelle M, Waharte F, Lizarraga F, Chavrier P (2011) HDAC6 is required for invadopodia activity and invasion by breast tumor cells. *Eur J Cell Biol* 90(2-3): 128–135.
51. Montagnac G, et al. (2011) Decoupling of activation and effector binding underlies ARF6 priming of fast endocytic recycling. *Curr Biol* 21(7):574–579.
52. Prat A, et al. (2013) Prognostic significance of progesterone receptor-positive tumor cells within immunohistochemically defined luminal A breast cancer. *J Clin Oncol* 31(2):203–209.
53. Wolff AC, et al. (2007) American Society of Clinical Oncology/College of American Pathologists guideline recommendations for human epidermal growth factor receptor 2 testing in breast cancer. *J Clin Oncol* 25(1):118–145.
54. Vincent-Salomon A, et al. (2007) HER2 status of bone marrow micrometastasis and their corresponding primary tumours in a pilot study of 27 cases: A possible tool for anti-HER2 therapy management? *Br J Cancer* 96(4):654–659.

Supporting Information

Rossé et al. 10.1073/pnas.1400749111

SI Experimental Procedures

Antibodies. Rabbit polyclonal anti-cortactin and mouse monoclonal anti-tubulin antibodies were purchased from Sigma. Anti-phosphoSer298 cortactin (P298) has been described previously (1). Monoclonal anti-cortactin (Clone 4F11), rabbit anti-p34Arc, and mouse anti–MT1-MMP monoclonal antibodies were obtained from Millipore. Rabbit anti-Rab7 and anti–phospho-aPKC (Thr410/403) antibodies were purchased from Cell Signaling. Monoclonal anti-VAMP7 and polyclonal anti–dynamin-2 antibodies were kind gifts of T. Galli (Institut Jacques Monod, Paris) and P. De Camilli (Yale University, New Haven, CT), respectively. Mouse monoclonal anti-PKCι antibody was purchased from BD Biosciences. Polyclonal antibodies against aPKCζ/ι (pan-aPKC) and GAPDH were purchased from Santa Cruz. AlexaFluor–phalloidin and anti-mouse IgG–Alexa488 antibody were from Invitrogen. Horseradish peroxidase-conjugated and fluorescently conjugated secondary antibodies were from Jackson ImmunoResearch Laboratories.

Plasmid Constructs. MT1-MMP–mCherry with the tag inserted in the extracellular domain to minimize interference with cytoplasmic domain trafficking motifs has been reported previously (2). Plasmid constructs expressing DsRed-tagged rat cortactin (wild-type and the deltaSH3mutant forms) and GFP–dyn-2 were kind gifts of M. A. McNiven (Mayo Clinic, Rochester, MI). Mouse GFP–cortactin expression construct was a kind gift of M. Way (London Research Institute, London). The cDNA encoding PKCι was inserted in the pEGFP vector. The plasmid construct expressing constitutively activated PKCι (caPKCι, containing an A120E mutation) was generated by site-directed mutagenesis of pEGFP–PKCι. Mutants of rat cortactin were made by site-directed mutagenesis of DsRed-tagged rat cortactin using the QuikChange Kit from Stratagene with the following oligonucleotides: For cortactin-S261A, 5′gagaagctgcagctgcatgaagcccaaaaagactat3′ (S261A sense); and 5′atagtctttttgggcttcatgcagctgcagcttctc3′ (S261A anti-sense). For cortactin S405A/S418A, 5′gcagacgccccctgcaGcccctagtcctca3′ (S405A sense); 5′tgaggactaggggCtgcagggggcgtctgc3′ (S405A anti-sense); 5′gacagaccaccctccgcccccatctatgagga3′ (S418A sense); and 5′tcctcatagatgggggcggagggtggtctgtc5′ (S418A anti-sense).

Cell Culture, Transfection, Stable Cell Lines, and Gene Silencing. The human breast adenocarcinoma cell line MDA-MB-231 (American Type Culture Collection, ATCC HTB-26) was maintained in L-15 culture medium (Sigma-Aldrich) with 2 mM glutamine and 15% (vol/vol) FCS at 37 °C in 1% CO_2 (2). MDA-MB-231 cells stably expressing MT1-MMP–mCherry were cultured in the presence of 0.5 mg/mL G418 (2). MDA-MB-231 cells were transfected with plasmid constructs by using Lipofectamine LTX (Invitrogen) or Amaxa nucleotransfection. Cells were analyzed 24 h after transfection.

For aPKCι/ζ knockdown, two independent pairs of siRNAs targeting both PKCζ and PKCι were used: siaPKCι/ζ-1 and siaPKCι/ζ-2 (PRKCZ, 5′AGAGGAUCGACCAGUCAGA3′; and PRKCI, 5′CGAAGAGCUCUUCACCAUG3′) as previously described (3). Small inhibitory RNAs targeting dyn-2–1 and MT1-MMP were SMARTpool ON-TARGETplus from Dharmacon. Cortactin and dynamin-2 siRNAs were purchased from Qiagen (4). Cells were treated with specific siRNA (25 nM final concentration) with Lullaby reagent (OZ Biosciences) and analyzed 72 h after treatment.

Indirect Immunofluorescence, Image Acquisition, and Analysis. Images were acquired with a wide-field Eclipse 90i Upright Microscope (Nikon) using a 100× Plan Apo VC 1.4 oil immersion objective and a highly sensitive cooled interlined charge-coupled device (CCD) camera (Roper CoolSnap HQ2). A z-dimension series of images was taken every 0.2 μm by means of a piezoelectric motor (LVDT; Physik Instrument), and images were deconvoluted (5). For quantification of cortactin on MT1-MMP–containing endosomes, a CellProfiler pipeline was constructed (6). First, the maximum intensity projection (MIP) of deconvoluted images of MT1-MMP–mCherry and cortactin was computed; then, cortactin spots were identified using a Laplacian of Gaussian filter, followed by a watershed on the automatically thresholded MIP image; the MT1-MMP–mCherry–containing endosomes were identified by thresholding and intensity based watershed; the number of cortactin spots was then checked in a neighborhood of three pixels around each MT1-MMP–mCherry vesicle.

3D Structured Illumination Microscopy. Acquisitions were performed in 3D structured illumination microscopy (SIM) mode with an N-SIM Nikon microscope before reconstructing the images with NIS Elements software (7). The system is equipped with an APO TIRF 100× 1.49 NA oil immersion objective, laser illumination (488 nm/200 mW and 561 nm/100 mW) and an EMCCD DU-897 Andor camera.

Electron Microscopy. For ultrathin cryosectioning and immunogold labeling, control and siRNA-treated cells were fixed with a 2% (vol/vol) paraformaldehyde or with a mixture of 2% (vol/vol) paraformaldehyde and 0.2% glutaraldehyde in 0.1 M phosphate buffer (pH 7.4). Cells were processed for ultracryomicrotomy and labeled with the indicated antibodies and Protein A conjugated to 10-nm gold particles (PAG10; purchased from Cell Microscopy Center) as reported previously (8). Samples were analyzed by using an FEI CM120 electron microscope (FEI Company) at 80 kV, and images were acquired with a digital camera (Keen View; Soft Imaging System).

RNA Extraction and RT-qPCR Analysis. We analyzed samples of 458 primary unilateral invasive primary breast tumors excised from women at the Institut Curie/René Huguenin Hospital (Saint-Cloud, France) from 1978 to 2008. Samples were examined histologically for the presence of tumor cells. A tumor sample was considered suitable for this study if the proportion of tumor cells was more than 70%. Estrogen receptor (ER), progesterone receptor (PR), and human epidermal growth factor receptor 2 (HER2) status was determined at the protein level by using biochemical methods (dextran-coated charcoal method, enzyme immunoassay, or immunohistochemistry) and confirmed by real-time quantitative RT-PCR assays (9). The population was divided into four groups according to HR (ER and PR) and HER2 status (Table S1).

Immediately following surgery, the tumor samples were stored in liquid nitrogen until RNA extraction. Ten specimens of adjacent normal breast tissue from breast-cancer patients or normal breast tissue from women undergoing cosmetic breast surgery were used as sources of normal RNA. Total RNA was extracted from breast-tumor and normal breast tissue samples by using the acid-phenol guanidium method. The quality of the RNA samples was determined by electrophoresis in agarose gels and staining with ethidium bromide. The 18S and 28S RNA bands were visualized under UV light. Primers for *TBP* (upper

primer, 5′-TGCACAGGAGCCAAGAGTGAA-3′; lower primer, 5′-CACATCACAGCTCCCCACCA-3′), *PKCι* (upper primer, 5′-CATTCTTTGCCACAGGAACCA-3′ ; lower primer, 5′-CCA-AACTCTCATGACTTGAAGGATT-3′), and *MT1-MMP* (upper primer, 5′-CAACATTGGAGGAGACACCCACT-3′; lower primer, 5′-CCAGGAAGATGTCATTTCCATTCA-3′) were selected with Oligo 6.0 (National Biosciences), and searches (2011) in dbEST and nr databases (NCBI) were used to confirm primer specificity and the absence of nucleotide polymorphisms. To avoid amplification of contaminating genomic DNA, one of the two primers was placed at the junction between two exons. The cDNA synthesis and PCR conditions have been described elsewhere (10).

Quantitative values were obtained from the cycle number (Ct value) at which the increase in fluorescent signal associated with an exponential growth of PCR products starts to be detected by the laser detector of the ABI Prism 7900 Sequence Detection System (Perkin-Elmer Applied Biosystems) using the PE Biosystems analysis software according to the manufacturer's manuals. The precise amount of total RNA added to each reaction (based on optical density) and its quality (i.e., lack of extensive degradation) were difficult to assess; therefore, we also quantified transcripts of the gene *TBP* (GenBank accession no. NM_003194) encoding the TATA box-binding protein (a component of the DNA-binding protein complex TFIID) as an endogenous control, and normalized each sample to its *TBP* content. Results, expressed as *N*-fold differences in target gene expression relative to the *TBP* gene, termed "N*target*," were determined by the formula: $N_{target} = 2^{\Delta Ct_{sample}}$, where ΔCt value of the sample was determined by subtracting the average Ct value of the target gene from the average Ct value of the TBP gene. The N*target* values of the samples were subsequently normalized such that the median of the 10 normal breast-tissue N*target* values was 1. Values of 3 or more were considered to represent overexpression of the target genes in tumor RNA samples.

1. De Kimpe L, et al. (2009) Characterization of cortactin as an in vivo protein kinase D substrate: Interdependence of sites and potentiation by Src. *Cell Signal* 21(2):253–263.
2. Sakurai-Yageta M, et al. (2008) The interaction of IQGAP1 with the exocyst complex is required for tumor cell invasion downstream of Cdc42 and RhoA. *J Cell Biol* 181(6): 985–998.
3. Rosse C, et al. (2009) An aPKC-exocyst complex controls paxillin phosphorylation and migration through localised JNK1 activation. *PLoS Biol* 7(11):e1000235.
4. Rossé C, et al. (2006) RalB mobilizes the exocyst to drive cell migration. *Mol Cell Biol* 26(2):727–734.
5. Sibarita JB (2005) Deconvolution microscopy. *Adv Biochem Eng Biotechnol* 95: 201–243.
6. Lamprecht MR, Sabatini DM, Carpenter AE (2007) CellProfiler: Free, versatile software for automated biological image analysis. *Biotechniques* 42(1):71–75.
7. Gustafsson MG, et al. (2008) Three-dimensional resolution doubling in wide-field fluorescence microscopy by structured illumination. *Biophys J* 94(12):4957–4970.
8. Raposo G, Kleijmeer MJ, Posthuma G, Slot JW, Geuze HJ (1997) Immunogold labeling of ultrathin cryosections: Application in immunology. *Handbook of Experimental Immunology*, eds Herzenberg LA, Weir DM, Herzenberg LA, Blackwell C (Blackwell Science, Oxford), pp 1–11.
9. Bièche I, et al. (1999) Real-time reverse transcription-PCR assay for future management of ERBB2-based clinical applications. *Clin Chem* 45(8 Pt 1):1148–1156.
10. Bieche I, et al. (2001) Identification of CGA as a novel estrogen receptor-responsive gene in breast cancer: An outstanding candidate marker to predict the response to endocrine therapy. *Cancer Res* 61(4):1652–1658.

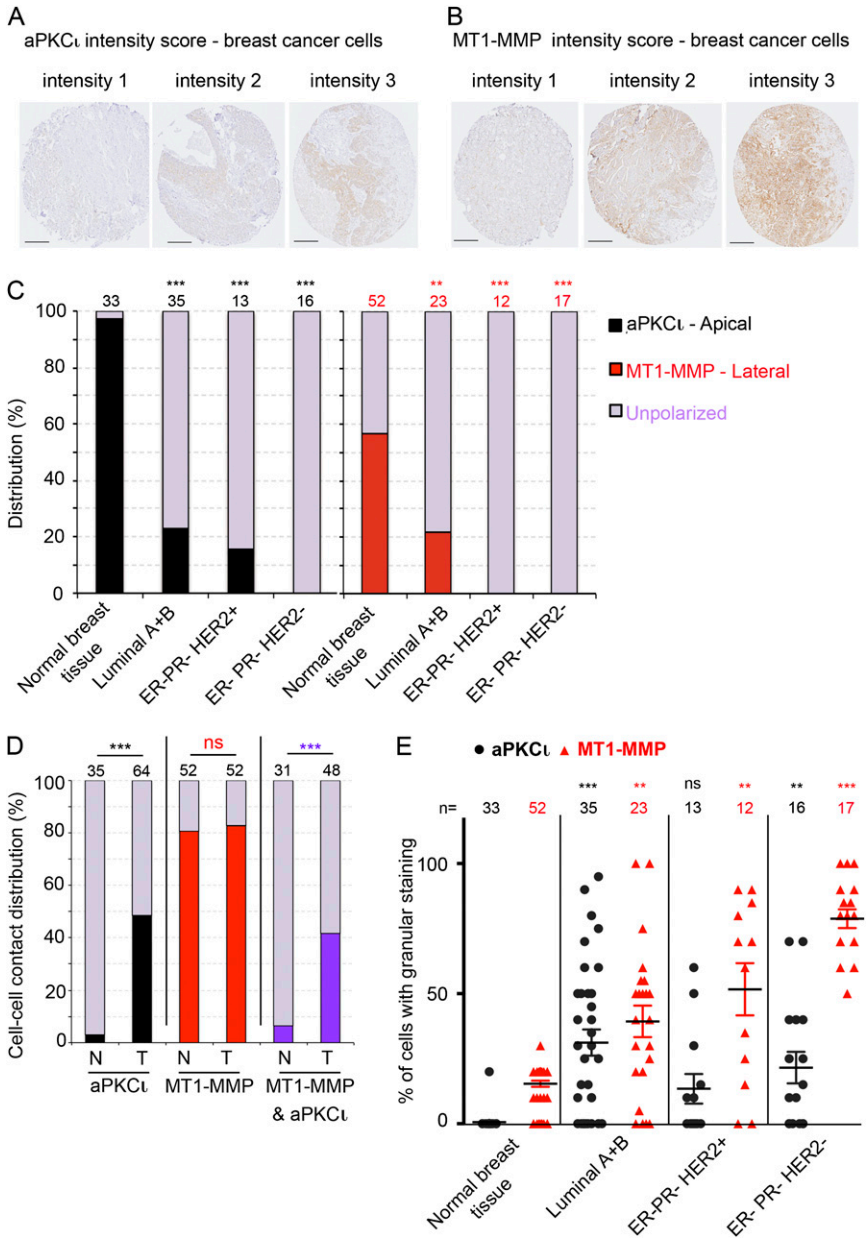

Fig. S1. Distribution of MT1-MMP and PKCι in breast-carcinoma cells. (*A* and *B*) Scoring intensity scale for aPKCι (*A*) and MT1-MMP (*B*) on tissue microarray (TMA) of human breast cancer. (*C*) Breast epithelial cells in adjacent nonneoplastic tissues and breast-cancer cells in representative luminal A, luminal B, HER2, or triple-negative tumor samples were scored for lateral, apical, or unpolarized distribution of MT1-MMP (red plots) and PKCι (black plots) based on immunohistocytochemistry (IHC) staining of TMA of human breast cancer. (*D*) Adjacent nonneoplastic tissues (N) and breast-tumor samples (T) were scored for the presence of MT1-MMP, PKCι, or both at cell–cell contacts. Only tumors with at least 20% of tumor cells with cell–cell contact staining were considered as positive. (*E*) Samples as in *C* were scored for cytoplasmic granular distribution of MT1-MMP (red triangles) and PKCι (black dots). *n*, number of tumors analyzed; ns, non significant; $^{**}P < 0.01$; $^{***}P < 0.001$ compared with adjacent nonneoplastic tissues (Kruskal–Wallis test). Only tumors positive for MT1-MMP and/or PKCι (intensity score ≥ 1) were considered for these analyses.

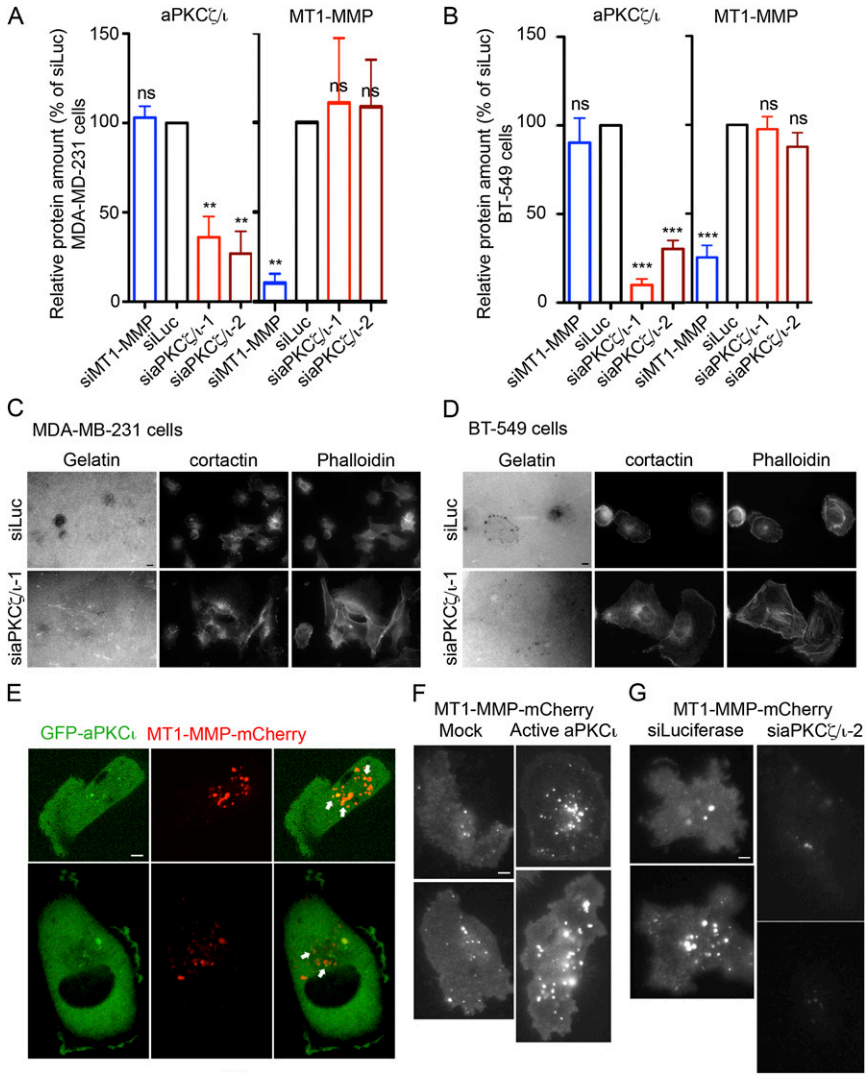

Fig. S2. aPKCζ/ι controlled matrix degradation and delivery of MT1-MMP at the surface of the cell. (*A* and *B*) The effects of MT1-MMP or aPKCζ/ι silencing on MT1-MMP and atypical PKC (aPKC) levels were quantified by Western blotting analysis and chemiluminescence signal detection with Bio-Rad ChemiDoc MP apparatus based on three independent experiments in MDA-MB-231 (*A*) and BT-549 cells (*B*). Graphs show the amount of MT1-MMP or aPKC normalized to the levels of GAPDH relative to levels in siLuc-treated cells. Values are means ± SEM from three independent experiments. $^{**}P < 0.01$; $^{***}P < 0.001$. (*C* and *D*) MDA-MB-231 cells (*C*) and BT-549 cells (*D*) treated with siRNAs against luciferase (siLuc) or aPKCζ/ι siRNA pair (siaPKCζ/ι-1) were plated for 5 h on fluorescently labeled cross-linked gelatin and then analyzed by labeling for cortactin and F-actin. Gelatin degradation (*Left*) was focal and coincided with cortactin-, F-actin–positive invadopodia forming at the adherent plasma membrane. Invadopodia formation and gelatin degradation were impaired in aPKCζ/ι-depleted cells. (Scale bar: 5 μm.) (*E*) Confocal spinning-disk microscopy image of MDA-MB-231 cell expressing GFP–aPKCι and MT1-MMP–mCherry. (Scale bar: 5 μm.) (*F*) MDA-MB-231 cells expressing MT1-MMP–mCherry alone or together with constitutively active aPKCι were imaged by total interference reflection fluorescence microscopy (TIRFM). (Scale bar: 5 μm.) (*G*) MDA-MB-231 cells overexpressing MT1-MMP–mCherry were transfected with siRNAs against luciferase or aPKCζ/ι (siaPKCζ/ι-2), plated onto gelatin, and imaged by TIRFM. To ensure that cells expressed similar levels of MT1-MMP, cells were imaged in wide-field mode (not shown). (Scale bar: 5 μm.)

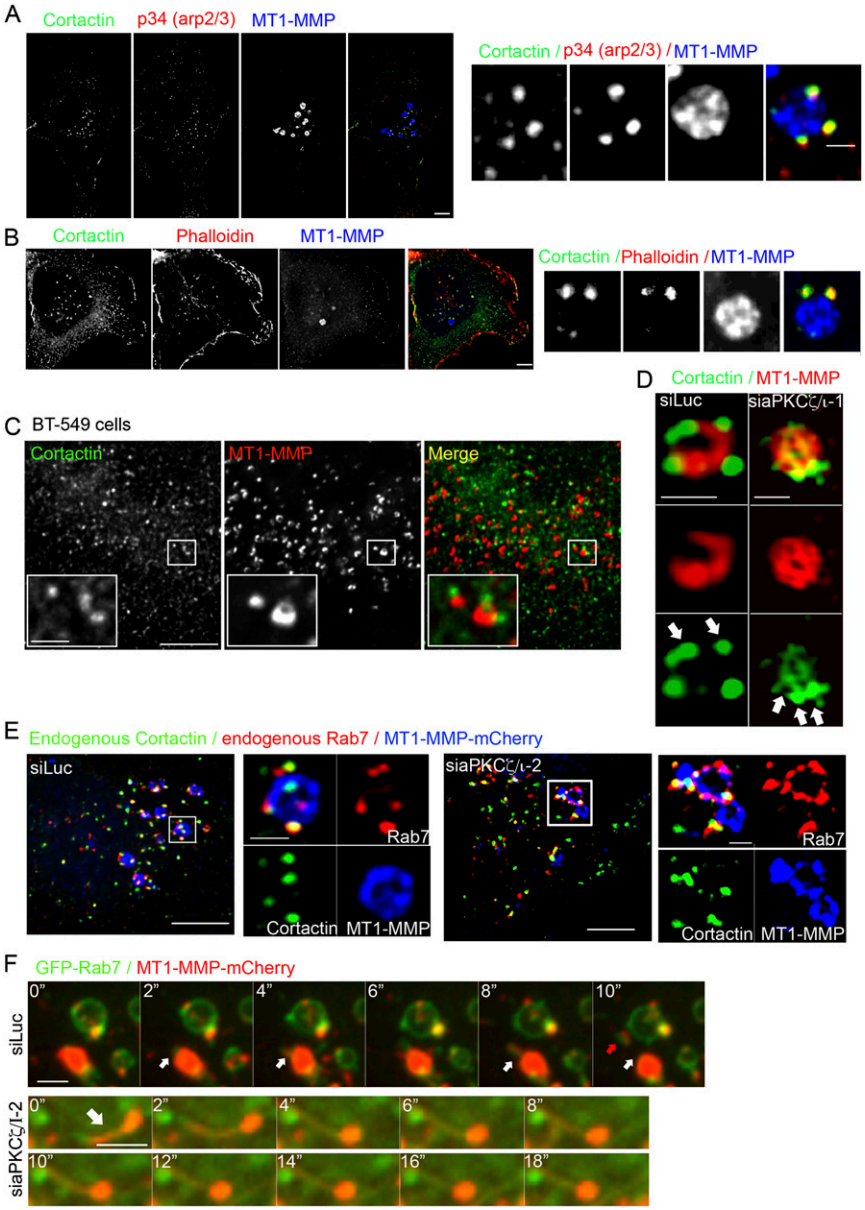

Fig. S3. Silencing of aPKCζ/ι affects endosomal cortactin recruitment and induces tubulation of MT1-MMP–positive late endosomes. (*A* and *B*) MDA-MB-231 cells stably expressing MT1-MMP–mCherry (blue) and immunolabeled for cortactin (green), and p34-Arc (an Arp2/3 complex subunit; red) (*A*) or labeled with phalloidin for F-actin (red) (*B*). *Right* in each series is a merge image of the three labels. [Scale bars: 5 μm (entire cell, *Left* rows) and 1 μm (*Right* rows). (*C*) BT-549 cells were immunolabeled with antibodies against cortactin (in green) and MT1-MMP (red). [Scale bars: 5 μm (entire cell) and 1 μm (*Insets* corresponding to boxed region at higher magnification).] (*D*) MDA-MB-231 cells treated with siRNAs against luciferase (siLuc) or aPKCζ/ι (siaPKCζ/ι-1) were labeled with antibodies against MT1-MMP (red) and cortactin (green) and imaged by 3D structured illumination microscopy (SIM). Arrows point to cortactin domains on MT1-MMP–containing endosomes. (*Left*) Merge images of the two labels. (Scale bars: 1 μm.) (*E*) MDA-MB-231 cells stably expressing MT1-MMP–mCherry (blue) treated with siRNAs against luciferase (*Left*) or aPKCζ/ι (siaPKCζ/ι-2, *Right*) were plated on gelatin and immunolabeled for cortactin (green) and Rab7 (red). [Scale bars: 5 μm (entire cell, *Left*) and 1 μm (boxed regions, *Right*). (*F*) MDA-MB-231 cells overexpressing GFP–Rab7 (green) and MT1-MMP–mCherry (red) were treated with siRNAs against luciferase (*Upper*) or aPKCζ/ι (siaPKCζ/ι-2, *Lower*), plated onto gelatin, and imaged by confocal dual-color spinning-disk microscopy. The images show time-lapse series at 2-s intervals. The white arrow in *Upper* (siLuc) points to a Rab7–MT1-MMP–positive membrane tubule. The red arrow points to fission of a transport vesicle. The white arrow in *Lower* (siaPKCζ/ι-2) points to a persistent MT1-MMP–Rab7–positive tubule. (Scale bar: 1 μm.)

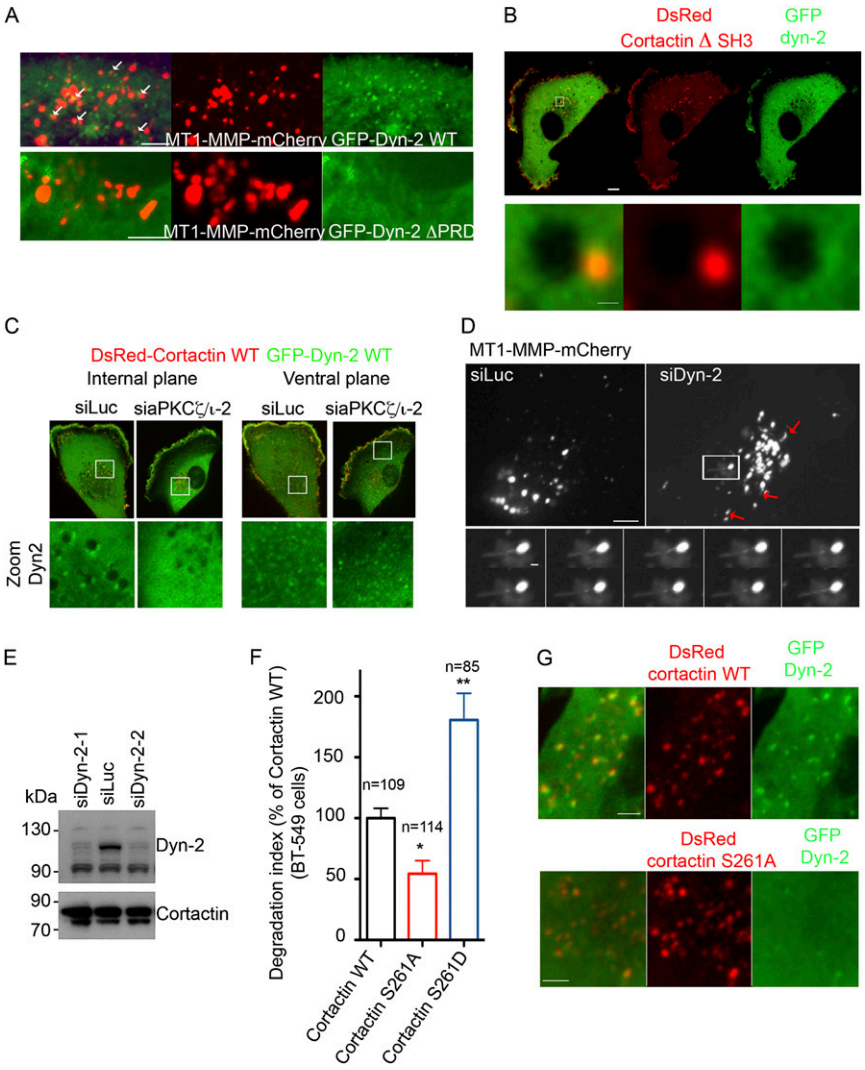

Fig. S4. aPKCζ/ι regulates cortactin and dynamin-2 association on MT1-MMP–positive endosomes. (*A*) Dual-color confocal spinning-disk microscopy of MDA-MB-231 cell expressing MT1-MMP–mCherry and wild-type dyn-2 fused with GFP (GFP–Dyn-2 WT, *Upper*) or GFP fused with a mutant of dyn-2 lacking the proline-rich domain (GFP–Dyn-2 ΔPRD, *Lower*). Arrows point to GFP–dyn-2 WT associated with MT1-MMP–positive endosomes. In contrast, GFP–dyn-2 ΔPRD does not associate with MT1-MMP–positive endosomes (*Lower*). (Scale bars: 5 μm.) (*B*) GFP–dyn-2 was expressed together with a fusion protein of DsRed with a mutant of cortactin lacking the SH3 domain (cortactinΔSH3) in MDA-MB-231 cells and visualized by using confocal dual spinning-disk microscopy. Expression of cortactinΔSH3 interferes with Dyn-2 association with endosomes (appearing as black vesicles in the GFP cytosolic signal). [Scale bars: 5 μm (entire cell, *Upper*) and 1 μm (*Lower*). (*C*) MDA-MB-231 cells expressing DsRed-cortactin and GFP–dyn-2 were treated with siRNA against Luciferase or both aPKCι and ζ (siaPKC-2). Silencing of aPKC leads to inhibition of dyn-2 recruitment on these compartments (*Left*, internal plane) whereas it does not affect dyn-2 localization to clathrin-coated pits at the ventral plasma membrane (*Right*, ventral plane). These data indicate that aPKC regulates specifically the interaction of cortactin and dyn-2 on late endosomes. Zooms (*Lower*) show only Dyn-2 signal. (*D*) MDA-MB-231 cells stably expressing MT1-MMP–mCherry treated with siRNAs against luciferase or dyn-2 were imaged by confocal spinning-disk microscopy. Red arrows point to tubulation of MT1-MMP–mCherry–positive endosomes in dyn-2–depleted cells (Movie S3). (*Lower*) A series of images of the boxed region at intervals of 2 s. [Scale bars: 5 μm (entire cell, *Upper*) and 1 μm (*Lower*). (*E*) Immunoblotting of dyn-2 in MDA-MB-231 cells treated with siRNAs against dyn-2 or luciferase, as indicated. Immunoblotting with an antibody against cortactin served as a control for loading. The mobilities of molecular mass markers are indicated in kDa. (*F*) Quantification of gelatin degradation by BT-549 cells expressing wild-type or S261A or S261D cortactin variants. Values are means ± SEM of the normalized degradation area from *n* (number of) cells analyzed from three independent experiments. (*G*) GFP–dyn-2 was expressed together with DsRed–cortactin or the cortactin point mutant S261A in MDA-MB-231 cells and visualized by using confocal dual-color spinning-disk microscopy. (Scale bars, 5 μm.)

Table S1. Correlation of PKCι and MT1-MMP mRNA levels with clinicopathological parameters of breast-cancer cases examined

Parameter	*n* (%)	No. of patients (%)				*P**
		Normal PKCι and MT1-MMP expression	Normal PKCι expression and MT1-MMP overexpression	PKCι overexpression and normal MT1-MMP expression	PKCι and MT1-MMP overexpression	
Total	458 (100.0)	265 (57.9)	40 (8.7)	86 (18.8)	67 (14.6)	
Age						
≤50	99 (21.6)	56 (21.1)	8 (20)	20 (23.3)	15 (22.4)	0.97 (NS)
>50	359 (78.4)	209 (78.9)	32 (80)	66 (76.7)	52 (77.6)	
SBR histological grade[†,‡]						
I	58 (12.9)	41 (15.8)	8 (20)	4 (4.8)	5 (7.6)	**0.0041**
II	230 (51.2)	142 (54.6)	19 (47.5)	40 (48.2)	29 (43.9)	
III	161 (35.9)	77 (29.6)	13 (32.5)	39 (47)	32 (48.5)	
Lymph node status[§]						
0	120 (26.2)	69 (26.0)	6 (15)	26 (30.6)	19 (28.4)	0.099 (NS)
1–3	237 (51.9)	134 (50.6)	25 (62.5)	49 (57.6)	29 (43.3)	
>3	100 (21.9)	62 (23.4)	9 (22.5)	10 (11.8)	19 (28.4)	
Macroscopic tumor size[¶]						
≤25 mm	223 (49.6)	131 (50.4)	18 (45)	39 (46.4)	35 (53)	0.79 (NS)
>25 mm	227 (50.4)	129 (49.6)	22 (55)	45 (53.6)	31 (47)	
ER status						
Negative	119 (26.0)	52 (19.6)	10 (25)	31 (36)	26 (38.8)	**0.0014**
Positive	339 (74.0)	213 (80.4)	30 (75)	55 (64)	41 (61.2)	
PR status						
Negative	195 (42.6)	94 (35.5)	16 (40)	46 (53.5)	39 (58.2)	**0.0010**
Positive	263 (57.4)	171 (64.5)	24 (60)	40 (46.5)	28 (41.8)	
HER2 status						
Negative	359 (78.4)	215 (81.1)	32 (80)	65 (75.6)	47 (70.1)	0.23 (NS)
Positive	99 (21.7)	50 (18.9)	8 (20)	21 (24.4)	20 (29.9)	
Molecular subtypes						
ER- PR- HER2- (TN)	69 (15.1)	27 (10.2)	5 (12.5)	20 (23.3)	17 (25.4)	**0.0030**
ER- PR- HER2+ (HER2+)	45 (9.8)	22 (8.3)	5 (12.5)	9 (10.5)	9 (13.4)	
ER+ PR+ HER2- (luminal A)	290 (63.3)	188 (70.9)	27 (67.5)	45 (52.3)	30 (44.8)	
ER+ PR+ HER2+ (luminal B)	54 (11.8)	28 (10.6)	3 (7.5)	12 (14)	11 (16.4)	

Estrogen receptor (ER), progesterone receptor (PR), and HER2 status were determined as described (1, 2). Overexpression is defined as greater than threefold over the level in normal tissue samples. In bold type, significant *P* values.

*χ^2 test.

[†]Scarff–Bloom–Richardson classification.

[‡]Information available for 449 patients.

[§]Information available for 457 patients.

[¶]Information available for 450 patients.

1. Bièche I, et al. (1999) Real-time reverse transcription-PCR assay for future management of ERBB2-based clinical applications. *Clin Chem* 45(8 Pt 1):1148–1156.
2. Bièche I, et al. (2001) Quantification of estrogen receptor alpha and beta expression in sporadic breast cancer. *Oncogene* 20(56):8109–8115.

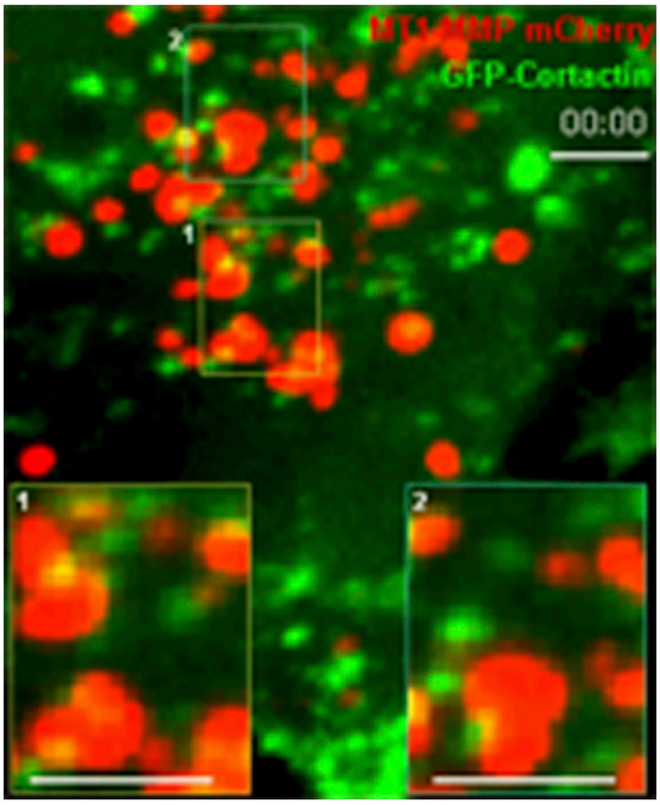

Movie S1. Dynamics of cortactin on MT1-MMP–mCherry–containing vesicles. MDA-MB-231 cells overexpressing MT1-MMP–mCherry and GFP–cortactin were plated onto gelatin and imaged by dual-color spinning-disk microscopy. Indicated time is in min:s. (Scale bar: 5 μm.)

Movie S1

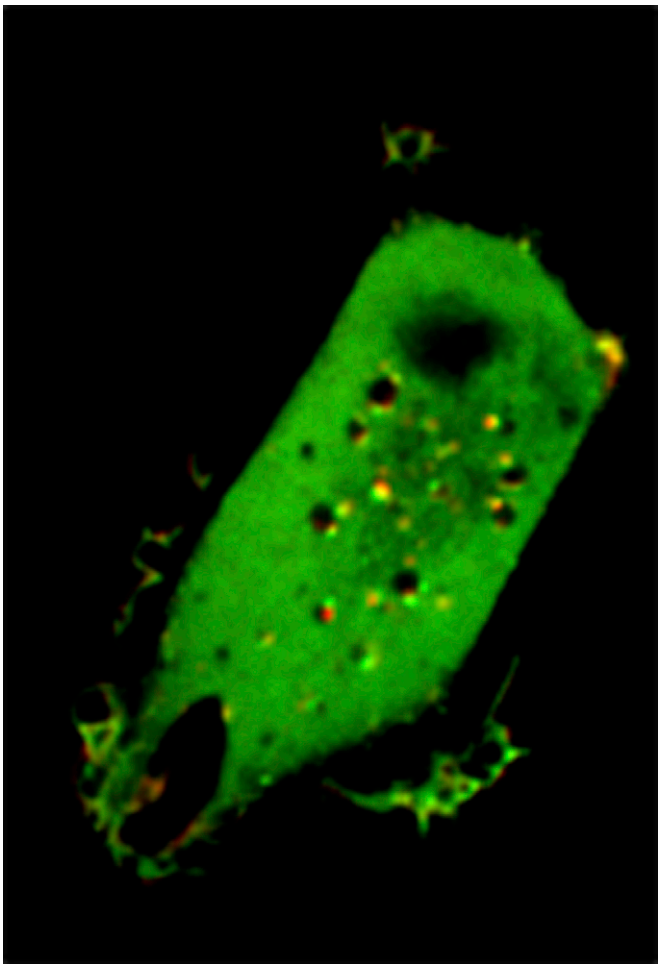

Movie S2. Dynamics of cortactin and dyn-2 on endosomes. MDA-MB-231 cells overexpressing GFP–dyn-2 and DsRed–cortactin were plated onto gelatin and imaged by dual-color spinning-disk microscopy. Images were taken every 2 s. (Scale bar, 5 μm.)

Movie S2

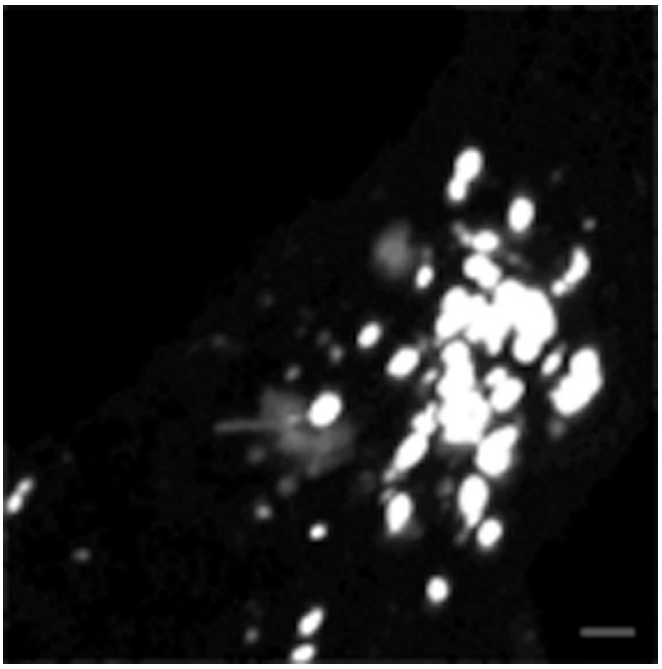

Movie S3. Tubulation of MT1-MMP–mCherry–containing vesicles in dyn-2–depleted cells. MDA-MB-231 cells overexpressing MT1-MMP–mCherry were treated with siRNAs against PKCζ/ι, plated on gelatin, and imaged by confocal spinning-disk microscopy. Images were taken every 2 s. (Scale bar: 5 μm.)

Movie S3

Dataset S1. Clinicopathological parameters of breast-cancer cases examined in the TMA

Dataset S1

Breast molecular subtypes were defined as follows: luminal A + B according to ref. 1, [luminal A, estrogen-receptor (ER) ≥ 10%, progesterone-receptor (PR) ≥ 20%, Ki67 < 14%; luminal B, ER ≥ 10%, PR < 20%, Ki67 ≥ 14%]; ER^- PR^- $HER2^+$: ER < 10%, PR < 10%, HER2 2+ amplified or 3+ according to ref. 2; ER^- PR^- $HER2^-$ (triple-negative): ER < 10%, PR < 10%, HER2 0/1+ or 2+ nonamplified according to American Society of Clinical Oncology (ASCO) guidelines (2). Mitotic index: low <11 mitotic figures from 10 high-magnification fields, intermediate 11–22 mitotic figures from 10 high-magnification fields, high >22 mitotic figures per 10 high-magnification fields.

1. Prat A, et al. (2013) Prognostic significance of progesterone receptor-positive tumor cells within immunohistochemically defined luminal A breast cancer. *J Clin Oncol* 31(2):203–209.
2. Wolff AC, et al. (2007) American Society of Clinical Oncology/College of American Pathologists guideline recommendations for human epidermal growth factor receptor 2 testing in breast cancer. *J Clin Oncol* 25(1):118–145.

Article 3

Exo70 Subunit of the Exocyst Complex Is Involved in Adhesion-Dependent Trafficking of Caveolin-1

Maud Hertzog, **Pedro Monteiro**, Gaëlle Le Dez, Philippe Chavrier

PLoS ONE (2012) 7(12): e52627. doi:10.1371/journal.pone.0052627

Contribution article PLoS One :

J'ai apporté ma contribution à ce papier dans la réalisation des expériences, de la culture cellulaire à l'observation des cellules au microscope, notamment en au travers de la microscopie TIRF permettant de visualiser les évènements se déroulant à proximité de la membrane plasmique.

Exo70 Subunit of the Exocyst Complex Is Involved in Adhesion-Dependent Trafficking of Caveolin-1

Maud Hertzog*¤a¤b, Pedro Monteiro¤a, Gaëlle Le Dez¤a, Philippe Chavrier*¤a

Membrane and Cytoskeleton Dynamics, Institut Curie, Research Center, CNRS- UMR144, Paris, France

Abstract

Caveolae are specialized domains of the plasma membrane, which play key roles in signaling, endocytosis and mechanosensing. Using total internal reflection fluorescent microscopy (TIRF-M), we observe that the exocyst subunit Exo70 forms punctuate structures at the plasma membrane and partially localizes with caveolin-1, the main component of caveolae. Upon cell detachment, we found that Exo70 accumulates with caveolin-1-positive vesicular structures. Upon cell re-adhesion, caveolin-1 traffics back to the plasma membrane in a multistep process involving microtubules and actin cytoskeleton. In addition, silencing of Exo70 redirects caveolin-1 to focal adhesions identified by markers such as α5 integrin or vinculin. Based on these findings, we conclude that Exo70 is involved in caveolin-1 recycling to the plasma membrane during re-adhesion of the cells to the substratum.

Citation: Hertzog M, Monteiro P, Le Dez G, Chavrier P (2012) Exo70 Subunit of the Exocyst Complex Is Involved in Adhesion-Dependent Trafficking of Caveolin-1. PLoS ONE 7(12): e52627. doi:10.1371/journal.pone.0052627

Editor: Joshua Z. Rappoport, University of Birmingham, United Kingdom

Received June 15, 2012; **Accepted** November 19, 2012; **Published** December 27, 2012

Copyright: © 2012 Hertzog et al. This is an open-access article distributed under the terms of the Creative Commons Attribution License, which permits unrestricted use, distribution, and reproduction in any medium, provided the original author and source are credited.

Funding: Support was provided to PC by Association pour la Recherche sur le Cancer.(grant # SL220100601356) and Agence Nationale pour la Recherche (grant # ANR-08-BLAN-0111). Core funding for this work was provided by Institut Curie and Centre National de la Recherche Scientifique (National Center for Scientific Research, France). The funders had no role in study design, data collection and analysis, decision to publish, or preparation of the manuscript.

Competing Interests: The authors have declared that no competing interests exist.

* E-mail: maud.hertzog@ibcg.biotoul.fr (MH); philippe.chavrier@curie.fr (PC)

¤a Current address: Laboratoire de Microbiologie et Génétique Moléculaire, LMGM-CNRS UMR 5100, Université Paul Sabatier, Toulouse, France
¤b Current address: CNRS, UMR 6061, Institut Génétique et Développement de Rennes, Université Rennes 1, UEB, IFR 140, Rennes, France

Introduction

Caveolae are bulb-shaped pits present in several mammalian cell types including adipocytes and muscle cells [1,2]. These structures play key roles in compartmentalization and organization of signaling pathways for cell growth and differentiation. In addition, caveolae were recently implicated in membrane-mediated mechanical responses [3,4]. Caveolin-1 (Cav1) is the main component of caveolae. Cav1 adopts a hairpin-like shape within the membrane bilayer with both the N and C-terminus facing the cytoplasm [1]. Recent studies showed that the Cav1 partner protein, Polymerase I and Transcript Release Factor (PTRF)/cavin-1 selectively associates with mature caveolae at the plasma membrane and is involved in caveolae formation and function [1,5]. Total internal reflection fluorescence microscopy (TIRF-M) allowed characterizing the dynamics of individual caveolae and revealed that caveolae can be stored in stationary multi-caveolar structures at the plasma membrane, or undergo kiss and run processes without disassembling the caveolar coat [6]. Moreover, caveolae can undergo long-range cytoplasmic transport during diverse regulated processes such as mitosis and during loss of integrin-based adhesion to the extracellular matrix (ECM) [1,7,8]. All together, these data suggest some interplay between caveolar trafficking and cell adhesion [9].

Initially identified in *Saccharomyces cerevisiae*, the exocyst complex comprises eight subunits named Sec3, Sec5, Sec6, Sec8, Sec10, Sec15, Exo70 and Exo84 [10,11]. This complex controls the docking and insertion of secretory and endocytic recycling vesicles to growing regions of the plasma membrane and impinges on diverse cellular processes requiring polarization of membrane trafficking such as cell motility and neuronal development [12,13]. In yeast, Exo70 interacts with phospholipids at the plasma membrane and is crucial for tethering of secretory vesicles for exocytosis [14]. Phospholipid binding and plasma membrane localization are conserved in mammalian cells suggesting a similar role of Exo70 in targeting of the exocyst complex to the plasma membrane and regulation of vesicle docking [14–16]. Previous studies showed that detachment of cells from integrin-mediated adhesion triggers the caveolin-dependent internalization of lipid rafts [9]. Conversely, re-adhesion of cells to the ECM induces the re-insertion of lipid rafts to the plasma membrane in a process that involves the Ras-related GTP binding proteins RalA and ARF6 and their downstream effectors, exocyst complex [17,18,19]. However, the specific contribution of Exo70 to Cav1 trafficking remains largely unknown.

Here, using TIRF-M we could show that Exo70 accumulates in punctuate plasma membrane domains where it co-localized with Cav1. Upon cell detachment, Exo70 localized to Cav1-positive intracellular compartments. When cells were allowed to re-adhere, silencing of Exo70 led to the accumulation of Cav1-positive structures at the cell periphery close to focal adhesions (FAs), suggesting that loss of Exo70 function results in Cav1 mistargeting during cell spreading.

Results

Exo70 co-localizes with Cav1 at the plasma membrane

TIRF-M revealed a punctuate distribution of Exo70-mCherry on the adherent surface of Hela cells and co-localization with a subset of Cav1-GFP-positive structures (representing 20 to 30% of

total Cav1-positive structures) and probably corresponding to caveolae (Fig. 1A and S1A). Live-cell confocal spinning disk microscopy confirmed this punctuate pattern and plasma membrane localization of Exo70-GFP whereas Cav1-mRFP associated predominantly with intracellular vesicular structures (Fig. 1B). It has been previously reported that Exo70 binds directly to phospholipids and that binding to PtdIns(4,5)P2 mediates interaction of Exo70 with the plasma membrane [14,16]. When we used the PtdIns(4,5)P2-binding protein tubby [20], tubby-GFP was present in plasma membrane punctuate structures observed by TIRF-M, which partially localized with Exo70-mCherry (Fig. S1B) indicating that Exo70 localization sites at the plasma membrane are enriched in PtdIns(4,5)P2.

Caveolae internalization can be triggered by several stimuli, including loss of integrin- mediated cell adhesion [21]. Upon cell detachment, Cav1-positive PM domains initiate an inward traffic to the perinuclear area. Hela cells expressing Cav1-mRFP and Exo70-GFP were detached from the substratum by trypsinization, maintained for 1 hr in suspension, replated onto fibronectin (FN)-coated substrate and visualized by spinning disk microscopy. Cav1-mRFP was observed in dynamic vesicles that shuttled between the perinuclear region and the cell periphery (Fig. 2A and movie S1). Analysis of the distribution and dynamics of Exo70-GFP during cell replating revealed that Exo70 was strongly associated with Cav1-positive vesicles throughout the cell (compare Fig. 1B and 2A). Thus, these results reveal a dynamic

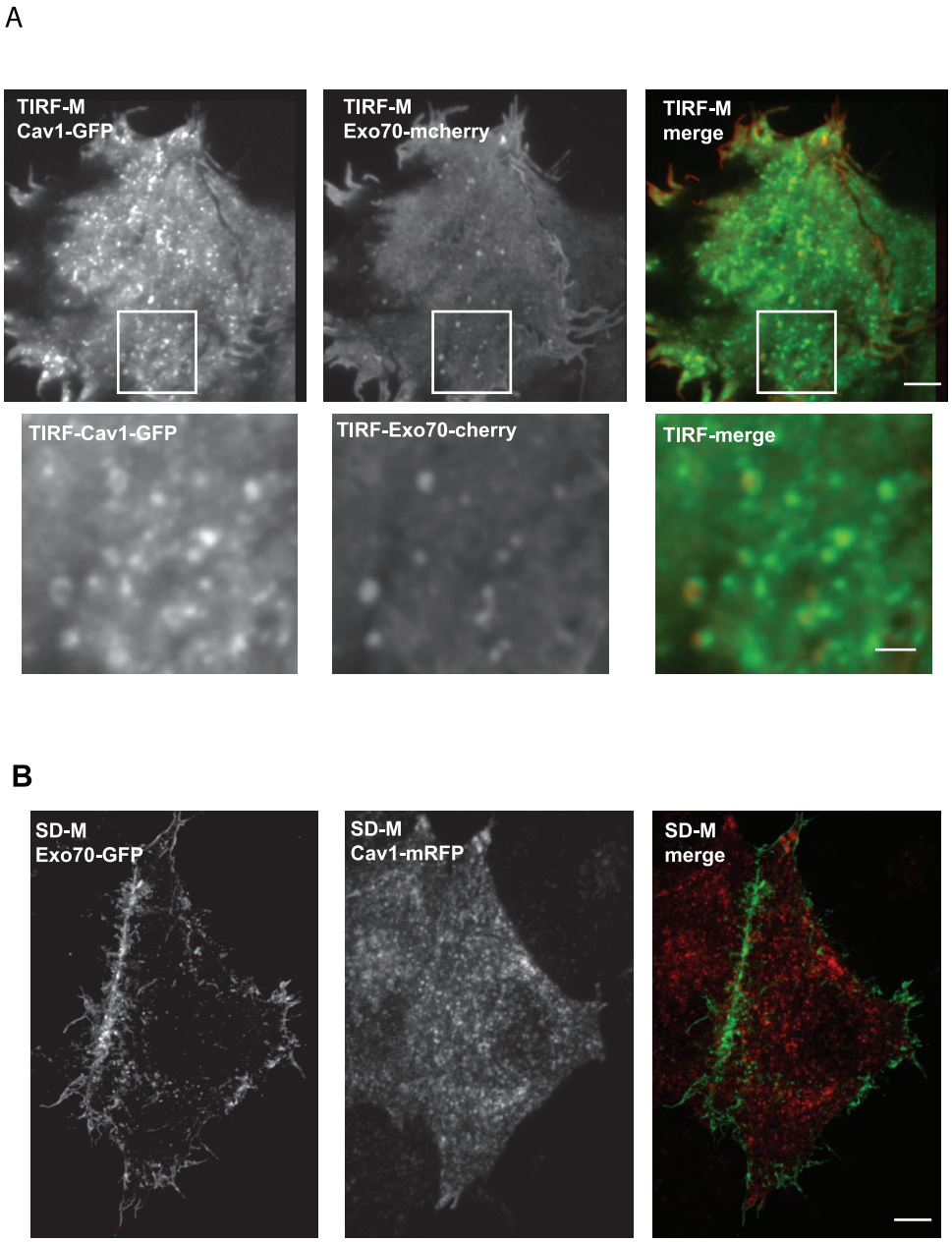

Figure 1. Partial co-localization and co-trafficking of Exo70 and Cav1 at the plasma membrane. (**A**) Hela cells expressing Cav1-GFP and Exo70-mCherry were visualized by TIRFM (upper panel); Scale bar, 5 μm. Higher magnification of the boxed region is shown (bottom panel). Scale bar, 1 μm. (**B**) Hela cells expressing Cav1-mRFP and Exo70-GFP were visualized using time-lapse confocal spinning disk microscopy. Scale bar, 5 μm.
doi:10.1371/journal.pone.0052627.g001

association of Exo70 with Cav1 transport intermediates following cell detachment and re-adhesion. In addition to Cav1, cavin-family proteins are required for caveolae formation and PTRF/cavin-1 associates with mature caveolae [22]. Interestingly, cavin-1 partially redistributed with Cav1 in intracellular vesicles in cells replated on FN-coated substrates after detachment, suggesting that mature caveolae are internalized and trafficked upon cell detachment (Fig. 2B). In addition, we acquired time-lapse sequences of HeLa cells expressing either Cav1-GFP and Exo70-mCherry or Cav1-mRFP and Exo70-GFP by TIRF-M (data not shown). These movies were acquired starting 1, 2, or 3 hours after cell detachment and replating. In all cases, we observed that 100% of Exo70-positive structures were Cav1-positive, while only a subset (20–30%) of Cav1-positive structures co-localized with Exo70 (data not shown).

Actin and microtubule cytoskeletons are involved in distinct steps of Cav1 trafficking

To identify mechanisms underlying cell detachment-induced Cav1 redistribution, we investigated the involvement of cytoskeleton components using nocodazole and cytochalasin-B (cytoB), which destabilize microtubule and actin networks, respectively. Treatment with nocodazole induced a blockade of Cav1 transport, which accumulated in a network of static tubulo-vesicular extensions extending towards the cell periphery (Fig. 3A, movie S2), indicating that recycling of Cav1 to the surface is a MT-dependent process. Inhibition of actin assembly by treatment with cytoB induced the redistribution of Cav1 to small, scattered vesicles in the central region of the cells and in some peripheral accumulations at the cell edges (Fig. 3B, movie S3). Remarkably, a network of radially extending tubular membranes connected the perinuclear vesicles and the peripheral Cav1 pools. Collectively,

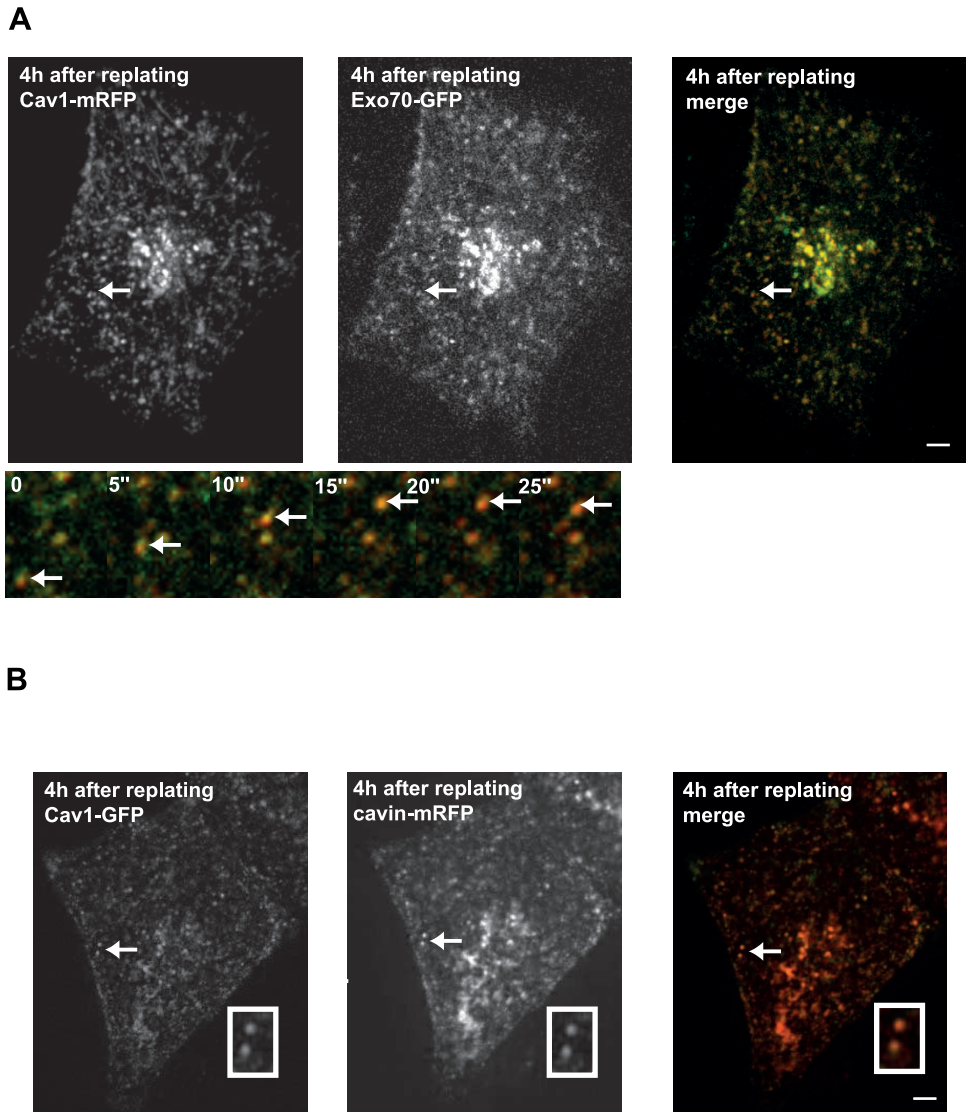

Figure 2. Exo70 redistributes in Cav1-positive compartments upon cell detachment. (**A**) Hela cells expressing Cav1-mRFP and Exo70-GFP were kept in suspension for 1 h and replated on fibronectin for 3 h, and then visualized by confocal dual-colour spinning-disk microscopy (see corresponding movie S1). Arrow points to a dynamic Cav1- and Exo70-positive vesicle. Bottom panel shows selected frames from the time-lapse series corresponding to the boxed region in the upper panel. Time is given in second. (**B**) Hela cells expressing Cav1-GFP and cavin-1-mRFP were treated as in panel A. Inset shows higher magnification of region indicated by an arrow. Scale bars, 5 μm.
doi:10.1371/journal.pone.0052627.g002

and in agreement with previous reports [23,24], these observations suggest that both MTs and actin cytoskeleton are involved in distinct steps of Cav1 trafficking: (i) a MT-dependent long range transport from perinuclear endosomal compartments that we identified as late endosomes (LEs) by co-localization with GFP-rab7 and GFP-VAMP7 (see Figure S2) (ii) and an actin-dependent step involved in Cav1 trafficking at the cell periphery.

Silencing of Exo70 leads to an accumulation of Cav1 in focal adhesions

Cav1 is internalized together with integrins upon cell detachment and β1 integrin regulates Cav1 trafficking and recycling to the plasma membrane for caveolae reassembly upon cell adhesion [25,26]. Consistent with these findings, we observed a partial co-localization of α5-integrin-GFP with Cav1-mRFP in cytoplasmic vesicles upon cell detachment and re-adhesion (Fig. 4A). In addition, α5-integrin-GFP associated with reforming focal adhesions at the cell edge, which were negative for Cav1 (Fig. 4A and A′). Noticeably, in 20% of the cells, Cav1-mRFP and α5-integrin-GFP associated with membrane tubules extending radially from the perinuclear compartments, and frequently targeting newly reformed focal adhesions (movies S3 and S4). All together, these findings indicate that Cav1 and integrins traffic together in tubulo-vesicular transport carriers to the cell periphery.

We investigated whether Exo70 may play a role in Cav1 trafficking and recycling upon cell adhesion [27]. Silencing of Exo70 using two independent siRNAs (Fig. S3) inhibited cell spreading on fibronectin-coated substratum during the early phase of replating (3 to 6 hrs after replating) (Fig. S4), Silencing of Exo70 caused the accumulation of Cav1-mRFP to peripheral α5-integrin-positive structures with a morphology typical of focal adhesions (Fig. 4, compare panels A and B and linescan profiles in panel A′ and B′). Co-localization of Cav1 and α5-integrin was quantified and compared between mock- and siExo70-treated cells in a peripheral region of the cells enriched in focal adhesions (see Material and Methods section) (Fig. 4C). In mock-treated cells, we observed a 26.6% co-localization of Cav1-mRFP and α5-integrin-GFP in the peripheral region. This percentage increased to 42–45% in cells depleted for Exo70 with two-independent siRNAs (Fig. 4C). These results suggest that, in the absence of Exo70, Cav1 (or Cav1-positive vesicles) is retained in focal adhesions. Next, we addressed the effect of Exo70 knockdown on the distribution of endogenous Cav1 protein. Hela cells were detached and maintained in suspension for 60 min before replating on

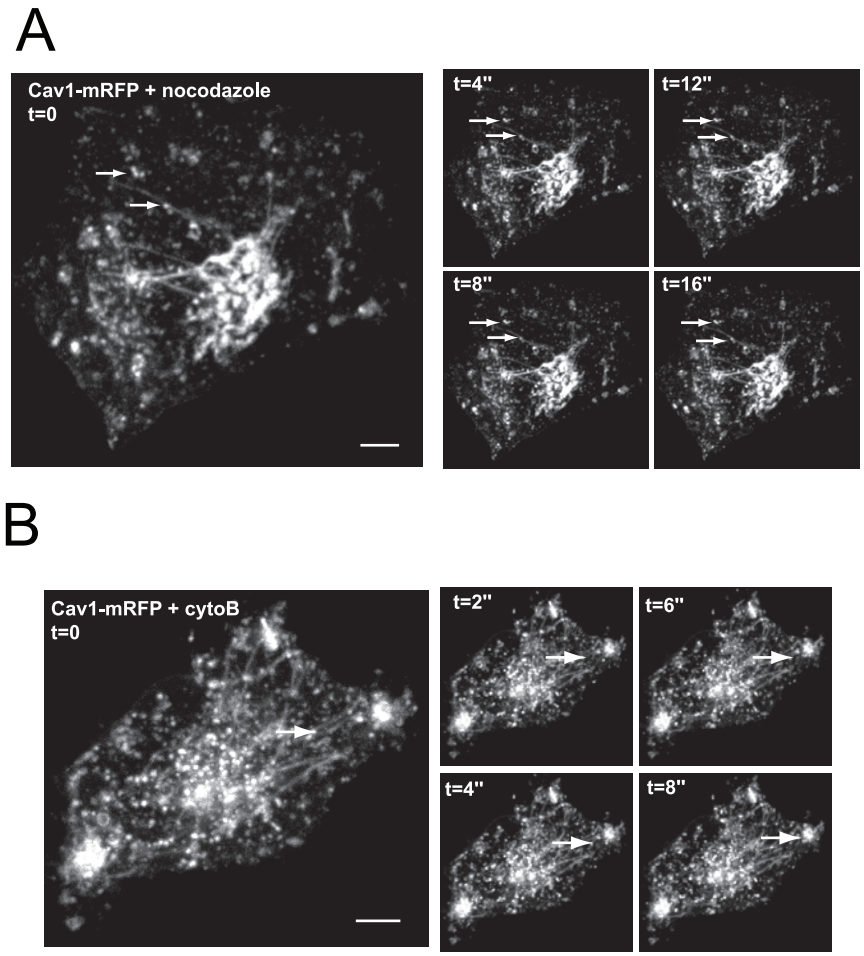

Figure 3. Actin and microtubule cytoskeletons act at distinct steps of Cav1 trafficking. (**A, B**) Hela cells expressing Cav1-mRFP maintained in suspension for 1 h, were replated on fibronectin for 3 h in the presence of 10 μM nocodazole (panel A) or 10 μg/ml cytochalasin-B (panel B) for 30 min. Cells were then analyzed by time-lapse confocal spinning disk microscopy. The right panels represent selected frames from the time-lapse series (time is given in second). Arrows point to Cav1-positive intracellular vesicles. See corresponding movie S2 (panel A) and movie 3 (panel B). Scale bars, 5 μm.
doi:10.1371/journal.pone.0052627.g003

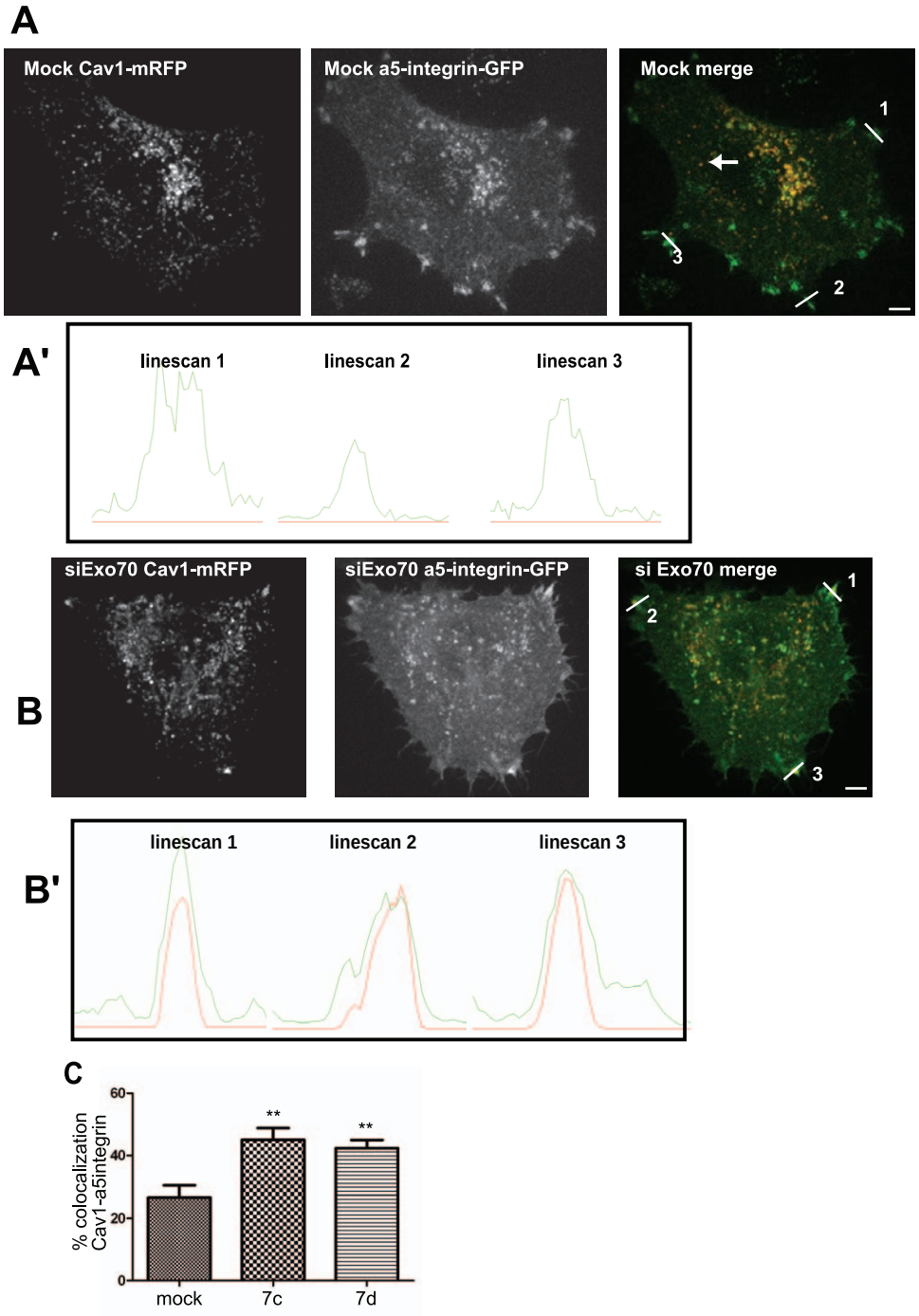

Figure 4. Exo70 is required for Cav1 transport to the plasma membrane. (**A, B**) Hela cells expressing Cav1-mRFP and α5-integrin-GFP either mock-treated (A) or treated with a specific siRNA to silencing Exo70 (B) were maintained in suspension for 1 h and replated on fibronectin for 3 h, and visualized using time-lapse spinning disk microscopy. Scale bars, 5 μm. (**A′, B′**) Intensity profile of Cav1 (red) and α5-integrin (green) along the white lines shown in panel A and B. (**C**) Co-localization analysis of Cav1-mRFP and α5-integrin-GFP in cells as in panels A and B in a 20-pixel width region along the cell periphery of mock- or Exo70 siRNA-depleted cells using two specific siRNAs (siRNA 7c and 7d). Results are the average of mean percentage of co-localization ± s.e.m. of three experiments. ** $P<0.05$. Experiment has been repeated three times; with number of cell analysed: n = 19 for mock cells, n = 17 for siRNA 7c, and n = 17 for siRNA 7d.
doi:10.1371/journal.pone.0052627.g004

fibronectin for 3h, and labeled for endogenous Cav1 and the focal adhesion protein vinculin. Using the quantification method described above, we found a 6.3% co-localization of Cav1 and vinculin at focal adhesions. This value increased to 10–12% in cells depleted for Exo70 (Fig. 5). Thus, these results suggest that depletion of Exo70 results in an accumulation of Cav1 at focal adhesions.

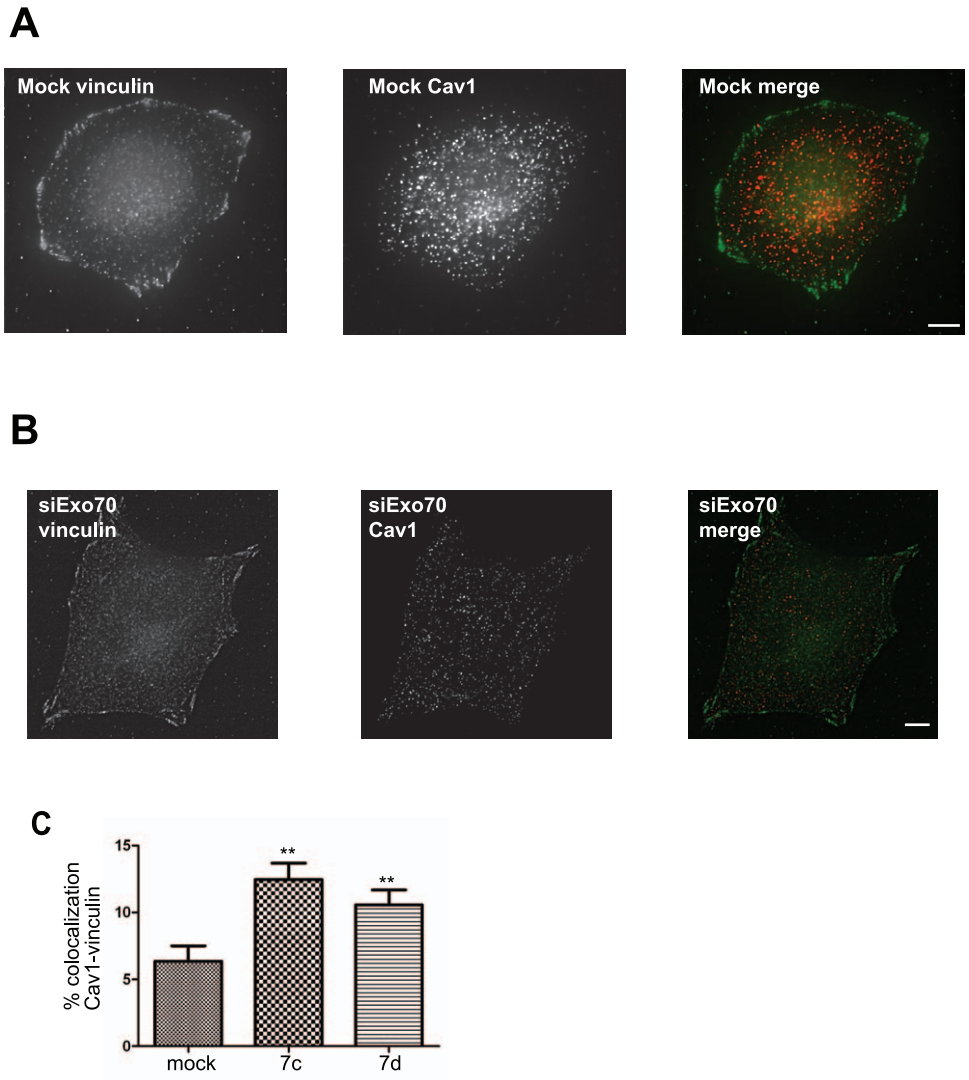

Figure 5. Silencing of Exo70 leads to Cav1 accumulation in focal adhesions. Mock-treated (**A**) or Exo70-depleted cells (**B**) were detached for 1 h and replated on fibronectin-coated substrate for 3 h, and then fixed and stained for endogenous vinculin and Cav1. Scale bars, 5 µm. Co-localization between Cav1 and vinculin was quantified in a 20-pixel width region from the cell periphery and compared in Exo70-depleted with two independent siRNAs *vs.* mock-treated cells (**C**). Results in panel C are the average of mean percentage of co-localization ± s.e.m. of three experiments. ** $P<0.05$. Experiment has been repeated three times with number of cells analysed: n = 25 mock cells, n = 9 for cells treated with Exo70 siRNA 7c, and n = 23 for siRNA 7d.
doi:10.1371/journal.pone.0052627.g005

Discussion

This study reveals that Exo70 accumulates in dotty structures, which are visible by TIRF-M at the plasma membrane. Exo70-positive plasma membrane domains are enriched in PtdIns(4,5)P2, a lipid known to mediate binding of Exo70 at the plasma membrane both in yeast and mammal cells [14,16]. In addition, in mammalian cells Exo70 has been shown to recruit other exocyst components to the plasma membrane and to control the tethering of secretory vesicles [15]. Thus, Exo70-positive puncta that we observed at the adherent plasma membrane of HeLa cells may represent some exocytic vesicles docking sites. Interestingly, these puncta also appear to be enriched for the main caveolar component, Cav1.

Whether caveolae can mediate endocytosis of specific cargo(es) is still a matter of debate [1]. In contrast, several studies have documented the internalization of caveolae in internal compartments during diverse cellular processes including mitosis and cell detachment [7,28]. Cell adhesion signaling through ß1 integrins seems to play a key role for the recycling of caveolar components and the formation of caveolae at the plasma membrane [6,20,23,24]. Keratinocytes from mice knockout for ß1 integrin or integrin-linked kinase (ILK) show a very low level of caveolae due to impaired traffic of Cav1-containing transport vesicles along microtubules [23,24]. ILK was shown to promote the recruitment of actin regulators allowing stable insertion of caveolae into the plasma membrane [24]. Our study confirms that intracellular transport of Cav1 is a multistep process controlled by cell adhesion. First, cell detachment leads to a massive redistribution of Cav1 and α5ß1 integrins in a perinuclear compartment. This compartment is rab7- and Vamp7-positive suggesting that upon cell detachment, Cav1 is internalized and trafficked to late endosome/lysosomal compartments. This is reminiscent of the effect of cholesterol depletion or serum deprivation, which trigger

caveolae accumulation into late endosomes/lysosomes [29]. Members of the cavin protein family, which comprise four proteins including cavin-1/PTRF are also crucial for caveolae formation [5,22]. Here, we observed that Cav1 partially redistributed with cavin-1 after cell detachment, suggesting that mature caveolae are internalized and traffic upon cell detachment (figure 2B). A recent study supports the conclusion that under normal conditions, upon docking and fusion of Cav1-positive transport carriers with the plasma membrane at nascent focal adhesions, Cav1 would be segregated away from focal adhesion to redistribute laterally along the plasma membrane bilayer for caveolae assembly [30]. Our data indicate that in adherent cells, at steady-state, Exo70 domains co-localize with a subset of Cav1-positive structures at the plasma membrane, very likely corresponding to caveolae, while these proteins show no association in the cytoplasm. Upon cell detachment and readhesion, Cav1 redistributes to late endosomes and strongly co-localizes with Exo70. Upon silencing of Exo70, Cav1 (or Cav1-positive transport carriers) are retained at focal adhesions and mistargeted, suggesting that Exo70 is involved in Cav1 recycling to the plasma membrane during readhesion of the cells to the substratum.

To conclude, functions for caveolae have been identified in biomechanical remodeling or mechanosensing [3,4,28]. Indeed, Cav1 and caveolae are abundant in cells experiencing high mechanical stress such as muscle, skin and endothelial cells. The fact that Cav1 and caveolae levels at the cell surface are regulated by cell adhesion provide a rational for the regulation of caveolae assembly by mechanical clues.

Materials and Methods

Cell Culture, transfection and siRNA treatment

Hela cells were cultured in DMEM medium (GIBCO) containing 15% FCS and 2 mM glutamine at 37°C and 5% CO_2. For treatment with cytoskeleton-disassembling drugs, cells were treated for 30 min with nocodazole (working concentration 10 μM) or cytochalasin-B (10 μg/ml). Drugs were purchased from Sigma.

Cells were transfected with following plasmids: Exo70-GFP or -mCherry, Exo84-GFP or -mCherry cloned in pcDNA3.1 plasmid; Cav1-GFP or mRFP constructs were a kind gift of Dr A. Helenius (ETH, Zürich) [31]; Cavin-1-mRFP was a kind gift of Dr C. Lamaze (Institut Curie, Paris) [3] and tubby-GFP was a kind gift L. Shapiro (Columbia University, New York) [20]. Transfections with plasmid DNA (1 μg) were carried out with Fugene (Roche) according to the manufacturer' instructions. Cells were analyzed 24 h after transfection.

Cells were transfected with two independent siRNAs (Dharmacon) specific for EXOC7 (Exo70) at a concentration 100 nM using Oligofectamine (Invitrogen). Sequences of the forward strand were as follows: EXOC7-duplexC: 5′-GAGAUGACAUGCUGGACGUUU-3′, EXOC7-duplexD: 5′-GGAAGGCCAUUGUGCGACAUU-3′. Mock or siRNA-treated cells were analyzed 3 days after transfection.

Western blot and antibodies

siRNA-treated cells were lysed in lysis buffer (50 mMTris-HCl [pH 7.4], 150 mM NaCl, 1% Triton X-100, 1 mM EDTA, and protease inhibitors Mini complete, Roche) and centrifuged at 16,000 g for 10 min at 4°C. Supernatants were separated by SDS-PAGE and analyzed by immunoblotting. Rabbit polyclonal antibodies against actin (A5060) and Cav1 (610060) were purchased from Sigma and BD Bioscience, respectively. Monoclonal antibody against EXOC7 was a generous gift of Dr S. Hsu (Rutgers University, NJ). Monoclonal against human vinculin was a kind gift of Dr Marina Glukhova (Institut Curie-Paris). HRP-conjugated anti-mouse IgG, Cy3-conjugated anti-mouse and Cy5-conjugated F(ab)2 anti-mouse antibodies were purchased from Jackson ImmunoResearch Laboratories. Alexa-Fluor-labeled anti-mouse IgG antibodies were purchased from Molecular Probes (Invitrogen).

Caveolin1 trafficking assay and quantification

Hela cells transfected with the indicated constructs were detached, held in suspension in culture medium supplemented with 20 mM Hepes at 37°C for 1 h and replated on fibronectin (10 μg/ml) coated glass dish. After the indicated time of replating, the cells were fixed for immunfluorescence analysis or observed in live using spinning disk or TIRF-M.

For quantification of co-localization between α5-integrin-GFP and Cav1-mRFP at the cell periphery, the area of cell surface was drawn with the Threshold command of MetaMorph 7. A 20-pixel width region from the cell periphery was created using both the Erode and Create Region commands of MetaMorph 7. The percentage of co-localization of the two proteins was measured using the Measure Colocalization command of MetaMorph 7 in the 20-pixel region. Statistical analyses were performed using Student's *t* test in GraphPad Prism 5 software.

Live cell imaging by TIRF and spinning disk confocal microscopy

For live cell imaging by TIRF-M, HeLa cells seeded onto glass-bottom dish were transfected with the indicated constructs and imaged the next day with a 100× 1.49 NA TIRF objective on a Nikon TE2000 (Nikon France SAS, Champigny sur Marne, France) inverted microscope equipped with a QuantEM EMCCD camera (Roper Scientific SAS, Evry, France/Photometrics, AZ, USA), a dual output laser launch which included 491 and 561 nm 50 mW DPSS lasers (Roper Scientific), and driven by Metamorph 7 software (MDS Analytical Technologies). A DV2 beam-splitter system (Roper Scientific/Photometrics) mounted on the light path enabled the simultaneous acquisition of the two emission channels. A motorized device driven by Metamorph allowed accurate positioning of the illumination light for evanescent wave excitation.

For spinning disk microscopy, HeLa cells plated onto a glass-bottom dish coated with fibronectin (Sigma, 10 μg/ml) and transfected with the indicated constructs. Images were acquired with 100 ms exposure time at 2 or 5 s interval as indicated using a spinning disk microscope based on a CSU22 Yokogawa head mounted on the lateral port of an inverted microscope Leica IRE2 equipped with a 100× 1.4NA Plan-Apo objective and a dual output laser launch which included 491 and 561 nm ERROL laser bench 491 nm, 561 nm (Roper Scientific). Images were acquired with a Camera EMCCD Cascade 512×512 (Photometrics). The system was steered by Metamorph 7 software.

Immunofluorescence analysis

For immunofluorescence analysis, Hela cells were plated on fibronectin coated coverslips, fixed and extracted with 0.3% Triton X-100 in 4% PFA for 20 min and further fixed for 20 min by 4% PFA. Then, cells were incubated with Cav1 antibodies in PBS and washed with PBS. Bound antibodies were detected with Cy3-conjugated mouse antibodies. Cells were then mounted in ProLong Gold antifade reagent (Invitrogen) containing DAPI. Images were taken using Eclipse 90i Upright Microscope with a

CCD Camera CoolSNAP HQ2 and a Piezo Flexure Objective Scanner. The system was steered by Metamorph 7 software.

Supporting Information

Figure S1 TIRF-M revealed specific structures positive for Cav1-GFP and Exo70-mCherry. (**A**) Hela cells expressing Cav1-GFP and Exo70-mCherry were visualized by TIRF-M (top panel). The bottom panel shows a wide-field image of the same field. (**B**) Hela cells expressing tubby-GFP and Exo70-mCherry were visualized by TIRF-M. Scale bars, 5 µm. Inset shows higher magnification of region indicated by an arrow.
(EPS)

Figure S2 Caveolin1 co-localizes with late endosomes markers, GFP-rab7 or GFP-VAMP7. (**A**) Hela cells expressing Cav1-mRFP and GFP-rab7 were detached and maintained in suspension for 1 h in culture medium at 37°C, and then replated on fibronectin for 3 h and visualized using time-lapse confocal spinning disk microscopy (upper panel). The lower panels represent selected frames from the time-lapse series (time is given in second). Arrows point to a Cav1-, rab7-positive intracellular vesicle. (**B**) Hela cells expressing Cav1-mRFP and GFP-VAMP7 were treated and analyzed as in panel A. Scale bars, 5 µm.
(EPS)

Figure S3 Exo70 silencing. Samples of Hela cells treated with two independent Exo70 siRNAs (7c and 7d) were analyzed by western blotting with the indicated antibodies. Levels of Exo70 were reduced by 1.9 and 2.2-fold upon treatment with Exo70 siRNA 7c and 7d, respectively. Actin immunoblotting staining was used as a loading control. Levels of Exo70 strongly decreased without affecting Cav1 levels.
(EPS)

Figure S4 Silencing of Exo70 inhibited cell spreading on fibronectin-coated substratum. Mock-treated cells or cells silenced for Exo70 were maintained in suspension for 60 min and replated on fibronectin for 3 or 6 h and fixed. The projected cell surface area was measured using Metamorph software. Graph represents the mean projected cell surface area ± S.E.M. in μm^2 measured before putting cell in suspension (t = 0); after 3 h (t = 3 h) and 6 h of replating (t = 6 h) on fibronectin coated substrates. ** $P<0.05$.
(EPS)

Movie S1 Microtubule disassembly interferes with Cav1-positive vesicle trafficking. Hela cells expressing Cav1-mRFP were kept in suspension for 1 h, and then replated on fibronectin-coated substrate for 3 h and further incubated in the presence of nocodazole for 30 min. Cells were visualized using time-lapse spinning disk microscopy. Images were taken every 2 s. Under Nocodazole treatment, Cav1- positive vesicles are static and concentrated in the cell center.
(MOV)

Movie S2 Cytochalasin-B treatment interferes with Cav1 trafficking. Hela cells expressing Cav1-mRFP are put in suspension for 1 h replated on fibronectin-coated substrates for 3 h, incubated with 10 µg/ml cytochalasin-B for 30 min, and visualized using time-lapse Spinning Disk Microscopy. Images are taken each 2 s. Under these conditions, an accumulation of Cav1-mRFP positive vesicles appeared at the cell periphery.
(MOV)

Movie S3 Cav1-positive tubules target peripheral focal adhesions. Hela cells expressing Cav1-mRFP and α5-integrin-GFP are put in suspension for 1 h replated on fibronectin-coated substrates for 3 h, and visualized using time-lapse confocal spinning disk microscopy. Images are taken each 5 s.
(MOV)

Movie S4 Cav1-positive tubules target peripheral focal adhesions. Hela cells expressing Cav1-mRFP and α5-integrin-GFP are put in suspension for 1 h replated on fibronectin-coated substrates for 3 h, and visualized using time-lapse confocal spinning disk microscopy. Images are taken each 5 s.
(MOV)

Acknowledgments

The authors wish to thank Drs C. Lamaze, M. Arpin, S. Hsu, M. Glukhova and L.Shapiro for providing reagents. We are indebted to Dr G. Scita for critical reading of the manuscript. We thank the staff of the Cell and Tissue Imaging Facility (PICT-IBiSA) for help with image acquisition. Members of PC's laboratory are thanked for helpful discussions.

Author Contributions

Conceived and designed the experiments: MH PC. Performed the experiments: MH GLD. Analyzed the data: MH PC. Contributed reagents/materials/analysis tools: GLD PM. Wrote the paper: MH PC.

References

1. Parton RG, Simons K (2007) The multiple faces of caveolae. Nat Rev Mol Cell Biol 8: 185–194.
2. Parton RG, Hanzal-Bayer M, Hancock JF (2006) Biogenesis of caveolae: a structural model for caveolin-induced domain formation. J Cell Sci 119: 787–796.
3. Sinha B, Koster D, Ruez R, Gonnord P, Bastiani M, et al. (2011) Cells respond to mechanical stress by rapid disassembly of caveolae. Cell 144: 402–413.
4. Goetz JG, Minguet S, Navarro-Lerida I, Lazcano JJ, Samaniego R, et al. (2011) Biomechanical remodeling of the microenvironment by stromal caveolin-1 favors tumor invasion and metastasis. Cell 146: 148–163.
5. McMahon KA, Zajicek H, Li WP, Peyton MJ, Minna JD, et al. (2009) SRBC/cavin-3 is a caveolin adapter protein that regulates caveolae function. EMBO J 28: 1001–1015.
6. Pelkmans L, Zerial M (2005) Kinase-regulated quantal assemblies and kiss-and-run recycling of caveolae. Nature 436: 128–133.
7. Boucrot E, Howes MT, Kirchhausen T, Parton RG (2011) Redistribution of caveolae during mitosis. J Cell Sci 124: 1965–1972.
8. del Pozo MA, Alderson NB, Kiosses WB, Chiang HH, Anderson RG, et al. (2004) Integrins regulate Rac targeting by internalization of membrane domains. Science 303: 839–842.
9. Echarri A, Muriel O, Del Pozo MA (2007) Intracellular trafficking of raft/caveolae domains: insights from integrin signaling. Semin Cell Dev Biol 18: 627–637.
10. He B, Guo W (2009) The exocyst complex in polarized exocytosis. Curr Opin Cell Biol 21: 537–542.
11. Munson M, Novick P (2006) The exocyst defrocked, a framework of rods revealed. Nat Struct Mol Biol 13: 577–581.
12. Hertzog M, Chavrier P (2011) Cell polarity during motile processes: keeping on track with the exocyst complex. Biochem J 433: 403–409.
13. Muriel O, Echarri A, Hellriegel C, Pavon DM, Beccari L, et al. (2011) Phosphorylated filamin A regulates actin-linked caveolae dynamics. J Cell Sci 124: 2763–2776.
14. He B, Xi F, Zhang X, Zhang J, Guo W (2007) Exo70 interacts with phospholipids and mediates the targeting of the exocyst to the plasma membrane. EMBO J 26: 4053–4065.
15. Zuo X, Zhang J, Zhang Y, Hsu SC, Zhou D, et al. (2006) Exo70 interacts with the Arp2/3 complex and regulates cell migration. Nat Cell Biol 8: 1383–1388.
16. Liu J, Zuo X, Yue P, Guo W (2007) Phosphatidylinositol 4,5-bisphosphate mediates the targeting of the exocyst to the plasma membrane for exocytosis in mammalian cells. Mol Biol Cell 18: 4483–4492.
17. Spiczka KS, Yeaman C (2008) Ral-regulated interaction between Sec5 and paxillin targets Exocyst to focal complexes during cell migration. J Cell Sci 121: 2880–2891.
18. Balasubramanian N, Meier JA, Scott DW, Norambuena A, White MA, et al. (2010) RalA-exocyst complex regulates integrin-dependent membrane raft exocytosis and growth signaling. Curr Biol 20: 75–79.

19. Balasubramanian N, Scott DW, Castle JD, Casanova JE, Schwartz MA (2007) Arf6 and microtubules in adhesion-dependent trafficking of lipid rafts. Nat Cell Biol 9: 1381–1391.
20. Santagata S, Boggon TJ, Baird CL, Gomez CA, Zhao J, et al. (2001) G-protein signaling through tubby proteins. Science 292: 2041–2050.
21. del Pozo MA, Balasubramanian N, Alderson NB, Kiosses WB, Grande-Garcia A, et al. (2005) Phospho-caveolin-1 mediates integrin-regulated membrane domain internalization. Nat Cell Biol 7: 901–908.
22. Hill MM, Bastiani M, Luetterforst R, Kirkham M, Kirkham A, et al. (2008) PTRF-Cavin, a conserved cytoplasmic protein required for caveola formation and function. Cell 132: 113–124.
23. Wickstrom SA, Fassler R (2011) Regulation of membrane traffic by integrin signaling. Trends Cell Biol 21: 266–273.
24. Wickstrom SA, Lange A, Hess MW, Polleux J, Spatz JP, et al. (2010) Integrin-linked kinase controls microtubule dynamics required for plasma membrane targeting of caveolae. Dev Cell 19: 574–588.
25. Wickstrom SA, Fassler R (2011) Regulation of membrane traffic by integrin signaling. Trends Cell Biol 21: 266–273.
26. Wickstrom SA, Lange A, Hess MW, Polleux J, Spatz JP, et al. (2010) Integrin-linked kinase controls microtubule dynamics required for plasma membrane targeting of caveolae. Dev Cell 19: 574–588.
27. Thapa N, Sun Y, Schramp M, Choi S, Ling K, et al. (2012) Phosphoinositide signaling regulates the exocyst complex and polarized integrin trafficking in directionally migrating cells. Dev Cell 22: 116–130.
28. Del Pozo MA, Schwartz MA (2007) Rac, membrane heterogeneity, caveolin and regulation of growth by integrins. Trends Cell Biol 17: 246–250.
29. Mundy DI, Li WP, Luby-Phelps K, Anderson RG (2012) Caveolin targeting to late endosome/lysosomal membranes is induced by perturbations of lysosomal pH and cholesterol content. Mol Biol Cell 23: 864–880.
30. Muriel O, Echarri A, Hellriegel C, Pavon DM, Beccari L, et al. (2011) Phosphorylated filamin A regulates actin-linked caveolae dynamics. J Cell Sci 124: 2763–2776.
31. Pelkmans L, Burli T, Zerial M, Helenius A (2004) Caveolin-stabilized membrane domains as multifunctional transport and sorting devices in endocytic membrane traffic. Cell 118: 767–780.